ANTIMICROBIAL BIOADHESIVE POLYMER COMPLEXES FOR THE ORAL CAVITY

GEMMA KEEGAN

A thesis submitted in partial fulfilment of the requirements of the University of Brighton for the degree of Doctor of Philosophy

March 2007

The University of Brighton in collaboration with GlaxoSmithKline.

ABSTRACT

Due to the problems associated with local antimicrobial delivery to the oral cavity, such as poor retention times, the use of bioadhesive polymers within oral healthcare products may significantly improve therapeutic efficacy. In the current study, bioadhesive antimicrobial-polymer complexes were investigated as a formulation strategy to improve the substantivity of antimicrobial compounds within the oral cavity.

Interactions between Carbopol™ polymers and antimicrobial metals were investigated using a dialysis technique. Carbopol 971P-zinc complexes exhibited ideal properties, with zinc retained by the polymer in deionised water and displaced in the presence of sodium chloride and calcium chloride at a rate determined by the pH of the solution. Carbopol 971P-silver and Carbopol 971P-copper complexes were both retained by the polymer in deionised water but did not demonstrate ideal displacement in the presence of competing ions. Both Carbopol 971P-zinc and Carbopol 971P-silver complexes exhibited bioadhesive properties comparable to the polymer alone when assessed using an *in vitro* staining technique and texture probe analysis, however Carbopol 971P-copper adhesion was significantly reduced.

Interactions between chitosan and fluoride did not prevent fluoride release in deionised water when using the dialysis technique, therefore microparticles were formulated using a water-in-oil solvent evaporation technique and by spray-drying. Spray-dried fluoride microparticles exhibited a smaller size distribution, sustained fluoride release, improved fluoride loading and bioadhesion to oesophageal epithelium when compared to particles prepared from a water-in-oil solvent evaporation technique. Scanning electron microscopy revealed the presence of crystals on the surface of particles prepared by water-in-oil solvent evaporation, which were absent in particles prepared by spray-drying. Higher starting concentrations of chitosan were found to improve the fluoride loading of spray-dried microparticles; however the addition of glutaraldehyde had no significant effect on the parameters measured.

Antimicrobial activity was initially assessed using a broth microdilution technique against a range of planktonic oral bacteria. Optimised chitosan-fluoride microparticles

demonstrated some activity at the highest concentration tested but was not effective against all species tested. Antimicrobial assessment of Carbopol 971P-zinc complexes suggested a lack of zinc bioavailability, possibly due to the lack of displacement. Subsequent assessment of metal salts alone established the antimicrobial activity of zinc and silver, with copper demonstrating the lowest efficacy. The use of a bioavailability model developed at GlaxoSmithKline found no improvement in zinc or silver efficacy when formulated with Carbopol 971P in preventing the formation of a biofilm on hydroxyapatite.

Despite the lack of significant antimicrobial effects, the potential for bioadhesive polymers in the improvement of antimicrobial retention within the oral cavity has been demonstrated through the characteristics of the complexes formed.

TABLE OF CONTENTS

ACKNOWLEGDEMENTS

My deepest gratitude goes to all of my supervisors who have been involved with the project over the years of my PhD, but first and foremost, to Professor John Smart, whose guidance and expertise has been a constant inspiration. To Dr Matthew Ingram and Dr Lara Barnes, your open doors, knowledge and coffee kept me going from when I arrived in Brighton, until the end. To Dr Gareth Rees and Dr Gary Burnett from GlaxoSmithKline, I could not have asked for better industrial supervisors, you have both been exemplary. I would also like to take the opportunity to thank both GlaxoSmithKline and the BBSRC for their funding and support of the project.

There are many other people who have helped me along the way and my first thank you must go to all my fellow PhD students both past and present. In particular Dominick Burton, Jenny Shackelford, Adam Heikal and Michael Maelzer. There was nothing quite like a good night out and bad hangover to get over a naff experiment. Much of the work I have achieved has been possible due to the dedication and support of numerous technical staff, so thank you to Val Ferrigan, Darren Gullick, Marcus Nash, Cinzia Dedi, Howard Dodd, and John Stephens. I would also like to thank Dr Gary Phillips for football conversations during those lengthy visits to the microscope room in Brighton, Gail Martin at GlaxoSmithKline for her help with the bioavailability model and scanning electron microscopy, and for the molecular biologists in laboratory 803, for putting up with someone who doesn't know whose chair it is anyway. I must also thank Louise Tait, the 4th year Pharmacy student whose dedication to the work reminded me during the last year what it was all about.

My friends Kelly Buckley, Polly Meldrum and Lisa Rusiecka, you have all listened to me moan on the phone for hours and that is a challenge in itself, many thanks go to all of you. I'd also like to thank the men in my life. My partner George for his constant support and love, even at times when I didn't deserve it. To my Dad and brothers, Karl and Sean, I love you, but really, what did you do again? And last but not least, my mum, my strength. Oh, and thanks for nagging.

Thank you.

AUTHOR'S DECLARATION

I declare that the research contained within this thesis, unless otherwise formally indicated within the text, is the original work of the author. The thesis has not been previously submitted to this or any other university for a degree, and does not incorporate any material already submitted for a degree.

Signature

Date

Chapter 1:
General Introduction

1.1 The Oral Cavity

1.1.1 Overview

The oral cavity is the first functional compartment of the alimentary tract, which consists of the lips, mouth, pharynx, oesophagus, stomach, small and large intestine, rectum and anus. These structures vary according to the specialised functions required to cause the mechanical fragmentation and chemical digestion of food in transit (Bloom and Fawcett. 1975). The oral cavity itself has numerous functions: mastication, taste, swallowing, lubrication, digestion, speech, the signalling of thirst, and protection of the body from harmful ingested substances (Smith and Morton. 2001).

1.1.2 The teeth

The main task of the oral cavity i.e. the fragmentation of large food masses, is performed by the teeth, which are arranged to allow food to be trapped between two opposing surfaces (Stevens and Lowe. 1997). Although the teeth appear different, each tooth has a basically similar structure (Figure 1.1). The crown protrudes into the oral cavity and is characterised by a layer of hard material called enamel, which is composed of hydroxyapatite ($Ca_5(PO_4)_3OH$) arranged in tightly packed hexagonal rods or prisms (Stevens and Lowe. 1997). This functions to provide the hardness to the teeth for the purpose of fragmenting food, and to protect the underlying dentine, a calcified tissue composed of crystalline hydroxyapatite that forms the bulk of each tooth. Dentine is formed by the mineralisation of predentine upon the discharge of small matrix vacuoles containing Ca^{2+} and PO_4^{2-} ions from odontoblasts (Stevens and Lowe. 1997). The pulp cavity is located at the centre of the tooth and contains blood vessels, which provide nourishment to the odontoblasts and nerve endings. These vessels enter and leave via the root canal. Cementum is a calcified bone-like tissue, which covers the dentine of the root. The upper region of cementum is thin and compact while the lower region is thicker and contains cementocytes, which lie within small cavities surrounded by calcified tissue (Stevens and Lowe. 1997). The dense collagen and fibrocytes of the periodontal ligament run between the cementum and alveolar bone, tethering the tooth

in the bony sockets of the mandible and maxilla. The periodontal ligament permits some movement of the tooth as well as acting as a biological shock absorber.

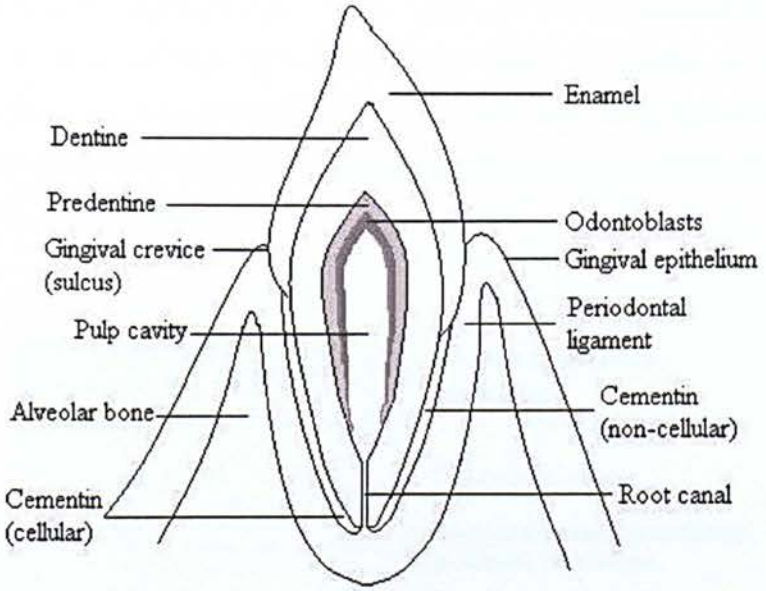

Figure 1.1 Basic structure of a tooth (adapted from Smith and Morton. 2001)

The gingival sulcus is a unique junction between two dissimilar tissues (Squier and Wertz. 1996). The epithelium surrounding the gingivae is keratinised; however within the sulcus this becomes non-keratinised. This epithelium is attached to the tooth surface by a stratified epithelium known as the junctional epithelium, which is undifferentiated and permeable to a variety of substances (Squier and Wertz. 1996). Gingival crevicular fluid (GCF) derived from serum components passes through the junctional epithelium. Within healthy sites, the flow of GCF is relatively slow but it increases during inflammation (Marsh and Martin. 1999). It is rich in serum proteins such as transferrin, haemoglobin and albumin. GCF also contains host defence components, these include: immunoglobulins (predominantly IgG), complement and leucocytes (predominantly neutrophils).

1.1.3 The oral mucosa

The oral mucosal (Figure 1.2) is covered by a stratified squamous epithelium, which is keratinised in some regions. This type of epithelium is characterised by a variable

number of cell layers, which undergo a morphological and functional transition from the cuboidal basal layer to the flattened surface layers (Stevens and Lowe. 1997). At the surface, degenerate cells are sloughed off and replaced by cells from the deeper layers. The rate at which the entire thickness of the epithelium can be replaced by this process is known as the turnover time (Squier and Wertz. 1996). In addition to keratinisation, both the thickness of the epithelium and its turnover time vary throughout different regions of the oral cavity. In general keratinising epithelium has a slower turnover time than non-keratinising epithelium.

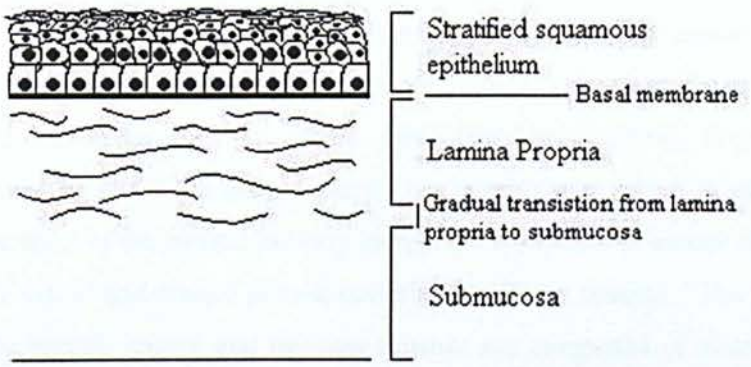

Figure 1.2 The oral mucosa, composed of a superficial layer of epithelium and a supporting layer of loose connective tissue, the lamina propria. The underlying submucosa contains numerous blood vessels, nerves and lymphatics within a connective tissue matrix. Image adapted from Bloom and Fawcett (1975).

Three different types of oral mucosa are recognised within the oral cavity (Squier and Wertz. 1996; Johnson and Moore. 1997):

- The lining mucosa covers the soft palate, ventral (lower) surface of the tongue, the floor of the mouth, the alveolar processes excluding the gingivae (gums), and the internal surfaces of the lips and cheeks. It is characterised by non-keratinising epithelium.
- The masticatory mucosa covers the gingivae and hard palate and is characterised by keratinised epithelium. These regions are subject to the mechanical forces of mastication, such as abrasion and shearing.

- The specialised mucosa covers the dorsal surface of the tongue. The anterior two-thirds are characterised by a keratinised epithelium bearing the papillae, or taste buds. The posterior third of the tongue is characterised by a non-keratinised epithelium, which covers lymphoid tissue nodules.

1.1.4 Saliva

Whole saliva is the collective product of secretions produced by the parotid, submandibular and sublingual salivary glands, in addition to the numerous minor glands located in the buccal mucosa and palate. Generally, glands can be considered in terms of the type of secretory cells located in the acini; serous, mucous or mixed (Bloom and Fawcett. 1975; Herrera *et al.*, 1988; Dowd. 1999; Hand *et al.*, 1999). Serous secretions are watery in nature due to the lack of mucin, but contain salts, proteins and the enzyme amylase. The acini of the parotid salivary glands are composed of serous cells. Mucous secretions are viscid and consist almost entirely of salivary mucins. The minor glands located in the buccal, lingual and palatine mucosa are composed of mucous cells and although the secretions from these glands account for only 10% of whole saliva, they can contribute up to 70% of the mucin content (Herrera *et al.*, 1988). Both the submandibular and the sublingual glands are composed of a mixture of secretory cells. The composition of whole saliva is highly variable and is dependant on a number of factors, including the time of day and the degree and type of stimulation (Bradley. 1995). Nervous stimulation accounts for 80-90% of the daily production of saliva and determines the salivary flow rate (Mandel and Wotman. 1976). During unstimulated states, saliva is secreted at a basal level, termed the resting flow rate.

The constituents that are found within whole saliva can be divided into two major categories: water and electrolytes (inorganic components) and macromolecules (organic components). The ions present within the oral cavity are derived from the blood plasma and include sodium, potassium, chloride and bicarbonate, amongst others. Bicarbonate is the major buffer in saliva and its concentration increases during nervous stimulation. The buffering capacity of saliva is important in the control of oral pH. Saliva is supersaturated with calcium phosphates, which help prevent the demineralisation of tooth enamel. Non-electrolytes such as urea, uric acid and ammonia are derived from

blood plasma and contribute to the buffering capacity of saliva (Dowd. 1999). Saliva contains many organic components, which contribute to functions such as, digestion (through enzymatic activity), lubrication and the protection of dental tissues (Table 1.1). Salivary components, in particular proteins, are multifunctional, redundant (performing similar functions but to different extents) and amphifunctional (acting both for and against the host) (Humphrey and Williamson. 2001).

The protective film that covers oral surfaces is known as the salivary pellicle; however the components that adsorb to different locations are not identical (Marsh and Martin. 1999). The pellicle that forms on mucosal surfaces is referred to as the mucus coat, while the pellicle that forms on enamel is referred to as the acquired enamel pellicle. The mucous coat is predominantly composed of salivary mucin and is approximately 53 μm thick (Slomiany *et al.*, 1996). Mucins have been shown to interact with the buccal mucosa via receptor proteins located within the epithelial cell membranes (Slomiany *et al.*, 1996). The function of the mucus coat is to preserve oral mucosal integrity through the modulation of intracellular calcium levels (Slomiany *et al.*, 1996). The mucus coat also limits the diffusion of various compounds, neutralises weak acids and resists proteolysis, protecting the mucosa underneath (Herrera *et al.*, 1988).

The acquired enamel pellicle is formed from the selective adsorption of specific salivary proteins on the enamel surface (Table 1.1). Protein adsorption is most likely facilitated through ionic interactions between hydroxyapatite and negatively charged residues such as serine and sialic acid (Boackle *et al.*, 1999). The acquired enamel pellicle has multiple functions; as well as lubricating the teeth it forms a chemical barrier, preventing the diffusion of acids, which can cause enamel demineralisation (Hannig *et al.*, 2004).

Table 1.1 Major organic components of human whole saliva (Slomiany *et al.*, 1996; Dowd. 1999; Humphrey and Williamson. 2001).

	Example	Molecular weight (approx)	Functions
Amylase	4-6 isoenzymes	67 kDa	Hydrolyses glycosidic links in starch.
Lipase	-	52 kDa	First phase digestion of lipids.
Mucous glycoprotein (Mucins)	MG1	>1000 kDa	Binds tightly to hydroxyapatite- provides physical and chemical barrier.
	MG2	120 kDa	Bind and aggregates oral bacteria. Forms complexes with other salivary components- concentrating them on oral surfaces.
Proline-rich protein	Acidic PRP	10-30 kDa	Bind tightly to hydroxyapatite. Aid in supersaturation of saliva.
	Basic PRP		Bind and aggregates oral bacteria.
Tyrosine-rich protein	Statherins	5.3 kDa	Bind to hydroxyapatite. Aid in supersaturation of saliva. Lubrication.
Histadine-rich protein	Histatin	3-4 kDa	Antifungal and antibacterial activity. Bind to hydroxyapatite. Aid in supersaturation of saliva.
Peroxidase	-	67 kDa (unglycosylated)	Produces hypothiocyanate from bacterial by-products, which inhibits glucose metabolism. Protects oral tissues from hydrogen peroxide.
Lysozyme	-	14 kDa	Binds salivary anions e.g. F^- Hydrolysis of polysaccharide component of bacterial cell wall.
Secretory IgA	2 isoforms	685 kDa dimer	Inhibits bacterial adherence. Neutralizes bacterial toxins and enzymes.
Protease inhibitors	Cystatins	15 kDa	Protect oral tissues from proteases. Bind to hydroxyapatite. Aid in supersaturation of saliva.

1.1.5 Microbial ecology of the oral cavity

Several different habitats that each supports a characteristic community of microorganisms can be identified within the oral cavity (Theilade. 1990; Marcotte and Lavoie. 1998; Marsh and Martin. 1999; Mager *et al.*, 2003). Within this ecosystem, a

variety of factors can influence the selection of microorganisms and help maintain the equilibrium among bacterial populations (Marcotte and Lavoie. 1998).

The oral mucosa represents a soft tissue site for the colonisation of oral bacteria. This surface is characterised by the desquamation of surface epithelial cells, and consequently the removal of surface bound microorganisms (Theilade. 1990). The gingival, palatine, buccal and lingual mucosa are colonised by few microorganisms (Marcotte and Lavoie. 1998). Frequent disruption accounts for the lack of complex microbial communities at these sites. The teeth represent a hard, non-shedding surface for microbial colonisation, which enables the accumulation of microorganisms (Marsh and Martin. 1999). Microorganisms exist in a complex matrix composed of microbial extracellular products and salivary compounds known as dental plaque (see 1.1.4.1).

The growth of oral microorganisms is influenced by a variety of physicochemical, host, microbial and external factors. These include: temperature, pH, oxidation-reduction potential, nutrients (both endogenous and exogenous), microbial adherence and agglutination, antimicrobial agents, host defences, and host genetics (Marsh and Martin. 1999; Marcotte and Lavoie. 1998).

All microorganisms that establish a more or less permanent residence within the human oral cavity are termed "resident" microflora (Theilade. 1990). The resident microflora is diverse comprising more than 200 species (Marsh and Martin. 1999). It can also be extremely variable, both qualitatively and quantitatively (Theilade. 1990). Some microorganisms may be isolated from the oral cavity without establishing residency; these are termed transient microflora, and are typically derived from other body surfaces or surroundings (Theilade. 1990). The oral microflora includes a wide range of species of viruses, mycoplasma, bacteria, fungi and protozoa (Table 1.2).

Table 1.2 The main groups of microorganisms found in the human oral cavity

Group	Genera	Examples	Abundance
Gram-positive cocci	Streptococcus	*Streptococcus mutans* *Streptococcus salivarius*	Isolated from all oral sites in high numbers, form a large proportion of resident microflora.
	Enterococcus.	*Enterococcus faecalis*	Low numbers, isolated in infected periodontal sites.
	Staphylcoccus	*Staphylococcus aureus*	Uncommon, usually transient- isolated from root caries sites, periodontal pockets and tongue.
	Micrococcus	*Micrococcus luteus*	
Gram-positive rods and filaments	Actinomyces.	*Actinomyces naeslundii*	Major portion of the microflora from dental plaque- numbers increase during infection.
	Eubacterium.	*Eubacterium yurii*	Comprise >50% anaerobic microflora of periodontal pockets.
	Lactobacillus.	*Lactobacillus casei*	Numbers rise in advanced caries lesions of the enamel and root surface.
	Propioni-bacterium.	*Propionibacterium propionicus*	Several species found in dental plaque.
	Others.	*Corynebacteria*	Isolated mainly in dental plaque.
Gram-negative cocci	Neisseria.	*Neisseria subflava*	Isolated in low numbers from all oral sites.
	Moraxella.	*Moraxella catharrhalis*	
	Veillonella.	*Veillonella parvula*	Isolated from many sites- but mainly from dental plaque.
Gram-negative rods	Facultative anaerobes and capnophilic genera.	*Haemophilus parainfluenzae*	Commonly present in saliva, epithelial surfaces and dental plaque.
	Obligate anaerobes.	*Porphyromonas gingivalis*	Found almost solely at sub-gingival sites- rarely isolated in healthy sites.
Fungi	Candida.	*Candida albicans*	Distributed throughout the oral cavity.
Mycoplasma	-	*Mycoplasma salivarium*	Isolated from saliva, oral epithelium and dental plaque.
Viruses	-	Herpes simplex (type I and II)	Commonest virus detected in the oral cavity.
Protozoa	Entamoeba Trichomonas.	*Entamoeba gingivalis*	Most common protozoan- isolated from periodontal tissue.

1.1.5.1 Dental plaque

Dental plaque is a non-mineralised microbial accumulation that adheres to the tooth surface. It shows structural organisation with a predominance of filamentous bacteria and is composed of an organic matrix made up of salivary proteins and extracellular microbial products (Listgarten. 1994). The development of dental plaque, through the attachment, growth, removal and reattachment of bacteria is a dynamic process and it undergoes continuous reorganisation (Marsh and Martin. 1999).

Saliva is responsible for the passive transport of bacteria to the pellicle-coated tooth surface. Initial long-range interactions between the bacteria and pellicle occur as a result of van der Waals attractive forces and electrostatic repulsion (Marsh and Martin. 1999). Bacteria that do not possess specific adhesins are easily removed from the surface at this stage. Primary colonisers of a pellicle-coated surface, mostly gram-positive cocci and coccobacilli such as *Actinomyces naeslundii* and *Streptococcus sanguinis*, can interact with salivary components within the pellicle, forming irreversible adhesion between the two (Marsh and Martin. 1999). Early colonisers co-aggregate with each other and each newly attached bacterium becomes a new surface for recognition by unattached bacteria (Prescott *et al.*, 1999). Extracellular polymers are synthesised by some bacteria and are important in maintaining the structural integrity of plaque (Marsh and Martin. 1999). These include branched chain polysaccharides known as glucans, which bind bacterial cells together forming a plaque ecosystem (Prescott *et al.*, 1999). As plaque develops, the metabolism of primary colonisers enables other bacteria to survive, increasing diversity. Plaque composition depends on several factors including the site within the oral cavity, and the synergistic and antagonistic interactions between the different bacteria (Marsh and Martin. 1999).

Bacteria experience a variety of benefits by existing in a biofilm, these include; wider habitat range, increased metabolic efficiency, increased resistance to environmental stresses and inhibitors, and enhanced virulence potential (Marsh. 2003). Bacteria growing in a biofilm have a phenotype that is distinct from the same bacteria grown planktonically. This confers an increased resistance of biofilm bacteria to antimicrobial agents (Marsh and Martin. 1999; Marsh. 2003). In addition, the structure of the biofilm

may restrict the penetration of antimicrobial agents and concentrate neutralising or drug-degrading enzymes produced by some species (Marsh. 2003).

Plaque is found naturally on the tooth surface, and forms part of host defences by excluding exogenous species through the competition of nutrients and attachment sites, production of inhibitory factors, and the creation of unfavourable growth conditions (Marsh. 2003). However, if plaque remains undisturbed then undesirable changes can occur which increase the likelihood of dental infection.

1.2 Dental Diseases

1.2.1 Dental caries

Dental caries can be defined as the localised destruction of the tissues of the tooth by bacterial fermentation of dietary carbohydrates (Marsh and Martin. 1999). It is one of the most prevalent infectious diseases to afflict mankind; in the United Kingdom alone, 55% of dentate adults had one or more teeth with visual or cavitated caries (Adult Dental Health survey. 1998). The caries process is dependant upon: 1) the interaction of protective and deleterious factors in saliva and plaque, 2) the balance between the cariogenic and non-cariogenic microbial population within saliva and in particular plaque, and 3) the physicochemical characteristics of enamel, dentine and cementum that make the dental hydroxyapatite more or less vulnerable to an acidogenic challenge (Hicks *et al.*, 2003).

Undissociated fermentation acids, particularly lactic acid, and possibly formic and acetic acids can diffuse into the tooth enamel (Prescott *et al.*, 1999). Once below the enamel surface, these acids dissociate and react with hydroxyapatite, releasing calcium and phosphate ions, which diffuse out of the tooth and are transported away into the surrounding environment. Calcium phosphate from supersaturated saliva can re-enter enamel and recrystallise. This process of demineralisation and remineralisation is continuous, and is intimately related to the presence of cariogenic bacteria within surface-bound plaque and the availability of fermentable carbohydrates (Hicks *et al.*, 2003).

Frequent consumption of a diet high in fermentable foods containing sucrose can result in prolonged periods of low pH, which can upset the demineralisation-remineralisation balance, increasing an individual's risk to dental caries. The corresponding reduction of plaque pH can also induce population shifts in the microbial community. Replacement of the resident microflora with acid tolerant species such as *Streptococcus mutans* and *Streptococcus sobrinus* and lactobacilli correlates with a significant increase in the incidence of dental caries (Marsh and Martin. 1999). These "cariogenic" bacteria possess several properties that determine their pathogenicity. These include: 1) the rapid transport of fermentable carbohydrates and conversion to organic acid, 2) production of extracellular and intracellular polysaccharides, and 3) maintenance of carbohydrate metabolism under adverse conditions and stress (Marsh and Martin. 1999; Hicks *et al.*, 2003). Extracellular polymers produced by acidogenic bacteria reduce the diffusion of molecules through dental plaque, which drives the process of demineralisation by limiting the uptake of proteins, calcium phosphate and buffers into plaque and the retaining organic acids at the tooth surface (Hicks *et al.*, 2003).

Sub-surface demineralisation and initial "white-spot" lesions represent the reversible stages of dental caries. If demineralisation continues then cavities can develop through enamel. Further progression through the dentine and into the pulp, may result in tooth death. Dental caries can also develop on the root surface if this area is exposed as a consequence of gingival recession. Cementum surfaces are particularly vulnerable to demineralisation by plaque acids (Marsh and Martin. 1999). Once cavities have developed, restorative dentistry is utilised to prevent infection of the more susceptible regions of the tooth. Infected material is removed by drilling or scraping and is replaced with a dental filling, which can be composed of composite resin, porcelain, dental amalgam or gold.

1.2.2 Periodontal disease

The term "periodontal disease" describes a group of conditions in which the supporting structures of the teeth are attacked (Marsh and Martin. 1999). Periodontal diseases can be divided into two main categories: gingivitis and periodontitis (Liebana *et al.*, 2004). Periodontal diseases are usually characterised by periodontal pockets formed by the

migration of the junctional epithelial tissue at the base of the gingival sulcus down the root of the tooth. In the United Kingdom, 54% of dentate adults had some periodontal pocketing while 43% had some loss of attachment between the tooth and periodontal tissue in 1998 (Adult Dental Health Survey. 1998). The development of periodontal disease is the direct result of plaque-associated microorganisms and subsequent inflammatory response of the human immune system.

1.2.2.1 Gingivitis

Gingivitis is a non-specific, inflammatory response to dental plaque involving the gingival margin. It is characterised by the swelling, redness and bleeding of the gingiva and is often linked with the onset of periodontitis. Gingivitis is associated with poor oral hygiene, which results in the development of more organised supragingival plaque (Sbordone and Bortolaia. 2003). Plaque contains many bioactive end products, such as fermented organic acid, sulphur components, tissue-digesting enzymes, peptidoglycan, and lipopolysaccharide. Diffusion of these products to the surface of the junctional epithelium increases the flow of gingival crevicular fluid and inflammatory fluid from periodontal tissue (Nishihara and Koseki. 2004). Inflammatory changes within the epithelium result in the deepening of the gingival sulcus, providing greater protection from mechanical and physiological removal of plaque and lowering the redox potential. Predominant streptococci typically found in the plaque located at the gingival margin are gradually replaced with *Actinomyces* species and the proportion of gram-negative capnophilic and obligate anaerobes increases (Marsh and Martin. 1999; Sbordone and Bortolaia. 2003; Liebana *et al.*, 2004). Calculus, or tartar, results from the calcification of dental plaque and is linked to the retention of bacterial antigens and further plaque accumulation (Listgarten. 2000). Consequently calculus at the gingival margin is associated with an increased risk of developing periodontal disease.

The removal of plaque and calculus from the gingival margin can often restore the tissue to normal. However, if inflammation of the gingival epithelium continues, the increased flow of gingival crevicular fluid can create a new microenvironment with an altered nutritional supply. This can modify the plaque ecosystem adjacent to the inflamed gingiva, supporting the colonisation and growth of proteolytic species, which

contribute to the destruction of surrounding tissue and development of deeper periodontal pockets.

1.2.2.2 Periodontitis

Periodontitis involves the loss of attachment between the root surface, the gingivae and the alveolar bone, and bone loss itself may occur (Figure 1.3). Periodontitis is classified in two ways; aggressive or chronic (Sbordone and Bortolaia. 2003). Chronic periodontitis is characterised by a slow to moderately slow progressive loss of attachment and bone, and is commonly identified in adults. Aggressive periodontitis is characterised by a rapid loss of attachment and bone in an otherwise clinically healthy individual. It is normally associated with host defects such as leukocyte impairment (Marsh and Martin. 1999).

Figure 1.3 Advanced periodontal disease in an adult patient. The inflamed gingivae have receded from the tooth surface and bone loss has resulted in gaps forming between the teeth. Excessive loss of attachment will eventually lead to tooth loss. Image obtained from http://webs.wichita.edu/mschneegurt/biol103/lecture22/periodontitis.jpg

Periodontitis is associated with subgingival plaque within the gingival sulcus or periodontal pocket and several species of bacteria are implicated in disease development. These include; *Porphyromonas gingivalis*, *Bacteroides forsythus*, *Actinobacillus actinomycetemocomitans*, *Campylobacter rectus* and *Treponema*

denticola (Listgarten. 1994; Marsh and Martin. 1999; Sbordone and Bortolaia. 2003; Liebana *et al.*, 2004; Nishihara and Koseki. 2004). Periodontal pathogens possess virulence factors that cause tissue destruction either directly or indirectly. Direct factors enable bacteria to colonise and multiply at subgingival sites, evade or inactivate the host defences, induce tissue damage, and on occasions, invade host tissues (Marsh and Martin. 1999; Sbordone and Bortolaia. 2003). Indirect factors contribute to an inflammatory host response, which can cause the destruction of tissues e.g. through the release of lysosomal enzymes during phagocytosis, or the production of cytokines, which can stimulate bone resorption (Marsh and Martin. 1999). In addition bacterial proteases can degrade important host control molecules, which modulate the potentially destructive forces of the inflammatory response (Marsh and Martin. 1999; Liebana *et al.*, 2004).

Periodontitis can be both prevented and treated by controlling the accumulation of plaque. In some instances, surgical intervention involving subgingival debridement is required to remove plaque and calculus from root surfaces. Incomplete removal of plaque and calculus, invasion of soft tissues and the intra-oral translocation of bacteria from untreated niches may allow rapid re-colonisation of these surfaces and indicate the need for post-surgical control with the use of antimicrobials, e.g. chlorhexidine or in some cases, antibiotics (Marsh and Martin. 1999; Quirynen *et al.*, 2003). The delivery of drugs to the periodontal pocket can either be via direct local placement or the systemic route (Mombelli. 2003). The maintenance of high concentrations within a well-confined area for a prolonged period remains a challenge in periodontal therapy.

1.3 Oral Healthcare

1.3.1 Oral healthcare products

The maintenance of oral hygiene is paramount to the prevention of plaque related infections and is facilitated with the use of oral healthcare products such as toothpastes, mouthwashes and dental floss. The use of oral healthcare products within the United

Kingdom has risen, with 74% of dentate adults regularly cleaning their teeth twice a day in 1998, compared with 67% in 1988 (Adult Dental Health Survey. 1998).

The term dentifrice describes a substance that is used to clean the accessible surfaces of the teeth and has been prepared in several forms including powders, pastes and gels (Reynolds. 1994). Toothpaste is an abrasive dentifrice and when used in conjunction with a toothbrush, facilitates the mechanical removal of plaque from the tooth surface (Hancock and Newell. 2001). The inclusion of active agents within toothpaste formulations results in specific activity directed toward the prevention of dental caries and gingivitis, the accumulation of plaque and the formation of calculus. Maintenance of oral hygiene with the regular use a toothbrush and dentifrice can significantly reduce the incidence of dental disease, however these measures are often inadequate for cleaning approximal tooth surfaces and the use of interdental devices such as dental floss, interdental brushes and toothpicks is recommended (Hancock and Newell. 2001). Mouthwashes are a common adjunct to mechanical hygiene measures and facilitate the control of supragingival plaque and gingivitis. Rinses are capable of flushing the oral cavity and may penetrate the approximal tooth surfaces. In general mouthwashes contain significant quantities of alcohol in which other substances are dissolved such as water, flavourings, colourings and active drugs (Eley. 1999; Steinberg and Friedman. 1999).

The maintenance of oral hygiene with the use of healthcare products is effective at controlling supragingival plaque, however subgingival plaque is less inaccessible to conventional supragingival delivery systems and active agents are more effective if introduced directly into the periodontal pocket (Friedman and Steinberg. 1990; Addy. 1994). Penetration of the drug into the periodontal pocket and rapid clearance by the flow of gingival crevicular fluid inhibit subgingival plaque control. Current strategies for periodontal therapy includes the use of sustained delivery systems that can be placed within the periodontal pocket and maintain an effective concentration of the active for prolonged periods. These include: fibres, films, bio-absorbable dental materials, gels and ointments, injectables and microcapsules. Sustained release devices are often based on polymeric delivery vehicles and have been used successfully for treating periodontal disease (Friedman and Steinberg. 1990; Addy. 1994; Southard and Godowski. 1998; Steinberg and Friedman. 1999; Vyas *et al.*, 2000; Schwach-Abdellaoui *et al.*, 2000).

1.3.2 Antimicrobials in oral healthcare

In general, tooth cleaning with brushing and dentifrices alone are usually insufficient over long periods to provide a level of plaque control compatible with oral health (Marsh. 1991; Addy. 1994). Antimicrobials are chemical anti-plaque agents, which reduce plaque accumulation by exerting a direct effect on the oral microflora (Table 1.3). Approaches include the inhibition of bacterial growth through various bactericidal or bacteriostatic mechanisms, such as inhibition of essential metabolic or synthetic events, or interference with membrane functions (Scheie. 1989). Ideal properties of antimicrobials formulated in oral healthcare products include: broad spectrum antimicrobial efficacy, retain high antimicrobial potency, fast acting, non-toxic to the host tissues, non-irritant, pleasant/neutral odour and taste, good oral retention properties, not too disruptive to the oral microbial ecology, globally regulatory approved, chemically defined, chemically stable and cost effective.

Table 1.3 Summary of the antimicrobials currently utilised in oral healthcare products (Collins and Stotzky. 1989; Hughes and Poole. 1989; Scheie. 1989; Marsh. 1991; Addy. 1994; Bhargava and Leonard. 1994; Gaffar *et al.*, 1997; Eley. 1999; Leke *et al.*, 1999; Schwach-Abdellaoui *et al.*, 2000; Sreenivasan and Gaffar. 2002; Hoang *et al.*, 2003).

Group	Examples	Mode of action
Anionic surfactants	Sodium lauryl sulphate (SLS)	Exhibits some activity against oral pathogens. Adsorbs onto bacterial surface and causes structural and functional changes. Penetrates and disrupts cell membranes. Enzyme inhibition has been reported.
Biguanides	Chlorhexidine Alexidine Octenidine	Chlorhexidine remains the most effective antimicrobial agent and is retained in the oral cavity. Effective against both gram –ve and +ve microorganisms. Alters bacterial adherence to teeth. Increases cell membrane permeability followed by coagulation of cytoplasmic macromolecules.
Cationic surfactants	Cetylpyridinium chloride Cetrimide Domiphen bromide	Effective against gram +ve and –ve bacteria. Cationic binding to phosphate groups of teichoic acid in gram +ve bacteria and membrane lipopolysaccharides in gram –ve causes membrane disruption and cytoplasmic leakage.
Iodophores	Povidone-iodine	Has antibacterial, antifungal and antiviral activity. Free iodine inhibits some enzymes through the binding of thiol groups.
Oxidising agents	Hydrogen peroxide	Have some activity against gram –ve bacteria. Acts by raising the redox potential.
Phenolics	Thymol Triclosan	Triclosan is the most commonly used antimicrobial in oral healthcare products. Effective against gram +ve and –ve bacteria and some fungi. Disrupts the cell wall and precipitation of cell proteins. Triclosan also inactivates some essential enzymes important in lipid biosynthesis.
Pyrimidines	Hexetidine	Exhibits antibacterial and antifungal activity. Inhibits the rate of ATP synthesis in mitochondria.
Metal Ions	Zinc Silver Copper	Less effective than chlorhexidine. Variety of antimicrobial mechanisms: alteration of surface charge through cell wall interactions, interference of glucan formation, and inactivation of enzymes. Activity is influenced by factors such as pH and temperature. The use of heavy metals is limited due to toxicity in humans.

1.3.3 Considerations and limitations in antimicrobial oral healthcare.

1.3.3.1 Human oral retention and clearance

The antimicrobial efficacy of oral healthcare products is directly related to the retention, or "substantivity" of the agent within the oral cavity. Substances that are introduced to the oral cavity are rapidly washed away or diluted with saliva and subsequently swallowed or expectorated (Weatherall *et al.*, 1996). Antimicrobial agents must achieve a suitable concentration for a sufficiently long period to have an effect. For some antimicrobial agents the duration of activity is little longer than the retention time of the delivery vehicle (Addy. 1994). This can result in a high initial concentration of the agent, which rapidly decreases to sub-therapeutic levels. Generally the most effective anti-plaque agents exhibit good substantivity within the oral cavity e.g. chlorhexidine is retained within the oral cavity for over 12 h (Addy. 1994). The substantivity of antimicrobial agents within the oral cavity may be achieved by two physicochemical mechanisms; absorption and adsorption. Antimicrobial agents exhibiting superior substantivity tend to carry a positive charge e.g. chlorhexidine, cetylpyridinium chloride (CPC) and metal ions. Negatively charged groups on salivary and plaque components facilitate the retention of positively charged agents through the provision of binding sites within the oral cavity.

The clearance of substances from the oral cavity is affected by physiological, anatomical and product related factors (Table 1.4). Antimicrobial agents that are released locally within the oral cavity through the use of oral healthcare products aim to provide uniform concentrations over the entire area (Weatherell *et al.*, 1994). Site-specific differences in the flow of saliva can alter the efficacy of antimicrobial agents within different regions of the oral cavity. For example, substances deposited close to the salivary ducts will be diluted and removed faster than those deposited in areas where salivary turnover is low (Weatherell *et al.*, 1996). However, substantive agents such as chlorhexidine tend to resist site-specific differences as a consequence of binding to salivary components. Formulation strategies could improve the substantivity of an agent thereby altering its clearance properties, however some parameters such as variations in salivary volume as a result of stimulation, are unavoidable. An

understanding of human oral retention and clearance can facilitate the optimisation of antimicrobial concentration within oral healthcare products with the target of achieving a therapeutic concentration within the oral cavity while avoiding toxicity.

Table 1.4 Parameters influencing the clearance of a product introduced in the oral cavity (Vivien-Castioni *et al.*, 1998).

Physiological and/or anatomical parameters:
• Salivary flow rate
• Swallowing frequency
• Residual volume of saliva
• Anatomical position of the salivary glands
• Anatomical factors (space between teeth, tongue position, etc)
• Oral muscular movements
Factors relating to the product and its administration:
• Dose and concentration of the product
• Duration and frequency of the administration
• Association between products and/or buccal substrates
• Dilution (drinking habits, rinsing, etc)
• Time of administration (day/night, proximity of a meal, etc)

1.3.3.2 Emerging microbial resistance

Microbial resistance has become a worldwide medical, economical and public health problem and the incidence is reportedly increasing continuously and at a high speed (Edlund *et al.*, 1996; Marsh and Martin. 1999; Quirynen *et al.*, 2003). The use of antibiotics in oral healthcare is only recommended during acute bacterial infections and aggressive forms of periodontal disease and therefore the incidence of antibiotic resistance among oral bacteria is rarely considered. However, the potential for microbial resistance towards oral antimicrobial agents and the implications for the development of cross resistance to antibiotics is relevant to the formulation of oral healthcare products. Quirynen *et al.* (2003) identified a study in which *Staphylococcus aureus* and *Escherichia coli* strains became resistant to triclosan, although these are not

typical oral microorganisms. Reviews by Russell (2003), Gilbert and McBain (2003) and Chapman (2003) have indicated that efflux pumps implicated in the development of antibiotic resistance are also able to remove antimicrobials including triclosan, chlorhexidine and quaternary ammonium compounds. However, the lack of resistant clinical isolates suggests the use of these agents is safe. Sreenivasan and Gaffer (2002) reviewed long term clinical studies conducted to evaluate the microbiological safety of dentifrices containing anti-plaque agents and concluded that their use does not result in microbial resistance. Cross-resistance has the potential to occur when different antimicrobial agents attack the same target, initiate a common pathway to cell death, or share a common route of access to their respective targets (Chapman. 2003). Of direct importance to oral healthcare is the tentative link between triclosan and the development of cross-resistance to antibiotics, reviewed by Aiello and Larson (2003). Conflicting reports on the incidence of antimicrobial resistance clearly indicates the need for continued investigation and vigilance, and should be considered when developing oral healthcare products, particularly as sub-therapeutic levels are often encountered.

1.3.3.3 In vitro vs. in vivo

The determination of antimicrobial activity within the laboratory does not necessarily reflect activity within the oral cavity. Conventionally, the sensitivity of bacteria to antimicrobial agents has been based solely on cells grown in liquid culture (planktonic cells) by the measurement of the minimum inhibitory concentration (MIC) or minimum bactericidal concentration (MBC) (Marsh and Martin. 1999). These parameters can be determined rapidly and are useful in preliminary assessment of antimicrobial agents; however biofilm bacteria that are present in dental plaque often exhibit different characteristics and antimicrobial sensitivities (Marsh and Martin. 1999; Marsh 2003). Antimicrobial assessment of oral formulations often indicates a significant reduction in activity when tested against sessile bacteria compared to planktonic cells (Fine *et al.*, 2001; Phan *et al.*, 2004).

The structure of dental plaque may restrict the penetration of an antimicrobial agent, providing protection to the organisms within the biofilm matrix (Marsh. 2003). The antimicrobial activity of chlorhexidine against experimental dental plaque was significantly reduced compared to tests on bacterial cell suspensions (Steinberg and

Rothman. 1996). This can be partially attributed to the presence of organic material within saliva and dental plaque, which can reduce bioavailability and block adsorption sites on the microbial cell surface (Collins and Stotzky. 1989; Smith. 2004). Bioavailability is defined as the degree or rate at which a drug becomes available or absorbed at the site of physiological activity after administration (Lund. 1994). By binding to organic material, antimicrobials are effectively unavailable to interact with microorganisms. Other factors that affect the activity of antimicrobials include; microbial density, concentration and exposure time, temperature, pH and the presence of divalent cations (Smith. 2004). These factors must be considered when selecting the appropriate *in vitro* method for the prediction of antimicrobial activity *in vivo*.

1.3.3.4 Formulation

The formulation of antimicrobials in oral healthcare products will affect both their bioavailability and activity within the oral cavity. The combination of some agents within a formulation may result in improved antimicrobial activity, greater than can be achieved separately. The addition of copper or zinc to CPC and PVP-I solutions significantly improved antimicrobial activity against a variety of bacterial species (Zeelie and McCarthy. 1998). Additive effects have also been observed within combinations of triclosan and zinc when tested against mixed bacterial cultures (Bradshaw *et al.*, 1993). This combination has been particularly successful in oral healthcare products and has frequently demonstrated improved effectiveness in the prevention and control of gingivitis (Marsh. 1991).

Development of triclosan-containing oral healthcare formulations has included the copolymer polyvinylmethyl ether maleic acid (PVM/MA), commercially known as Gantrez®). Volpe *et al.* (1996) reviewed the studies on the use of dentifrices containing triclosan and PVM/MA and reported a variety of benefits, including reductions in plaque, gingivitis and salivary bacterial numbers. Triclosan bioavailability has also been significantly improved in experimental studies following the incorporation of cyclodextrin and carboxymethylcellulose (Loftsson *et al.*, 1999). Cyclodextrin improved the solubility of triclosan while carboxymethylcellulose enhanced substantivity, resulting in a significantly improved toothpaste formulation.

By improving the formulation of antimicrobials in oral healthcare products significant enhancements can be achieved, increasing the efficacy of such products against the rapidly rising incidence of dental disease. Whereas the current situation often requires high antimicrobial concentrations within the vehicle to achieve a therapeutic effect at the physiological target site, improving formulation may enable lower concentrations to be administered, reducing the risk of adverse side effects or unforeseen future events. Formulation strategies could target specific limitations in current therapies, such as oral retention to achieve desired clinical outcomes.

1.4 Bioadhesion

Bioadhesion is the term used to describe the attachment of a synthetic or natural macromolecule to a biological substrate. The term "mucoadhesion" is employed when the biological substrate is mucus and/or an epithelial surface (Gu *et al.*, 1988). Bioadhesion has received particular attention in the field of formulation as a strategy to modify the drug delivery characteristics of pharmaceutical dosage forms. The incorporation of bioadhesive polymers into a formulation may fulfil the following desirable features of a controlled drug delivery system: 1) prolonged residence time at the site of drug absorption, 2) increased intimate contact to the absorbing mucosa, resulting in a steep concentration gradient to favour drug absorption, and 3) localisation in specified regions to improve and enhance the bioavailability of the drug. Bioadhesive polymers have been used successfully in nasal (Ugwoke *et al.*, 2005), ophthalmic (Ludwig. 2005) and oral (Smart. 2004a; Birudaraj *et al.*, 2005) drug delivery to achieve either a local or systemic effect.

1.4.1 The theories of adhesion

There are five classic theories that are used to describe the fundamental mechanisms of adhesion (Gu *et al.*, 1988; Ahuja *et al.*, 1997; Lee *et al.*, 2000; Smart. 2005a), these include; electronic, adsorption, diffusion, wetting and fracture. A sixth theory based on the postulation that adhesion arises from an interlocking of a liquid adhesive into irregularities on a rough surface has also been described. However, research

investigating the effect of surface roughness rarely results in enhanced adhesion as a direct consequence of mechanical interlocking (Peppas and Sahlin. 1996). Instead, the increased surface area associated with roughness often accounts for improved adhesion due to the enhanced physicochemical interactions between the adhesive and substrate and enhanced viscoelastic and plastic dissipation of energy at the interface during joint failure. Fundamental differences exist between the adhesive and bioadhesive phenomena that arise between two surfaces, namely that the latter usually occurs in the presence of water (Park and Robinson. 1985; Mortazavi and Smart. 1993; Marshall *et al.*, 2004). However in a particular system, one or more theories can equally well explain or contribute to the formation of bioadhesive bonds.

1.4.1.1 The electronic theory

The electronic theory states that electron transfer occurs upon contact of adhering surfaces due to differences in their electronic structures. This results in the formation of a double layer of electrical charge at the adhesive interface. Subsequently, adhesion occurs due to the presence of attractive forces across the electrical double layer.

1.4.1.2 The adsorption theory

The adsorption theory states that after initial contact between two surfaces, the material adheres because of surface forces acting between the atoms in the two surfaces. Secondary chemical bonds such as hydrogen bonds, electrostatic forces, van der Waals forces and hydrophobic bonds are common contributors to the adhesive interaction. In some instances, primary chemical bonds are formed which are considerably stronger than secondary bonds. These include covalent bonds and ionic bonds.

1.4.1.3 The diffusion theory

The diffusion theory describes the interpenetration of chains from the adhesive and substrate to a sufficient depth to create a semi-permanent adhesive bond. The penetration rate depends on the diffusion coefficients of each interacting polymer and the time of contact. The diffusion coefficient is known to be dependant on molecular

weight and decreases significantly as cross-linking density increases. The segmental mobility of the polymer generally governs the strength of adhesion.

1.4.1.4 The wetting theory

The wetting theory analyses adhesive and contact behaviour in terms of the ability of a liquid or paste to spread spontaneously on a substrate. It is primarily applied to liquid systems and considers the interfacial and surface energies responsible for the contact and adhesive strength between two surfaces. Interactions that occur across an interface between two arbitrary phases determine the interfacial (free) energy and are composed of polar and dispersive contributions (Bodde and Leiden. 1990). Surface energy, termed surface tension in a liquid, arises because of intermolecular forces and represents the tendency of surfaces to contract to the minimum surface area. The spreading coefficient (SAB) can be calculated from the surface energies of the solid and liquid using the equation:

$$SAB = \gamma B - (\gamma A + \gamma AB)$$

Where: γA is the surface tension of the liquid A, γB is the surface energy of the solid B and γAB is the interfacial energy between the solid and the liquid. SAB should be positive for the liquid to spread spontaneously over the solid. The work of adhesion (WA) represents the energy required to separate the two phases, and is calculated using the equation:

$$WA = \gamma A + \gamma B - \gamma AB$$

The greater the individual surface energies of the solid and the liquid relative to the interfacial energy the greater the work of adhesion.

1.4.1.5 The fracture theory

The fracture theory relates to the detachment of two surfaces after adhesion due to the adhesive bond strength. Fracture strength (σ) can be calculated using the equation:

$\sigma = \sqrt{(E\varepsilon/L)}$

Where: E is the Young's modulus of elasticity, ε is the fracture energy, and L is the critical crack length upon separation of the two surfaces. The work required to fracture an adhesive bond at the interface is greater when molecular weight is higher, or the degree of crosslinking smaller. This theory assumes that the fracture will occur at the interface between the two surfaces; however this almost never occurs (Duchene *et al.*, 1988).

1.4.2 Mucoadhesion

Investigations into the interaction between mucoadhesive materials and a mucous membrane have resulted in the identification of two steps in the mucoadhesive process: the contact stage and the consolidation stage (Smart. 2004a, 2005a). These stages have been identified mainly from investigations between mucous membranes and dry or partially hydrated dosage forms and may not accurately represent the processes that occur with liquid or semi-solid dosage forms. The specific processes that occur during mucoadhesion are influenced by the physical properties of the dosage form e.g. hydration and the physiological target site e.g. mucus composition (Smart. 2004a, 2005a).

1.4.2.1 The contact stage

Intimate contact must exist between the mucoadhesive and mucous membrane for an adhesive bond to develop (Duchene *et al.*, 1988; Gu *et al.*, 1988; Ahuja *et al.*, 1997; Smart. 2005a). Contact can be initiated through mechanical manipulation in which the mucoadhesive is placed and held in position. However, mucoadhesive drug delivery to inaccessible areas relies on intimate contact formed as a result of physiological and physiochemical properties of the target site or dosage form. Mucoadhesion of particles in suspension is thought to occur as a result of adsorption to the mucosae surface.

It has been proposed that the physicochemical adsorption of small particles to a mucous membrane is similar to the long-range interactions experienced by oral bacteria when

attaching to a surface (Gu et al., 1988; Smart. 2005a). The DLVO theory (described by Derjaguin and Landau and separately by Verwey and Overbeek in the 1940's) states that as two rigid bodies of like charge approach one another they are subjected to both attractive and repulsive forces which are additive and vary with the distance of separation (Gu et al., 1988; Smart. 2005a). Repulsive forces arise from osmotic pressure, steric effects and electrostatic interactions. Attractive forces arise from van der Waals' forces, surface energy effects and electrostatic interactions if the particle and the surface carry opposing charges.

The establishment of intimate contact between the mucoadhesive and the mucous membrane can be affected by the surface characteristics e.g. surface roughness, the composition of the adhesive and substrate, the applied force and the duration of that force (Gu *et al.*, 1988). The composition of the adhesive and substrate will dictate the physicochemical processes that occur between them e.g. surface energy, charge and viscosity, although the adhesive and/or substrate may be altered *in vivo* by the presence of biomolecules (Smart. 2005a). Wetting and swelling properties of the mucoadhesive material are important in initiating intimate contact (Duchene et al., 1988; Gu et al., 1988; Ahuja et al., 1997). Adhesives with good wetting properties will spread sufficiently on a substrate, increasing the surface area for contact and penetrating tissue anomalies. The ability of a material to swell results in the relaxation of stretched, entangled or twisted molecules through the dissociation of pre-existing hydrogen bonds. This increases chain mobility and liberates sites i.e. functional groups, which are capable of forming bonds in the later stages of mucoadhesion.

1.4.2.2 The consolidation stage

The consolidation of the mucoadhesive bond occurs following the contact stage. Interfacial bonds are formed between the mucoadhesive and the mucous membrane; these are primarily secondary chemical bonds (Duchene et al., 1988; Gu et al., 1988; Ahuja et al., 1997; Smart. 2005a). Hydrophilic mucoadhesives containing hydrogen bond-forming groups, such as carboxyl, hydroxyl and amine groups, are known as "wet" adhesives as they need to be activated by hydration (Smart. 2005a; Smart. 2005b). The importance of water in the strengthening of a mucoadhesive bond has been described by the dehydration theory. This theory states that when a material capable of

rapid gelation in an aqueous environment is brought into contact with a second gel, water movement occurs between gels until equilibrium is achieved (Smart. 2005a). This has been demonstrated visually by Marshall *et al.* (2004) using confocal laser scanning microscopy and nuclear magnetic microscopy. During the development of a mucoadhesive bond between sodium alginate and purified pig gastric mucin, an area of increased mucin concentration formed adjacent to the interface between the different materials, which was attributed to the movement of free water from the mucus gel to the hydrating alginate matrix. This region corresponded with a decreased self-diffusion coefficient, which relates to the mobility of water with a decrease indicating water restriction. The bond was monitored for 30 min in which time further dehydration of the mucus gel and hydration of the alginate matrix was observed. It is probable that water movement from the mucus layer to a dry or partially hydrated mucoadhesive represents the initial, rapid consolidation of the mucoadhesive bond but subsequent durability and strength may depend on the extent of mucoadhesive hydration, as over-hydration in some instances can lead to the development of slippery mucilage (Smart. 2005a). The movement of water within the mucoadhesive bond may also initiate the interpenetration of polymer and mucin chains, outlined in the second theory of consolidation, the macromolecular interpenetration effect.

The macromolecular interpenetration effect describes the interdiffusion of mucus and polymer chains across the mucoadhesive interface. The two phases involved must be compatible, and for interdiffusion to occur a concentration gradient must exist across the interface (Duchene *et al.*, 1988). Experimental evidence for the macromolecular interpenetration effect is generally rare in current literature, although some papers indirectly indicate that this phenomenon is likely in the formation of mucoadhesive bonds. For example, in the work by Marshall *et al.* (2004) an area of restricted water mobility adjacent to the alginate/mucin boundary may indicate interaction between the different polymer chains. Park and Robinson (1985) found that the mucoadhesion of a polycarbophil hydrogel to freshly excised rabbit stomach tissue increased significantly following exposure of a mucolytic agent to the tissue surface. This suggests that partial mucolysis increases the flexibility of the mucin chains which improves their interaction or entanglement with the hydrogel. Conversely, when the tissue surface was treated with glutaraldehyde, a protein cross-linking agent, the mucoadhesion of the polycarbophil hydrogel significantly decreased probably as a result of the reduction in

mucin chain flexibility. Mortazavi (1995) found that the rheological behaviour of Carbopol 934P-mucus mixture suggested an intermediate between a physically entangled system and a cross-linked system. Small polymer chains tethered to a larger polymer structure such as poly(acrylic acid) has been shown to improve mucoadhesive properties, which is most likely accounted for by an improvement in penetration and anchoring of the chains with the mucosa (Peppas and Huang. 2004; Bromberg *et al.*, 2004). Peppas and Sahlin (1995) examined the theoretical and experimental support for the interpenetration effect and found that a combination of surface and diffusional phenomena contribute to the formation of adequately strong interchain bridges between the mucoadhesive and biological substrate.

It is apparent that much of the work supporting the macromolecular interpenetration effect utilises polymer hydrogels as the mucoadhesive, while, as previously mentioned, the dehydration theory is primarily applicable to dry or partially hydrated dosage forms. Importantly, upon conclusion all authors accept that the mucoadhesive bond is unlikely to be governed by any one mechanism and interplay of mucoadhesive properties and mucus/epithelial properties will dictate the contact and consolidation stages that are observed.

1.4.3 Factors important to mucoadhesion

Several factors have been identified which significantly affect the strength of mucoadhesion (Duchene *et al.*, 1988; Gu *et al.*, 1988; Ahuja *et al.*, 1997; Lee *et al.*, 2000; Smart. 2005a). These factors can be separated into two categories; polymer-related factors and environment-related factors (Table 1.5). Typically, polymer-related factors require optimisation to achieve the desired mucoadhesive outcome. For example, at low molecular weight interpenetration of the polymer chains is favoured, while higher molecular weights favour chain entanglement (Ahuja *et al.*, 1997). Hence an optimum molecular weight would allow sufficient interpenetration while favouring chain entanglement. Highly cross-linked polymers have reduced chain flexibility, which can negatively affect the interaction of the polymer with the mucosa. However polymers with low cross-linking density tend to hydrate rapidly, significantly reducing the duration of mucoadhesion. Properties of the polymer will influence the effect of

environment-related factors on mucoadhesion, e.g. polymers with ionisable groups will be greatly affected by the pH of the surrounding medium. Each factor should be considered when selecting mucoadhesive polymers for pharmaceutical applications in order to obtain an optimum platform for local or systemic drug delivery.

Table 1.5 Summary of the factors that influence mucoadhesive strength.

Polymer-related factors:
Molecular weight
Concentration of active polymer
Polymer chain flexibility
Spatial conformation
Environment Related factors:
pH
Applied strength
Initial contact time
Swelling
Physiological variables e.g. mucus/epithelial cell turnover, disease states

1.4.4 Methods to determine mucoadhesion

The determination and quantification of mucoadhesion has been assessed in multiple ways, particularly *in vitro*. Despite the extensive research into suitable methodology, a standardised test remains elusive and as such the assessment of mucoadhesives varies accordingly between authors. This reflects the specific interplay between polymer-related and environment-related factors, which determine the observations reported in the literature.

1.4.4.1 In vitro test methods

By far the most popular *in vitro* method of quantifying bioadhesion is the measurement of the force (energy) required to break a formed adhesive joint, namely the maximum detachment force (N) and work of adhesion (N mm^{-1}), known collectively as adhesive

strength. In general the mucoadhesive and substrate are placed on two platforms, which are brought into contact at a pre-determined force and duration, following which one platform is removed at a constant rate. The force (N) exerted during the separation of the two materials is measured to obtain a force-displacement curve. Previously, these measurements have been conducted using modified tensiometers (Park and Robinson. 1985; Dyvik and Graffner. 1992; Mortazavi and Smart. 1995; Grabovac *et al.*, 2005), however more recently texture analyser equipment has become accepted due to the accuracy and control exerted over experimental variables such as contact force and withdrawal speed (Jones *et al.*, 1997a; Tamburic and Craig. 1997; Wong *et al.*, 1999; Eouani *et al.*, 2001). The methodology employed for adhesive strength testing is varied throughout the literature, which can make comparisons impossible. Wong *et al.* (1999) found that varying the contact time, contact force and withdrawal speed could influence the adhesive strength measured. Selection of the model biological substrate and surrounding media specific to adhesive target sites may allow some prediction of *in vivo* characteristics and some correlations have been reported. The majority of adhesive strength testing studies the mucoadhesion of solid formulations such as tablets, compacts and microparticles. The assessment of gels using adhesive strength testing is often inaccurate as the molecular force exerted across a surface within the gel, resisting internal rupture is frequently less than the gel-substrate adhesive bond, resulting in cohesive failure rather than adhesive failure (Jones *et al.*, 1997a).

Direct assessment of the binding of mucoadhesive polymers to epithelial cells has been investigated and often involves the use of hydrated dispersions rather than dry formulations. Park and Robinson (1984) incorporated pyrene, a lipid soluble fluorescent molecule, which localises in the lipid bilayer, into cultured human conjunctival epithelial cells to detect changes in viscosity and membrane fluidity. This method was able to determine the binding of polymers to cells; although this was based on the assumption that polymer binding or adsorption caused an increased, detectable viscosity. Patel *et al.* (1999) detected bound polymer on the surface of buccal cells using a biotinylated lectin following exposure to aqueous polymer dispersions. Lectin binding was detected using o-phenylenediamine dihydrochloride and a reduction in the rate of oxidation from the saline control indicated masking of sugar groups at the buccal cell surface due to polymer binding. Kockisch *et al.* (2001) also visualised adhered polymer on the surface of isolated buccal cells using a similar procedure to Patel *et al.*

(1999). Following exposure to aqueous polymer dispersions, cells were stained with either Alcian blue or Eosin and the extent of polymer binding was quantified by measuring the relative stain intensity by image analysis. These methods are particularly valuable in the assessment of polymer adsorption from solution and require no modification to the polymer prior to mucoadhesion.

The retention of mucoadhesive formulations on mucosal surfaces under dynamic test conditions has been utilised in several studies, including Rango Rao and Buri (1989), Kockisch *et al.* (2004) and Batchelor *et al.* (2004). The use of fluorescent labels to detect polymer adhesion, which was adopted by Kockisch *et al.* (2004), may affect the observed mucoadhesive properties through the occupation of functional groups and alterations in spatial conformation. However, the use of these models can be easily modified to recreate conditions encountered at target mucosal surfaces such as humidity, the flow of physiological fluid i.e. saliva, and presence of mucin. Microscopy techniques such as atomic force (Patel *et al.*, 2000) and scanning force (Schwender *et al.*, 2005) microscopy have also been used to detect polymer adhesion to the surface of biological substrates. The measurement of surface energy using contact angle goniometry (Lehr *et al.*, 1993; Esposito *et al.*, 1994) and the characterisation of mucoadhesive flow properties using rheology (Needleman *et al.*, 1998) have both been used with varying degrees of success, to predict the mucoadhesive performance of polymers. Recent techniques involving surface plasmon resonance have been used to detect interactions between chitosan and mucin (Takeuchi *et al.*, 2005). This method may represent an exciting technique for detecting the mucoadhesion of liquid systems.

1.4.4.2 In vivo test methods

Gamma scintigraphy has been used successfully to measure the *in vivo* behaviour of pharmaceutical dosage forms in the oral cavity, oesophagus and gastrointestinal tract (Wilson and Nottingham. 1989). Gamma cameras can be used to detect gamma rays emitted through the body of test subjects, which enable the visualisation of radio-labelled formulations *in situ*. Scintillation counting can also be used to count emissions from labelled formulations collected from test subjects e.g. saliva to determine the rate of release or disintegration of buccal formulations. Radionuclides must be safe and

require specialist equipment. Difficulties can arise with availability, radioactive half-life and their formulation into pharmaceuticals.

More recently, *in vivo* methods have been employed which utilise alternative detection techniques. Needleman *et al.* (1998) assessed the *in vivo* retention of mucoadhesive periodontal gel formulations within the periodontal pockets of 8 patients using insoluble fluorescein-free acid. Released fluorescein was collected at the gingival margin and the percentage fluorescein remaining in the gel was calculated as a function of the fluorescein concentration. Kockisch *et al.* (2001) investigated the *in vivo* retention of mucoadhesive polymers to the oral cavity. Subjects rinsed with mucoadhesive solutions for 30 s and harvested buccal cells were stained to detect bound polymer. Techniques such as these can be used to observe the behaviour of mucoadhesive formulations *in vivo* and the use of appropriate fluorescent markers is a safe and cost-effective method of visualising delivery characteristics such as retention.

1.4.4 Mucoadhesive polymers

Mucoadhesive polymers that adhere to the mucin/epithelial surface may significantly improve the characteristics of drug delivery systems through the retention and localisation of the active ingredient at a target site. An ideal polymer for a mucoadhesive drug system should have the following characteristics (Ahuja *et al.*, 1997):

- The polymer and its degradation products should be non-toxic and non-absorbable from the gastrointestinal tract.
- Non-irritant to the mucous membrane.
- Form strong non-covalent bonds with the mucin/epithelial surface.
- Adhere quickly to moist tissue and possess some site specificity.
- Compatible with the active ingredient, allowing easy incorporation and desired *in vivo* release.
- Long shelf life.
- Cost-effective.

1.4.4.1 Poly(acrylic acid)-based polymers

The polymerisation of acrylic acid to form poly(acrylic acid), a comparatively simple polymer consisting of a hydrocarbon backbone, has led to the development of a range of synthetic polymers that are commonly included in mucoadhesive formulations. Poly(acrylic acid) is polyanionic due to the ionisable carboxylic acid groups on each repeat unit (Figure 1.4), and has water absorbent properties. Commercially available high molecular weight cross-linked poly(acrylic acid) derivatives Carbopol and polycarbophil, manufactured by Noveon Inc (Cleveland, USA), are amongst the most important mucoadhesive molecules (Smart. 2004b). Both have regulatory approval and have been used extensively in pharmaceutical formulation for a range of purposes for use in both drug and cosmetic applications.

1.4.4.1a Carbopol

Carbopol is a homopolymer of acrylic acid cross-linked with allyl sucrose (Noveon. 2002a). Carbopol is a flocculated powder averaging 2-7 microns in diameter and is not soluble in water; instead these polymers can swell in water up to 1000 times their original volume and form a gel when exposed to a pH environment above 4.0-6.0 (Dittgen *et al.*, 1997). Since the pH at which the concentration of dissociated and associated carboxylic acid groups are equal (pKa) is 6.0 ± 0.5, the carboxylate groups on the polymer ionise, resulting in repulsion between the negative particles, adding to the swelling of the polymer. Several grades of Carbopol are recommended for use as oral and mucosal adhesives, these include Carbopol 934P, Carbopol 971P and Carbopol 974P. Different Carbopol grades vary according to molecular weight and cross-linking density. However the actual molecular weight is unavailable due to the nature of the cross-linked polymer network although theoretical estimations are typically within the range 700,000 to 3 or 4 billion (Noveon. 2002a). Carbopol polymers exhibit low potential for toxicity (Noveon. 2002b) and have demonstrated excellent bioadhesive properties for drug delivery to the oral cavity (Patel *et al.*, 1999; Wong *et al.*, 1999; Kockisch *et al.*, 2001).

1.4.4.1b Polycarbophil

Polycarbophil is a homopolymer of acrylic acid cross-linked with divinyl glycol and shares many physicochemical characteristics with Carbopol, due to the poly(acrylic acid) backbone common to both polymers. Polycarbophil AA-1 is typically used in oral and mucosal formulations, although polycarbophil calcium salts (CA-1 and CA-2) have been used as bulk laxatives due to their swelling behaviour in the intestinal tract. The mucoadhesion of polycarbophil is generally of the same order as Carbopol and other cross-linked poly(acrylic acid) polymers (Patel *et al.*, 1999; Wong *et al.*, 1999; Eouani *et al.*, 2001; Kockisch *et al.*, 2001; Grabovac *et al.*, 2005). Lehr *et al.* (1992) demonstrated that the adhesive strength of polycarbophil to porcine intestinal mucosa was highest in non-buffered saline (pH 6.6-7.0), intermediate in gastric fluid (pH 1.2-1.4) and minimal in intestinal fluid (pH 7.4-7.5). Generally, the resting pH of saliva is under pH 7.0, which should confer optimal polycarbophil mucoadhesion.

1.4.4.2 Chitosan-based polymers

Chitosan is a natural polysaccharide produced by the partial deacetylation of chitin, a major component of crustacean shells. Chitosan is a copolymer of glucosamine and N-acetyl glucosamine (Figure 1.4), and a variety of molecular weights (50 kDa – 2000 kDa), viscosity and degree of acetylation (> 75%) are produced commercially. Chitosan is a linear polyamine with a number of amine groups that are readily available for chemical reaction and salt formation with acids (Singla and Chawla. 2001). It is insoluble at alkali and neutral pHs and is typically prepared in dilute organic acid solutions. Upon dissolution, amine groups of the polymer become protonated, with a resultant positively charged soluble polysaccharide (RNH_3^+). Due to its cationic nature, chitosan is not compatible with anionic compounds. High electrolyte concentrations can cause precipitation of chitosan from solution in a "salting out" effect (Singla and Chawla. 2001). Unfortunately, the safety of chitosan has been questioned and several authors have highlighted biocompatibility issues. Cytotoxicity, cytokine release and complement activation have all been observed in response to chitosan exposure (Carreno-Gomez and Duncan. 1997; Mori *et al.*, 1997; Minami *et al.*, 1998; Suzuki *et al.*, 2000). However, careful selection of chitosan properties i.e. organic acid used in chitosan dissolution and molecular weight, may avoid biocompatibility issues.

Chitosan has been proposed for a number of medical and pharmaceutical applications including tissue engineering (Di Martino *et al.*, 2005), and most notably, gene and peptide delivery (Issa *et al.*, 2005). Its high charge density enables complexes to be formed with anionic drug(s)/excipient(s), although the amount must be carefully controlled to avoid polymer precipitation. Chitosan exhibits mucoadhesive properties (Needleman and Smales. 1995; Takeuchi *et al.*, 2005), mainly based on ionic interactions with anionic substructures of the mucus layer although other attractive forces such as hydrogen bonding and/or hydrophobic interactions may be involved (Qaqish and Amiji. 1999). Chitosan itself has antimicrobial properties, with an increased efficacy exhibited with increased molecular weight (Ikinci *et al.*, 2002; No *et al.*, 2002).

1.4.4.3 Other mucoadhesive polymers

1.4.4.3a Cellulose-based polymers

Cellulose $(C_6H_{10}O_5)_n$ is an insoluble complex carbohydrate composed of glucose units and forms the constituent of the cell wall in most plants. Cellulose contains numerous hydroxyl groups, which can react with acids to form esters or alcohols to form ethers. Water-soluble cellulose derivatives (Figure 1.4) important in the pharmaceutical industry include; sodium carboxymethyl cellulose, hydroxypropyl cellulose, hydroxypropylmethyl cellulose and hydroxyethyl cellulose. These cellulose derivatives have been used in the formulation of solid dosage forms, aqueous disperse systems as viscosity enhancing agents and in products for topical application (Ahuja *et al.*, 1997).

1.4.4.3b Natural polysaccharides

Other than chitosan and cellulose, a wide variety of (semi) natural polysaccharides exist that have potential uses in mucoadhesive drug delivery, these include; guar and xanthan gums, pectin, carrageenan, hyaluronic acid and sodium alginate (Ahuja *et al.*, 1997; Lee *et al.*, 2000; Smart. 2004b). These polysaccharides have a range of applications in pharmaceutical formulation. Sodium alginate (Figure 1.4) is currently used in the management of gastro-oesophageal reflux and particles are retained from suspension on the oesophageal mucosa during swallowing (Richardson *et al.*, 2004). However, these

polymers are generally characterised as being poor mucoadhesives with short adhesion times when compared to superior adhesives such as Carbopol (Grabovac *et al.*, 2005).

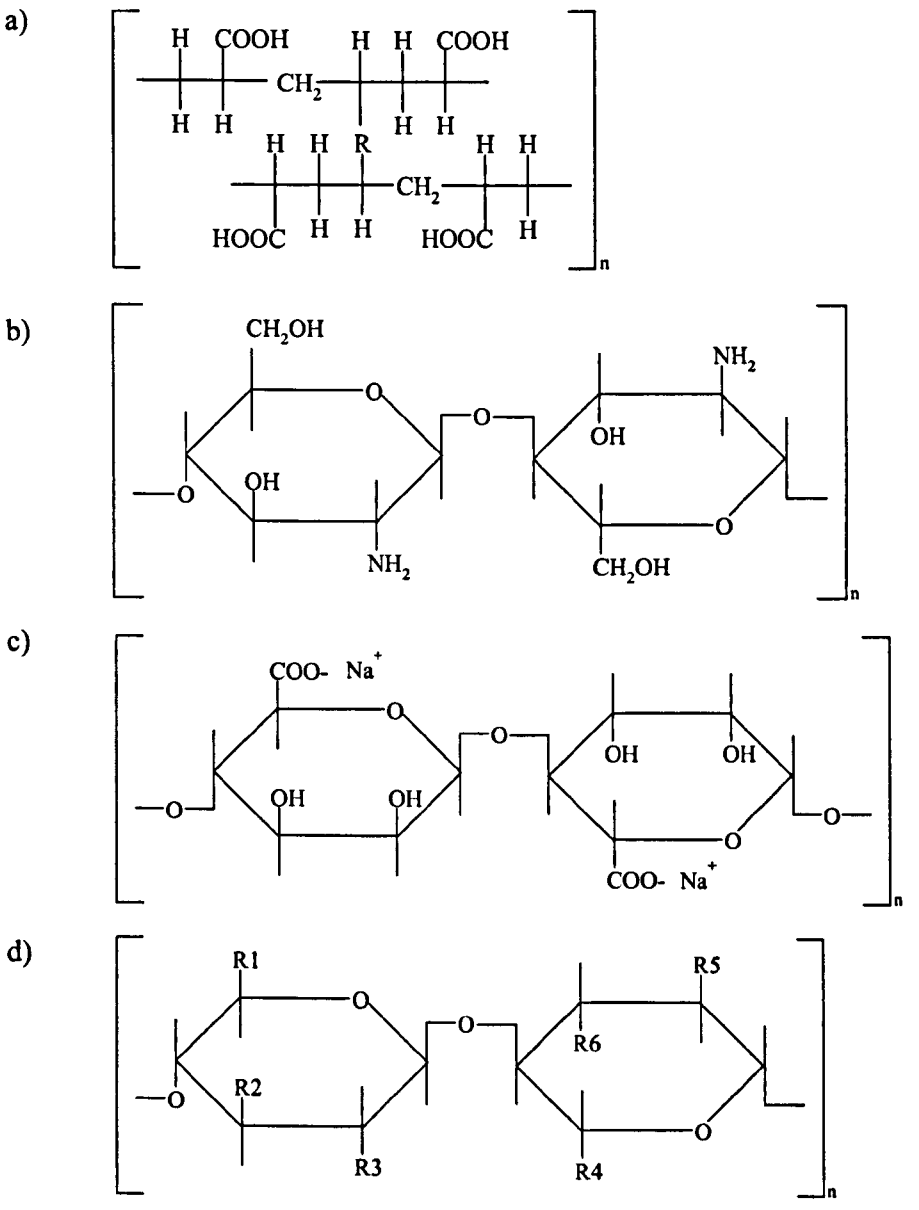

Figure 1.4 The structure of some common mucoadhesive polymers; a) polyacrylic acid, R = allyl sucrose (Carbopol) or divinyl glycol (polycarbophil); b) Chitosan; c) Sodium alginate, and d) Cellulose derivatives e.g. sodium carboxymethyl cellulose, R1, R4 = CH2OH; R2, R3, R5 = OH; R6 = OCH2CO2-Na+, or hydroxypropylmethyl cellulose, R1 = CH2OCH3; R2 = OH; R3 = OCH2CHOHCH3; R4 = CH2OH; R5, R6 = OCH3

1.4.4.3c Other synthetic polymers

These include polyethylene oxide (PEO), polyvinylalcohol polyvinyl-pyrrolidone (PVP), polymethacylate (Eudragit®) and Gantrez®. Typically these polymers exhibit poor mucoadhesion (Grabovac *et al.*, 2005). Despite the use of Gantrez® in various toothpaste formulations to increase the retention of triclosan in the oral cavity; Kockisch *et al* (2001) could find no evidence of adhesion to buccal cells either *in vitro* or *in vivo*.

1.4.5 Mucoadhesive drug and antimicrobial delivery in the oral cavity

Mucoadhesive drug formulations for the oral cavity can be categorised into three main forms; solid dosage forms which include tablets and lozenges, semi-solid dosage forms which include hydrogels and pastes, and liquid dosage forms which include rinses. Particulate systems can be administered in a variety of dosage forms. Typically particles are delivered in aqueous suspension but can also be applied by aerosol, incorporated into a paste or ointment, or compressed to form tablets. Due to their versatility, particulates will be considered separately.

1.4.5.1 Solid dosage forms

Mucoadhesive tablets for oral drug delivery are typically prepared with the compression of powder mixes that can be placed into contact with the oral mucosa and allowed to adhere (Smart. 2005b). Drug release from tablets can either be multidirectional or unidirectional (Figure 1.5). In multidirectional tablets, the drug is incorporated into a bioadhesive polymer matrix, which hydrates and releases the drug upon contact with the mucosa. These are often used to obtain local delivery within the oral cavity, with drug release directed toward to oral cavity. In unidirectional tablets, an impermeable layer, which contains no drug, protects the underlying drug/polymer matrix, which is positioned against the mucosa. These are often found in systemic formulations, where drug permeation across the oral mucosa is favoured by unidirectional drug release.

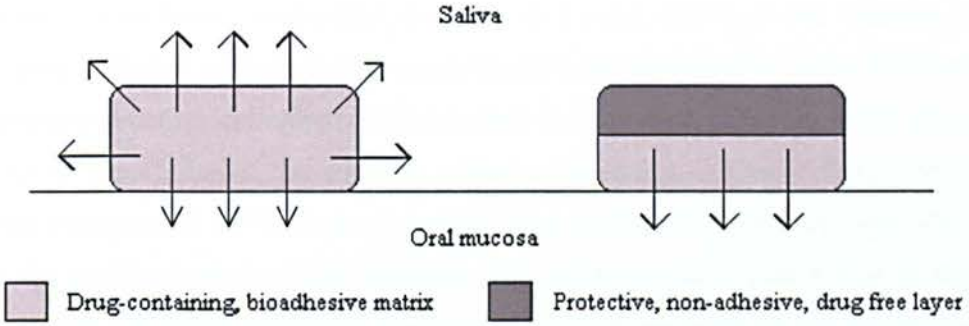

Figure 1.5 Typical mucoadhesive tablet formulations: a) the drug is incorporated throughout the tablet matrix, allowing multidirectional drug release upon polymer hydration, and b) the drug-containing polymer matrix is protected by the non-adhesive backing layer, favouring unidirectional drug release toward the mucosa. Image adapted from Smart (2005b).

Drugs absorbed via the oral mucosa avoid low gastric pHs and proteases and first pass hepatic degradation, which must be overcome in enterically administered drugs (Zhang *et al.*, 2002). Absorption of drugs across the oral mucosa provides a rapid onset of action, similar to that of intravenous administration. Bioadhesive strategies attempt to immobilise the drug on the oral mucosa long enough for drug absorption to occur. Systemic administration of antimicrobials for the treatment of dental diseases demonstrates several disadvantages, including:

- Inadequate concentration at the site of the periodontal pocket,
- Rapid decline of the plasma concentrations to sub-therapeutic levels,
- The development of microbial resistance due to sub-therapeutic drug levels,
- Peak plasma concentrations, which may be associated with various side effects, such as hypersensitivity, gastrointestinal intolerance and drug interactions with alcohol.

Sustaining the local delivery of antimicrobials within the oral cavity is an attractive alternative to the systemic administration of agents such as antibiotics. Llabot *et al.* (2002) designed a biphasic buccal adhesive tablet for the delivery of nystatin, an antibiotic used in the treatment of fungal infections such as oral candidosis. Tablets were prepared by direct compression; the immediate release layer was composed of

lactose (100 mg) and nystatin (30 mg); the sustained release layer was composed of Carbopol and hydroxypropylmethyl cellulose (9:1 ratio, 200 mg) and nystatin (33.3 mg). Mucoadhesion of the tablets to a gelatin gel layer showed that higher Carbopol to hydroxypropylmethyl cellulose ratios resulted in improved adhesive bond strength, suggesting that Carbopol has superior adhesive properties. *In vitro* drug release in distilled water caused 50% release of nystatin from the immediate release layer after 1 h while the sustained release layer achieved 80% nystatin release after 8 h at an almost constant rate. Biphasic release of nystatin was clearly observed during dissolution of the double-layered tablets. The drug release characteristics observed within this study are unlikely to reflect the *in vivo* situation due to the selection of the release medium. Mucoadhesive polymers are influenced by the presence of electrolytes such as those present in saliva, which would affect water uptake and adhesion to the mucosa. Drug release from tablets is dependent on diffusion through the hydrated polymer matrix and polymer relaxation, which would ultimately be affected *in vivo* by saliva.

Ali *et al.* (2002) prepared buccoadhesive erodible disks for the sustained delivery of CPC in the treatment of oro-dental infections. The disks were prepared by direct compression using different combinations of hydroxypropylmethyl cellulose, sodium carboxymethyl cellulose, magnesium stearate, mannitol, and CPC. *In situ* drug release studies were carried out in flow-through apparatus by applying the buccoadhesive disk to bovine cheek mucosa in isotonic phosphate buffer. Optimised tablet formulations were shown to maintain the concentration of CPC above its MIC for 6 h, which was confirmed by growth inhibition of commonly isolated oral bacterial strains. *In vivo* investigations confirmed that the concentration of CPC in saliva was elevated above the MIC over a period of 8 h. The tablets were shown to completely erode with minimal discomfort felt by volunteers and a correlation between *in situ* and *in vivo* drug release was observed. Perioli *et al.* (2003) prepared mucoadhesive tablets containing metronidazole, an antibiotic agent selective against anaerobic bacteria, for the treatment of periodontal disease. Suitable mucoadhesion, hydration and *in vitro* drug release characteristics were identified in tablets containing hydroxylethyl cellulose and Carbopol 940 in a 2:2 weight ratio. Salivary levels of metronidazole were maintained above its MIC for over 12 h. Arora *et al.* (2003) characterised the *in situ* release of secnidazole, an antibiotic effective against anaerobic bacteria, from tablets composed of Carbopol 934P and sodium carboxymethyl cellulose. Samples collected from the *in situ*

release studies inhibited the growth of planktonic *Bacteroides fragilis* and *Fusobacterium*. It is uncertain whether these tablets would exhibit clinical efficacy as microbiological evaluation was judged using planktonic organisms only, which is not an accurate reflection of their growth *in vivo*. Despite this, mucoadhesive and drug release properties from these solid dosage forms are ideal for local drug delivery to the oral cavity.

One of the main disadvantages of antimicrobial delivery with buccoadhesive tablets is patient acceptability i.e. mouth feel, taste and irritation (Smart. 2004a). The popular use of poly(acrylic acid) polymers, such as Carbopol, in mucoadhesive tablets results in strong acid characteristics, increasing the chance of mucosal irritation. Llabot *et al.* (2004) used a mixture of Carbopol and lyophilised Carbopol sodium salt to prepare mucoadhesive tablets for the delivery of nystatin to avoid the acidity of Carbopol-only preparations. Although these tablets exhibited good *in vitro* drug release, water uptake, and mucoadhesive properties, no information was presented regarding the benefits of using Carbopol sodium salts such as the measurement of surface pH. The control of water uptake into mucoadhesive tablets is important. Poly(acrylic acid)s and cellulose derivatives, which are commonly used in tablet formulation, hydrate to form an outer gel layer which increases the size of the tablets negatively affecting patient compliance and in some cases the drug bioavailability (Singla *et al.*, 2000). The amount of drug incorporated into a tablet matrix is also often limited due to possible interference with mucoadhesive characteristics.

1.4.5.2 Semi-solid dosage forms

These typically contain a mucoadhesive polymer and drug plus any excipient dissolved or suspended as a fine powder in an aqueous or non-aqueous base, depending on their solubility and concentration (Smart. 2004a). Hydrogels have become a commonly investigated semi-solid dosage form, typically formed from a cross-linked polymer, which upon application, either topically with the finger or via a syringe, swell slowly in the presence of water releasing any drug entrapped within (Peppas and Sahlin. 1996). Jones *et al.* (1997b, 1997c, 2000) developed and characterised a range of mucoadhesive, antimicrobial gels using texture probe analysis for the treatment of periodontal disease. Assessment of hardness, compressibility, adhesiveness and cohesiveness were all used

to characterise the physical properties of the mucoadhesive gels and resulted in the selection of an optimal bioadhesive formulation; hydroxylethyl cellulose (3% w/w), polyvinylpyrrolidone (3% w/w) and polycarbophil (1% w/w) (Jones *et al.*, 1997b, 2000). Formulations containing tetracycline hydrochloride (5% w/w) were evaluated for clinical efficacy in two subjects exhibiting periodontal pockets ≥ 5 mm in depth (Jones *et al.*, 2000). Sub-gingival plaque samples were taken from each site both before and 1 week following application of the formulation with a syringe. The bacterial content of collected plaque samples were analysed using dark-field microscopy and growth on Wilins-Chalgren agar. The composition of the plaque collected 1 week after application had changed considerably, obligate anaerobes constituted 49.01% of total bacteria morphocytes, whereas previously these organisms were the dominant (84.41%) bacterial type. The number of black-pigmented anaerobes and spirochaetes were also significantly reduced, with cocci species becoming the dominant species, indicating a shift in plaque composition towards a microflora which is associated with periodontal health.

Senel *et al.* (2000) used chitosan gels prepared in lactic acid for the topical delivery of chlorhexidine to the oral cavity. The viscosity, *in vitro* chlorhexidine release and microbiological studies against *Candida albicans* were used to evaluate the potential use of the formulation in the topical treatment of candidosis. Unfortunately, no data on the mucoadhesive properties of these gels were included in the study and the antimicrobial efficacy of these gels was assessed using MIC values against planktonic species only. Interestingly, 0.1% chlorhexidine in a 2% chitosan gel gave a lower MIC value (indicating a higher toxicity to *Candida albicans*) than 0.2% chlorhexidine in a 2% gel. This may indicate some reduction in chlorhexidine bioavailability when higher chlorhexidine concentrations are incorporated into the 2% chitosan gels, although the author did not comment upon this. Aksungur *et al.* (2004) used chitosan gels to deliver nystatin for the prevention of *Candida albicans* infection in patients' suffering from oral mucositis: an inflammatory condition often caused by radiation or chemotherapy used in the treatment of cancer. *In vivo* studies were carried out in healthy human subjects and a hamster model for chemotherapy-induced mucositis. Nystatin saliva levels were maintained above the MIC for *Candida albicans* for 90 min in samples collected from three different sites in the oral cavity. Nystatin delivered by suspension remained at therapeutic levels for 30-45 min, indicating rapid clearance. Although no obvious

advantage could be attributed to the formulation of nystatin with chitosan when assessed using an experimental animal model, chitosan gels did prolong salivary levels of nystatin in the human volunteers at higher concentrations than the suspension. This suggests that chitosan gels are able to improve the substantivity of an active drug.

1.4.5.3 Liquid dosage forms

The use of liquid dosage forms for the delivery of antimicrobials increase the likelihood that the formulation will reach all areas of the oral cavity, including the distal, hard to reach crevices and surfaces. However, few liquid bioadhesive dosage forms have been investigated. Generally, the focus of many drug delivery strategies concerning the use of mucoadhesion have focused on dry and semi-solid dosage forms. This may be due to the vast amount of theoretical and experimental evidence supporting the adhesion and clinical efficacy of these formulations *in vivo*. Although the adsorption of polymers from solution has been demonstrated (Patel *et al.*, 1999, 2000; Kockisch *et al.*, 2001), the contact time of liquid formulations within the oral cavity is rarely longer than 60 s. A sufficient amount of adsorption from solution is therefore required within this time to achieve prolonged local therapeutic concentrations.

Ungphaiboon and Maitani (2001) prepared mucoadhesive mouthwash formulations containing the corticosteroid triamcinolone acetonide for the treatment of oral lichen planus, a chronic inflammatory condition that manifests itself as lesions on the oral mucosa. Carbopol 934 was incorporated into a cosolvent system and the *in vitro* permeation of triamcinolone acetonide across hamster cheek pouch was analysed following a 1 minute contact time using a Franz type diffusion cell. Only formulations containing Carbopol 934 resulted in the permeation of triamcinolone acetonide through the hamster cheek pouch. However a significantly higher amount of triamcinolone acetonide was present within the mucosa after the application of an aqueous suspension, which suggests that the inclusion of Carbopol has little effect on triamcinolone acetonide retention and resulted in permeation rather than mucosal accumulation. Furthermore the viscosity of the mucoadhesive formulation was high, indicating an incompatibility in clinical situations.

1.4.5.4 Particulate systems

The incorporation of drugs into polymeric microparticles has become a popular method for obtaining bioadhesive, controlled delivery formulations for a number of target sites including the eye, nasal cavity, oral cavity and gastrointestinal tract. In the oral cavity, microparticles may become lodged in sites, which are notoriously difficult to reach e.g. approximal tooth surfaces. Giunchedi *et al.* (2002) prepared chitosan microparticles loaded with chlorhexidine to achieve prolonged therapeutic concentrations within the oral cavity. The microparticles were prepared by spray-drying solutions of chlorhexidine and chitosan in 1:2 and 1:4 weight ratios. Particle characterisation showed drug incorporation and small particle sizes were achieved using this method. Large particles may cause patient discomfort due to "mouth feel" issues. *In vitro* drug release from the microparticles significantly improved the dissolution of chlorhexidine when compared to chlorhexidine diacetate powder. These particles were compressed with sodium alginate, mannitol and saccharine to form tablets which were then assessed *in vivo*. Elevated chlorhexidine concentration in saliva was evident for over 3 h, which was comparatively longer than a chlorhexidine mouthwash (2 h).

Kockisch *et al.* (2003, 2005) compared microparticles prepared with a range of mucoadhesive polymers; Carbopol 974P, polycarbophil AA-1, chitosan and Gantrez. Polymeric microparticles were prepared using a "water-in-oil" solvent evaporation technique and their mucoadhesive properties were characterised using swelling studies and tensile testing and retention on porcine oesophageal tissue (Kockisch *et al.*, 2003). Particles prepared from Gantrez and chitosan demonstrated significantly higher retention times on the oesophageal model, despite the lower tensile strengths observed when compared to the particles prepared from poly(acrylic acid) polymers. Triclosan-loaded particles were prepared using an "oil-in-water-in-oil" double-emulsion technique, and the *in vitro* release kinetics evaluated (Kockisch *et al.*, 2005). Particles prepared from the poly(acrylic acid)s and Gantrez exhibited burst-release characteristics, with Gantrez particles depleted within 2.5 min and poly(acrylic acid) particles within 15 min. Chitosan particles however exhibited prolonged release characteristics; with less than 80% total triclosan released over 8 h. These particles showed potential for achieving good sustained delivery within the oral cavity, however

triclosan-loading may affect the mucoadhesive properties exhibited by these particles in the previous work.

Govender *et al.* (2005) statistically optimised the formulation of tetracycline-loaded chitosan microparticles prepared by tripolyphosphate cross-linking based on adhesive strength testing and *in vitro* drug release. Increasing the concentration of tripolyphosphate and therefore the degree of chitosan cross-linking increased the maximum detachment force exhibited by the microparticles. In addition, higher chitosan concentrations decreased the maximum detachment force. The optimal formulation; 3% w/w chitosan, 10% w/w tetracycline hydrochloride, 9% w/w tripolyphosphate, was then characterised in terms of hydration, release kinetics, antimicrobial activity, thermal properties, morphology and surface pH. Tetracycline was released at concentrations above the MIC of *Staphylococcus aureus* for over 8 h. By optimising the formulation according to mucoadhesive and drug release properties the potential for clinical efficacy is enhanced. Other authors have reported a positive correlation between *in vitro* and *in vivo* drug release and although microbiological evaluation was based solely on planktonic experiments the use of chitosan microparticles for controlled drug delivery seems promising.

1.4.6 A new development in antimicrobial therapy within the oral cavity

Dental diseases of a bacterial origin continue to be prevalent among western populations as a consequence of poor diet and inadequate standards of oral hygiene. In addition, only 59% of the UK population attended regular dental check-ups in 1998 (Nuttall *et al.*, 2001). The observation stated by Marsh (1991) and Addy (1994) regarding the insufficiency of cleaning techniques to provide a level of plaque control compatible with oral health over long periods suggests that modern healthcare products need to be improved. The use of triclosan appears to offer benefits in terms of enhanced antimicrobial efficiency; however concerns have been raised about the possible development of cross resistance. Therefore future formulations should target the growth of complex bacterial biofilms within the oral cavity over sustained periods of time using antimicrobials that have low potential for adverse effects including toxicity and cross resistance. It is important to note that the antimicrobials used should not completely

eradicate bacterial populations within the oral cavity as the resident flora can have protective effects competing for nutrients and space with potentially pathogenic bacterial species.

Toothpastes are typically the oral healthcare product of choice for the majority of consumers; however the supplementary use of mouthrinses is also popular, particularly in the developed world. The use of other dosage forms, such as tablets and films, for the delivery of antimicrobials to the oral cavity is generally less acceptable to patients and consequently not widely used. This is partly due to discomfort experienced by the patient during the residence of the formulation on oral surfaces; this is particularly applicable to solid dosage forms such as tablets, which are positioned either on the tooth or mucosal surface until dissolved. Formulations that are likely to be the most successful and widely accepted should probably be based on a toothpaste/mouthwash principle. In addition, relatively few studies have examined the use of bioadhesive strategies in formulations other than those based on solid dosage forms.

Therefore the idea explored in this thesis is to develop a retentive delivery system for the various alternatives to triclosan that could be included into a toothpaste or mouthwash formulation allowing enhanced antimicrobial action. This could have a significant impact on the development of oral cavity infections.

1.5 Aims and Objectives

- To optimise the delivery and substantivity of different actives using strategies based on bioadhesive formulations, most particularly where poor retention in the oral cavity is known to compromise the *in vivo* antimicrobial efficacy.
- To design bioadhesive complexes that may improve the effectiveness of oral healthcare formulations through preventative activity e.g. prevention of dental diseases and plaque accumulation, rather than treatment.
- To obtain bioadhesive antimicrobial-polymer complexes that can be formulated into a paste or mouthwash to improve the antimicrobial efficacy of oral healthcare products.
- Investigate antimicrobial-polymer complexes which are based on secondary chemical interactions such as electrostatic or hydrogen bonding rather than covalent bonding.
- Utilise known mucoadhesives such as chitosan and poly(acrylic acid) which do not require regulatory approval.
- Attempt to create complexes which are responsive to local environmental changes, particularly low pH, to target specific oral pathogens.
- Characterise the complexes in terms of drug release and develop relevant methods to analyse mucoadhesive properties both before and after antimicrobial incorporation.
- To use microbiological assays based on both planktonic and sessile organisms commonly implicated in the aetiology of dental disease to evaluate the potential of antimicrobial-polymer complexes for use in oral healthcare.

Chapter 2

In vitro assessment of bioadhesive polymers

2.1. Introduction

2.1.1 Background

The development of *in vitro* test methods for the assessment of bioadhesion is an important step in the design of mucoadhesive, oral drug delivery systems. The aims of *in vitro* testing are to predict the behaviour of a formulation *in vivo* and hence such techniques should be reflective of the delivery target. Polymers intended for use as mucoadhesive platforms for drug delivery must be assessed for bioadhesion before development continues.

Many methods have been utilised for the determination of polymer bioadhesion to a model surface, and are reviewed in section 1.4.4.1. Research has focused mainly on the determination of adhesive bond strength by means of tensile testing, which has remained an important tool in the classification of mucoadhesive performance (Dyvik *et al.*, 1992; Esposito *et al.*, 1994; Mortazavi and Smart. 1995; Tobyn *et al.*, 1995, 1996, 1997; Tamburic and Craig. 1997; Wong *et al.*, 1999; Eouani *et al.*, 2001). In addition to the mechanical characterisation of the adhesive bond, the adsorption and binding of mucoadhesive polymers from aqueous dispersion to a model surface is important, particularly when considering liquid formulation strategies (Park and Robinson. 1984; Patel *et al.*, 1999, 2000; Kockisch *et al.*, 2001). The demonstration of adsorbed molecules on a surface is at most semi-quantitative and such methods could provide a better understanding of mucoadhesive performance when coupled with other techniques.

High molecular weight cross-linked poly(acrylic acid) polymers and chitosan exhibit good bioadhesive and physicochemical properties (Smart. 2004b), ideal for the intended application. In this section a range of such polymers were purchased and characterised in terms of bioadhesive properties using a direct staining technique adapted from a study by Kockisch *et al.* (2001) and texture analyser equipment. Model substrates were selected to represent soft tissue surfaces within the oral cavity. Polymers that demonstrated the most promising behaviour were selected for further investigations.

2.1.2 Detecting polymer on cell surfaces: Histological staining and dyes

The adsorption of aqueous polymer dispersions onto the surface of buccal cells has been analysed using a direct staining technique (Kockisch *et al.*, 2001). The quantification of bound polymer on the buccal cell surface relies on the analysis of digital images captured using light microscopy. Cells are virtually colourless and so need to be stained with a suitable dye for light microscopy (Stevens and Lowe. 1997). To quantify the amount of polymer on the buccal cell surface a dye must be selected that causes an intense stain of the polymer, differential to that of the buccal cell.

Alcian blue has been employed to identify the presence of acidic mucins secreted by some epithelial cells using light microscopy. In solution, this stain is positively charged (cationic) (Figure 2.1) and therefore binds to negatively charged (anionic) structures through the formation of reversible electrostatic interactions. These electrostatic interactions can be readily broken revealing a variation in bonding among different types of glycosominoglycans. When the concentration of electrolyte required to break the bond is increased progressively, then neutral, sulphated and phosphated mucopolysaccharides may be identified in tissue sections.

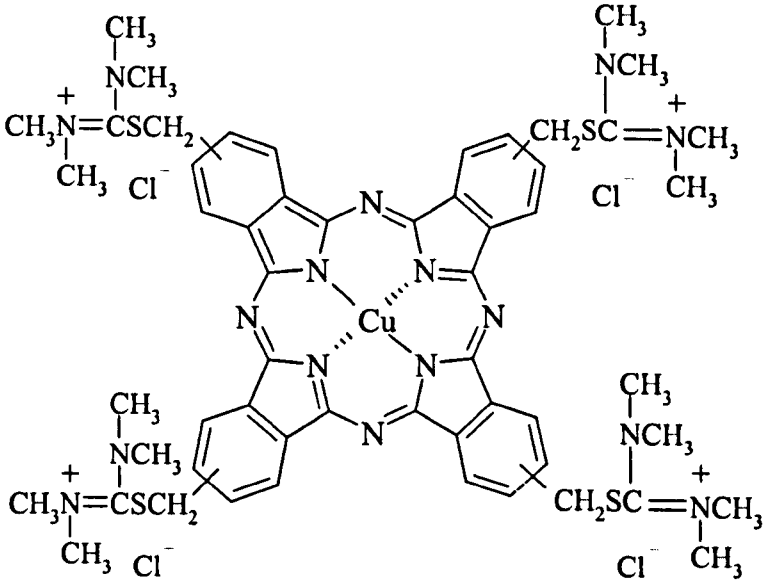

Figure 2.1 Chemical structure of Alcian blue 8GX.

Alcian blue is water-soluble and its interaction with polyanionic glycoproteins is influenced by pH; both sulphate and carboxylate groups will react at pH 2.5, but sulphate groups alone react at pH 1. Carbopol and polycarbophil are homopolymers of acrylic acid lightly cross-linked with allyl sucrose and divinyl glycol respectively. When aqueous polymer dispersions are adjusted to pH 7.0, the polymer carries a net negative charge as a consequence of ionised carboxylate groups along the polymer backbone. Alcian blue prepared in sucrose acetate buffer (pH 5.8) will bind to polyanionic structures (Corne *et al.*, 1974). Therefore Alcian blue would be retained with the polymer if it were present on the surface of the buccal cells; this has been demonstrated in previous studies (Patel *et al.*, 1999; Kockisch *et al.*, 2001).

Eosin is a pink stain commonly used throughout histology in conjunction with haematoxylin. Eosin stains the cytoplasm of cells amongst other acidophilic materials. It is weakly acidic, with each molecule carrying one carboxylic acid group (Figure 2.2) which can complex with free terminal amino groups by simple salt formation. Chitosan has a high concentration of amine groups and has been shown to form complexes with eosin, as demonstrated through light microscopy (Patel *et al.*, 1999; Kockisch *et al.*, 2001) and adsorption onto chitosan hydrobeads (Chatterjee *et al.*, 2005).

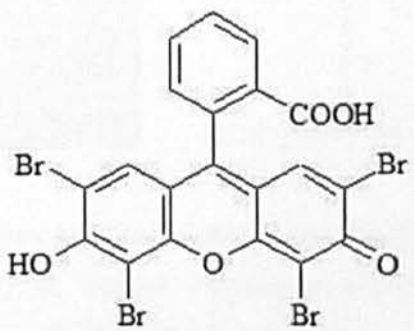

Figure 2.2 Chemical structure of Eosin Y.

2.1.3 Measuring adhesive bond strength: Texture probe analysis

Tensile testing is a widely used method for the assessment of the bioadhesive joint strength. The measurement of the tensile strength of the adhesive bond can be divided into two components; the maximum detachment force (mN) and the work of adhesion

(mN mm^{-1}). Previously, tensile measurements have been determined using modified tensiometers (Dyvik *et al.*, 1992; Esposito *et al.*, 1994) or rheometers (Smart *et al.*, 1995). Texture analyser equipment (Figure 2.3) is capable of quantifying adhesive bond strength and enables the user specific control over a range of experimental parameters, including probe speed and applied force.

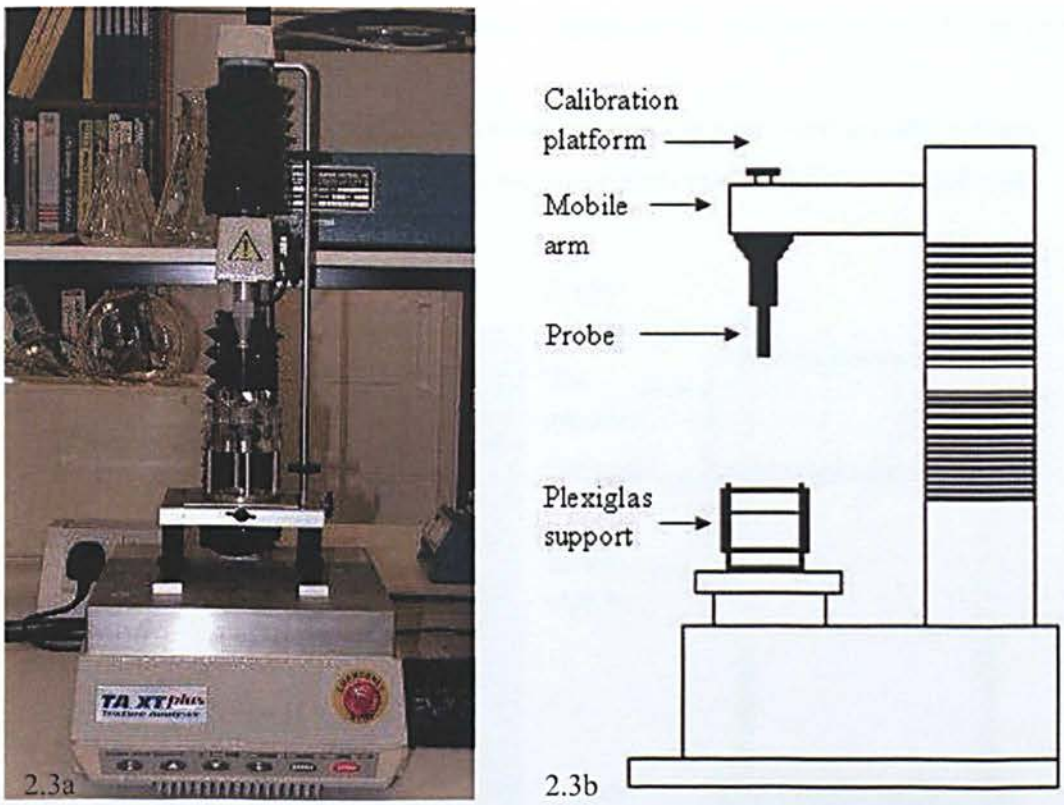

Figure 2.3 TA.XT plus texture analyser instrument by Stable Micro Systems (2.3a) and schematic diagram (2.3b) to outline instrument components important in the determination of tensile strength of an adhesive bond.

Texture analysis is a technique that has been extensively employed in the mechanical characterisation of food materials (Tamburic and Craig. 1997). It has since emerged as a useful technique in the field of pharmaceutical gel characterisation (Jones *et al.*, 1996) and as a means of quantifying bioadhesion (Tobyn *et al.*, 1995). Texture analyser equipment consists of a probe, which is fixed to the mobile arm of the instrument (Figure 2.3). The base of the probe is often used to attach compact polymer samples by means of an adhesive (Tobyn *et al.*, 1996; 1997; Wong *et al.*, 1999; Eouani *et al.*, 2001)

and this is then bought into contact with a suitable substrate i.e. model mucosa. The probe has also been used for adhesive substrates such as mucin (Tamburic and Craig. 1997). The movement of the probe is computer controlled, and is able to define:

- Probe speed (mm s^{-1}) - the speed of the probe during force determinations, this is separated into pre-test, test and post-test speed,
- Applied force (N) - the constant force applied to the probe once contact has been established,
- Contact time (s) – the duration of contact between the probe and a model surface,
- Return distance (mm) – the distance the probe must reach before test completion.

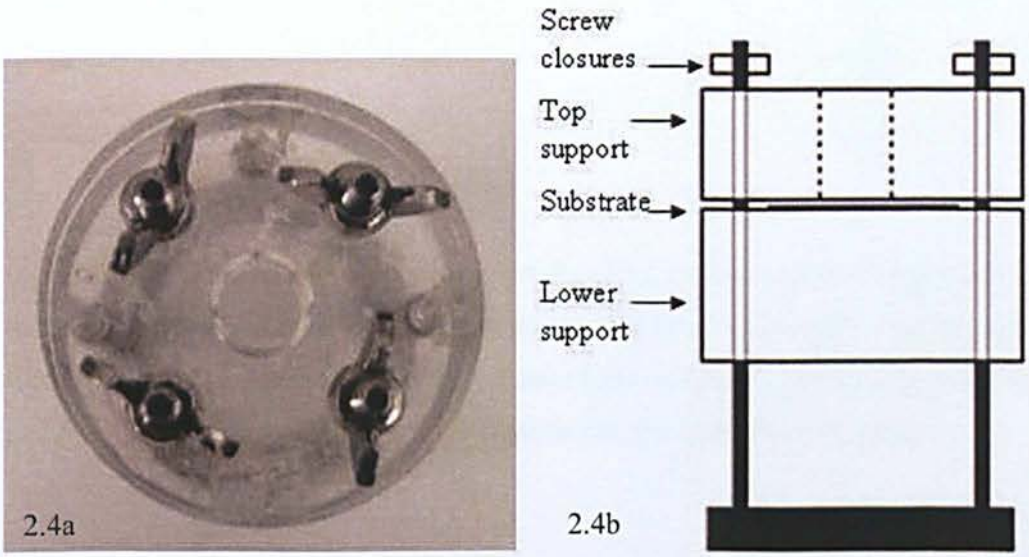

Figure 2.4 Plexiglas support used in tensile strength determinations: top-down photograph (2.4a) and side-on schematic diagram (2.4b). The substrate to be tested is held securely in the support, leaving an area exposed for adhesion.

Most mucoadhesive studies involve the attachment of a compact polymer sample to the probe using an adhesive such as cyanoacrylate or double-sided tape. Substrates can range from dialysis membrane to mucosa of animal origin. These are normally fixed in place using a platform (Figure 2.4), which exposes an area of the surface for contact to be made, and bathed in a medium suited to the application. The probe is then bought into contact with the fixed substrate for a pre-determined duration and contact force.

The force required to remove the probe from the surface is measured and a force-distance curve obtained (Figure 2.5). From this curve both the maximum detachment force and work of adhesion can be determined.

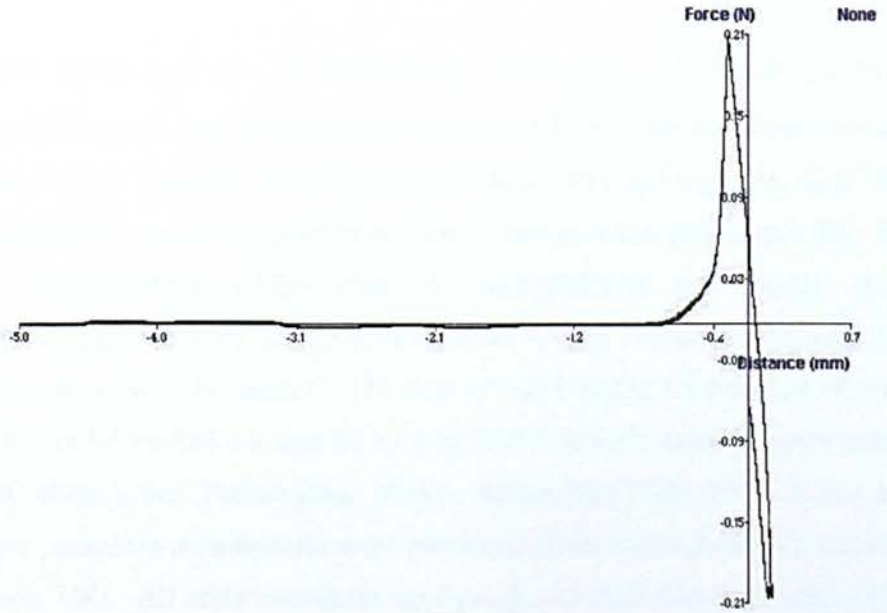

Figure 2.5 Typical force-distance curve produced by texture analyser equipment in the determination of the tensile strength between Carbopol 971P and a model mucosal surface. The highest peak on the graph determines maximum detachment force (mN) and work of adhesion (mN mm^{-1}) is determined by the area under the graph.

2.2 Materials and methods

2.2.1 Materials

Carbopol™ (974P Lot Nº CC24MAB482, 971P Lot Nº CC29MAJ126) and polycarbophil™ (AA-1 Lot Nº CC17MAW025) were kindly donated from Noveon Inc, (Cleveland, USA). Medium viscosity (Lot Nº 408499/1) and high viscosity chitosan (Lot Nº 414555/1) were purchased from Fluka Chemicals Ltd (Glossop, UK). HCMF (Lot Nº GR23238901), CMFP (Lot Nº GR23238903) and DCMF (Lot Nº GR23238902) chitosan were kindly donated from Cognis Deutschland GmbH Co.KG (Illertissen, Germany). Protasan CL113 (Lot Nº FP-110-02), CL213 (Lot Nº FP-104-02), G113 (Lot Nº FP-108-04) and G213 (Lot Nº FP-103-07) chitosan were purchased from FMC Biopolymer (Philadelphia, USA). Alcian blue 8GX, Eosin Y and sodium dihydrogen phosphate monohydrate were purchased from Sigma-Aldrich Company Ltd (Gillingham, UK). All other chemicals were purchased from Fisher Scientific UK Ltd (Loughborough, UK) unless otherwise stated. All chemicals were used as received without further treatment unless otherwise stated.

2.2.2 Methods

2.2.2.1 In vitro direct staining technique

2.2.2.1a Preparation of aqueous polymer dispersions

Carbopol™ and polycarbophil™ aqueous dispersions were prepared by adding 0.1 g to 40 mL deionised water under constant stirring using a magnetic stirrer at 300 rpm (Stuart, Heat-Stir CB192). After 4 h, the pH of the dispersion was adjusted to 7.0 using 0.1 M sodium hydroxide and made up to 100 mL volume with deionised water in order to obtain a concentration of 0.1% w/v. Chitosan (Fluka, Cognis) aqueous dispersions were prepared by adding 0.1 g to 40 mL 1% v/v acetic acid under constant stirring using a magnetic stirrer at 300 rpm. Chitosan salts obtained from FMC Biopolymer were dispersed in deionised water. After stirring for 4 h, the pH of the dispersions were adjusted to 4.5 using 0.1 M sodium hydroxide and made up to 100 mL volume using

deionised water to obtain 0.1% w/v concentration. Aqueous polymer dispersions were sealed and stored at 4°C overnight to allow the hydration of polymer chains and an expiry date set at 1 week from preparation.

2.2.2.1b *In vitro* mucoadhesion of polymer dispersions to human buccal cells in sucrose

Buccal cells were collected from healthy individuals 2 h post-prandial by gently scraping the inside of the cheek with a wooden tongue depressor. Collected cells were suspended in 0.25 M sucrose solution (20 mL) and stirred using a magnetic stirrer at 500 rpm for 30 min in order to prevent cell aggregates. Aliquots of cell suspension (5 mL) were dispensed into 15 mL glass test tubes and centrifuged at 200 g for 15 min (Juoan B4i centrifuge). The supernatant was removed and the resultant cell pellet was re-suspended in 5 mL fresh 0.25 M sucrose solution. This process was repeated three times in order to remove debris and unbound proteins from the cell surface.

After the final wash, the cell pellet was re-suspended with gentle vortexing in 0.1% w/v aqueous polymer dispersion (5 mL) or the negative control; 0.25 M sucrose solution (5 mL) and incubated at 32°C for 30 min. Cells were separated from excess polymer by centrifuging at 400 g for 15 min. Increasing the centrifugal force had no detrimental affect on the buccal cells. The supernatant was removed and the resultant cell pellet was washed five times in 0.25 M sucrose solution using the process previously described.

2.2.2.1c *In vitro* mucoadhesion of polymer dispersions to human buccal cells in artificial saliva

Buccal cells were collected as before from healthy individuals 2 h post-prandial and suspended in 20 mL artificial saliva (5 mM sodium bicarbonate, 7.36 mM sodium chloride, 20 mM potassium chloride, 6.6 mM sodium dihydrogen phosphate monohydrate, 1.5 mM calcium chloride dihydrate) under constant stirring with a magnetic stirrer at 500 rpm for 30 min to avoid cell aggregation. The composition of the artificial saliva was based on the ionic component of submandibular saliva (excluding magnesium) at a flow of 0.26 mL min^{-1} (Lentner. 1981). Aliquots (5 mL) were dispensed into 15 mL glass test tubes and centrifuged at 200 g for 15 min. The

supernatant was removed and replaced with fresh artificial saliva and this washing procedure was repeated as above.

The resultant cell pellet was incubated with either 0.1% w/v polymer dispersion (5 mL) or the negative control; artificial saliva (5 mL) at 32°C for 15 min. Cells were separated from excess polymer by centrifugation at 400 g for 15 min. The cell pellet was washed once in 0.25 M sucrose solution, three times in artificial saliva and once more in 0.25 M sucrose solution. Sucrose was used for the initial wash, as large polymer precipitates would form following an initial artificial saliva wash. Artificial saliva was not used for the final wash due to potential disruption of Alcian blue staining by the presence of free ions.

2.2.2.1d Cell staining and analysis

Sucrose acetate buffer was prepared by adding a sucrose solution (0.15 M, 10.26 mL) to sodium acetate solution (0.05 M, 0.82 mL). Cells treated with poly(acrylic acid) based polymers were stained with 0.05% w/v Alcian blue 8GX in 0.16 M sucrose acetate buffer (pH 5.8 using 0.1 M hydrochloric acid) for 30 min at 32°C. Cells treated with chitosan were stained with 0.1% w/v eosin Y prepared in deionised water and incubated for 30 min at 32°C. Uncomplexed dye was removed by washing the cells with 0.25 M sucrose solution, until the supernatant was clear.

Cells were transferred to a microscope slide and examined using light microscopy (Nikon eclipse E600). Images of 20 different cells selected randomly were captured using a digital camera (Leica DC 200) at x200 magnification and converted to greyscale using Image Converter and Editor Software (v1.87, Copyright Global General Computer, Inc., 2001-2003). Image analysis was carried out using Scion Image (vBeta 4.0.2, Copyright Scion Corporation., 2000). An area within the cell containing 10,000 pixels was measured and analysed according to the average pixel intensity based on a scale (white = 0, black = 255). The experiment was repeated three times.

2.2.2.2 Texture probe analysis

2.2.2.2a Preparation of polymer samples

Polymer disks were prepared by accurately weighing out 30 mg of polymer (Carbopol 974P, 971P and polycarbophil AA-1, Protasan CL113, CL213, G113 and G213) and applying 2 tons of pressure for 10 s using a KBr press (Specac) and a KBr disk assembly unit (8 mm diameter). Ethylcellulose was prepared for use as a negative control.

Chitosan obtained from Fluka chemicals and Cognis were initially dispersed in 1.0% v/v acetic acid and the pH adjusted to 4.5 using 0.1 M sodium hydroxide at a concentration of 0.5% w/v. Chitosan dispersions were then transferred to a 250 mL round bottom flask and frozen in liquid nitrogen. The chitosan samples were then lyophilised by freeze drying for 48 h (Edwards, Micro Modulyo). Polymer disks were prepared by accurately weighing out 30 mg of lyophilised chitosan and applying 2 tons of pressure for 10 s using a KBr press. All samples were stored in a desiccator before use.

2.2.2.2b Preparation of porcine oesophageal tissue

Oesophagi excised from freshly slaughtered pigs were collected from the local abattoir (P.C Turner, Farnborough, UK) and stored in saline solution (0.9% w/v sodium chloride) during transportation. Oesophageal epithelial tissue was separated from the surrounding smooth muscle using dissecting equipment within 2 hours of collection and flash frozen in liquid nitrogen to prevent the formation of large ice crystals. Frozen oesophageal tissue was then stored at -40°C until use.

2.2.2.2c Texture probe analysis

Porcine oesophageal tissue was removed from the -40°C freezer and defrosted in saline solution at room temperature. Tissue sections (3 cm by 6 cm) were cut and fixed to a plexiglas support (Stable Micro Systems, Surrey, UK) covered with black electrical tape, using cyanoacrylate glue (Loctite III). Artificial saliva (1 mL), prepared as

described in section 2.2.2.1c, was added to the surface of the tissue prior to the measurement of adhesive strength to hydrate the surface. The polymer disk to be tested was fixed onto a movable probe using a circle of double-sided tape (4 mm diameter).

Maximum detachment force and work of adhesion were determined using a TA.XTplus texture analyser with a 5 kg load cell (Stable Micro systems Ltd, Surrey, UK). The test conditions were as follows: pre-test probe lowering speed, 0.6 mm s^{-1}, test speed, 0.1 mm s^{-1}, applied force, 0.2 N, contact time, 300 s, post-test speed, 0.1 mm s^{-1}, return distance, 5.0 mm, trigger force, 0.05 N. Data was recorded on a force-distance graph using texture exponent software (v.2.0.0.3, Copyright Stable Micro systems Ltd., 1996-2005). Maximum detachment force (mN) and work of adhesion (mN mm^{-1}) were recorded for six samples of each polymer.

2.2.3 Statistical analysis

Values obtained for the average stain intensity of cells treated with aqueous polymer dispersions were standardised by calculating a percentage increase from the negative control for each value of n. Average percentage increases and standard deviations were calculated using Microsoft Excel 2003 (Copyright Microsoft corporation., 1985-2002). The Kolmogorov-Smirnov test was used to test the goodness of fit of the normal distribution to the data. One-way analysis of variance (ANOVA) was used to determine the variation between data collected for the mean pixel intensity of the untreated control on three separate occasions. ANOVA was then used to determine significant differences between the average stain intensity of cells treated with different polymers and those subjected to an artificial saliva challenge using SPSS (v.14.0, Copyright SPSS Inc., 1989-2005). Average work of adhesion and maximum detachment force (± standard deviation) were calculated for each polymer sample. Due to the unequal variance, significant differences between data obtained for each polymer sample was determined using the Kruskal-Wallis ANOVA. Where a significant difference was evident, the Mann-Whitney U test was used to test each pair wise location. For a full justification of the statistics employed within this thesis please refer to Appendix 1.

2.3 Results and discussion

2.3.1 *In vitro* staining technique

The adsorption of polymers from aqueous dispersions onto buccal cells collected from the oral cavity was assessed *in vitro*. Cells treated with poly(acrylic acid) based polymers had clearly visible darker staining regions on the cell surface when compared to the negative control.

The analysis of chitosan polymers with this staining technique proved unsuccessful in both 0.25 M sucrose solution and artificial saliva. There appeared to be no visible difference between untreated and treated cells (Figure 2.6), which was contradictory to previous work (Patel *et al.*, 1999; Kockisch *et al.*, 2001). During the experimental procedure, material deposits on the surface of the test tube, particularly evident following staining with eosin Y, were observed. In addition, the recovery of buccal cells for analysis was greatly reduced when compared to cells treated with poly(acrylic acid) based polymers. Samples of the material adhered to the glass test tube wall were removed by gently scraping with a spatula and examined using light microscopy (Figure 2.6). Based on appearance, samples were identified as a mixture of chitosan and buccal cells, accounting for the reduced amount of cells available for analysis. This may be a consequence of electrostatic interactions between the positive charge carried by the aqueous dispersion of the chitosan and the negative surface charge of the glass.

Adaptations to the technique were employed to improve specimen recovery, these included; silanising the glass and using increased and reduced chitosan concentrations. However, these proved to be unsuccessful. Previous work with this technique had concluded the adsorption and detection of chitosan on the buccal cell surface with CL113 chitosan, although individual cells could not be identified due to cell agglutination as a consequence of bound chitosan (Kockisch *et al.*, 2001). In this procedure, high viscosity and medium viscosity chitosan (Fluka) were initially used. Although actual molecular weight is not defined for these chitosans, there is a substantial difference in the apparent viscosity of CL113 and high viscosity and medium viscosity chitosan; 16 mPa.s, > 400 mPa.s and > 200 mPa.s respectively. It is

likely that the increased viscosity of chitosan causes a reduction of cell separation from the polymer during the washing. This could lead to a reduction in cell numbers during supernatant removal. In addition, CL113 is a chitosan chloride salt (β(1-4) linked *N*-acetyl-D-glucosamine and D-glucosamine chloride) and therefore interactions with the surface of the glass may be decreased as a consequence of a reduced net positive charge.

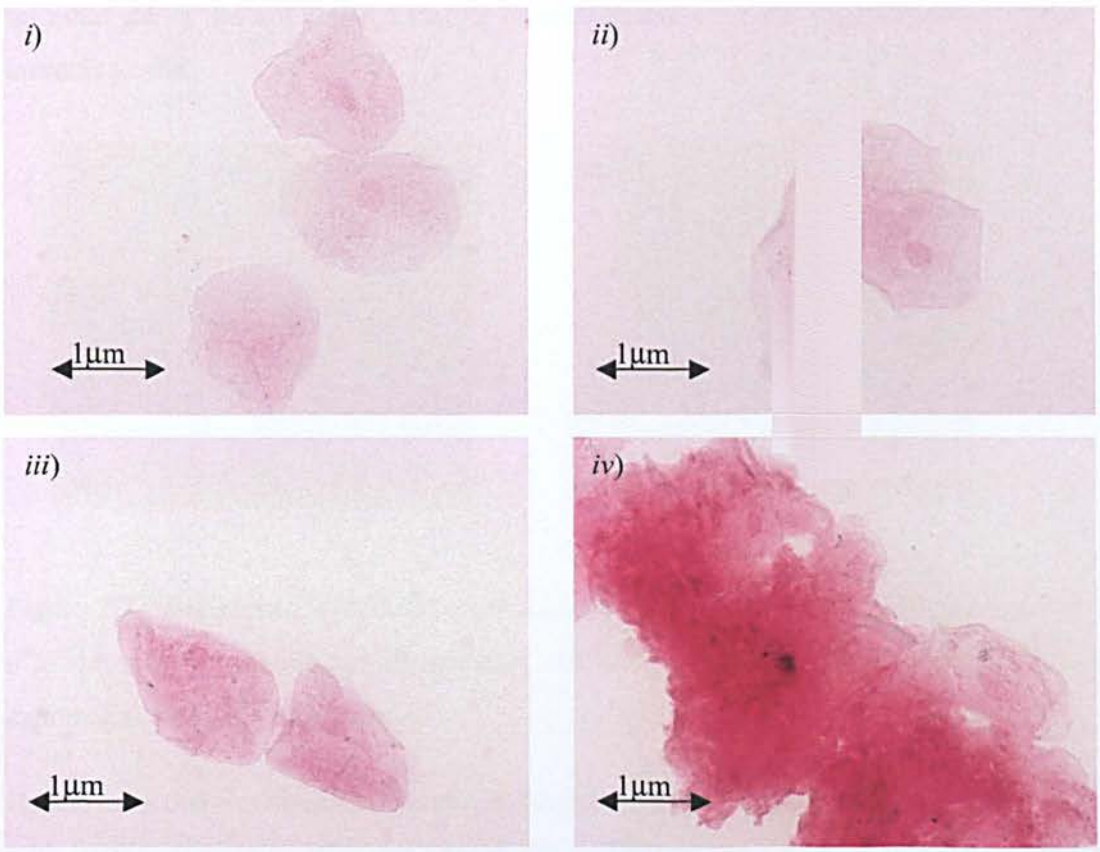

Figure 2.6 Digital images of buccal cells stained with 0.1% w/v eosin Y following incubation with, i) 0.25M sucrose, ii) 0.1% w/v medium viscosity chitosan and, iii) 0.1% w/v high viscosity chitosan (Fluka). A significant reduction in cell numbers may have been due to the adhesion of buccal cells and chitosan to the test tube surface (iv). Images were captured at x200 magnification

As a result of the problems encountered, chitosan samples were not assessed in this way.

2.3.1.1 Microscopy of treated cells

Light microscopy was used to analyse the cell samples collected. Untreated cells (negative control) retained the Alcian blue dye; the cytoplasm stained light blue whilst the nucleus of the cell was clearly discernible, appearing darker in coloration (Figure 2.7). In general, Alcian blue staining following an experimental procedure with artificial saliva did not cause a visible increase/decrease in the blue coloration of the untreated cells.

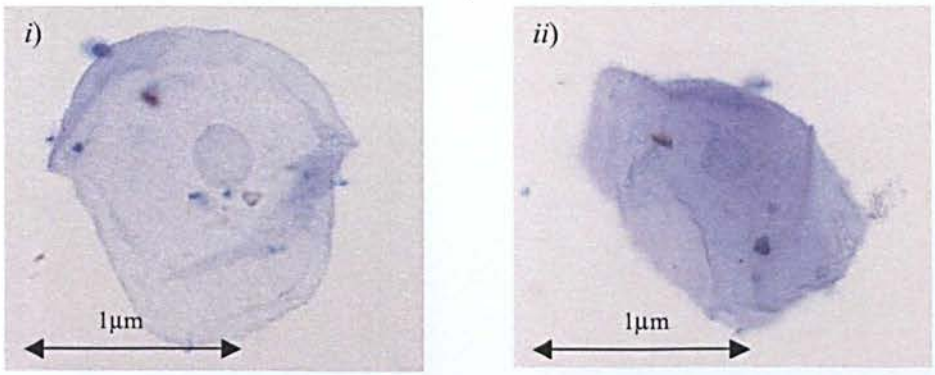

Figure 2.7 Cells stained with 0.05% w/v Alcian blue 8GX following incubation with i) 0.25 M sucrose solution, or ii) artificial saliva for 30 min at 32°C. Images were captured at x200 magnification.

Buccal cells that were incubated with poly(acrylic acid) based polymers prior to staining with 0.05% w/v Alcian blue appeared darker in colour when compared to the negative control (Figure 2.8). In all instances, lightly stained buccal cells were partially or completely obscured by a densely dark blue stained region, identified as bound polymer as per previous studies (Kockisch *et al.*, 2001). Magnification of the optical microscope had to be limited to x200 when examining buccal cells treated with aqueous polymer dispersions as decreased depth of field resulting from an increased magnification had a detrimental effect on the image quality.

Areas of dark staining can be easily identified in treated buccal cells washed with 0.25 M sucrose and artificial saliva suggesting that the polymer can adhere to the cell under both conditions. However, cells washed with a sucrose solution appear to retain higher

amounts of stained polymer when compared to those washed in artificial saliva (Figure 2.8*)*.

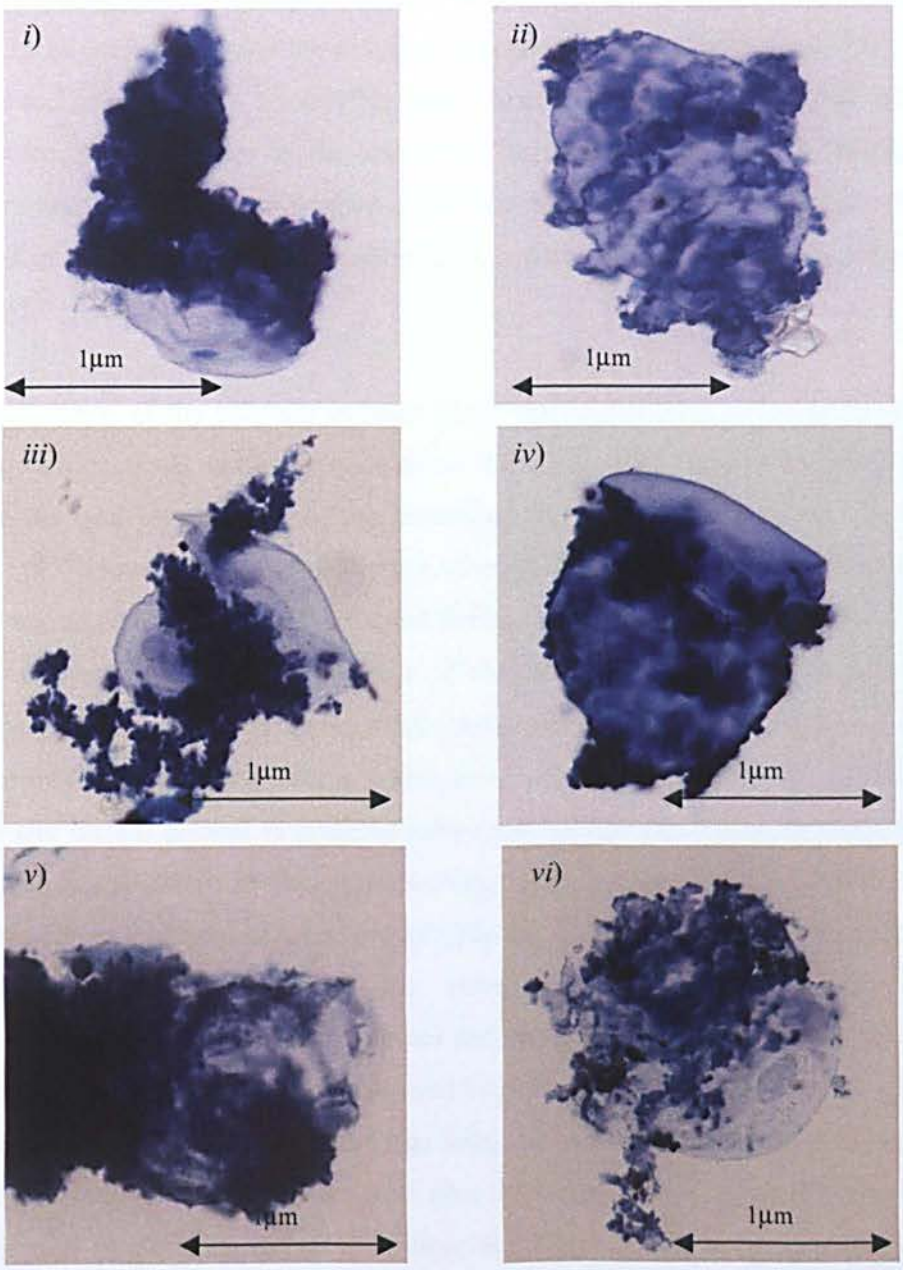

Figure 2.8 Cells stained with 0.05% w/v Alcian blue 8GX following incubation with 0.1% w/v aqueous polymer dispersions (pH 7.0) using 0.25 M sucrose solution (left) or artificial saliva (right) for excess polymer removal. Three PAA based polymers were analysed; i-ii, Carbopol 974P, iii-iv, polycarbophil AA-1, and v-vi, Carbopol 971P. Images were captured at x200 magnification.

However, most of the adsorbed polymer does not appear to be in intimate contact with the cell surface. In addition to the amount of material adhered to the cell, there is also a noticeable difference in the appearance of the polymer on the surface. In cells washed with 0.25 M sucrose solution the polymer structure appears to extend out from the cell surface and has an almost "cloudy" texture. In cells washed with artificial saliva, the appearance of the polymer on the buccal cell surface does not seem to resemble the structure detected on sucrose washed cells. The polymer is easily identified, however its extension from the surface is minimal and areas of less intense staining can be observed.

The appearance of the polymer is most likely due to the ions in the artificial saliva binding to the ionised carboxylate groups of the acrylic acid backbone, either resulting in a decrease in bioadhesion, or the precipitation of some of the polymer. Tur and Ch'ng (1998) found that the bioadhesion of cross-linked poly(acrylic acid) was linked to the degree of ionisation that occurred during the interaction of the polymer with a mucin/epithelial surface. The addition of electrolytes to aqueous polycarbophil has previously been shown to reduce particle size; particularly in the presence of calcium (Kriwet and Kissel. 1996). Ionic interactions between negatively charged carboxyl groups and cations present in artificial saliva may reduce the degree of ionisation and, consequently the extent of polymer swelling. This is caused by a reduction in the repulsive forces that exist between poly(acrylic acid) chains at high pH. Further to this, divalent ions such as calcium can serve as polymer cross-linkers, reacting simultaneously with the same or different poly(acrylic acid) chains. Since polymer is still detectable on the surface of the buccal cells, it is unlikely that adhesion to the cell surface is disrupted. It is more likely that artificial saliva caused a reduction in polymer swelling during the washing procedure after adhesion had occurred. Dehydration or precipitation of polymer chains extending from the surface may have occurred in artificial saliva, contributing to the different appearance of the polymer on the buccal cell surface.

Based on the visual inspection of the treated cells, there does not appear to be any difference between the adhesion of the various grades of Carbopol and polycarbophil to the buccal cell surface.

2.3.1.2 Stain intensity

Semi-quantitative data was collected by analysing the digital images (x200 magnification) of treated and untreated buccal cells for pixel intensity. A rectangular area containing 10,000 pixels was positioned on each image to determine mean pixel intensity. Collection of the digital images was subject to user bias. During microscopy, collection bias was reduced by selecting cells at random; this was achieved by moving the objective vertically down the coverslip and capturing an image of the first cell to pass directly underneath the centre cross-hair. It should be noted however that this precaution does not totally eliminate bias from this technique.

The variation between data collected for the mean pixel intensity of the untreated control on three separate occasions was investigated. Untreated cells that had been washed only in 0.25 M sucrose resulted in no significant difference in mean pixel intensity ($P > 0.05$). Conversely, untreated cells that were washed in artificial saliva resulted in significantly different mean pixel intensities ($P < 0.05$). This may be due to variation in Alcian blue retention due to the presence of electrolytes following a washing procedure with artificial saliva, as electrolytes can disrupt the bond between Alcian blue and the negatively charged retention sites. In order to minimise this effect, mean pixel intensities obtained for the treated buccal cells were standardised relative to the mean pixel intensity of the untreated control.

Values for mean pixel intensity of treated cells were expressed as percentage increase relative to the untreated control prepared during the same experiment (Figure 2.9). In all instances, there was at least a 50% increase in the mean pixel intensity of the treated buccal cells, with the highest percentage increase caused by Carbopol 974P in sucrose. Data obtained from treated cells using an experimental procedure incorporating a sucrose washing solution produce higher variation than those obtained using an artificial saliva wash. This increase in variation is most likely due to the structure of the polymer deposit on the buccal cell surface, as it tends to be less uniform and extends out from the surface. There was no statistically significant difference between treated cells prepared using an experimental procedure involving sucrose solution or artificial saliva, or cells treated with different polymers ($P > 0.05$). Therefore, using this technique there is no difference in the adsorption of Carbopol 974P, 971P and polycarbophil AA-1 onto

the surface of the buccal cells. This is most likely due to the physicochemical properties that are common to each of these polymers. Each was designed specifically for oral and mucosal contact applications and are proven bioadhesives (Noveon Inc. 2002a).

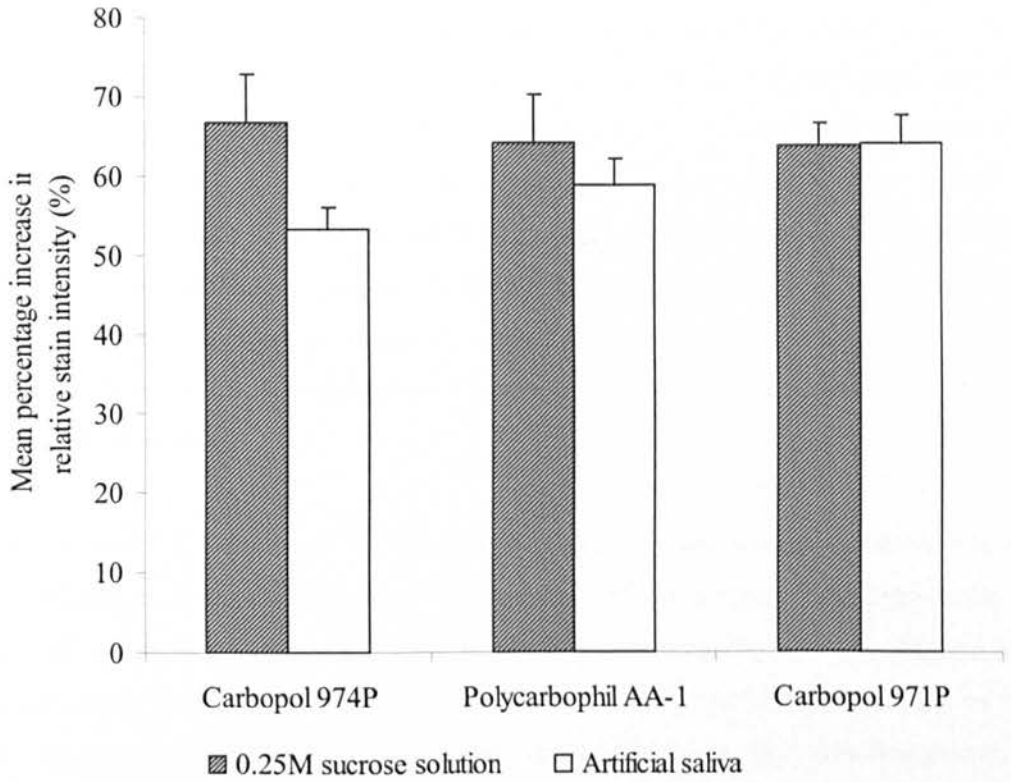

Figure 2.9 Percentage increase in mean pixel intensity of cells treated with aqueous poly(acrylic acid) based polymer dispersions in i) 0.25M sucrose solution, or ii) artificial saliva, relative to an untreated negative control. (n=60, ± SE).

2.3.2 Texture probe analysis

Texture probe analysis was used to determine the adhesion of poly(acrylic acid) and chitosan polymers to porcine oesophageal tissue in artificial saliva. Assessment was based on the determination of the maximum detachment force and the work of adhesion of the adhesive bond. These parameters have been used extensively as an *in vitro* tool for the prediction of bioadhesive formulations *in vivo*.

Porcine oesophageal tissue has been previously used as a model for the buccal mucosa in drug permeation studies as they share structural properties (Diaz del Consuelo *et al.*, 2003). Both are composed of stratified squamous epithelium with membrane coating granules within the superficial layers. Due to swallowing, mucus that coats the oesophagus has a similar composition to the mucus coat found within the oral cavity. With regards to mucoadhesion, both oesophageal and sublingual mucosa show similar surface characteristics. The degree of keratinisation and the carbohydrate residues expressed on the mucosal surface are important parameters in bioadhesion as these can influence the hydration state and surface roughness (Accili *et al.*, 2004). Areas of keratinisation and the presence of terminal sialic acid residues were evident in both oesophageal and sublingual mucosa. In this study, it was concluded that Carbopol 974P adhered more strongly to sublingual mucosa than oesophageal mucosa. However oesophageal mucosa is easily prepared and provides a large, mostly undamaged surface area for bioadhesion.

Previous work has considered the instrument parameters appropriate for texture probe analysis studies of mucoadhesion. Wong *et al.* (1999) investigated the importance of instrument variables when using texture analysis to determine the work of adhesion and the maximum detachment force. Contact force was found to have little effect on the work of adhesion and maximum detachment force, however contact time was proven to be an important parameter as increasing the contact time resulted in significantly larger adhesion forces. Probe withdrawal speed was also found to be a critical factor with reportedly higher variations occurring at lower withdrawal speeds. Significant increases in adhesion forces were seen when probe speed was increased from 0.1 mm s^{-1} to 1.0 mm s^{-1}, however there was no significant increase in adhesion force when the probe speed was increased from 0.1 mm s^{-1} to 0.3 mm s^{-1}. The quantification of mucoadhesion in recent studies has used a probe withdrawal speed of 0.1 mm s^{-1} (Tobyn *et al.*, 1995, 1996, 1997; Tur and Ch'ng., 1998; Cilurzo *et al.*, 2003; Bromberg *et al.*, 2004; Grabovac *et al.*, 2005). Based on these works, a probe speed of 0.1 mm s^{-1} was selected for this study. Contact time (300 s) and force (0.2 N) were selected to ensure intimate contact with the mucosa whilst allowing adequate time for the polymer disks to hydrate. It is clear from the literature that numerous instrument parameters have been used to assess mucoadhesion using texture analysis; this has an obvious disadvantage when comparing results from other works. Experimental conditions and

instrument parameters used to analyse bioadhesion of the polymers to porcine oesophageal tissue were employed throughout the project to allow direct comparison of data.

2.3.2.1 Poly(acrylic acid) based polymers

Polycarbophil AA-1 and Carbopol 974P and 971P all produced measurable adhesion to porcine oesophageal mucosa under the experimental conditions (Figures 2.10 and 2.11). Carbopol 971P exhibited the highest mean work of adhesion (165 mN mm^{-1}) with the least variation between results. Polycarbophil AA-1 produced the highest amount of variation between results while Carbopol 974P produced the lowest mean work of adhesion. A significant difference was detected between the work of adhesion for each polymer tested ($P < 0.01$). In particular, all polymers exhibited a work of adhesion that was significantly different to the negative control, ethylcellulose, a material known to have no bioadhesive properties ($P < 0.01$). However, the work of adhesion measured during detachment of Carbopol 971P, polycarbophil AA-1, and Carbopol 974P were not significantly different to each other ($P > 0.05$).

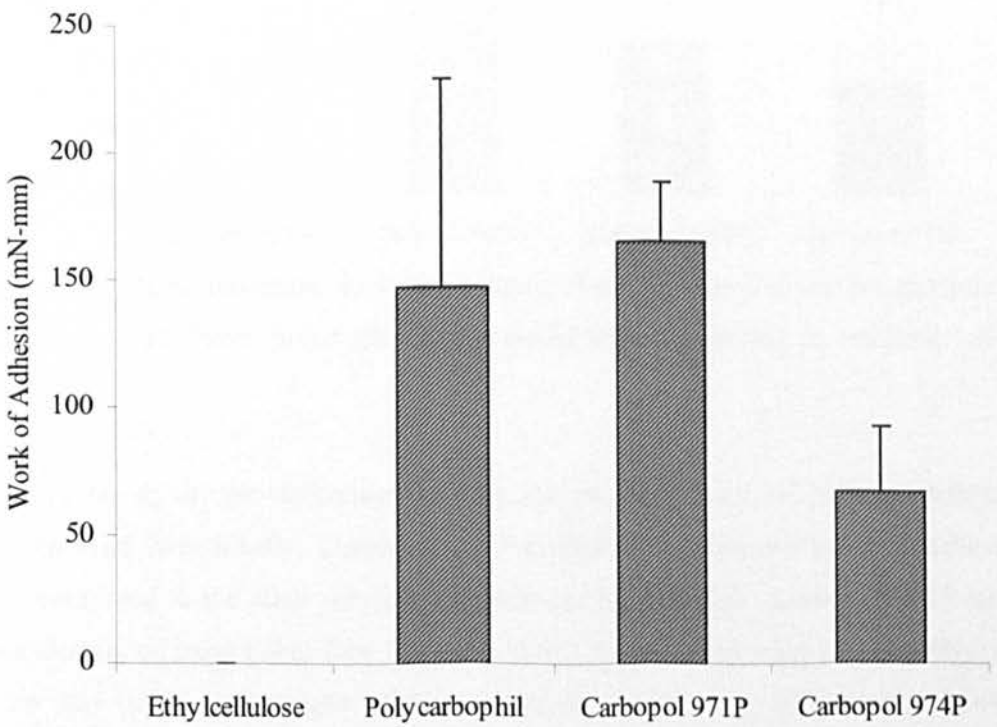

Figure 2.10 Mean work of adhesion obtained from texture probe analysis of poly(acrylic acid) based polymers using a model mucosal surface in artificial saliva. (n=6, ± SD).

The measurement of the maximum detachment force produced higher variation in the data than the work of adhesion. Polycarbophil AA-1 produced the highest mean maximum detachment force (524 mN) however; variation was also the highest. All poly(acrylic acid) polymers exhibited a significantly higher mean maximum detachment force than the negative control ($P < 0.01$). However, as with the work of adhesion, the polymer samples were not significantly different to each other in terms of the maximum detachment force ($P > 0.05$).

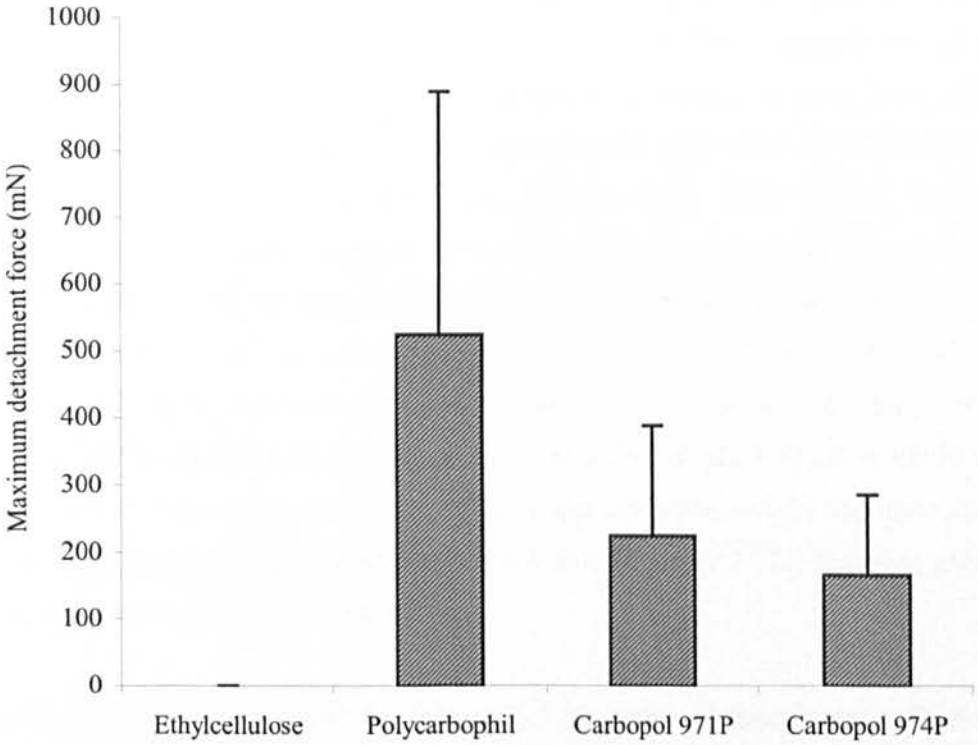

Figure 2.11 Mean maximum detachment force obtained from the texture analysis of poly(acrylic acid) based polymers using a model mucosal surface in artificial saliva. (n=6, ± SD).

Although no significant difference between the tensile strength of polymer adhesion was observed directionally, Carbopol 971P exhibited the greatest work of adhesion when compared to the other poly(acrylic acid) polymers tested. Carbopol 971P has a lower density of cross linker than Carbopol 974P, indicated by a significant difference in the M_C (molecular weight between adjacent cross-links), 237600 and 104400 respectively (Noveon Inc., 2002a; Gomez-Carracedo *et al.*, 2004). Carbopol 971P also has a lower density of cross linker than polycarbophil AA-1. A reduction in the cross

linker density allows for greater flexibility of the polymer chains, which enables a more rapid rate of hydration and a high level of interaction between polymer and the adhesive substrate, allowing intimate contact and possibly chain interpenetration/secondary bond formation. Tamburic and Craig (1997) concluded that Carbopol 971P showed the greatest evidence, determined by dynamic oscillatory rheology and texture analysis, for positive synergy with type III mucin, despite its low adhesiveness in their investigation. Wong *et al.* (1999) utilised an optimum contact time, force and probe withdrawal speed, to measure the adhesion of poly(acrylic acid) polymers to chicken pouch mucosa in simulated saliva. A rank order of Carbopol 971P > Carbopol 974P > polycarbophil AA-1 was given for work of adhesion, which is similar to this study. Eouani *et al.* (2001) investigated the swelling properties and mucoadhesive properties of a selection of polymers including polycarbophil AA-1 and Carbopol 971P. After 15 min, Carbopol 971P displayed higher values for both the work of adhesion and maximum detachment force. Poly(acrylic acid) polymers swell rapidly in water, particularly at high pH as this causes the ionisation of the carboxylic groups and hence uncoiling of the polymer chains due to charge repulsion (Tur and Ch'ng. 1998; Tamburic and Craig. 1997). Following a five-minute contact time in artificial saliva at pH 6.87, it is likely that Carbopol 971P uncoils more rapidly due to its lower molecular weight and cross linker density when compared to polycarbophil AA-1 and Carbopol 974P, allowing greater interactions with the mucosal surface.

Previous studies have indicated the following rank order of adhesiveness; Carbopol 974P > polycarbophil AA-1 > Carbopol 971P (Grabovac *et al.*, 2005; Tamburic and Craig. 1997). Differences in experimental conditions are the likely source of contradiction between these findings and those of other studies, in particular the composition and pH of the hydrating fluid. The presence of multiple electrolytes at high pH can exert an influence on the mucoadhesive properties of the polymers. Cations such as sodium and potassium cause a detrimental affect on the mucoadhesive interaction by reducing the hydration state of the polymer through compensation of the electronegative charge, potentially disrupting the formation of hydrogen bonds (Tur and Ch'ng. 1998; Kriwet and Kissel. 1996; Tobyn *et al.*, 1997). The presence of calcium has previously been shown to reduce the mucoadhesion of polycarbophil AA-1 due to the chelation of the ions by carboxylic acid groups (Kerec *et al.*, 2002). This can cause cross-linking of the polymer, reducing chain flexibility and chain interpenetration with

mucus glycoproteins. Consequently, interactions between the functional groups of polycarbophil and mucus are lowered due to the interactions of calcium with carboxylic groups. The presence of multiple cations may have caused the high variation associated with this technique due to the range of interactions with the polymer compact. Interestingly however, the presence of multiple cations within the artificial saliva may also be the reason why bioadhesion did not deteriorate due to the formation of slippery mucilage, as can occur when anionic polymers become over-hydrated (Smart. 2005a). This has been observed by Cilurzo *et al.* (2005) when the addition of magnesium and calcium salts reduced the dissolution of mucoadhesive polymethylmethacrylate sodium salt formulation.

2.3.2.2 Chitosan polymers

Chitosan polymers selected for this investigation all produced measurable adhesion forces when removed from the surface of porcine oesophageal mucosa bathed in artificial saliva (Figure 2.12 and 2.13). The values obtained for the work of adhesion and maximum detachment force were compared to polycarbophil AA-1, a well known mucoadhesive material.

Medium viscosity chitosan exhibited the greatest mean work of adhesion (224 mN mm^{-1}), while HCMF, DCMF and CL113 all yielded values higher than the reference polymer, polycarbophil AA-1 (Figure 2.12). A highly significant difference was detected between the polymer samples ($P < 0.001$). Post-hoc analysis found that all chitosan polymers exhibited a highly significant difference when compared to the negative control ($P < 0.01$). Both HCMF and medium viscosity chitosan produced a work of adhesion that was significantly greater than the positive control, polycarbophil AA-1 ($P < 0.01$) (Figure 2.12). CL113, CL213 and high viscosity chitosan produced mean values that were comparable to the reference polymer (147 mN mm^{-1}) and were not significantly different ($P > 0.05$). Although G213, G113, DCMF, and CMFP produced values that were lower than the positive control, these were also not significantly different ($P > 0.05$). Results obtained by medium and high viscosity chitosan produced the greatest amount of variation, suggested by the SD bars in Figure 2.12. Rank order according to the results obtained for the work of adhesion is as

follows: medium viscosity chitosan > HCMF > DCMF > CL113 > high viscosity chitosan > CL213 > G113 > G213 > CMFP.

Medium viscosity chitosan exhibited the greatest mean maximum detachment force (776 mN), while CL213 and high viscosity chitosan both obtained mean values higher than the reference polymer (Figure 2.13). Results produced from the measurement of the maximum detachment force were more variable, as seen previously with the assessment of poly(acrylic acid) based polymers. All chitosan samples were highly significantly different to the negative control, ethylcellulose ($P < 0.01$). Only medium and high viscosity chitosan elicited a maximum detachment force that was significantly different to the positive control, polycarbophil AA-1 ($P < 0.05$). Compared to this control (524 mN), G213, G113 and CMFP displayed low maximum detachment forces when compared to the reference polymer, which is consistent with the results obtained for the work of adhesion. Rank order according to the results obtained for the maximum detachment force is as follows: medium viscosity chitosan > CL213 > high viscosity chitosan > DCMF > CL113 > HCMF > G213 > G113 > CMFP.

Chitosan, in its commercial flake form, has poor wetting properties and requires an acidic medium to ionise the amine groups and allow the polymer to disperse in water. The preparation of an aqueous dispersion therefore requires the addition of an acid such as glycolic acid, benzoic acid, acetic acid or lactic acid to solubilise the chitosan. The analysis of chitosan in its commercial form yields no measurable adhesive forces due to a lack of hydration (Wong *et al.*, 1999), therefore DCMF, HCMF, CMFP (Cognis) and medium and high viscosity chitosan (Fluka) were prepared in 1% acetic acid and lyophilised to produce a highly porous acidified chitosan matrix, which would improve the matrix-solvent interaction (Risbud *et al.*, 2000). The solubilisation of chitosan in acetic acid would produce a lyophilised chitosan acetate salt, which would considerably improve the wetting properties of the chitosan when compared to the free base. Previous studies have identified chitosan as having weak and short-lasting mucoadhesive properties (Grabovac *et al.*, 2005), however a contact time of 30 min was used in this study, which is significantly longer when compared to this work. This might cause over-hydration of the lyophilised polymer which is detrimental to the adhesive bond formed (Smart. 2005a). Adhesion forces measured were comparable to that of polycarbophil AA-1, with the noticeable exception of CMFP.

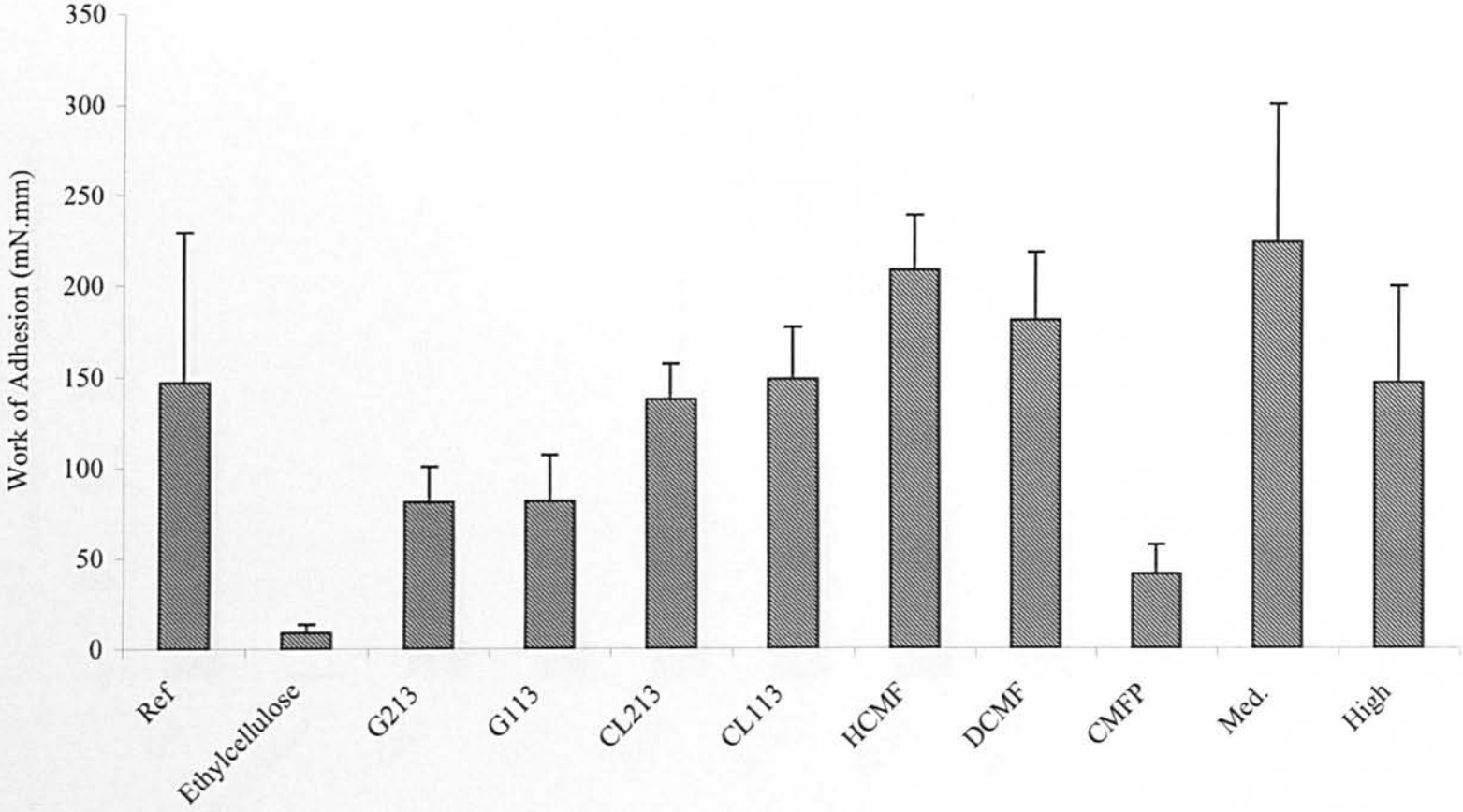

Figure 2.12 Mean work of adhesion from the texture probe analysis of 30mg compacts made from different grades of chitosan using a model mucosal surface in artificial saliva. Polycarbophil AA-1 (Ref.) was used as a positive control (n=6, ± SD).

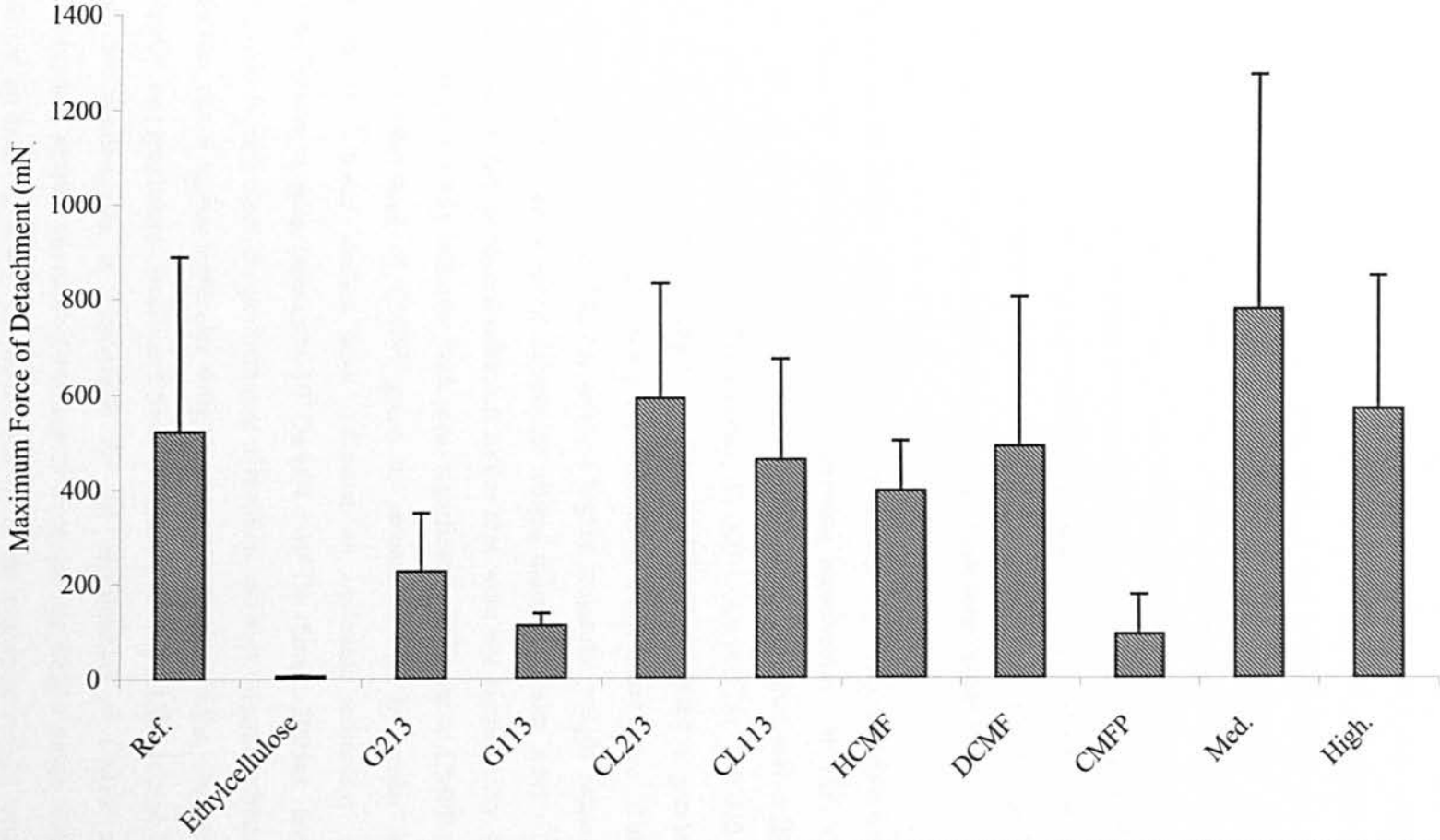

Figure 2.13 Mean maximum detachment force from the texture probe analysis of several grades of chitosan using a model mucosal surface in artificial saliva. Polycarbophil AA-1 (Ref.) was used as a positive control. (n=6, ± SD)

The mucoadhesive properties of chitosan are predominantly the result of ionic interactions between the positively charged amino groups of chitosan and the negatively charged sialic acid residues of mucins (Qaqish and Amiji. 1999; Grabovac *et al.*, 2005), and are therefore dependent on environmental pH (Singla and Chawla. 2001). Both G213 and G113 displayed poor mucoadhesion, both in terms of maximum detachment force and work of adhesion, when compared to the positive control. Chitosan glutamate salt is prepared by reacting chitosan with the amino acid, glutamic acid. During contact with the mucosa, the pH of the artificial saliva would result in the ionisation of the carboxylic groups of glutamic acid (pI = 3.1) resulting in a negative charge. The presence of positive and negatively charged groups within the hydrated polymer compact makes the interaction with the mucosal surface potentially very complex, and the potential for intramolecular interactions may explain the low values obtained for both the work of adhesion and maximum detachment force.

High molecular weight chitosans would be expected to provide multiple binding sites for interactions with mucin, therefore improving bioadhesion. HCMF, DCMF and CMFP grades of chitosan have identical molecular structures and differ only in molecular weight according to the supplier; 50 000-1 000 000 Da, 300 000-2 000 000 Da and 500 000-5 000 000 Da respectively. HCMF exhibited a greater work of adhesion while DCMF exhibited a greater maximum detachment force. This was also observed with CL113 and CL213, where a higher molecular weight caused a greater detachment force and a lower molecular weight induced greater work of adhesion. HCMF and DCMF produced adhesion forces that were not significantly different to each other ($P > 0.05$); however both were significantly different to CMFP ($P < 0.05$). The low performance of CMFP, given its preparation and molecular weight was unexpected. Some studies have indicated an optimum molecular weight for mucoadhesion, ranging from circa 10^4 Da to 4×10^6 Da (Smart. 2005a). Indeed, when compared to each other, the performance of medium and high viscosity chitosan (Fluka) indicates that a higher molecular weight causes a reduction in the observed work of adhesion and maximum detachment force (Figures 2.12 and 2.13). It may be possible that this phenomenon is responsible for the performance of CMFP within this investigation, despite the distinct overlap of its molecular weight range with the range reported by Smart (2005a). The determination of the molecular weight (and viscosity) of each of these grades of chitosan would enable a better understanding of observed

differences in adhesive strength performance. Accurate characterisation is difficult in high molecular weight polymers and manufacturer's guidelines mainly provide a description of a range rather than specific values. In some cases, this information is substituted with viscosity, as this characteristic is often directly related to the molecular weight of the polymer. It is worth noting that the degree of deacetylation is at least 80% for each chitosan investigated here, making this an unlikely source of observed differences in tensile strength.

It is interesting to note that materials that were retained on buccal cells in the *in vitro* study were also adhesive in the texture probe analysis study. The first study evaluates a polymer adsorption phenomenon at an interface, the second is a classic adhesive force measurement study, yet the same class of materials show an affinity in both cases. This confirms previous studies (Patel *et al.*, 1999; Kockisch *et al.*, 2001), although, in the cell adsorption study, the grades of chitosan used appeared to bind effectively to every surface that they come into contact with. The lack of information regarding the adsorption of chitosan from an aqueous dispersion due to the failure of the *in vitro* staining technique mean results obtained from the tensiometers study are unsupported. It must be noted that rank orders obtained from a tensiometer study are highly dependent on contact time and water availability in the test system, as the materials used need to swell to become adhesive but can over-hydrate to form slippery mucilage if left in contact with sufficient water for extended periods.

2.4 Conclusions

- Each grade of poly(acrylic acid) based polymer demonstrated adsorption from aqueous dispersion to a buccal cell surface, which could be detected using Alcian blue.
- The adsorption of poly(acrylic acid) based polymer was unaffected by the presence of artificial saliva determined by image analysis, although there was a change in the appearance of the polymer on the buccal cell surface which suggested a reduction in the amount present.
- No significant difference was found between the adsorption of each poly(acrylic acid) based polymer to the cell surface.
- Carbopol 971P exhibited the greatest work of adhesion and polycarbophil AA-1 exhibited the greatest maximum detachment when determined by texture probe analysis.
- The adsorption of chitosan from aqueous dispersion could not be evaluated using the direct staining technique due to the ability of this polymer to bind to the test tube surface.
- Medium viscosity chitosan exhibited the greatest work of adhesion and the greatest maximum detachment force when determined by texture probe analysis.
- Chitosan glutamate and CMFP exhibited the lowest adhesion to porcine oesophageal tissue.
- Values obtained for the maximum detachment force had high standard deviations, possibly caused by the presence of artificial saliva.
- Polymers of lower molecular weight and/or lower cross-linker density produced higher values of adhesion. Results for chitosan suggest an optimum molecular weight for mucoadhesion.
- Tensiometer studies could be used as an indicator of the ability of polymers to adsorb from solutions onto a mucosal surface.

Chapter 3

Development of a poly(acrylic acid)-metal ion oral delivery system

3.1 Introduction

3.1.1 Background

In Chapter 2 the bioadhesive properties of Carbopol 971P and other polymers was demonstrated *in vitro* using a variety of test systems. In this section the use of these materials as carriers of antimicrobial agents will be investigated in terms of their potential to allow enhanced *in vivo* activity. The ability to form complexes that permit sustained release of the antimicrobial agent while retaining their bioadhesive nature are key factors to be investigated.

A range of antimicrobial agents have been used within the oral cavity. Triclosan is commonly found in oral healthcare products as well as many other personal hygiene products and household cleaners. It has a broad spectrum of antimicrobial activity and is effective at low concentrations. However, more recently its use within such a large array of domestic products has become controversial due to reports of the development of bacteria which are cross-resistant to clinically relevant antibiotics (Aiello and Larson, 2003). Metal ions such as zinc and copper are toxic to microorganisms above certain concentrations and are less likely to cause cross-resistance to antibiotics because of their mechanism of action. In particular the use of zinc has been extensively reviewed in the literature due its well-established synergistic effects with triclosan (Bradshaw *et al.*, 1993) and its ability to inhibit acid production in oral bacteria (Phan *et al.*, 2004). The human diet typically includes a variety of metal ions and as such *in vivo* toxicity is unlikely.

Positively charged metal ions should bind to negatively charged poly(acrylic acid)s such as Carbopol. Kriwet and Kissel (1996) have previously demonstrated that sodium and calcium ions compete for negatively charged sites on the cross-linked poly(acrylic acid), polycarbophil. It is proposed that metal ion-polymer complexes could be substantive and exhibit controlled release through metal ion displacement from the polymer as a result of direct competition for binding sites by other cations present within saliva.

3.1.2 Dialysis: A method of evaluating the rate of active agent release.

Dialysis is a separation process for substances in solution driven by a concentration gradient and their varying diffusion rates through a semi-permeable membrane. Dialysis is employed to retain large molecules while exchanging small ones and has been used for the following applications:

- Concentration: removal of solvent.
- Desalting: removal of high or low molecular weight solutes.
- Fractionation: separation of macromolecular mixtures.

Dialysis membranes are typically made from cellulose however more recently specialist membranes have been developed that are resistant to high temperatures and organic solvents, such as polyvinylidene difluoride. Dialysis membranes are characterised by their molecular weight cut-off; the molecular weight at which 90% of the solute will be retained by the membrane.

Equilibrium dialysis is a specific application of dialysis, which is important in the study of the binding of small molecules and ions by proteins. The binding characteristics of a macromolecule are determined by selecting a dialysis membrane that is permeable to the small molecules. Typically, the macromolecule is placed on one side of the dialysis membrane and the small molecule on the other. Equilibrium is reached when the concentration of small molecule is equal on both sides of the dialysis membrane. Debon and Tester (2001) examined the binding of zinc and calcium to a variety of non-starch polysaccharides using an equilibrium dialysis technique. Polysaccharide solutions were immobilised within a standard length of dialysis tubing and immersed in a solution containing a known concentration of zinc or calcium. After 60 min, the concentration of ion remaining in the outer solution was analysed and from this the extent of binding to the polysaccharide was normalised with a reference where the polysaccharide solution was replaced with water.

Dialysis techniques have also been used to evaluate *in vitro* drug release from semi-solid and liquid formulations (Senel *et al.*, 2000; Martin *et al.*, 2003; Aksungur *et al.*, 2004). Typically, the formulation is placed within dialysis tubing, which is subsequently immersed in a suitable release medium (Figure 3.1). The dialysis tubing must have a sufficiently large molecular weight cut-off to allow diffusion of the small molecule/ion of interest. The receiver phase is continuously stirred to prevent the formation of an unstirred water layer at the membrane/outer solution interface, which can affect the concentration gradient across the membrane. At regular intervals samples are removed from the receiver phase and replaced with drug-free release medium to maintain sink conditions, which ensures a concentration gradient remains across the dialysis membrane. This enables calculation of drug/ion released from the formulation as a function of time.

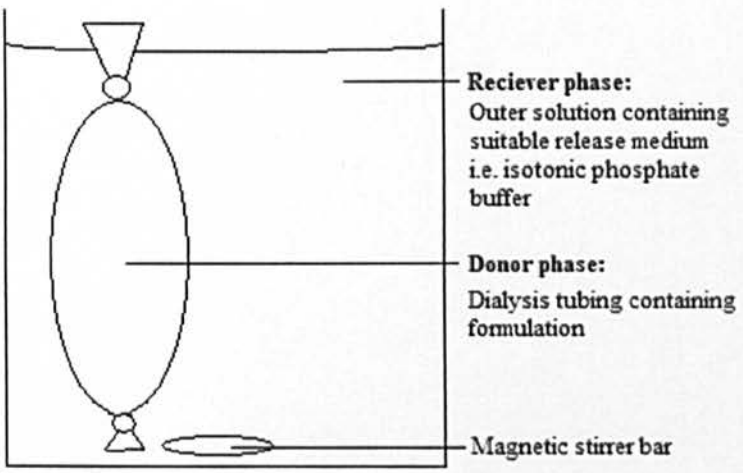

Figure 3.1 A dialysis method to assess the in vitro release of small molecules and ions from a macromolecular carrier.

Several factors can influence the rate of diffusion across a dialysis membrane; these include: dialysis buffer volume, buffer composition, temperature and the molecular size relative to the pore size. The rate of diffusion will be faster at higher temperatures and at larger buffer to sample volume ratios. Substances that are much smaller than the molecular weight cut-off will pass through the dialysis membrane at a faster rate than substances that are only slightly smaller. Osmosis is the passage of water between two solutions separated by a semi-permeable membrane, flowing from the lower to the

higher concentration solution. In some instances a net movement of water into the sample will occur when dialysing high solute concentrations, which will affect the rate of diffusion out of the membrane and increase the volume of the sample. This may result in the membrane bursting during dialysis and therefore precautions should be taken to minimise the difference in concentration. Some substances may interact with the dialysis membrane, which will affect the concentration of the substance in solution. Initial investigations to establish non-specific binding to the dialysis membrane are recommended when designing a dialysis protocol.

3.1.3 Metal ion detection in solution - Atomic absorption spectroscopy

Atomic absorption spectroscopy is a technique used for the qualitative and quantitative determination of single elements in analytical samples. Atoms are volatised in a flame and radiation is passed through this. Volatised atoms, which are mainly in their ground state and thus not emitting energy, will absorb radiation with an energy corresponding to the difference between their ground state and the excited state (Watson, 1999). For example, volatised atoms of zinc will absorb radiation at 214 nm (Figure 3.2).

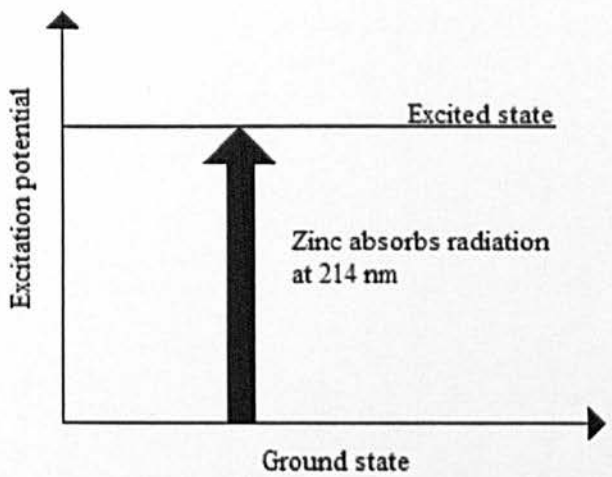

Figure 3.2 The excitation of zinc by absorption of radiation at the first resonance line.

Usually the transition between the ground state and the first excited state, known as the first resonance line, has the line with the strongest absorptivity (Willard *et al.*, 1988). The wavelength of the first resonance line for metals and many metalloids is longer than

200 nm, for non-metals the wavelength falls under 200 nm in the vacuum ultraviolet region. Therefore, atomic absorption spectroscopy is typically applicable to metals and metalloids only. Further consideration of the theory and practice of atomic absorption spectroscopy is given in Appendix 2.

In this chapter, zinc, silver and copper were investigated for both their interaction with, and displacement from Carbopol 971P (Noveon Inc, USA) using a modified dialysis technique. Samples were analysed using atomic absorption spectroscopy. The bioadhesion of the metal ion-polymer complexes were compared to the polymer alone using both the direct staining technique and texture probe analysis described in the previous chapter.

3.2 Materials and Methods

3.2.1 Materials

Carbopol® 971P NF (Lot Nº CC29MAJ126) was kindly donated by Noveon Inc (Cleveland, USA). Polyvinylidene fluoride (PVDF) dialysis membrane, molecular weight cut-off 250,000 Da 1.8 $mLcm^{-1}$, was purchased from Spectrum laboratories (Rancho Dominguez, USA). Zinc sulphate heptahydrate, copper sulphate and sodium dihydrogen phosphate monohydrate were all of ACS standard and purchased from Sigma-Aldrich Company Ltd (Gillingham, UK). All other chemicals used in this investigation were purchased from Fisher Scientific UK Ltd (Loughborough, UK). All chemicals were used as received without further treatment unless otherwise stated.

3.2.2 Methods

3.2.2.1 Preparation and characterisation of metal ion-polymer complexes

3.2.2.1a Preparation of aqueous polymer dispersions and metal ion solutions

Carbopol 971P (0.10 g) was dispersed in 40 mL deionised water under magnetic stirring at 300 rpm (Stuart, Heat-Stir CB192) for 4 h. The pH of the resultant dispersion was adjusted to 7.0 using 0.1 M sodium hydroxide and the volume made up to 100 mL with deionised water to give a final concentration of 0.10% w/v. Aqueous polymer dispersions were sealed and stored overnight at 4°C until use with an expiry date set at 1 week from preparation.

Based on the formula weight of acrylic acid (FW, 72.06), the estimated molar concentration of 0.10% w/v Carbopol 971P was determined as 13.9 mM. Although this value is inaccurate due to the presence of allyl sucrose cross-links and the length of Carbopol chains, it provides a useful estimation of carboxyl group concentration. The

initial concentration of the metal salt solutions was twice that of the polymer solution. Hence, zinc sulphate, copper sulphate and silver nitrate were prepared at a concentration of 27.8 mM in deionised water. Dilutions were prepared in deionised water to obtain the following concentrations of each metal salt; 27.8 mM, 13.9 mM, 6.95 mM, 2.78 mM, 1.39 mM, 0.28 mM and 0.14 mM.

3.2.2.1b Development of Carbopol 971P-metal salt solution

Aqueous Carbopol 971P (10 mL of 0.10% w/v) was transferred to a 100 mL glass beaker and stirred at approximately 300 rpm with a magnetic stirrer. Metal salt solution (10 mL) was added slowly to the aqueous polymer dispersion while stirring and the resultant solution observed for changes in turbidity over 30 min. All concentrations of each metal salt were used with Carbopol 971P and repeated at least three times.

3.2.2.1c Stability of metal-polymer complex

PVDF dialysis membrane (approx. 25 cm) was prepared as per manufacturer's instructions; the dialysis tubing was soaked for 30 min in deionised water and 30 min in 100% ethanol. The dialysis tubing was then washed repeatedly in deionised water and pre-equilibrated overnight in either 1.39 mM zinc sulphate/copper sulphate or 2.78 mM silver nitrate depending on the metal ion-polymer complex to be investigated. Gloves were worn during the handling of the dialysis membrane to prevent possible contamination.

Prior to the experiment, dialysis tubing was washed in deionised water. Control experiments determined that any metal ions bound to the dialysis tubing were not released into deionised water during exhaustive dialysis over a period of 24 h using the experimental volumes. Carbopol 971P-metal salt solution (20 mL) prepared 30 min prior to dialysis was transferred into the dialysis tubing using a bulb pipette (20 mL, Fisherbrand) and secured with dialysis clips. The dialysis tubing was subsequently immersed in 480 mL release medium (deionised water) under constant stirring at 400 rpm using a multi-position magnetic stirrer (Fisherbrand) at room temperature. The

beakers were covered with Parafilm® to minimise evaporation from the surface. Aliquots of 20 mL were removed at hourly intervals for 6 h to determine the concentration of metal within the release medium, and replaced with fresh deionised water. After 6 h, the dialysis tubing was transferred to fresh deionised water (480 mL) under stirring and a final sample was removed after 24 h. Samples were stored for a maximum of 48 h at 4°C in acid-treated glass bottles (35 mL capacity, Fisherbrand). The detection of metal ions within the release medium was compared to a control composed of 10 mL deionised water and 10 mL metal salt solution. This procedure was repeated six times for each metal ion-polymer complex and corresponding experimental controls.

3.2.2.1d Displacement of metal from the polymer complex

PVDF dialysis membrane was prepared as described above. A solution of 1.56 mM calcium chloride adjusted to isotonicity with sodium chloride was used as the release medium for the analysis of zinc sulphate and copper sulphate polymer complexes (0.229 g calcium chloride, 8.913 g sodium chloride in 1 L deionised water). Due to the insolubility of silver chloride, an isotonic solution (1 L) prepared from calcium nitrate (0.357 g) and sodium nitrate (12.857 g) in deionised water was used for the analysis of the silver nitrate polymer complex.

Carbopol 971P-metal salt solution (10 mL) was added to double strength isotonic solution (10 mL) immediately prior to the experiment and transferred into the dialysis tubing. This was subsequently immersed in 480 mL single strength isotonic solution under constant stirring at 400 rpm. Samples were collected as described previously. The displacement of the metal ions from Carbopol 971P was compared to a control composed of metal salt solution (5 mL), deionised water (5 mL) and double strength isotonic solution (10 mL).

Each experiment was performed six times at three different pHs: 4.0, 5.5 and 7.0. The pH of the isotonic solution was adjusted with 0.1 M sodium hydroxide or 0.1 M hydrochloric acid.

3.2.2.1e Atomic absorption spectroscopy

The concentration of metal from samples collected during dialysis was determined using a Hitachi Z800 atomic absorption spectrometer at the School of Pharmacy and Biomedical Sciences, University of Portsmouth (Portsmouth, UK) using a flame atomiser fuelled with an air-acetylene mixture at a flow rate of 1.5 l min^{-1}. Lamp current and slit width was fixed for all metal analysis at 5.0 mA and 1.3 nm respectively. Calibration of the instrument was by means of calibration standards (Appendix 2):

- Zinc- 1000 ppm (µg mL^{-1}) zinc in nitric acid (Fisher Scientific) was diluted in deionised water to obtain the following concentrations: 0.0, 0.2, 0.4, 0.5, 0.6, 0.8 and 1.0 ppm.
- Silver- 1000 ppm silver in nitric acid (Fisher Scientific) was diluted in deionised water to obtain the following concentrations: 0.0, 0.5, 1.0, 1.5, 2.0, 2.5 and 10.0 ppm.
- Copper- 1000 ppm copper in nitric acid (Fisher Scientific) was diluted in deionised water to obtain the following concentrations: 0.0, 0.2, 0.4, 0.6, 0.8 and 1.0 ppm.

Cumulative release was calculated by the sum of the uncorrected concentration of the previous samples from the first to the $n^{th} - 1$ sample relative to the sample volume. This is given by:

$$c_n = c_{n_{meas}} + \left[\frac{x}{y} \times \sum_{s=1}^{n-1} c_{s_{meas}} \right]$$

Where:

c_n = expected concentration of the n^{th} sample if previous samples had not been removed,

$c_{n\,meas}$ = measured concentration of the n^{th} sample,

$c_{s\,meas}$ = un-corrected concentration of the previous sample,

x = sample volume collected for analysis (20 mL),

y = volume of the receptor phase (480 mL).

The amount (μg) of metal released from within the dialysis tubing following each time interval was calculated from the corrected metal concentrations (μg mL^{-1}) of the release medium (480 mL). The mean cumulative amount of metal released at each sampling time was calculated and expressed in terms of mean percentage (%) (± SD) total metal released from the dialysis tubing. Metal salt solutions used to prepare the donor phase were diluted in deionised water by a factor of 100 and measured using atomic absorption spectroscopy to determine the amount of metal introduced at time 0 h. Atomic absorption spectroscopy measurement of the Carbopol 971P-metal salt solution was not possible due to the adhesive nature of the polymer and likelihood of contamination within the atomic absorption spectroscopy sampling mechanism.

3.2.2.2 In vitro assessment of bioadhesion I: Direct staining technique

3.2.2.2a *In vitro* mucoadhesion of polymer dispersions to human buccal cells in sucrose

The method used was that described in section 2.2.2.1b. Following their preparation, buccal cells were incubated with Carbopol 971P-metal salt solution (5 mL) and compared with cells incubated with a negative control, 0.25 M sucrose, and a positive control, 0.05% w/v Carbopol 971P (pH 7.0). No further deviations were made from this methodology. Each Carbopol 971P-metal salt solution was assessed in this manner on three separate occasions.

3.2.2.2b *In vitro* mucoadhesion of polymer dispersions to human buccal cells in artificial saliva

The method used was that described in section 2.2.2.1c. Following their preparation, buccal cells were incubated with Carbopol 971P-metal salt solution (5 mL) and compared with cells incubated with a negative control, artificial saliva, and a positive control, 0.05% w/v Carbopol 971P (pH 7.0). No further deviations were made from this methodology. Each Carbopol 971P-metal salt solution was assessed in this manner on three separate occasions.

3.2.2.2c Cell staining and analysis

The method used was that described in section 2.2.2.1d.

3.2.2.3 In vitro assessment of bioadhesion II: Texture probe analysis

3.2.2.3a Preparation of texture probe analysis samples

Metal salt solution (1.39 mM zinc sulphate, 2.78 mM silver nitrate or 1.39 mM copper sulphate, 50 mL) was added gradually to Carbopol 971P (0.1% w/v, 50 mL, pH 7.0) under stirring. The Carbopol 971P-metal salt solutions were dialysed against deionised water for 6 h with repeated water changes in order to remove counter-ions and excess metal ions from the dispersion. In addition, Carbopol 971P (0.1% w/v, 100 mL) was prepared for use as a positive control. Each Carbopol 971P-metal salt solution was transferred to a 250 mL round bottom flask and frozen in liquid nitrogen. Flasks were transferred to a vacuum freeze dryer immediately for a period of 48 h (Edwards, Micro Modulyo).

Polymer disks were prepared by accurately weighing out 30 mg of each sample into a KBr disk assembly (Specac). Disks (8 mm diameter) were formed following compression at 2 tons of pressure for 10 s using a KBr press (Specac). Ethylcellulose (30 mg) was prepared for use as a negative control. In total, six disks were prepared for each sample and stored in a desiccator until use.

3.2.2.3b Porcine oesophageal tissue

The tissues were prepared as described in section 2.2.2.2b.

3.2.2.3c Texture probe analysis

The method used was that described in section 2.2.2.2c.

3.2.3 Statistical analysis

Values obtained for the average stain intensity of buccal cells treated with Carbopol 971P-metal salt solution and the positive control (0.05% w/v Carbopol 971P) were standardised by calculating a percentage increase from the negative control for each value of n. Results were expressed in terms of mean (± SD) percentage increase in stain intensity. Significant differences between the percentage increase in stain intensity observed from cells treated with Carbopol 971P-metal salt and Carbopol 971P were identified using an unpaired student's *t*-test, P = 0.05 (Microsoft Excel 2003). Mean (± SD or SE) work of adhesion and maximum detachment force was calculated for each polymer sample. Significant differences between adhesive forces measured from lyophilised Carbopol 971P-metal salt and Carbopol 971P were identified using a two-sample student's *t*-test (Microsoft Excel 2003). Prior to each statistical analysis, the Kolmogorov-Smirnov test was used to determine the normality of the data.

3.3 Results and Discussion

3.3.1 Development of Carbopol 971P-metal salt solutions

In the hydrated state, Carbopol 971P particles uncoil to a limited extent due to extensive intra and inter-chain hydrogen bonding between associated carboxyl groups (R-COOH) on the polymer backbone (Dittgen *et al.*, 1997; Noveon. 2002a). With the addition of sodium hydroxide, carboxyl groups dissociate ($R\text{-}COO^-$) and the negative charges cause chain repulsion, fully uncoiling the polymer. This results in the expansion of the polymer network, or swelling. The compatibility of an aqueous Carbopol 971P dispersion with cations is concentration dependent, with high concentrations resulting in the collapse of the uncoiled polymer network and the precipitation of tightly coiled polymer particles. The optimum concentration of metal salt that could be added to 0.10% w/v Carbopol 971P aqueous dispersion in a 1:1 volume ratio was investigated visually (Table 3.1).

Table 3.1 Visual inspection of 0.10% w/v Carbopol 971P aqueous dispersion following addition of various concentrations of metal salt solution. The viewer graded polymer precipitation. Grades were based on the precipitation of large aggregates (***), precipitation of small aggregates (**), no precipitation accompanied by an increase in polymer turbidity (*), and no visible changes (-).

Concentration (mM)	Estimated metal:carboxyl group ratio	Observed precipitation after 30 min		
		Zinc sulphate	silver nitrate	copper sulphate
27.80	2:1	***	***	***
13.90	1:1	**	**	**
6.95	1:2	**	*	**
2.78	1:5	*	-	*
1.39	1:10	-	-	-
0.28	1:50	-	-	-
0.13	1:100	-	-	-

At 1.39 mM both zinc sulphate and copper sulphate caused no visible changes to the Carbopol 971P aqueous dispersion. Based on the formula weight of acrylic acid, this corresponds to an estimated 1:10 ratio between the metal and carboxyl group concentration. Silver nitrate could be added at a concentration of 2.78 mM (estimated 1:5 metal:carboxyl concentration) without causing any changes to the polymer dispersion. Neutralised polycarbophil has previously been shown to bind sodium and calcium ions through negatively charged carboxyl groups (Kriwet and Kissel, 1996). The valence of the metal ion has a significant influence on the concentration of metal salt solution that can be added to the polymer dispersion without causing precipitation. Divalent ions i.e. Cu^{2+} and Zn^{2+} are capable of cross-linking Carbopol through interactions with two carboxyl groups while monovalent ions i.e. Ag^{+} may interact with only one. Therefore, lower concentrations of divalent metal salt solutions will interact with twice as many carboxyl groups as a monovalent metal salt solution of the same concentration. This explains why the concentration of silver nitrate that caused no visible changes to the polymer dispersion was twice that of copper sulphate and zinc sulphate.

The precipitate formed following the addition of high concentrations of metal salt solution to the aqueous polymer dispersion was characteristically white, except when using copper sulphate, which resulted in a pale blue precipitate. Complex copper (II) ions exhibit blue colouration due to the presence of bound ligands, which in this instance are most likely deprotonated carboxyl groups on the polymer chains. The presence of copper within the precipitate suggests that both zinc and silver would also be found in the precipitate of the corresponding Carbopol 971P-metal salt solutions and that these metals cations are key in the collapse of the polymer chains. Lele and Hoffman (2000) have previously used the cationic drug levobetaxolol to precipitate insoluble complexes with partially neutralised poly(acrylic acid). They observed that without poly(acrylic acid) neutralisation with sodium hydroxide, precipitation would not occur, indicating that the drug loading in the precipitated complex is only due to ionically bound drug molecules to charged carboxyl groups. When high metal salt concentrations are added to the aqueous Carbopol 971P dispersion, the negative charges that exist between adjacent polymer chains diminish causing the expanded polymer network to collapse to a turbid dispersion. Above a critical concentration, the distance

between adjacent polymer chains has become sufficiently reduced to cause the formation of tightly coiled polymer particles.

Previous authors have investigated the interactions between poly(acrylic acid) and drug molecules using equilibrium dialysis (Sandri *et al.*, 2006), ultrafiltration (Tomida *et al.*, 2001) and turbidometric techniques (Lele and Hoffman, 2000; Nurkeeva *et al.*, 2004). It is worth noting however that the majority of these studies were performed using linear poly(acrylic acid) rather than cross-linked polymer networks, which are less susceptible to precipitation in salt solutions. Due to these properties of Carbopol, it was deemed unsuitable to use techniques such as equilibrium dialysis, which may result in the precipitation of the polymer before equilibrium has been reached. Turbidometric analysis was also deemed unsuitable due to the immediate formation of large precipitates formed on addition of high concentrations of metal salt, which would not enable accurate measurement with visible spectroscopy due to settling.

3.3.2 Stability of Carbopol 971P-metal salt complex

To ensure that metal ions had interacted with neutralised Carbopol 971P following the addition of the metal salt solution a dialysis technique was employed. The dialysis tubing employed to study these interactions was constructed from polyvinylidene difluoride (PVDF) instead of the commonly used regenerated cellulose. PVDF dialysis membranes are relatively inert and are purchased in a high purity form without the necessity of complex preparation procedures. Previous experiments with regenerated cellulose dialysis tubing (Biodesign Inc, New York, USA) required pre-treatment of the membrane with sodium carbonate and ethylenediaminetetraacetic acid to remove contaminants prior to dialysis. Following the experimental procedure it was observed that the recovery of metal in the release medium from the metal salt solution control was particularly low. This may have been due to metal ions binding to the regenerated cellulose, resulting in reduced recovery in the receptor phase. Pre-equilibration in metal salt solution had no effect on this observation. Metal recovery from the control solution was significantly improved when the PVDF dialysis tubing was used and as a consequence this type of dialysis membrane was selected for use within the investigation. To minimise any possible metal binding by the dialysis membrane, pre-

equilibration in metal salt solution was undertaken to occupy possible binding sites. The volume of the release medium was optimised to ensure that diffusion from the dialysis tubing into the receptor phase was not limited by a significantly reduced concentration gradient over the experimental period. No difference in zinc detection over 24 h was observed when the receptor phase was increased from 480 mL to 980 mL, indicating that the release medium used in the investigation still maintained sink conditions after 24 h and did not restrict the diffusion of zinc out of the donor phase.

The release of zinc from a 0.695 mM zinc sulphate control and Carbopol 971P-zinc sulphate solution was analysed over 24 h (Figure 3.3). The release of zinc from the control was used to assess the behaviour of zinc under the experimental conditions without the inclusion of the polymer; hence the final concentration of zinc sulphate within the polymer dispersion was used for this purpose. During the first 4 h, 44.5% ± 3.6 of total zinc was detected within the release medium at a near constant rate (11.9% h^{-1}, $R^2 = 0.97$), which began to drop slightly between 4 and 6 h after which 58% ± 4.9 of total zinc had been released. This may be due to a slight reduction in the concentration gradient after 4 h, which can decrease the rate of diffusion. Following full replacement of the release media, the zinc remaining within the dialysis tubing was dialysed overnight (18 h) to reach equilibrium, confirmed by the equal concentration of zinc in the donor and receptor phase. At 24 h, 90% ± 3.2 of total zinc had been released from the PVDF dialysis tubing. In comparison, zinc was not detectable within the release medium throughout the 24 h period when dialysing the Carbopol 971P-zinc sulphate solution (Figure 3.3). This indicates that zinc is retained within the dialysis tubing due to some interaction with the negatively charged polymer. As zinc remained beneath detectable levels throughout the 24 h period, it can be assumed that the polymer binds all of the zinc.

Silver released from 1.39 mM silver nitrate control was considerably rapid, with 51.5% of total silver released within the first hour of dialysis (Figure 3.4). The rate of diffusion decreased during the susequent 5 h, following which 84.8% ± 8.0 of total silver had been detected within the release medium. After 24 h, equilibrium was reached and 87.3% ± 8.1 of total silver had been released from the dialysis tubing. Contrary to the observations with the Carbopol 971P-zinc sulphate solution, silver was

detected within the release medium when dialysing the Carbopol 971P-silver nitrate solution (Figure 3.4). However, following 24 h the amount of silver released was only 2.4% ± 1.8 of total silver, which was considerably less than the control after this time. This suggests that a small fraction of the silver added to Carbopol 971P remains unbound by the polymer and is therefore able to diffuse out of the dialysis membrane.

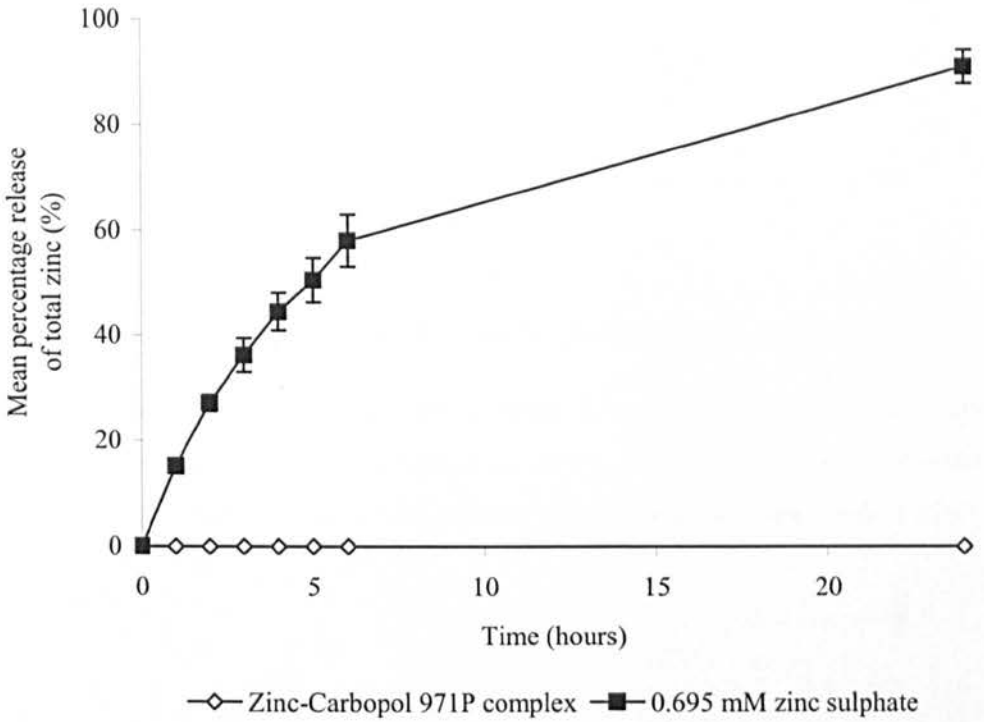

Figure 3.3 Cumulative release of zinc detected in the release medium when dialysing Carbopol 971P-zinc complex in deionised water. The diffusion of zinc from the polymer complex was compared to an aqueous zinc sulphate solution (n=6, ± SD).

The recovery of copper from the 0.695 mM copper sulphate control was higher than both zinc and silver; with 90.3% ± 3.3 of total copper detected after the first 6 h and 97.1% ± 4.1 after 24 h, when equilibrium was reached (Figure 3.5). No copper was detected within the release medium after 24 h when dialysing the Carbopol 971P-copper sulphate solution. As with zinc, this indicates that copper is retained within the dialysis tubing due to some interaction with Carbopol 971P and all the copper is bound.

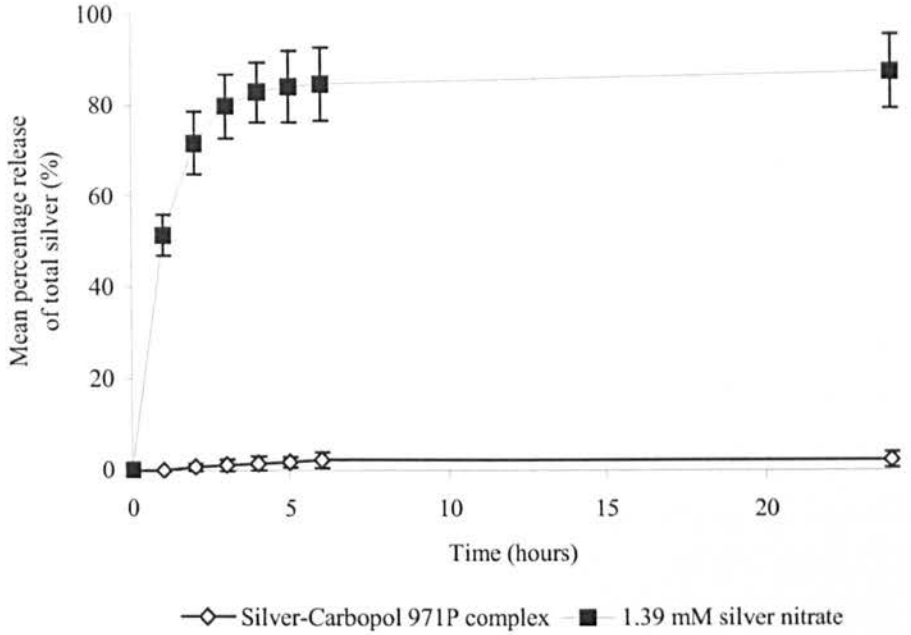

Figure 3.4 Cumulative amount of silver detected in the release medium when dialysing Carbopol 971P-silver complex in deionised water. The diffusion of silver from the polymer complex was compared to an aqueous silver nitrate solution. (n=6, ± SD)

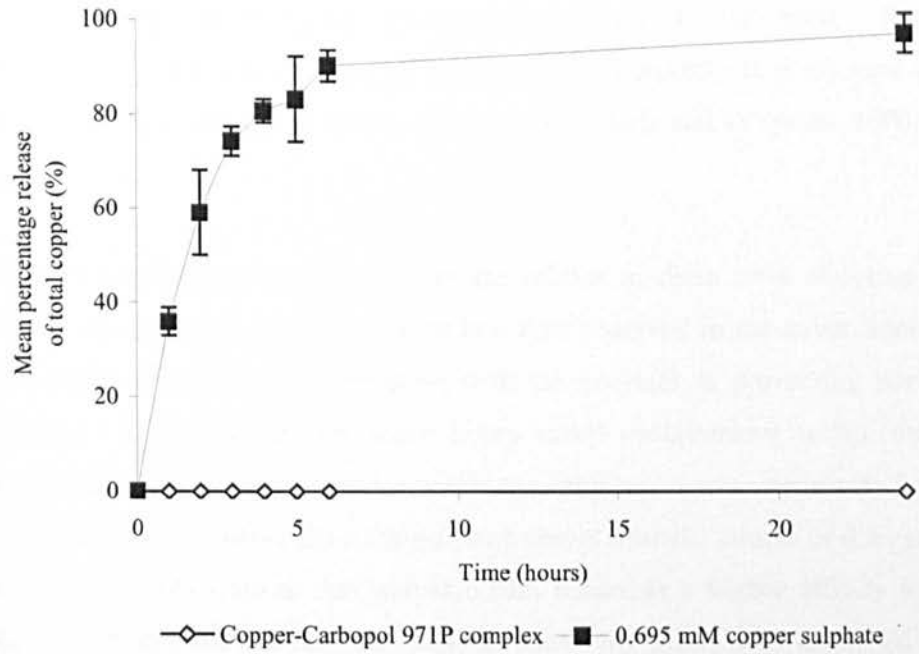

Figure 3.5 Cumulative amount of copper detected in the release medium when dialysing Carbopol 971P-copper complex in deionised water. The diffusion of copper from the polymer complex was compared to an aqueous copper sulphate solution. (n=6, ± SD)

The dialysis of Carbopol 971P-zinc sulphate and Carbopol 971P-copper sulphate in deionised water confirms that metal ions are bound by the polymer, characterised by the absence of either metal within the release medium after 24 h. It is probable that the type of interaction that exists between the polymer carboxyl groups and the divalent metal ions ($Metal^{2+}$) is ionic. The interaction can be expressed as follows:

$$COO^- + Metal^{2+} \rightleftharpoons COOMetal^+ \quad (1)$$

$$2COO^- + Metal^{2+} \rightleftharpoons COO_2Metal \quad (2)$$

The mononuclear interaction (2) may occur between carboxyl groups located on the same polymer chain or on adjacent chains and may increase the degree of polymer cross-linking (Kriwet and Kissel. 1996). Tomida *et al.* (2001) investigated the binding properties of poly(acrylic acid) (molecular weight 240,000) with divalent metal ions using an ultrafiltration technique. They proposed a third complex between poly(acrylic acid) and divalent metal ions involving coordinate bonds between a central metal ion with two or more carboxyl groups. However the numbers of these types of bond decreased with increasing pH and increasing metal ion concentration and are not likely to be found in the complexes investigated within this experiment. Experimental formulations between cationic drug molecules and poly(acrylic acid) have concluded that the nature of the interaction is typically ionic (Lele and Hoffman. 2000; Sandri *et al.*, 2006).

Although some silver was detected in the release medium after dialysing Carbopol 971P-silver nitrate the amount was far less than observed in the silver nitrate control, which suggests that some interaction with the polymer is preventing normal silver diffusion. It is possible that some heavy metal contaminants within the aqueous polymer dispersion or ionic species within the deionised water source may have caused the displacement of silver from the polymer chains over the course of dialysis. Kriwet and Kissel (1996) showed that polycarbophil possesses a higher affinity for divalent ions than monovalent ions. This may explain why silver was displaced while the divalent metal ions remained bound. As silver is not detected until 2 h rather than immediately, this explanation appears the most plausible. However it is also possible that upon addition of 1.39 mM silver nitrate solution to the aqueous Carbopol 971P dispersion that there is an excess of silver ions relative to the available carboxyl binding

sites. Due to the valence of silver this small amount of excess ions (2.4% of total silver) does not cause precipitation of the polymer and is able to diffuse with the negatively charged nitrate ions out of the dialysis membrane.

3.3.3 Displacement from the metal-polymer complex

Within the oral cavity, it is proposed that electrolytes present in saliva will displace the metal ions from the polymer carboxyl groups to maintain a sustained antimicrobial concentration. Therefore the displacement of the metal from each of the polymer complexes was investigated using a solution containing electrolytes commonly found in salivary secretions. It was crucial to place the same concentration of electrolytes in the donor and receptor phases to reduce osmosis into the dialysis tubing. Initially, artificial saliva (2.2.2.1c) both with and without calcium chloride was used to assess the displacement of metal ions from the polymer complex. However during dialysis of the zinc sulphate control, the recovery of zinc over 24 h was persistently low. Increasing the ratio within the dialysis tubing between 0.695 mM zinc sulphate and artificial saliva did improve zinc recovery e.g. 1:1 resulted in 13.6% zinc recovery and 1:4 resulted in 29.1% zinc recovery, as did the omission of calcium chloride from the artificial saliva e.g. 1:1 resulted in 58% zinc recovery. However adequate zinc recovery from the control using artificial saliva could not be achieved. Based on these observations, it was concluded that the artificial saliva was either limiting the diffusion of zinc from the donor phase or interfering with atomic absorption analysis. The appearance of white precipitate during the dialysis with the zinc sulphate control does indicate some incompatibility with artificial saliva, possibly due to the formation of insoluble zinc phosphate. Therefore an alternative isotonic solution containing 1.56 mM calcium chloride adjusted to isotonicity with sodium chloride was employed as the release medium to analyse Carbopol 971P-zinc sulphate solutions. Unfortunately due to the insolubility of silver chloride a solution containing 1.56 mM calcium nitrate adjusted with sodium nitrate had to be used to analyse the Carbopol 971P-silver nitrate solutions. The concentration of calcium corresponds to the calcium content of saliva secreted at the resting rate from the submandibular gland (Lentner. 1981). Saliva from this gland comprises 80% of whole saliva during unstimulated states (Bloom and Fawcett. 1975).

The effect of release medium pH on the displacement of metal ions from Carbopol 971P was also investigated. Three physiologically relevant pHs were selected: pH 5.5- the critical demineralisation pH of enamel (Marsh and Martin. 1999) , pH 4.0- the lowest plaque pH measured after the consumption of a 10% sucrose solution following salivary stimulation (Edgar and O'Mullane. 1996) and, pH 7.0- the upper range of resting salivary pH (Lentner. 1981).

The release of zinc from the zinc sulphate control is shown at pH 5.5 as no change in the rate of zinc diffusion at pH 4.0 or pH 7.0 was observed (data not shown). The rate of zinc released from the control is initially very high, with 42.9% ± 2.3 of total zinc detected within the release medium after 1 h (Figure 3.6). After 24 h 89.2% ± 4.6 of total zinc was released from within the dialysis tubing and equilibrium had been reached. When the Carbopol 971P-zinc sulphate solution was dialysed against the sodium chloride/calcium chloride release medium, zinc was detected within all the samples removed (Figure 3.6). This indicates that zinc is being displaced from the polymer as a direct result of the electrolytes present in the release medium. At pH 5.5 the rate of release of zinc was significantly slower than the zinc sulphate control, with only 56.4% ± 5.7 of total zinc released after the first 6 h. After 24 h an average of 77.2% ± 5.6 had been displaced from the Carbopol 971P-zinc sulphate solution, which was 12% less than the zinc sulphate control. At pH 4.0 the rate of release of zinc from the polymer complex had increased from that observed at pH 5.5, with 77.9% ± 8.0 of total zinc released after 6 h. The rate of zinc release was only slightly reduced from the zinc sulphate control, with a difference of only 3.3% of total zinc released after 24 h. Conversely, at pH 7.0 the rate of release of zinc from the polymer complex had slightly decreased from that observed at pH 5.5, with 56.4% ± 5.7 of total zinc released after 6 h and 77.2% ± 5.6 after 24 h. It is apparent that the rate of zinc release from the polymer is affected by the pH of the release medium, with more rapid displacement occurring at lower pH.

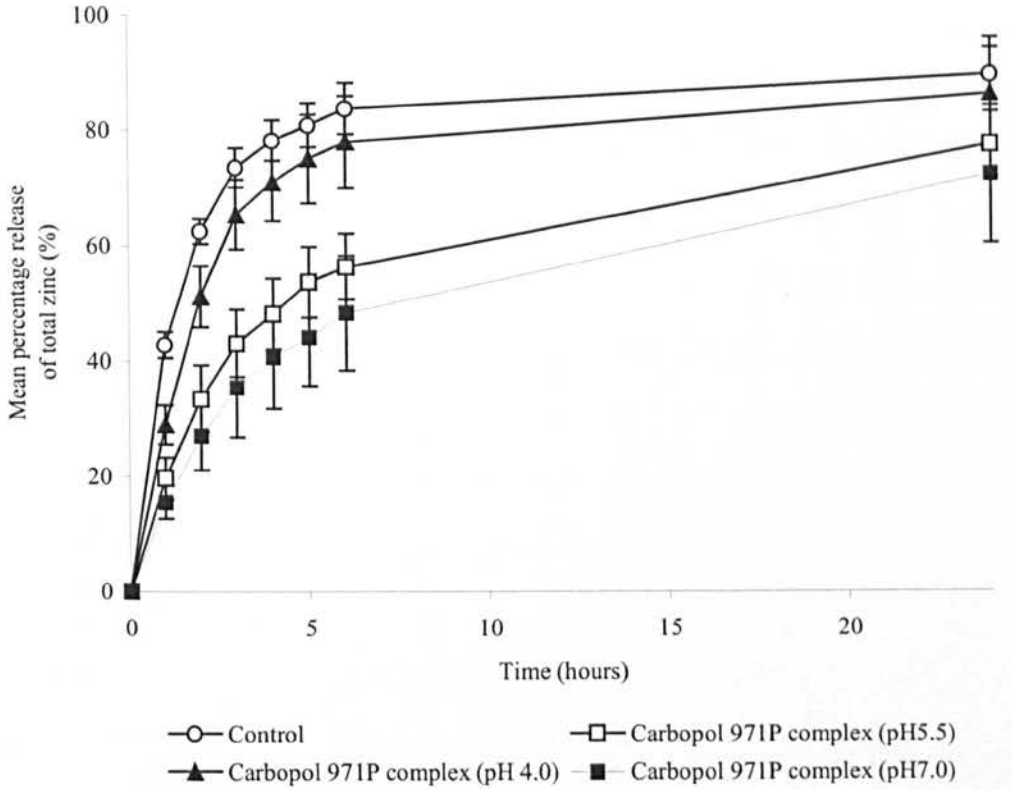

Figure 3.6 Cumulative displacement of zinc from the Carbopol 971P-zinc sulphate solution and the effect of pH compared to a zinc sulphate control at pH 5.5 (n=6, ± SD).

The rate of silver released from the silver nitrate control was rapid, with 87.9% ± 3.6 of total silver detected in the release medium after 6 h and 90.8% ± 3.8 after 24 h (Figure 3.7). When dialysing the Carbopol 971P-silver nitrate solution against the release medium silver was detected in the receptor phase at all time points. As with the Carbopol 971P-zinc sulphate solution, this indicates that the electrolytes present in the release medium are displacing the silver from the polymer carboxyl groups. However, no difference could be observed in the rate of silver displacement from the Carbopol 971P-silver nitrate solution and the silver nitrate control. Changing the pH of the release medium had no effect on the rate of silver displacement with 90.2% ± 4.3, 89.3% ± 1.3 and 84.3% ± 0.7 of total silver released after 6 h at pH 5.5, 4.0 and 7.0 respectively. It is clear that the pH of the release medium has no effect on the rate of silver displacement from the polymer.

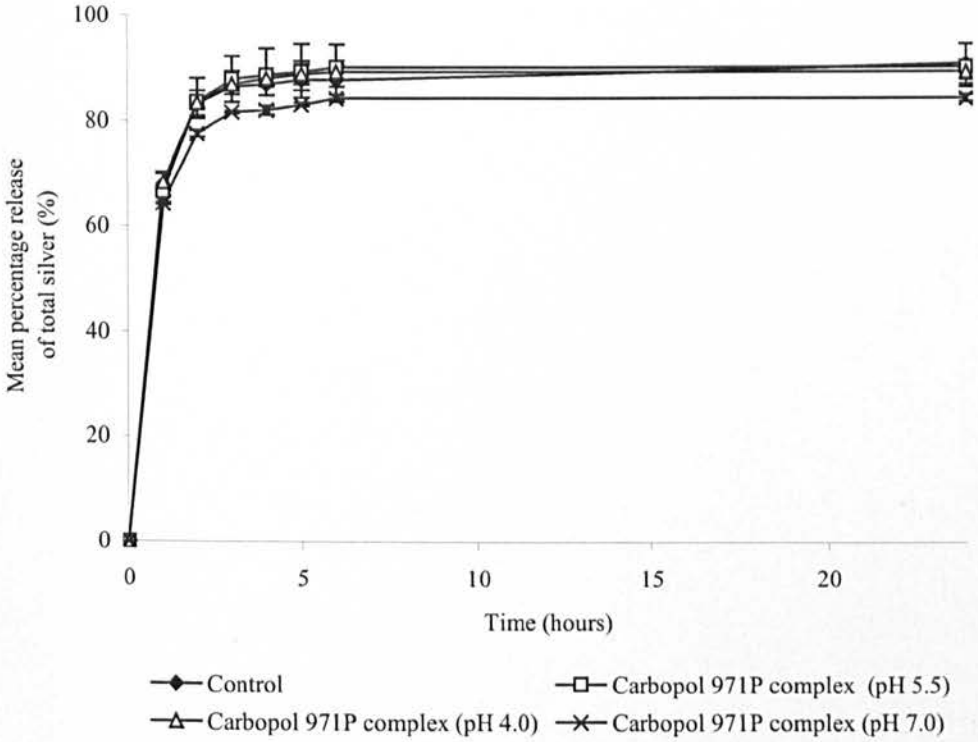

Figure 3.7 Cumulative displacement of silver from the Carbopol 971P-silver nitrate solution and the effect of pH compared to a silver nitrate control at pH 5.5 (n=3-6, ± SD).

Unfortunately, the Carbopol 971P-copper sulphate solution could not be analysed using this dialysis technique due to the formation of precipitate during the experiment. The Carbopol 971P-copper sulphate solution was dialysed against the sodium chloride/calcium chloride release medium. During the dialysis procedure, blue precipitate became slowly visible within the dialysis tubing and limited the amount of copper detected throughout the course of the experiment. This seems to be a direct consequence of electrolytes from the release medium diffusing into the dialysis tubing, as no precipitate formed following the addition of double strength isotonic sodium chloride/calcium chloride solution and the development of precipitation was not immediate. The nature of copper-polyelectrolyte interactions has been previously investigated with poly(acrylic acid) (Francois *et al.*, 1997) and poly(methacrylic acid)

(Heitz and Francois, 1999). It was determined that at low pH a binuclear complex between four carboxyl groups and two copper ions is predominant:

$$4COO^- + 2Cu^{2+} \rightleftharpoons COO_2Cu_4 \quad (3)$$

The formation of these complexes is dependant on the chain expansion of the polymer; hence at low pH the conformation of the polymer chains allows the formation of the binuclear complex (3) over the mononuclear complex (2), while at high pH the charge repulsion between the polymer chains causes an extended conformation, which favours the mononuclear complex (2) (Francois *et al.*, 1997). It is likely that the mononuclear complex is predominant during the dialysis in deionised water and therefore no precipitation of the Carbopol 971P-copper sulphate solution was observed. The addition of sodium chloride and calcium chloride to an aqueous dispersion of polycarbophil causes both dehydration of the polymer and compensation of the negative carboxyl charges (Kriwet and Kissel, 1996). Therefore upon addition of the release medium to the aqueous dispersion of Carbopol 971P-copper sulphate solution a reduction in both polymer hydration and chain expansion takes place, changing the conformation of the polymer. As precipitation of the complex does not occur immediately it can be assumed that cations diffuse into the dialysis tubing following immersion in the receptor phase and the polymer chains become increasingly coiled, allowing the formation of the binuclear complex (3) leading to precipitation. As this is not observed during dialysis of the zinc and silver polymer complexes it can be assumed that copper interacts to a greater extent with Carbopol 971P. Tomida *et al.* (2001) calculated that the overall complexation constants, which represent the stability and binding equilibria of divalent metal ions to poly(acrylic acid), decrease in the order of Cu > Pb > Zn > Ni, Co. This seems to agree with the observations in this study, whereby copper remained bound to Carbopol 971P causing precipitation as sodium and calcium concentration increased within the dialysis tubing.

The release of zinc from the Carbopol 971P complex during dialysis in sodium chloride/calcium chloride solution, as a result of the need for displacement of zinc from the polymer, gave a slower rate of transport across the dialysis membrane relative to the zinc sulphate control. Lele and Hoffman (2000) found that the dissociation of ionic

complexes between levobetaxolol and poly(acrylic acid)acrylic acid) only occurred in the presence of both the common ions i.e. sodium and chloride ions. Vilches *et al.* (2002) investigated the release of fluoroquinolone from a Carbopol 934P hydrogel. They found that the release of fluoroquinolone occurred more rapidly in sodium chloride solution than distilled water and suggested that the dissociation of ion pairs formed between fluoroquinolone and the poly(acrylic acid) carboxyl groups is the limiting step that controls the rate of fluoroquinolone release. Kriwet and Kissel (1996) also observed that calcium was displaced from polycarbophil by sodium ions, which increased as the concentration of sodium ions increased. It is reasonable to conclude that an ion exchange mechanism is causing the displacement of zinc from the Carbopol 971P polymer and explains why zinc remains bound during dialysis against deionised water. Sodium and calcium ions compete for the negatively charged binding sites on the polymer and cause the displacement of zinc, which is then detected within the release medium. The rate of displacement from Carbopol 971P was affected by the pH of the release medium, with a lower pH resulting in a faster rate. At low pH, the concentration of dissociated carboxyl groups ($R\text{-}COO^-$) would decrease as hydrogen ion concentration increases, causing a corresponding increase in associated carboxyl groups (R-COOH). As available binding sites decrease on the polymer, competition increases for the negatively charged carboxyl groups, which results in a faster rate of zinc displacement. Conversely, as pH increases the concentration of dissociated carboxyl groups ($R\text{-}COO^-$) also increases reducing competition for negatively charged binding sites, which results in a slower rate of zinc displacement. It is likely that calcium ions present in the release medium compete more efficiently with zinc for negatively charged binding sites compared to sodium ions. Sodium ions would also compete for binding sites but due to the higher affinity of poly(acrylic acid) for divalent ions, is less likely to displace zinc at the same rate as calcium (Kriwet and Kissel, 1996).

The release of silver from the Carbopol 971P complex during dialysis in sodium nitrate/calcium nitrate solution resulted in the displacement of silver from the polymer at a rate equal to the silver nitrate control. The displacement of silver from the negatively charged carboxyl groups on the polymer probably occurs through a similar ion exchange mechanism observed during the dialysis of the Carbopol 971P-zinc sulphate solution. However the rate of silver displacement from the polymer was rapid when compared to zinc displacement, indicating that the affinity of the polymer for the

silver ions is relatively low when compared to sodium and calcium. For this reason, silver is almost immediately displaced when the Carbopol 971P-silver nitrate solution is initially mixed with the release medium prior to transfer into the dialysis tubing resulting in normal silver diffusion across the membrane as observed with the silver nitrate control. These observations support claims that the affinity of poly(acrylic acid) is higher for divalent ions than monovalent ions. The rate of silver displacement from Carbopol 971P is not affected by the pH of the release medium. Changes in the concentration of dissociated carboxyl groups within the polymer dispersion do not affect the rate displacement of silver due to effective competition from both sodium and calcium ions and the low affinity of silver for Carbopol 971P.

3.3.4 *In vitro* assessment of bioadhesion I: Direct staining technique.

3.3.4.1 Bioadhesion in sucrose

Carbopol 971P and Carbopol 971P-metal salt complex were detected on the surface of isolated buccal cells using Alcian blue and visualised using light microscopy (Figure 3.8). The negative control retains the Alcian blue stain to produce a light blue staining of the cytoplasm and nucleus, probably through electrostatic interactions with negatively charged structures such as proteins. After exposure to each of the polymer samples, a significant increase in stain retention can be observed, with densely staining dark blue regions easily identifiable on the buccal cell surface. These cells appear vastly different from the negative control due to the adsorption of polymer on the surface. Evidence of bound polymer on the surface of the buccal cells can be seen after exposure to all of the polymer samples. Visible differences between the stained buccal cells are not obvious following incubation with each of the Carbopol 971P-metal salt solutions. However cells incubated with the positive control do appear to be more lightly stained than those incubated with the Carbopol 971P-metal salt solutions (Figure 3.8), although the difference appears insignificant.

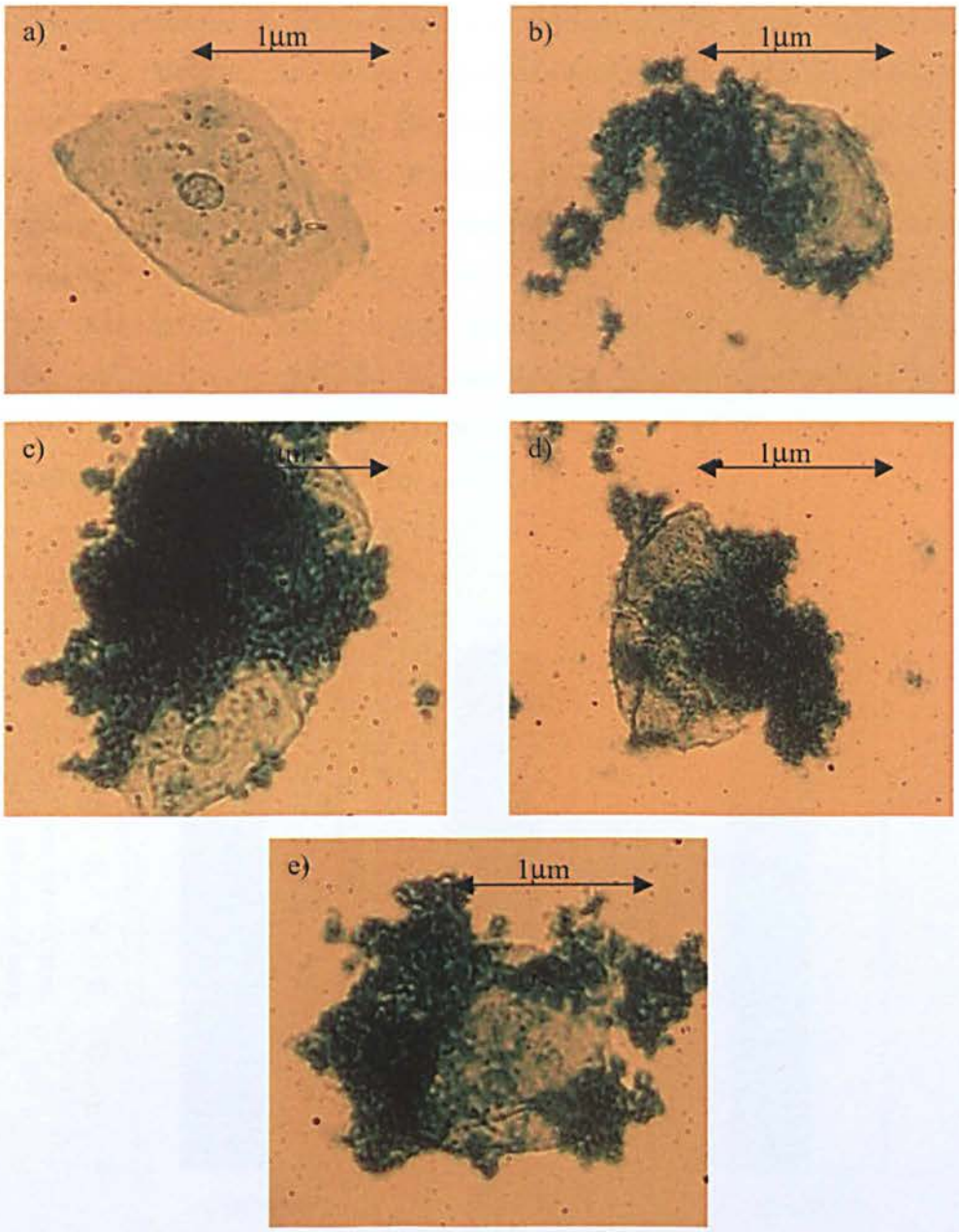

Figure 3.8 Human buccal cells stained with 0.05% w/v Alcian blue after exposure to a) 0.25 M sucrose solution, b) 0.05% w/v Carbopol 971P, c) Carbopol 971P-silver nitrate solution, d) Carbopol 971P-copper sulphate solution and, e) Carbopol 971P-zinc sulphate solution at x200 magnification.

The percentage increase in stain intensity relative to the negative control was calculated for buccal cells exposed to the positive control and each of the Carbopol 971P-metal salt solutions. The negative control was tested simultaneously with the positive control and each of the Carbopol 971P-metal salt solutions to ensure that variation between

experiments conducted on different days was eliminated. For buccal cells incubated with each of the polymer samples and the positive control a percentage increase in stain intensity was detected (Figure 3.9). This confirms that exposure to the polymer samples results in increased stain intensities relative to the negative control caused by bound polymer on the buccal cell surface. The percentage increase in stain intensity detected following exposure to the Carbopol 971P-metal salt solution was not significantly different to the stain intensity caused by exposure to the positive control ($P > 0.05$). This suggests that the presence of metal ions bound to the carboxyl groups of Carbopol 971P does not result in reduced adsorption to the buccal cell surface when the cells are prepared with 0.25 M sucrose solution.

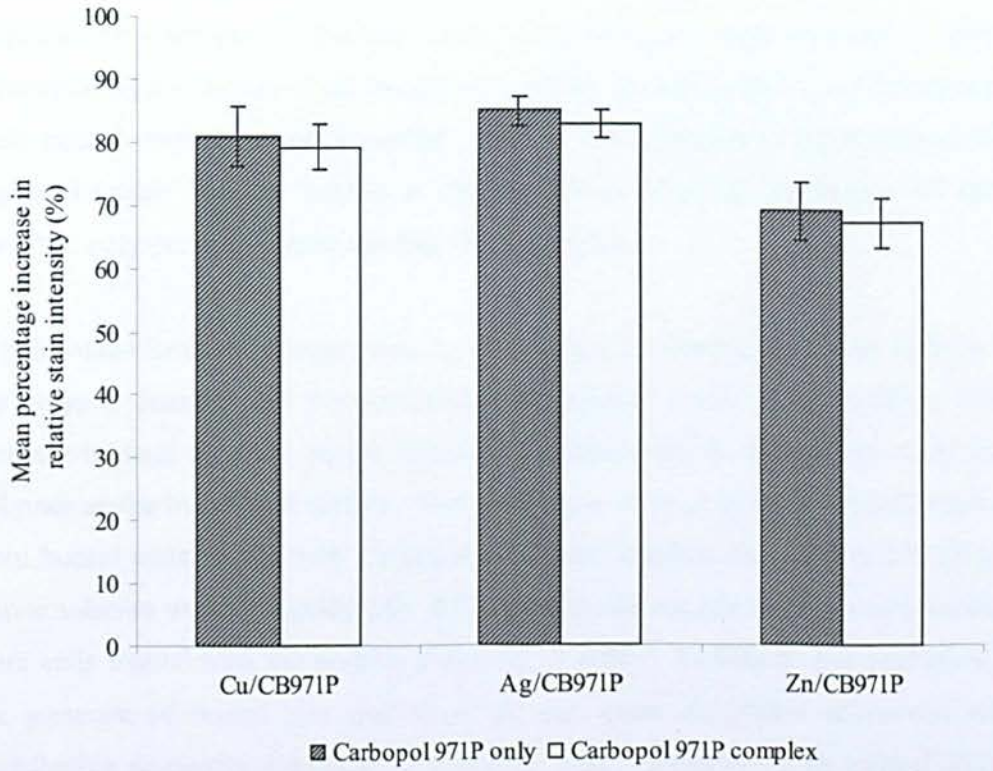

Figure 3.9 Mean percentage increase in relative stain intensity of buccal cells stained with 0.05% w/v Alcian blue following exposure to Carbopol 971P and Carbopol 971P-metal salt solutions, with copper, silver and zinc complexes denoted as Cu/CB971P, Ag/CB971P, and Zn/CB971P respectively (n=60, ± SE).

3.3.4.2 Bioadhesion in artificial saliva

Buccal cells prepared in artificial saliva were used to assess the adsorption of metal-polymer complexes to the cell surface in the presence of electrolytes found in salivary secretions. Control cells not exposed to the polymer retained the Alcian blue stain to a similar extent as cells prepared in sucrose, which suggests preparation in artificial saliva does not interfere with the staining protocol (Figure 3.10). Bound polymer is evident on all cells exposed to the positive control and Carbopol 971P-metal salt solutions.

Following treatment with the positive control, densely stained regions on the buccal cell surface representing the bound polymer are visible. Exposure to Carbopol 971P-zinc sulphate and Carbopol 971P-silver nitrate solution caused large amounts of polymer adsorption on the surface of the buccal cells, which appear similar to the appearance of cells treated with the positive control. Buccal cells exposed to the Carbopol 971P-copper sulphate solution exhibit a slightly altered physical appearance of surface adsorbed polymer with lighter staining characteristics.

A percentage increase in stain intensity was detected following treatment with each of the polymer samples and the positive control (Figure 3.11). This confirms that an increase in stain intensity occurs following treatment due to the adsorption of bound polymer on the buccal cell surface. The percentage increase in stain intensity measured from buccal cells treated with Carbopol 971P-zinc sulphate and Carbopol 971P-silver nitrate solution was not significantly different from the relative stain intensity measured from cells treated with the positive control ($P > 0.05$). As before, this confirmed that the presence of bound zinc and silver do not cause significant alterations to the bioadhesive properties exhibited by Carbopol 971P. However, cells treated with the Carbopol 971P-copper sulphate solution exhibited an increase in stain intensity that was significantly different from the positive control ($P < 0.001$). Although cells treated with the Carbopol 971P-copper sulphate solution did exhibit some adsorption on the buccal cell surface (Figure 3.10), the mean percentage increase in relative stain intensity was lower than that seen when the polymer was tested alone (Figure 3.11). This suggests that when buccal cells are prepared and washed in artificial saliva, polymer adsorption to the surface is affected by the presence of bound copper, but no significant effect was seen with zinc and silver.

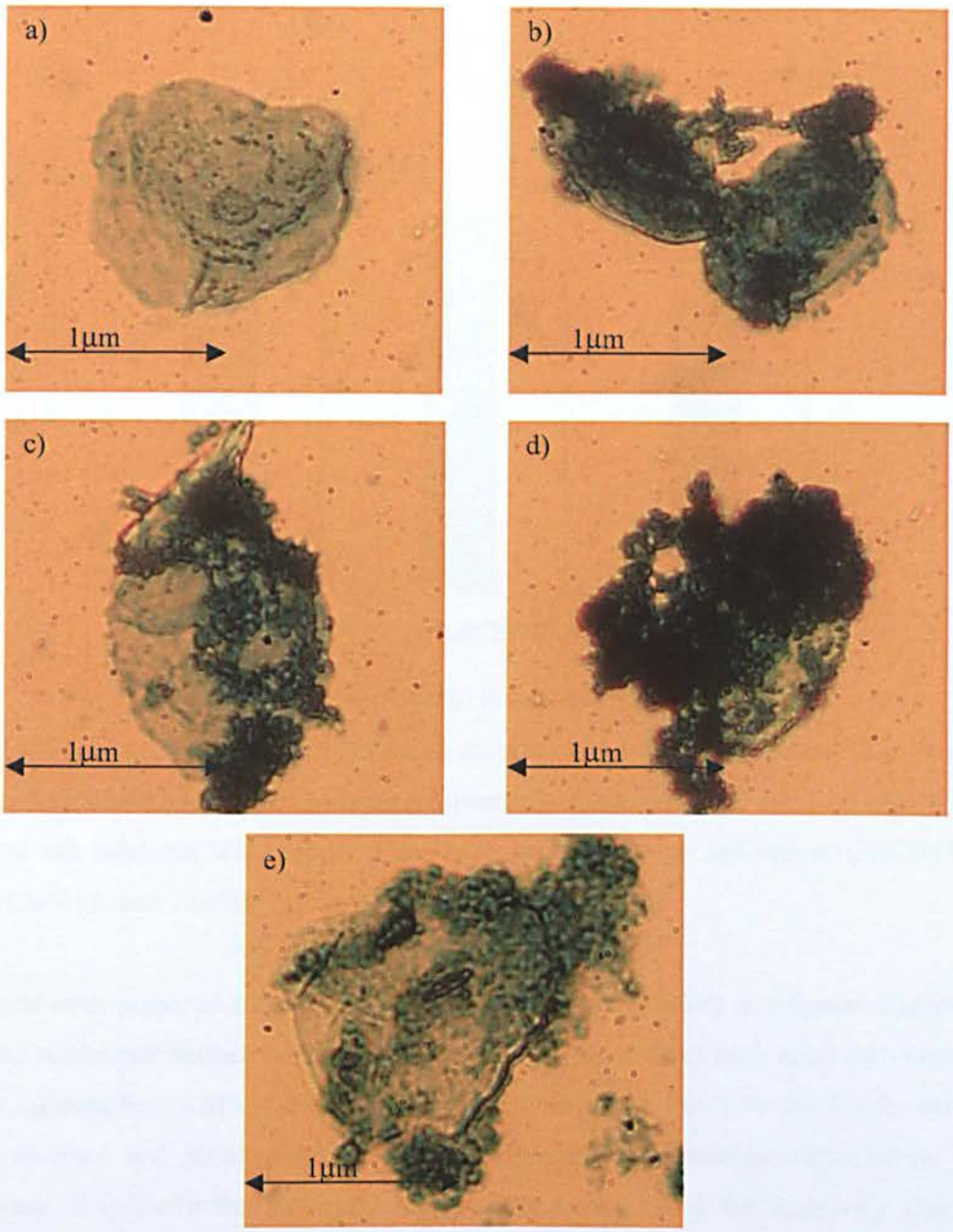

Figure 3.10 Human buccal cells, prepared in artificial saliva, stained with 0.05% w/v Alcian blue after exposure to a) 0.25 M sucrose solution, b) 0.05% w/v Carbopol 971P, c) Carbopol 971P-zinc sulphate solution, d) Carbopol 971P-silver nitrate solution and, e) Carbopol 971P-copper sulphate solution, at x200 magnification.

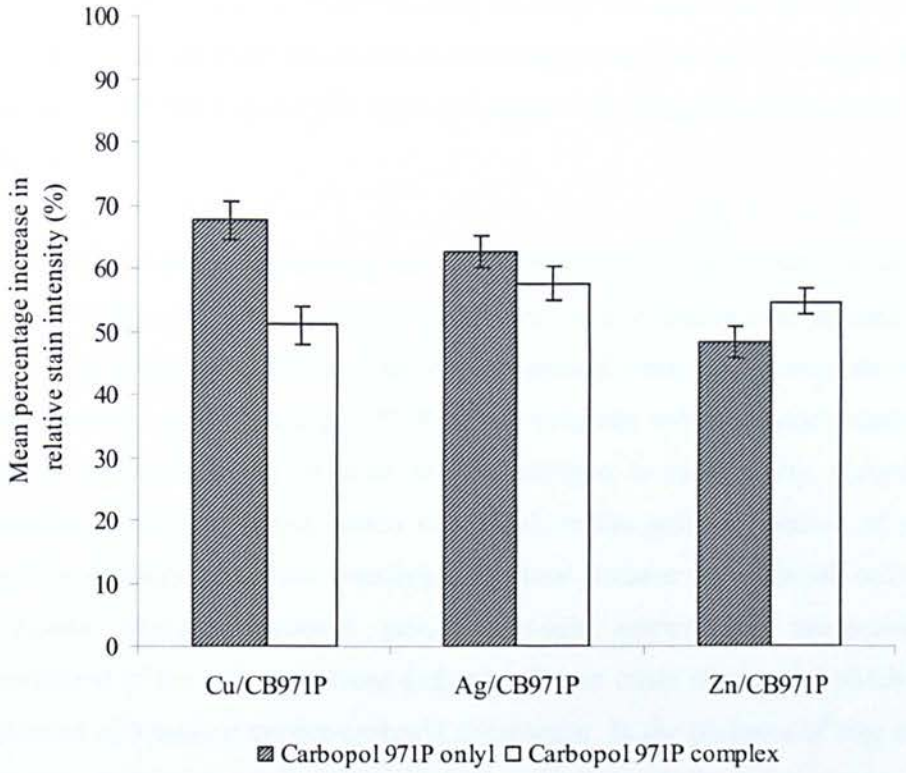

Figure 3.11 Mean percentage increase in relative stain intensity of buccal cells stained with 0.05% w/v Alcian blue following exposure to Carbopol 971P and Carbopol 971P-metal salt solutions with copper, silver and zinc complexes denoted as Cu/CB971P, Ag/CB971P, and Zn/CB971P respectively (n=60, ± SE).

Buccal cells prepared and washed with 0.25 M sucrose resulted in polymer adsorption to the buccal cell surface that was unaffected by the presence of each metal salt solution. The estimated ratio of metal:carboxyl group concentration was 1:10 and 1:5 for the for the divalent and monovalent Carbopol 971P-metal salt solutions respectively. In sucrose, it is likely that the metal ions remain associated to the negatively charged carboxyl groups of the polymer through electrostatic interaction as no direct competition arises from the presence of sucrose. Carbopol 971P exhibits good bioadhesive properties due the high density of carboxyl groups within the polymer chains which enable the formation of hydrogen bonds with the mucosal surface. The positive control demonstrates that the availability of carboxyl groups within the aqueous Carbopol 971P dispersion (pH 7.0) available for hydrogen bond formation are sufficient to enable bioadhesion to the buccal cell surface. The addition of metal salts to the polymer dispersion reduces the negative charges associated with dissociated carboxyl

groups but still allows hydrogen bonding to occur via undissociated groups. It is also possible that the divalent cations could encourage cross-linking by bridging between the negatively charged poly(acrylic acid) and negatively charged groups on the buccal cell surface.

Buccal cells prepared and washed with artificial saliva resulted in polymer adsorption to the cell surface that was unaffected by the presence of bound zinc sulphate and silver nitrate, but a highly significant reduction was caused when copper sulphate was present. The behaviour of the Carbopol 971P-copper sulphate solution during dialysis against sodium chloride/calcium chloride release medium is most likely occurring in the presence of artificial saliva, which may result in the gradual removal of precipitated complex through repetitive washing. Cations present in artificial saliva bind to negatively charged carboxyl groups through electrostatic interaction causing dehydration of the polymer chains and reduction in chain expansion, which enable the formation of binuclear copper-carboxyl complexes. In the presence of zinc sulphate the reduction in chain expansion may result in an increase in the polymer cross-linking by the divalent zinc ions, which is also caused by calcium in the artificial saliva (Kriwet and Kissel. 1996). This may result in some precipitation of the polymer, although this does not cause a significant reduction in the adsorption to the surface measured by stain intensity. In addition, repetitive washing in artificial saliva may cause some displacement of the zinc ions through direct competition. Silver nitrate would be affected to a lesser extent by the washing procedure with artificial saliva as direct competition through other cations would cause a rapid removal of silver ions from the negatively charged carboxyl groups, as demonstrated earlier. Therefore no difference between the positive control and Carbopol 971P-silver nitrate solution would be expected.

3.3.5 *In vitro* assessment of bioadhesion II: Texture probe analysis

Texture probe analysis was used to measure the adhesive forces between lyophilised polymer samples and porcine oesophageal mucosa. The negative control ethylcellulose demonstrated no measurable work of adhesion or maximum detachment force following contact with the mucosa for 5 min in artificial saliva (Figure 3.12 and Figure 3.13).

Lyophilised Carbopol 971P was compared with lyophilised Carbopol 971P-metal complex to elucidate any potential disruption to the process of bioadhesion through the interruption of bond formation and chain interpenetration. The work of adhesion and maximum detachment force exhibited by lyophilised Carbopol 971P-zinc and Carbopol 971P-silver complexes were not significantly different to the positive control ($P > 0.05$). However, the work of adhesion and the maximum detachment force demonstrated by the Carbopol 971P-copper complex were significantly different to the positive control, with $P < 0.01$ and $P < 0.05$ respectively. This confirms the observations made for the direct staining experiment utilising artificial saliva as the washing solution and further supports the use of both techniques simultaneously to examine bioadhesion.

The work of adhesion provides information regarding the extent of polymer chain interpenetration (Park and Munday. 2002). The use of lyophilised polymer samples greatly increases the rate of hydration due to the porous structure produced by the lyophilisation process (Risbud *et al.*, 2002; Llabot *et al.*, 2004). It is less likely therefore that differences in adhesive forces measured are the result of substantial differences in hydration rate and polymer swelling. The work of adhesion measured by the Carbopol 971P-zinc complex was slightly lower than both the positive control and the Carbopol 971P-silver complex (Figure 3.12). Although this difference is not significant it does lend support to the theory regarding the influence of divalent zinc ions on the polymer chains in artificial saliva. Ionic-cross-linking by divalent zinc and calcium ions occurs to a greater extent as chain expansion reduces under conditions of increased ionic strength. This decreases the mobility of the chains, which may limit chain interpenetration. The average work of adhesion exhibited by the positive control and Carbopol 971P-silver complex are close in value (Figure 3.12), expected if the processes occurring at the bioadhesive interface are similar. Increased variation in the measured work of adhesion of the Carbopol 971P-silver complex may be due to the formation of insoluble silver chloride within the polymer structure, lower values may be obtained when these insoluble salts are gathered near the bioadhesive interface. In the case of the Carbopol 971P-copper complex, the highly significant reduction in work of adhesion may be attributed to either: 1) the formation of an insoluble precipitate at the bioadhesive interface which then interferes with the interactions between the two surfaces, or, 2) the formation of a binuclear copper-carboxyl complex which reduces the

chain flexibility to a greater extent than the zinc and calcium ions, which affects chain interpenetration.

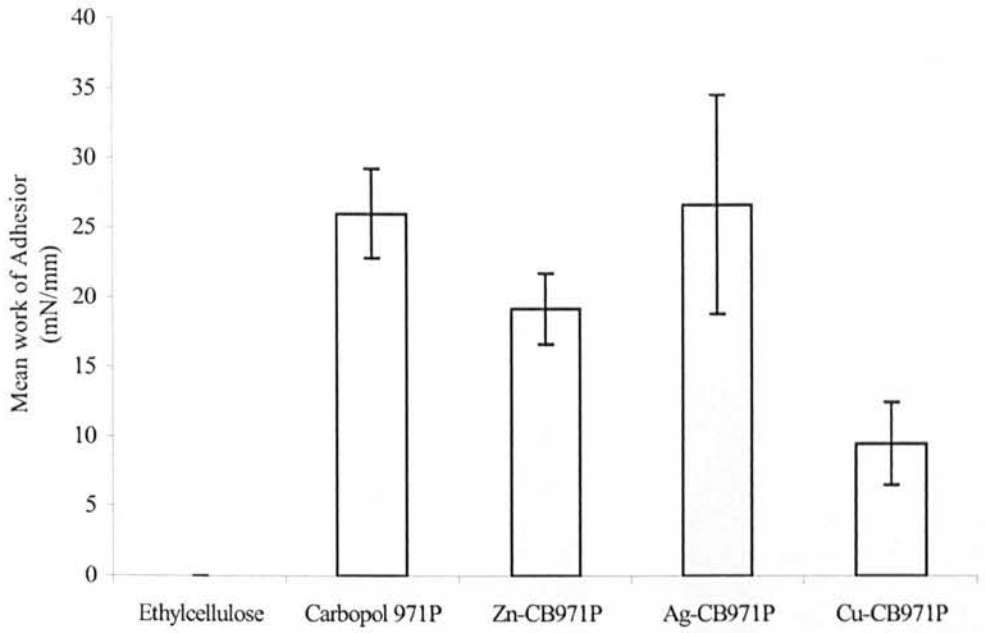

Figure 3.12 Texture probe analysis of lyophilised polymer samples using a model mucosal surface in artificial saliva to give the work of adhesion. Polymer samples are represented as Zn-CB971P, Ag-CB971P and Cu-CB971P for Carbopol 971P-zinc, Carbopol 971P-silver, and Carbopol 971P-copper complexes respectively. (n=6, ± SD)

The maximum detachment force provides information regarding the development of secondary bonds between the material and the substrate (Park and Munday. 2002). The values obtained for the maximum detachment force exhibited by the positive control and the Carbopol 971P-zinc and Carbopol 971P-silver complexes were almost identical, indicating that both silver and zinc ions do not interfere with the formation of secondary bonds (Figure 3.13). Although zinc may cause a reduction in chain flexibility, it is unlikely to affect the carboxyl groups available for secondary bonding to the mucosal surface. Likewise, silver may be rapidly removed from the hydrated polymer through direct competition with other cations within the artificial saliva, resulting in a limited interference in secondary bond formation. The presence of copper however did cause a significant reduction in the maximum detachment force; this may again be due to the formation of an insoluble Carbopol 971P-copper interaction product, probably due to

the formation of binuclear complexes as previously described. If insoluble products are forming at the bioadhesive interface then carboxyl groups become unavailable for interaction with the mucosal substrate. The behaviour of the Carbopol 971P-copper complex under experimental conditions where multivalent cations are present suggests that copper is binding to the polymer more effectively than both zinc and silver, which become unfavourable for good bioadhesion to occur.

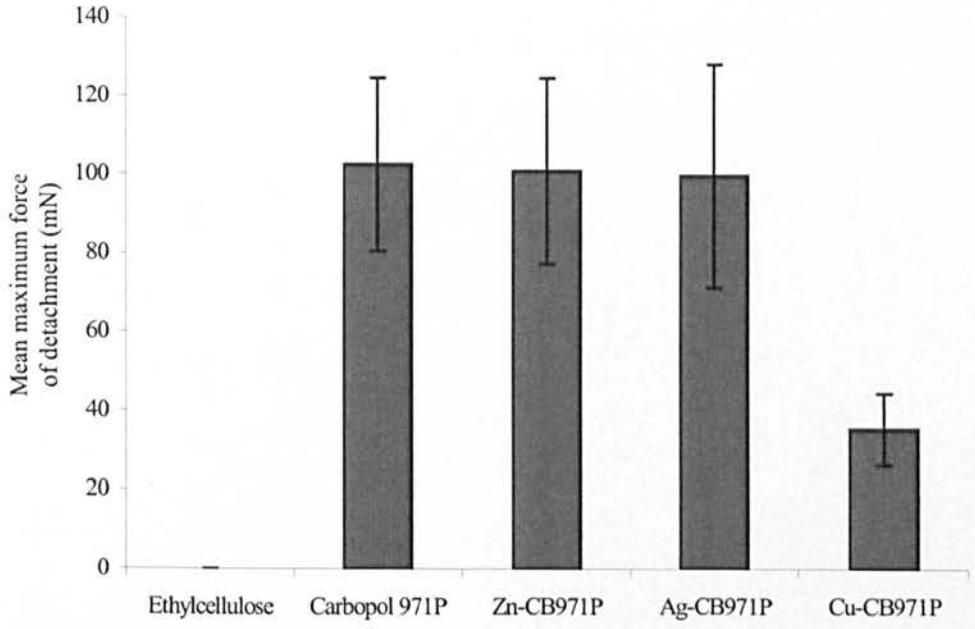

Figure 3.13 Texture probe analysis of lyophilised polymer samples using a model mucosal surface in artificial saliva to give maximum detachment force. Polymer samples are represented as Zn-CB971P, Ag-CB971P and Cu-CB971P for Carbopol 971P-zinc, Carbopol 971P-silver, and Carbopol 971P-copper complexes respectively. (n=6, ± SD)

3.4 Conclusions

- Copper, silver and zinc ions can interact with Carbopol 971P through electrostatic interactions with the negatively charged carboxyl groups on the polymer backbone.
- The metal ions remain associated with the polymer in deionised water.
- Zinc is displaced from the polymer in the presence of sodium and calcium ions at a rate which is affected by the pH of the release medium. The rate of zinc displacement is controlled by the dissociation of ion pairs through competition with cations.
- Silver is displaced from the polymer in the presence of sodium and calcium at a rate which is not altered from the rate of silver diffusion from an aqueous solution. Changing the pH of the release medium had no effect on the rate of displacement.
- Copper forms an insoluble interaction product in the presence of cations demonstrating a clear incompatibility. This may be due to the formation of binuclear complexes following a reduction in polymer chain expansion.
- Both silver and zinc ions had no significant detrimental effect on the adsorption of the Carbopol 971P-metal complex to buccal cells from solution and the tensile strength measured between porcine oesophageal mucosa and lyophilised polymer discs using texture probe analysis.
- Copper did not cause a reduction in the adsorption of the polymer complex onto the surface of buccal cells prepared in sucrose. However, under artificial saliva a significant reduction was detected. This was mirrored in the texture analysis of the lyophilised polymer samples in artificial saliva.

Chapter 4

Development of a chitosan-fluoride oral delivery system

4.1 Introduction

4.1.1 Background

In Chapter 3, Carbopol 971P was investigated as a potential bioadhesive carrier of the antimicrobial metals, zinc, silver, and copper. The interaction between the polymer and the metal ions was ionic in nature and, in the case of zinc and silver, did not diminish the bioadhesive properties of the polymer. In this section, chitosan was investigated as a potential carrier of negatively charged fluoride compounds. The formulations produced were evaluated in terms of *in vitro* drug release and bioadhesion. Both are important factors in determining the suitability of the formulation for the application.

The inclusion of fluoride in water and oral healthcare products produces an anti-caries effect by preventing demineralisation of enamel and driving remineralisation through the formation of fluoroapatite and fluoridated calcium phosphate phases. The formation of fluoroapatite lowers the dissolution pH and promotes remineralisation (Cowan. 1992; Vivien-Castioni *et al.*, 1998). Fluoride had previously been considered only in this capacity; however research has clearly indicated that anti-caries activity is the result of a combination of both its effect on tooth mineral and antimicrobial activity (Marquis *et al.*, 2003). Fluoride ions or hydrofluoric acid modulate microbial physiology, which alters the cariogenic behaviour of oral bacteria through several mechanisms, these include the sensitisation of biofilms to acid damage, reduction of acid production through the inhibition of enzymes involved in glycolysis and the disruption of bacterial adherence and glucose incorporation (Zameck and Tinanoff. 1987; Cox *et al.*, 1994; Balzar Ekenback *et al.*, 2001; Marquis *et al.*, 2003). Fluoride is included in almost all oral healthcare preparations, most commonly as sodium fluoride and/or sodium monofluorophosphate. Sodium fluoride is considered by some to be superior to sodium monofluorophosphate in terms of relative anticaries efficacy (Stookey *et al.*, 1993; Johnson. 1993).

The continuous presence of low fluoride concentrations in the fluid phase surrounding the teeth is considered essential to have an optimal cariostatic effect and forms the basis

of fluoride controlled release formulations such as tablets (Diarra *et al.*, 2003; Owens *et al.*, 2005). Achieving sustained low fluoride concentrations following the use of oral healthcare products may significantly improve anticaries efficacy through the prevention of enamel demineralization, promotion of remineralisation, and modulation of bacterial growth.

Chitosan is a cationic polysaccharide that exhibits moderate bioadhesion within the oral cavity from aqueous dispersion (Patel *et al.*, 1999, 2000; Kockisch *et al.*, 2001). Lyophilised chitosan disks demonstrated measurable adhesion forces against porcine oesophageal mucosal in artificial saliva (section 2.3.2.2). Chitosan microparticles prepared using a water in oil (W/O) solvent evaporation technique remained adhered to mucosal tissue longer than poly(acrylic acid) microparticles and exhibited favourable controlled-release behaviour of triclosan over 8 h (Kockisch *et al.*, 2003, 2005). In addition, chitosan demonstrates toxicity towards several species of oral bacteria (Singla and Chawla. 2001; Ikinci *et al.*, 2002; No *et al.*, 2002) and reduces plaque formation and counts of salivary Streptococci after a 14-day rinsing period (Sano *et al.*, 2003). The formulation of chitosan and fluoride in combination may produce desirable results through both the control of dental plaque and the maintenance of enamel integrity.

4.1.2 Detecting free fluoride using potentiometry-Fluoride ion selective electrodes

Electrodes with a selective response to particular ions have been widely used for many years, e.g. pH electrodes. A number of ion selective electrodes have been fabricated to monitor selectively the activity of certain ions in solution both continuously and non-destructively (Willard *et al.*, 1988). Ion selective electrodes sensitive to ions such as Ca^{2+}, K^{+}, CN^{-}, S^{2-} and F^{-}, have all been developed and have numerous applications in laboratory analysis, industry, process control, physiological measurements and environmental monitoring. The potential of an ion selective electrode is actually composed of two or more discrete contributions arising from the various processes at the interface and in the bulk of the active membrane material (Willard *et al.*, 1988). If charge separation occurs between ions at an interface, a potential difference is generated across that interface. In the fluoride ion selective electrode, a single crystal of lanthanum fluoride doped with europium (II) forms the selective interface, which allows

specific interaction with the fluoride ion (Figure 4.1). Within the fluoride ion selective electrode, 0.1 M sodium fluoride controls the potential of the inner surface of the lanthanum fluoride crystal and is known as the internal solution. When the ion selective electrode is placed in contact with a sample, the activity of the fluoride ion will govern the response of the external surface of the lanthanum fluoride crystal, generating a potential difference across the interface. The electrode potential is related to the logarithm of the concentration of the measured ion, described by the Nernst equation. An internal reference electrode composed of a silver/silver chloride wire in 0.1 M potassium chloride is located within the fluoride ion selective electrode and has a known and constant potential at a particular temperature, which is independent of the sample solution composition. In practice, the potential difference i.e. the electromotive force (emf) is measured between an ion selective electrode and an external reference electrode placed in the sample solution. The determination of fluoride concentration within this investigation utilised a silver/silver chloride reference electrode (Figure 4.1). Electrical contact between the sample and the reference electrode occurs at the liquid junction.

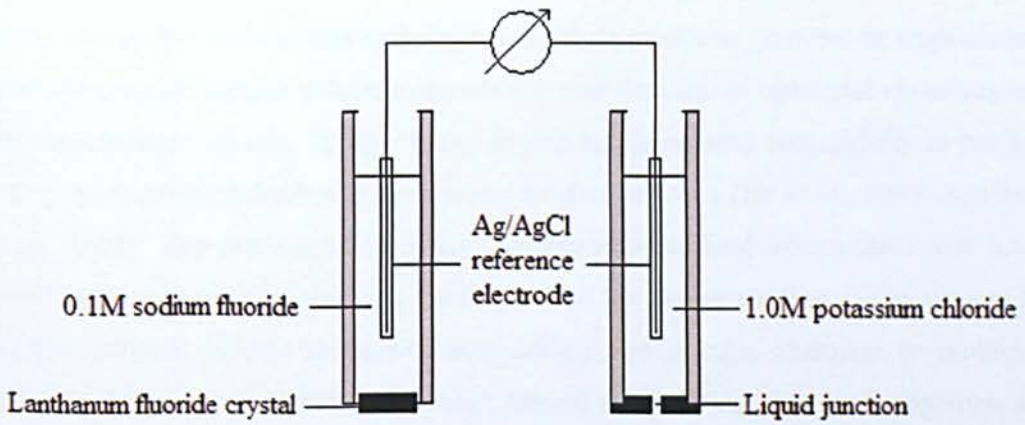

Figure 4.1 Experimental set-up for the determination of fluoride within a sample using an ion selective electrode.

The concentration of fluoride within an unknown sample solution can be determined using direct potentiometry and a calibration curve generated using a series of standard fluoride solutions. To produce a linear response between the signal measured (emf) and the Log^{10} fluoride concentration (mol dm^3), a constant ionic strength must be maintained between each calibration standard and the samples to be measured. Ion

selective electrodes measure the concentration of ions in equilibrium at the membrane surface (Koryta. 1975; Willard *et al.*, 1988). The activity coefficient (γ) is the ratio of the activity, described as the effective concentration measured at the electrode membrane, divided by the concentration. In dilute solutions the concentration of ions is directly related to the total number of ions, hence the activity coefficient is equal to 1. However at higher concentrations, inter-ionic interactions between all ions in solution reduce their mobility, causing inaccurate determinations of electromotive force. Increasing ionic strength therefore reduces the activity coefficient towards 0. The use of a total ionic strength adjustment buffer in known standard solutions and unknown samples produces a uniform ionic strength, allowing direct determination of sample fluoride concentration from the calibration curve. Itota *et al.* (2004) used a direct potentiometry technique utilising a fluoride ion selective electrode to analyse the release of total fluoride from resin-based dental materials.

4.1.3 Manufacturing microparticles by spray drying

Spray drying is a widely used technique to produce powders, granules or agglomerates from aqueous or organic solutions, emulsions and the like, in industrial chemistry and the food industry (Buchi. 2002). Spray drying has been used successfully to produce micro- and nanoparticles based on chitosan for drug delivery (He *et al.*, 1999; Agnihotri *et al.*, 2004). The process involves the transformation of feed from a fluid state into a dried particulate form by spraying the feed into a hot drying medium. The aims of the method include; volume reduction, easy dosing and storage, chemical or biological stability, defined particle size distribution, altered physical and chemical properties, and a large specific surface (Buchi. 2002).

Four main process steps make up the spray drying procedure; 1) feeding, 2) dispersion, 3) evaporation, and 4) separation. The feed used for the production of chitosan microparticles typically involves the dissolution of chitosan in aqueous acetic acid solution; drug is then dissolved or dispersed in the solution following which, a suitable cross-linking agent is added if required (He *et al.*, 1999; Giunchedi *et al.*, 2002; Agnihotri *et al.*, 2004). The solution is fed into the spray dryer using a peristaltic pump, which draws the sample to the spray nozzle at a defined rate. Dispersion of the sample

solution is achieved using a pressure nozzle, a two fluid nozzle, a rotary disk atomiser or an ultrasonic nozzle. In the Buchi B-290 bench-top spray dryer a two fluid nozzle is employed for the atomisation of the sample solution. The sample is dispersed, or atomised, through the spray nozzle and is sprayed in the same direction as the flow of hot air through the apparatus, this is known as co-current flow (Figure 4.2). The air stream is sucked through the device by the aspirator motor and heated electrically to achieve the desired inlet temperature, which is measured prior to flowing into the spray cylinder. As soon as droplets of the spray come into contact with the drying air, evaporation takes place from the saturated vapour film, which is quickly established at the droplet surface (Buchi. 2002). The outlet temperature of the air and solid particles is measured before entering the cyclone and is governed by the inlet temperature, aspirator flow rate, peristaltic pump rate and the concentration of the sample solution. Separation of the dried product from the air stream occurs both at the base of the spray cylinder and in the cyclone (Figure 4.2). In the cyclone, particles are separated based on inertial forces and are collected in the collecting vessel.

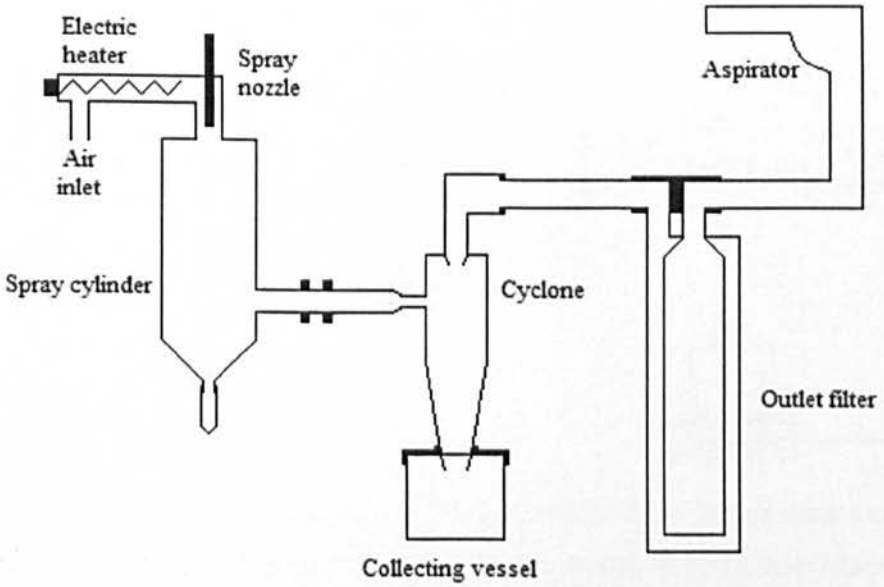

Figure 4.2 Functional components of the spray dryer, which operates according to a co-current air and product stream. Image adapted from Buchi (2002).

Control of various process parameters can be used to obtain a desired particle size; these include the size of the nozzle, spray flow rate, atomisation pressure and inlet air

temperature (Agnihotri *et al.*, 2004). For example, higher spray flow rates and a smaller nozzle size tend to result in smaller particles. In addition, the residual moisture content of the dried product is governed by specific interaction of individual process parameters, for example, larger temperature differences between the inlet and outlet temperatures result in a larger amount of residual moisture (Buchi. 2002).

4.1.4 Particle sizing using laser diffraction

Laser light scattering, termed laser diffraction, is used to measure the size structure of any one material phase in another. For reliable measurements, each phase must be distinct optically from the other and the medium must be transparent to the laser wavelength. Laser diffraction has been used in numerous studies to characterise the size of bioadhesive microparticles in drug delivery research (He *et al.*, 1999; Lim *et al.*, 2000; Giunchedi *et al.*, 2002; Kockisch *et al.*, 2003).

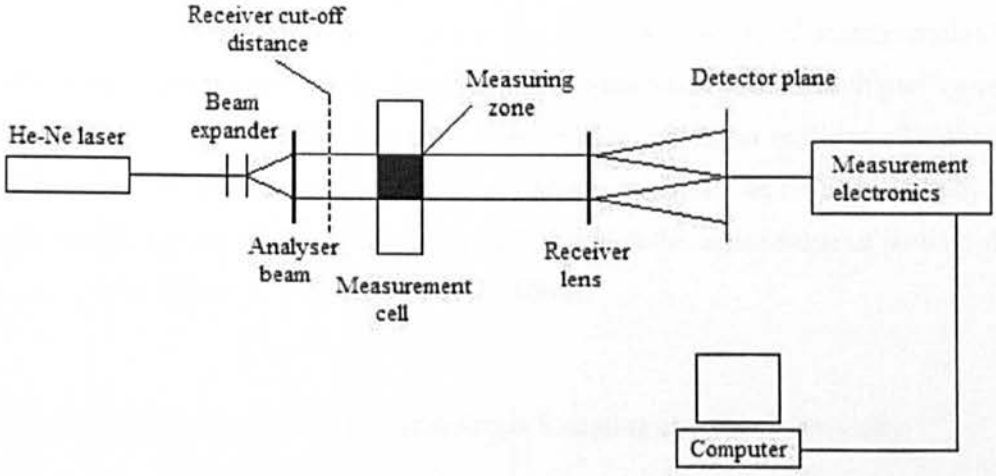

Figure 4.3 Laser diffraction set-up utilising a conventional Fourier optics configuration for the measurement of particle size distribution. Image adapted from Malvern (1992).

For the purposes of this work conventional Fourier optics was suitable for the application and the set-up of the laser diffraction experiment is shown in Figure 4.3. The light from a low power Helium-Neon laser (632.8 nm wavelength) is used to form a collimated and monochromatic beam of light known as the analyser beam, typically 18 mm in diameter (Malvern. 1992). The particles are introduced to the analyser beam by

a cell system that pumps the sample to the measurement cell. The sample is continuously stirred during measurements to keep the particles suspended; a single motor, which also pumps the sample around a circulation loop containing the measurement cell, provides this. The receiver lens operates as a Fourier transform lens, forming the far field diffraction pattern of the light scattered by the particles at its focal plane. Unscattered light is focused on the detector and passes through a small aperture, which passes out of the optical system and allows the sample volume concentration to be determined. The detector is composed of a series of 31 concentric annular sections, which gathers the scattered light over a range of solid angles of scatter (Malvern. 1992). The light energy is measured over each of these annular sections and converted to an electronic output signal, which then passes to the computer for analysis. Particle size was determined using the Fraunhofer diffraction model, which states that, independent of size, a particle will extinguish two times the light incidence upon it, half being absorbed within the particle and half being diffracted into non-zero scattering angles (Malvern. 1992).

The use of laser diffraction to determine the size distribution of microparticles has several advantages which include: i) a short time of analysis in which multiple "sweeps" can build up an integral light scattering characteristic based on millions of individual particles, ii) no calibration is required as calculations are based on fundamental physical properties, iii) a wide range of size fractions into which the entire range of particle sizes can be divided (Malvern. 1992; Eshel *et al.*, 2004).

4.1.5 Investigating microparticle morphology- Scanning electron microscopy

The scanning electron microscope has been used to study a range of surfaces in great detail through the production of a three-dimensional image with high resolution (<7 nm) and depth of focus (Prescott *et al.*, 1999). The scanning electron microscope constructs an image by detecting electrons emitted from an objects surface, unlike other forms of electron microscopy, in which electrons transmitted through the sample form the image. Air-dried samples do not require preparation before viewing with the scanning electron microscope, although specimens can be coated with metal such as gold, known as sputter coating, to; i) prevent the charge build-up on the specimen surface, and ii)

increase the emission of secondary electrons. Sputter coating is used to improve the quality of the image produced.

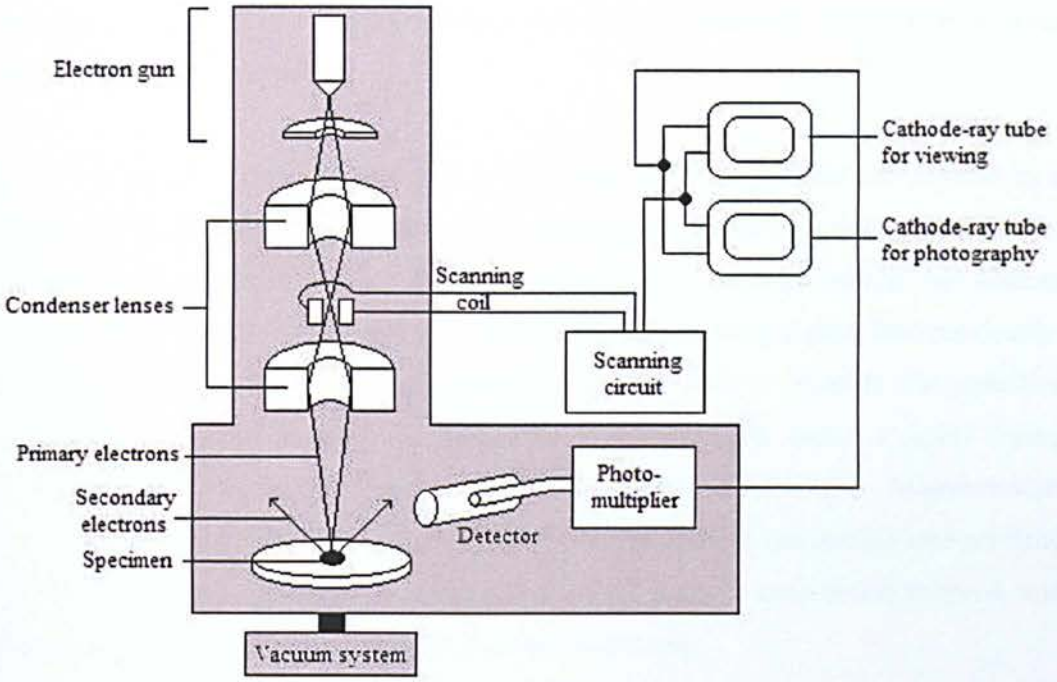

Figure 4.4 Schematic presentation of a scanning electron microscope. Image adapted from Prescott *et al.* (1999).

Primary electrons are generated by an electron gun, situated at the top of the scanning electron microscope (Figure 4.4). Typically, a tungsten filament functions as the cathode and is heated by applying a voltage. The anode, which is positive with respect to the cathode, causes electrons to be emitted from the surface of the filament, which are then accelerated by an electric field. In general, electrons are accelerated in a potential difference of the order 10-20 keV. Electromagnetic condenser lenses are used to focus the electron beam, which is scanned back and forth over the specimen by the scanning coil. When the primary electrons strike the specimen, surface atoms discharge a tiny shower of electrons known as secondary electrons (Prescott *et al.*, 1999). Secondary electrons that enter the detector hit a scintillator causing it to emit light flashes, which are converted into electrical signals and amplified by the photomultiplier (Figure 4.4). The signal is then passed to a cathode-ray tube, which produces an image of the surface. The number of electrons that enter the detector modulates the image produced by the

scanning electron microscope. The impact of primary electrons on a raised surface will cause a large amount of secondary electrons to enter the detector; therefore these areas appear lighter in the image. Secondary electrons generated at a depression in the surface are less likely to escape the surface and enter the detector; therefore these areas appear darker in the image.

In this chapter, the use of a chitosan and fluoride combination was investigated as a potential antimicrobial complex for local delivery to the oral cavity. Initially, the interaction between chitosan and fluoride in the form of sodium fluoride and sodium monofluorophosphate was investigated using a dialysis technique described previously. Fluoride was quantified using direct potentiometry with a fluoride ion selective electrode. Chitosan-fluoride microparticles were prepared using a spray-drying technique and a water-in-oil emulsion solvent evaporation technique. Microparticles were characterised according to particle size, fluoride loading and release into artificial saliva, bioadhesion to porcine oesophageal mucosal using texture probe analysis, and morphology, determined by scanning electron microscopy.

4.2 Materials and Methods

4.2.1 Materials

Medium (Lot Nº 408499/1) and high viscosity (Lot Nº 414555/1) chitosan were purchased from Fluka Chemicals Ltd (Derbyshire, UK). HCMF (Lot Nº GR23238901) was kindly donated by Cognis Deutschland GmbH Company (Illertissen, Germany). Protasan CL113 chitosan chloride salt (Lot Nº FP-110-02) was purchased from FMC Biopolymer (Philadelphia, USA). Sodium monofluorophosphate (sodium monofluorophosphate) was kindly donated by GlaxoSmithKline R&D (Weybridge, UK). Glutaraldehyde solution (50% w/v in water) was purchased from BDH Chemicals (Poole, UK). Polyvinylidene fluoride (PVDF) dialysis membrane, molecular weight cut-off 250,000 Da 1.8 $mLcm^{-1}$, was purchased from Spectrum laboratories (Rancho Dominguez, USA). Sodium fluoride, sodium acetate trihydrate, ethylenediaminetetraacetic acid, tetrasodium salt dihydrate and sodium dihydrogen phosphate monohydrate were all of ACS reagent grade and purchased from Sigma-Aldrich Company Ltd (Gillingham, UK). All other chemicals used in this investigation were purchased from Fisher Scientific UK Ltd (Loughborough, UK). All chemicals were used as received without further treatment unless otherwise stated.

4.2.2 Methods

4.2.2.1 Preparation and characterisation of chitosan-fluoride complexes

4.2.2.1a Preparation of polymer dispersions and fluoride solutions

Medium and high viscosity chitosan and HCMF (0.1 g) were dispersed in 1% v/v acetic acid (40 mL) under constant stirring at 300 rpm using a magnetic stirrer (Stuart, Heat-Stir CB192). CL113 (0.1 g) was dispersed in deionised water (40 mL) due to the solubility of the chitosan chloride salt. After stirring for 4 h, the pH of the dispersions were adjusted to 4.5 using 0.1 M sodium hydroxide and made up to 100 mL volume

using deionised water to obtain 0.1% w/v concentration. Aqueous chitosan dispersions were sealed and stored at 4°C until use with an expiry date set at 1 week from preparation.

Fluoride solutions were prepared in deionised water at a concentration of 23.2 mM (1.65 g sodium monofluorophosphate in 500 mL, 0.49 g sodium fluoride in 500 mL). Chitosan-fluoride solutions were prepared by slowly adding 23.2 mM sodium monofluorophosphate or sodium fluoride (10 mL) to 0.10% w/v aqueous chitosan dispersions at pH 4.5 (10 mL) stirred at approximately 300 rpm with a magnetic stirrer.

4.2.2.1b Stability of chitosan-fluoride complexes

PVDF dialysis membrane (approx. 25 cm) was prepared as previously described (section 3.2.2.1c) and pre-equilibrated overnight in either sodium monofluorophosphate or sodium fluoride, according to the complex being dialysed.

Prior to the experiment, dialysis tubing was washed in deionised water. Chitosan-fluoride solution (20 mL) prepared 30 min prior to dialysis was transferred to the dialysis tubing using a bulb pipette (20 mL, Fisher) and secured with dialysis clips. The dialysis tubing was subsequently immersed in 480 mL deionised water under constant stirring at 400 rpm using a magnetic stirrer. Aliquots of 20 mL were removed at 2 hourly intervals for 8 h and were replaced with fresh deionised water. After 8 h, the dialysis tubing was transferred to fresh deionised water (480 mL) under stirring and a final sample was removed after 24 h. The detection of fluoride within the receptor phase was compared to an experimental control composed of either aqueous 11.6 mM sodium fluoride or 11.6 mM sodium monofluorophosphate solution (20 mL).

High viscosity and medium viscosity chitosan, HCMF and CL113 were each assessed with sodium monofluorophosphate against deionised water. High viscosity chitosan only was assessed for stability with sodium fluoride. Each chitosan-fluoride solution was tested a minimum of three times.

4.2.2.1c Displacement of fluoride from the chitosan complex

PVDF dialysis membrane was prepared as before. A solution of 1.5 mM calcium chloride adjusted to isotonicity with sodium chloride (0.22 g calcium chloride, 8.913 g sodium chloride in 1 L deionised water) was used as the release medium for the analysis of high viscosity chitosan-sodium monofluorophosphate and sodium fluoride complexes.

Chitosan-sodium monofluorophosphate solution (10 mL) was added to double strength isotonic solution (10 mL) immediately prior to the experiment and transferred to the dialysis tubing as previously described. The dialysis tubing was secured with dialysis clips and immersed in 480 mL single strength isotonic solution under constant stirring at 400 rpm. Samples were collected as before. The displacement of fluoride from high viscosity chitosan was compared to a sodium monofluorophosphate control comprising aqueous 11.6 mM sodium monofluorophosphate or sodium fluoride solution (10 mL) and double strength isotonic solution (10 mL).

Each experiment was performed three times at three different pHs; 4.0, 5.5 and 7.0. The pH of the isotonic solution was adjusted with 0.1 M sodium hydroxide or 0.1 M hydrochloric acid.

4.2.2.2 Analysis of fluoride samples using an ion selective electrode

4.2.2.2a Preparation of ionic strength (IS) adjustment buffers

Ionic Strength (IS) adjustment buffers were prepared as follows:

IS diluent: 100.0 g ethylenediaminetetraacetic acid, 100.0 g sodium acetate and 15.0 g sodium hydroxide were added to 800 mL deionised water in a plastic 1 L plastic volumetric flask. Concentrated hydrochloric acid (50 mL) was added and the solution stirred on a magnetic stirrer until mixed. The pH of the resultant solution was adjusted to 7.25 (±0.03) using concentrated hydrochloric acid and made up to 1 L volume with deionised water.

80\20 diluent: 200 mL deionised water was measured into a 1 L plastic volumetric flask and made up to volume with IS diluent. The solution was stirred for 5 min to ensure adequate mixing.

No-acid Added Ionic Strength (NAIS) diluent: 100.0 g ethylenediaminetetraacetic acid, 100.0 g sodium acetate, and 15.0 g sodium hydroxide were added to 800 mL deionised water in a plastic 1 L volumetric flask and stirred using a magnetic stirrer until fully dissolved. The volume was made up to 1 L with deionised water.

4.2.2.2b Preparation of calibration standards

Stock fluoride standard (100 ppm) was prepared by accurately weighing sodium fluoride (0.221 g) and dissolving in 80/20 diluent (1 L) in a plastic volumetric flask. Working standards were prepared by diluting the stock standard with 80\20 diluent to produce fluoride concentrations of 50, 20, 10, 5 and 1 ppm ($\mu g\ mL^{-1}$). Standards were stored at room temperature and expiry dates were set at 56 days from preparation.

4.2.2.2c Calibration of the ion selective electrode

The fluoride ion selective electrode (Hach Loveland CO 80537) was pre-conditioned in 0.1 M sodium fluoride for at least 30 min before use at room temperature. The electromotive force (mV) of each calibration standard was measured by immersing the fluoride ion selective electrode and silver/silver chloride reference electrode (Fisher) into the solution under stirring and recording a steady reading (mV) on an ionic strength analyser (Phillips PW9416). The electrodes were rinsed in deionised water and gently blotted with a tissue between measurements. The temperature of the calibration standards was measured using a pH/mV/°C meter (Accumet- AP6) to ensure that solution temperatures were within ± 1°C of each other. The calibration standards were measured from the lowest to the highest fluoride concentration.

Electromotive force (mV) was plotted against Log^{10} fluoride concentration (mol dm^{-3}) to yield a linear calibration curve (Appendix 3). The reproducibility of fluoride analyses and limits of detection of the fluoride ion selective electrode was assessed to

ensure data reliability. The fluoride ion selective electrode was calibrated prior to sample analyses to compensate for electrode drift and variations in ambient temperature between days.

4.2.2.2d Analysis of fluoride samples

Samples (15 mL) were transferred into a 100 mL plastic volumetric flask using a bulb pipette (Fisher). Following the addition of concentrated hydrochloric acid (4 mL) and deionised water (1 mL) the samples were stirred for 1 h to ensure adequate hydrolysis and liberation of free fluoride. Samples were then diluted to volume (100 mL) with NAIS diluent and the electromotive force (emf) was measured using the calibrated fluoride ion selective electrode. Log^{10} fluoride concentration (mol dm^{-3}) of the sample was calculated from the calibration curve using the following equation:

$$Log^{10}F^{-}concentration = \left(\frac{\varepsilon - c}{m}\right)$$

Where ε = emf (mV)

c = y-axis intercept of calibration curve

m = gradient of calibration curve

Cumulative release was calculated by the sum of the uncorrected concentration of prior sampling from the first sample to the n^{th} – 1 sample relative to the sample volume (section 3.2.2.1e). The amount (μg) of fluoride released from within the dialysis tubing following each time interval was calculated from the corrected fluoride concentration of the release medium (480 mL). The mean cumulative amount of fluoride released at each sampling time was calculated and expressed in terms of percentage (%) total fluoride released from the dialysis tubing. Fluoride solutions used to prepare the donor phase were diluted in deionised water by a factor of 5 and prepared as per the samples for fluoride analysis described previously. Six replicates were measured to determine total fluoride added to the chitosan dispersion.

4.2.2.3 Preparation of chitosan-fluoride microparticles

4.2.2.3a Preparation of aqueous phase

The composition of the aqueous phases used to produce a range of chitosan-fluoride microparticles are described in Tables 4.1 and 4.2. To prepare the aqueous phase chitosan (HCMF) was initially solubilised in 1% v/v acetic acid (40 mL), sealed and stirred overnight using a magnetic stirrer (Fisher). Sodium fluoride or sodium monofluorophosphate were dissolved in deionised water (10 mL) and added drop wise to the aqueous chitosan dispersion to give a final volume of 50 mL. Glutaraldehyde solution was diluted in deionised water to produce working concentrations of 0.5% w/v and 0.05% w/v. Appropriate volumes of working glutaraldehyde solutions were added to the aqueous phase 5 min prior to spray drying (Table 4.1).

4.2.2.3b Preparation of microparticles using spray drying

Chitosan-fluoride microparticles were prepared by spray drying using a Buchi B290 mini spray drier with a 0.7 mm nozzle at the School of Pharmacy and Biomedical Sciences, University of Portsmouth (Portsmouth, UK). The aqueous phase (Table 4.1) was fed to the nozzle using a peristaltic pump with a feed flow of 8 mL min^{-1}. The drying conditions were as follows: spray flow rate of 35 m^3 h^{-1}, compressed air flow rate of 600 Nl h^{-1}, inlet air temperature of 130°C and outlet air temperature of 65°C. The dry product was then collected in a collection bottle, weighed and stored in a desiccator until use. Deionised water (50 mL) was aspirated both before and after aqueous samples were spray dried to clean the feed lines. Initially one batch of each sample was prepared for preliminary evaluation. Three batches were later prepared from an optimum aqueous phase formulation both with and without sodium fluoride.

Table 4.1 Composition of the aqueous phase for the production of chitosan-fluoride microparticles using a spray drying technique.

Sample ID	Chitosan (g)	Glutaraldehyde (g)	Sodium Fluoride (g)
HCMF I	0.5	-	0.1
HCMF II	0.5	0.0005	0.1
HCMF III	0.5	0.025	0.1
HCMF IV	1.0	-	0.2
HCMF V	1.0	0.001	0.2
HCMF VI	1.0	0.05	0.2

Table 4.2 Composition of the aqueous phase used for the production of chitosan-fluoride microparticles using water in oil solvent evaporation technique.

Sample ID	Chitosan (g)	Sodium fluoride (g)	Sodium monofluorophosphate (g)
HCMF VII	1.0	-	0.05
HCMF VIII	1.0	0.2	-
HCMF IX	1.0	-	-

4.2.2.3c Preparation of microparticles using water in oil (W/O) emulsion solvent evaporation technique

Light white mineral oil (250 mL) containing 2% v/v Span 80 was placed in a 600 mL glass beaker and stirred using a magnetic stirrer bar (50 x 8 mm) and stirrer (Stuart, Heat-Stir CB192). The oil was heated to a constant temperature of 60°C and monitored using a temperature probe (Accumet- AP6). The aqueous phase (25 mL) was added to the heated oil drop wise using a hypodermic syringe (cap. 50 mL) and the emulsion left under constant temperature and speed for a minimum of 8 h.

Once adequate time had elapsed the W/O emulsion was removed from the heat and allowed to cool slightly. Aliquots (50 mL) were centrifuged at 1300 g for 5 min (Sorvall RT6000B) to separate the microparticles from the oil. The oil was decanted

carefully using a 10 mL pipette (Fisher) and the collected microparticles were re-suspended in hexane (25 mL). Suspensions were centrifuged at 1300 g for 5 min and the supernatant discarded. This process was repeated three times to remove oil residues from the microparticles, which were subsequently dried at 50°C for 6 h, weighed and stored in a desiccator until use. Three batches of each sample (Table 4.2) were prepared using this technique.

4.2.2.4 Characterisation of chitosan-fluoride microparticles

4.2.2.4a Particle size

Spray dried microparticles (10 mg) and W/O microparticles (100 mg) were accurately weighed into glass bottles (30 mL) using a precision balance (Mettler Toledo). Microparticle samples were suspended in carrier fluid (20 mL) containing 1% v/v Tween 20 in methanol. Samples were sonicated for 2.5 min prior to particle sizing measurements to ensure adequate suspension of the microparticles within the carrier fluid.

Particle size was determined using a Malvern MasterSizer series 2600 particle sizer with a MS1 small volume cell system and MS23 measurement cell operating on BØ software. Background scattering of the laser was determined prior to measurement of particle size with 80 mL carrier fluid. Initially, the mean particle size was determined following four replicates for each type of microparticle. Microparticles selected for further development were measured six times.

4.2.2.4b Fluoride loading

Chitosan-fluoride and chitosan-only microparticles (10 mg) were suspended in 8 mL deionised water in a 50 mL polycarbonate centrifuge tube (Fisher), and left to swell for 30 min at room temperature. Concentrated hydrochloric acid (2 mL) was added to the samples and placed on an orbital shaker at 200 rpm (Denley orbital shaker) for 60 min at 32°C. NAIS diluent (40 mL) was then added to the solution and the mixture agitated for a further 30 min, after which each sample was centrifuged at 1300 g for 15 min to

collect insoluble chitosan as a pellet. The supernatant was decanted and analysed for fluoride concentration using a calibrated fluoride ion selective electrode (section 4.2.2.4d) within 6 h.

4.2.2.4c *In vitro* fluoride release

Chitosan-fluoride or chitosan-only microparticles (40 mg) were accurately weighed into a 35 mL centrifuge tube (Nalgene, PPCO tubes) and suspended in isotonic solution (10 mL) comprising sodium chloride and 1.5 M calcium chloride at pH 5.5 with gentle mixing. The suspension was then placed on an orbital shaker and incubated at 32°C for 6 h. The amount of fluoride released from the microparticles was measured after 10, 30, 60, 120, 240, and 360 min. Each tube was centrifuged at 6000 g for 10 min (Sorvall RC-5B) and samples (7.5 mL) were removed using a pipette and replaced with fresh isotonic solution. Samples were stored in 35 mL polycarbonate bottles and analysed for fluoride concentration after sample preparation within 24 h.

Samples were transferred to a 50 mL plastic volumetric flask for preparation for fluoride ion selective electrode analysis. Concentrated hydrochloric acid (2 mL) and deionised water (0.5 mL) were added and the solution stirred for 1 h to ensure adequate hydrolysis of the sample. Treated samples were then diluted to 50 mL volume with NAIS diluent and the fluoride concentration measured. The fluoride ion selective electrode was calibrated as previous (section 4.2.2.2c).

Mean fluoride release following each time interval was initially determined following three replicates at pH 5.5. Cumulative fluoride release was calculated as previously described (section 3.2.2.1e). Data was converted into percentage total fluoride released using values determined by fluoride loading experiments (section 4.2.2.4b). Microparticles selected for further development were analysed at pH 4.0 and 7.0 on at least three separate occasions.

4.2.2.4d Texture probe analysis

Microparticle disks were prepared by accurately weighing chitosan-only or chitosan-fluoride microparticles (50 mg) into a KBr disk assembly unit (8 mm diameter) and applying 2 tons of pressure for 10 sec using a KBr press (Specac). The resultant polymer disks were stored in a desiccator before use.

Porcine oesophageal tissue was prepared as previously described in 2.2.2.2b. Texture probe analysis was carried out as described in 2.2.2.2c. In initial studies, the maximum detachment force and work of adhesion was determined following three replicates for each type of microparticle. Microparticles selected for further development were measured six times.

4.2.2.4e Scanning electron microscopy

The morphology of microparticles produced by the spray drying and W/O emulsion solvent evaporation techniques were compared using scanning electron microscopy. Dried microparticles were applied to an adhesive surface mounted onto a scanning electron microscopy stub using a spatula and the excess removed by gently tapping. Samples were viewed using a Zeiss EVO 50EP scanning electron microscope (at GlaxoSmithKline R&D, Weybridge, UK) operating at 10-12.5 keV with Windows® XP based SmartSEM™ control software.

4.2.3 Statistical analysis

Data is presented as the mean ± standard deviation in all protocols within this chapter. Particle size analysis and fluoride loading data produced data that fitted the normal distribution, confirmed by the Kolmogorov-Smirnov test (SPSS v.14), and were analysed using the one-way ANOVA (SPSS v.14) or unpaired two-sample *t*-test assuming unequal variance (Microsoft Excel 2003) to determine significant differences at the 5% probability level. Due to the unequal variance encountered during texture analysis, significant differences between the multiple data sets were determined using Kruskal-Wallis ANOVA test (SPSS v.14). Subsequent significant differences occurring

between each paired location were analysed using the Mann-Whitney U test (SPSS v.14). Both were analysed at the 5% probability level. Comparison of the optimised formulation using texture probe analysis was analysed using the unpaired two-sample *t*-test assuming unequal variance (Microsoft Excel 2003).

4.3 Results and Discussion

4.3.1 Development and stability of aqueous chitosan-fluoride complexes

Chitosan is a linear polyamine with a number of amino groups that are readily available for chemical reaction (Singla and Chawla. 2001). The cationic nature permits it to form complexes with oppositely charged drug(s)/excipient(s). For this reason, chitosan was selected for investigation with the fluoride compounds, sodium fluoride and sodium monofluorophosphate. Both have been used successfully in oral healthcare products as effective anticaries agents (Weyant. 2004). It was hypothesised that chitosan and fluoride would interact ionically as observed previously with negatively charged Carbopol 971P and positively charged metal ions (Chapter 3). Initial investigations into the compatibility of aqueous sodium monofluorophosphate solutions with 0.1% w/v chitosan dispersions yielded a concentration of 23.2 mM sodium monofluorophosphate. Higher concentrations of sodium monofluorophosphate caused chitosan precipitation. However no such observation was noted during the addition of sodium fluoride solutions as high as 148.8 mM to chitosan dispersions. In the previous chapter, the concentration of monovalent silver ions compatible with 0.1% w/v Carbopol 971P was twice that of divalent zinc or copper ions. If the concentration of sodium fluoride compatible with chitosan was twice that of sodium monofluorophosphate, then the difference could be attributed to the valence of the ion. However, since this was not observed it could be assumed that fluoride does not interact with chitosan in a manner similar to sodium monofluorophosphate. To observe the behaviour of the chitosan-sodium fluoride solution in deionised water using the dialysis technique, a concentration of 23.2 mM was selected in order for direct comparisons to be made with the chitosan-sodium monofluorophosphate solution.

The release of fluoride from an 11.6 mM sodium monofluorophosphate control and chitosan-sodium monofluorophosphate solutions was analysed over 24 h in deionised water (Figure 4.5). The fluoride ion selective electrode was used to analyse the concentration of fluoride within the samples. Treatment of the samples removed from the dialysis experiment with concentrated hydrochloric acid ensured that free fluoride

ions were liberated for analysis. It was calculated that the fluoride ion selective electrode had a limit of detection of 0.09 ppm ($\mu g\ mL^{-1}$) (Appendix 3), which equates to a receptor phase concentration of 0.6 ppm as a result of sample preparation. Apart from time 0 h, no sample was found to be below this concentration; hence the fluoride ion selective electrode was deemed suitable for the assessment of fluoride within the dialysis samples. Fluoride released from the sodium monofluorophosphate control was rapid during the first 2 h. The rate of diffusion after 2 h slowed considerably and after 8 h, 89.8% ± 0.7 of total fluoride had been detected within the receptor phase (Figure 4.5). Fluoride was detected within the receptor phase after time 0 h, with a range of 72.7% - 86.2% total fluoride released from the chitosan-sodium monofluorophosphate solutions after 24 h. The rate of diffusion of fluoride from the chitosan-sodium monofluorophosphate solutions was however greatly reduced when compared to the control (Figure 4.5). This indicates that weak interactions between the positively charged amine groups of chitosan and the sodium monofluorophosphate may exist in solution. The release of sodium monofluorophosphate from the chitosan-sodium monofluorophosphate solutions under deionised conditions may be the result of sodium ion diffusion into the receptor phase. This will change the distribution of ions between the donor and receptor phases, possibly resulting in the gradual diffusion of sodium monofluorophosphate into the receptor phase to maintain electrical neutrality.

There is relatively little difference in the rate of fluoride release from each of the chitosan grades, although high viscosity chitosan (Fluka) does retain the greatest amount of fluoride after 24 h (Figure 4.5). This may be due to differences in molecular weight between the chitosan grades. High viscosity chitosan has a higher molecular weight than medium viscosity chitosan, although accurate descriptions of these values are not available from the manufacturer. A higher molecular weight will result in an increased number of amine groups and therefore a higher charge density at pH 4.5, relative to a lower molecular weight. This difference may therefore be the product of a slightly altered equilibrium achieved after 24 h, as a higher charge density would increase the amount of anions retained by chitosan. High viscosity chitosan was therefore selected for investigation with sodium fluoride.

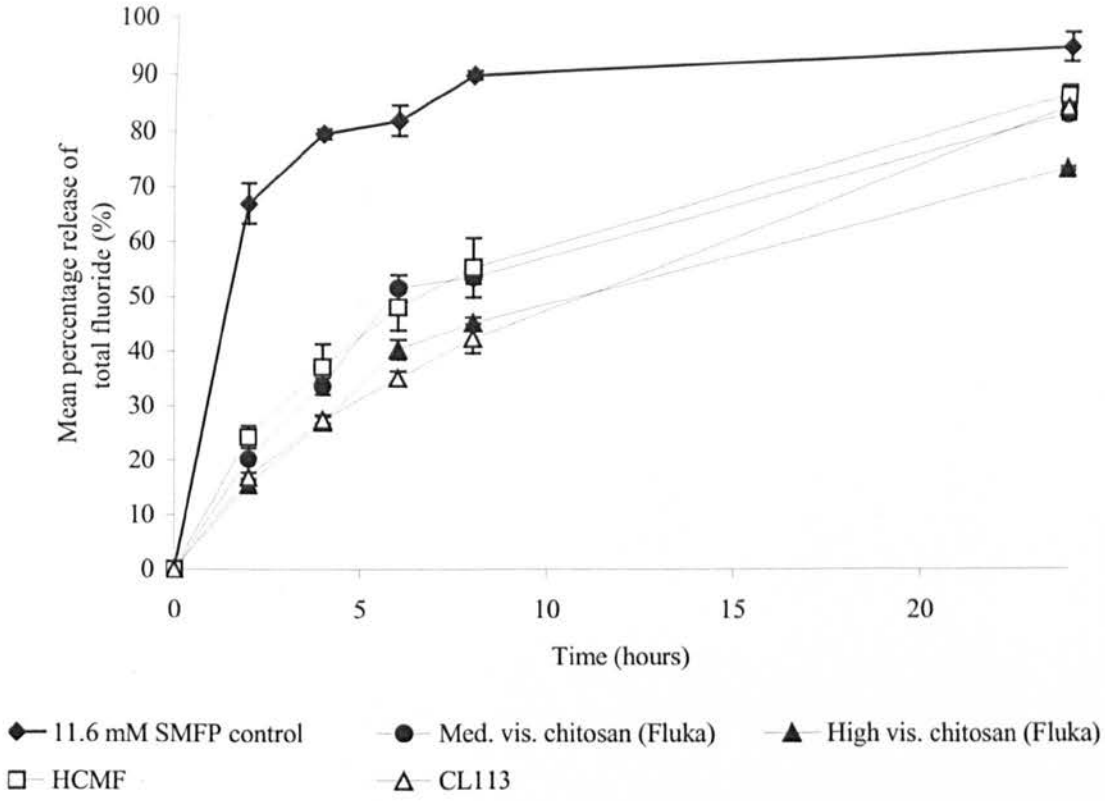

Figure 4.5 Cumulative release of fluoride detected in the release medium when dialysing chitosan-sodium monofluorophosphate solutions in deionised water. The diffusion of fluoride from the polymer solution was compared to an aqueous sodium monofluorophosphate solution. (n=3, ± SD)

The release of fluoride from an 11.6 mM sodium fluoride control and high viscosity chitosan-sodium fluoride solution was analysed over 24 h in deionised water (Figure 4.6). No difference was observed between the rates of diffusion of fluoride throughout the 24 h period. This outcome is in agreement with the earlier interpretation regarding the compatibility of aqueous sodium fluoride solutions with chitosan. It is apparent that no ionic interaction between fluoride and the positively charged amino groups of chitosan exists in solution.

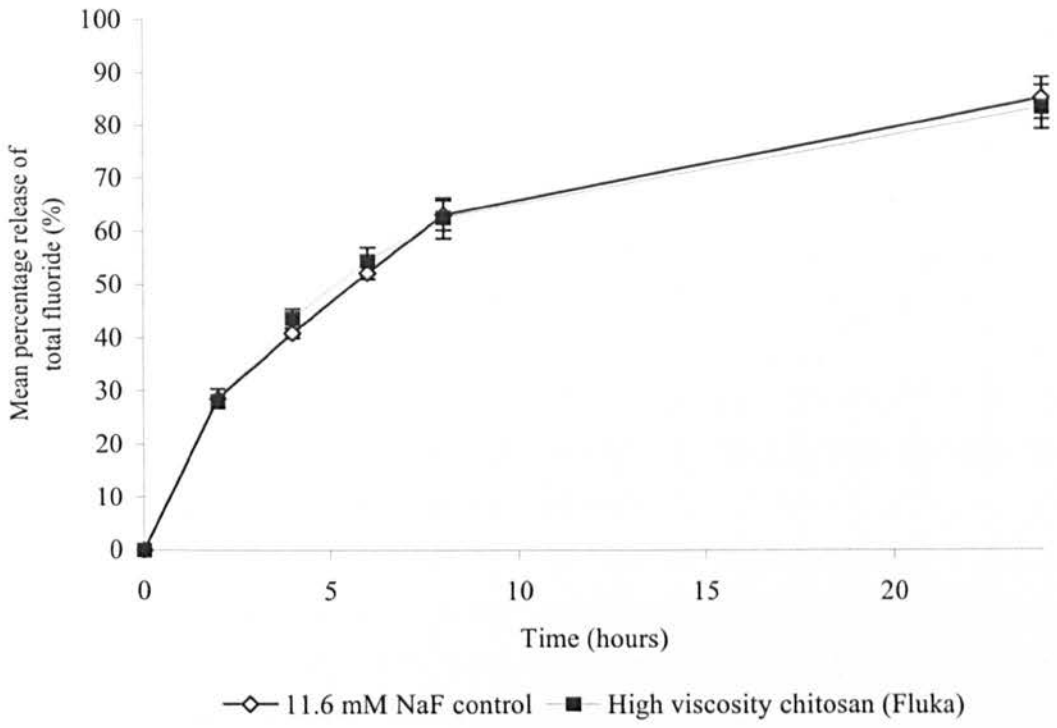

Figure 4.6 Cumulative release of fluoride detected in the release medium when dialysing high viscosity chitosan-sodium fluoride solution in deionised water. The diffusion of fluoride from the polymer solution was compared to an aqueous sodium fluoride solution. (n=3, ± SD)

4.3.2 Displacement of sodium monofluorophosphate from chitosan in isotonic solution

The displacement of sodium monofluorophosphate from high viscosity chitosan-sodium monofluorophosphate solution was assessed in isotonic 1.5 M calcium chloride/sodium chloride solution at clinically relevant pHs over 24 h (Figure 4.7). The rate of sodium monofluorophosphate released during dialysis of the control between 2-8 h achieved a steady state with 4.5% total fluoride detected per h. After 24 h 98.2% ± 1.6 of total fluoride had diffused from the control into the release medium. At all time points, the amount of sodium monofluorophosphate detected in the release medium during the dialysis of high viscosity chitosan-sodium monofluorophosphate solution was lower than the control (Figure 4.7). Despite this, the rate at which sodium monofluorophosphate was released from the chitosan solution was not notably reduced

from the control. For example, after 8 h the amount of free fluoride detected in the release medium from the control was 58.2% ± 1.4, with 45.7% ± 3.0, 51.8% ± 3.6, and 51.9% ± 1.9 released from the chitosan-sodium monofluorophosphate at pH 4.0, 5.5 and 7.0 respectively. The rate of release of sodium monofluorophosphate from chitosan-sodium monofluorophosphate solution in isotonic solution was increased compared to previous observations in deionised water. This suggests that the presence of competing ions increases the rate of displacement of fluoride from the positively charged amino groups of chitosan. However, due to the detection of fluoride throughout the 24 h time period during the dialysis of chitosan-sodium monofluorophosphate solution in deionised water (Figure 4.5), the interaction of sodium monofluorophosphate with the positively charged groups of chitosan is questionable.

After 24 h, the amount of fluoride released at pH 5.5 and 4.0 from the chitosan-sodium monofluorophosphate solution were approximately 10-13% lower than both the control and chitosan-sodium monofluorophosphate solution at pH 7.0. This may be due to an altered conformation of the chitosan polymer as a consequence of release medium pH. The positive charge carried by deacetylated units at a pH < 6.5 causes repulsion between neighbouring units within the chitosan molecule, therefore extending the conformation of the polymer within solution (Singla and Chawla. 2001). Within an isotonic solution at pH 7.0 the charge density of chitosan may be reduced, which could account for the difference between sodium monofluorophosphate released in the control and at pH 7.0, and pH 4.0 and 5.5.

Texture analysis of freeze-dried chitosan- sodium monofluorophosphate did not produce any measurable adhesion forces when using the protocol described in 2.2.2.2c. Initially, this effect was attributed to the amount of sodium monofluorophosphate with respect to chitosan. Reducing the concentration of sodium monofluorophosphate to 1.2 mM however did not improve the adhesion of the freeze-dried chitosan- sodium monofluorophosphate solution. The adhesion of chitosan to mucosal epithelium depends primarily on the interaction of positively charged amino groups with negatively charged glycoproteins i.e. mucin (Singla and Chawla, 2001) although hydrogen bonding and/or hydrophobic interaction are thought to contribute (Qaqish and Amiji. 1999). Disruption of chitosan adhesion to the porcine oesophageal mucosal by sodium

monofluorophosphate is most likely due to the presence of sodium monofluorophosphate, further reducing the quantity of positively charged groups for adhesive bond consolidation. This observation does suggest an ionic interaction between sodium monofluorophosphate and chitosan, although the loss of the adhesive properties does render this formulation undesirable.

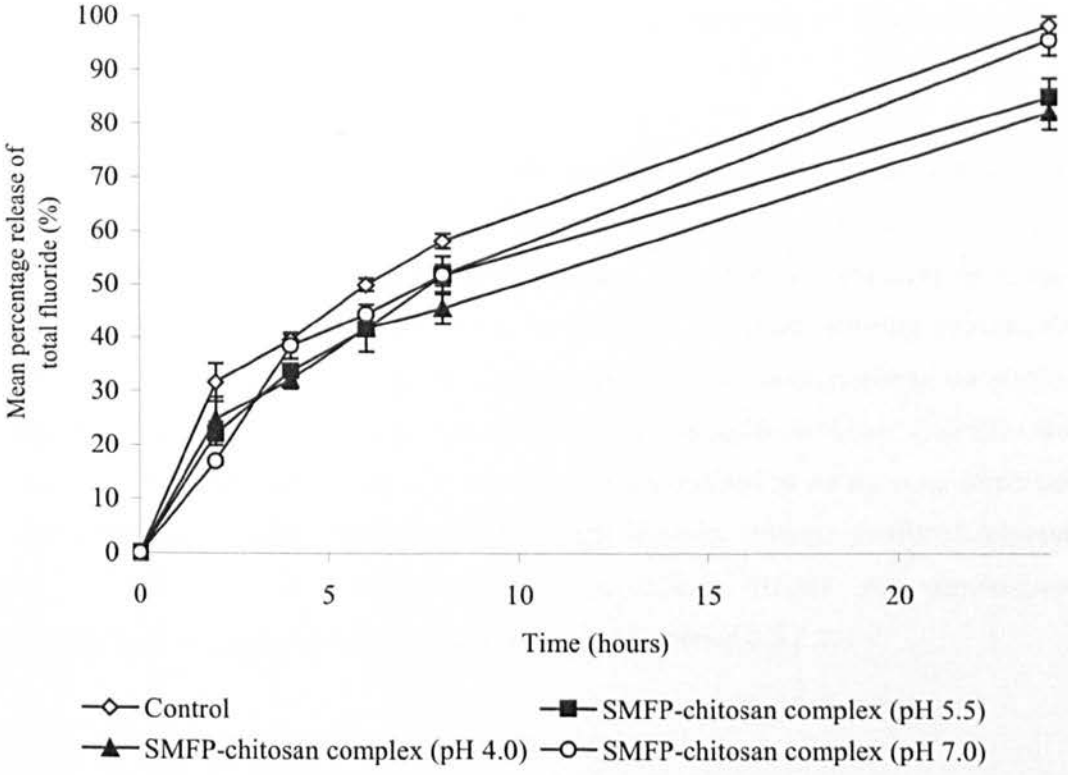

Figure 4.7 Cumulative release of fluoride during the dialysis of high viscosity chitosan-sodium monofluorophosphate solution and the effect of release medium pH compared to a 5.8 mM sodium fluoride control. (n=3, ± SD)

4.3.3 Preliminary investigation into fluoride-containing microparticles

Research into the use of chitosan microparticles to entrap and deliver drugs has been extensive (He *et al.*, 1999; Agnihotri., 2004; Sinha *et al.*, 2004). Chitosan is a suitable candidate for microparticle production due to its low toxicity and bioadhesive properties. The properties exhibited by chitosan microparticles can be influenced by certain production characteristics (Sinha *et al.*, 2004). Increasing the molecular weight

and/or cross-linking of chitosan results in sustained drug release properties due to the swelling behaviour of the particle. Higher molecular weight polymers require longer hydration times while cross-linking reduces the swelling capacity; both act to delay drug diffusion out of the polymer matrix. Chitosan can be cross-linked easily with the addition of chemicals such as glutaraldehyde, and anions such as tripolyphosphate. Changes in the polymer to drug ratio has an affect on the rate of drug release from the particle. An increased polymer to drug ratio causes a reduced rate of drug release due to increased drug entrapment efficiency.

Chitosan microparticles containing sodium fluoride or sodium monofluorophosphate were prepared using two different techniques; spray drying using a Buchi B290 spray dryer and a W/O solvent evaporation technique. Microparticles obtained from each method were characterised to determine the effect of the manufacturing process, the addition of glutaraldehyde, and the concentration of the aqueous phase on particle properties. HCMF (Cognis) was selected to prepare the aqueous phase. Selection was based on the molecular weight and viscosity, which resulted in an aqueous dispersion that could be processed. Both medium and high viscosity chitosan produced solutions that were highly viscous, making preparation difficult. HCMF also demonstrates moderate adhesion to porcine oesophageal mucosal (section 2.3.2.2).

4.3.3.1 Spray-dried chitosan microparticles

Due to the availability of the spray dryer at the University of Portsmouth, a thorough investigation into production variables such as inlet temperature and spray flow rate was unjustifiable. Therefore, spray drying parameters were selected based on work published by Ganza-Gonzalez *et al.* (1999), who utilised a B290 Buchi spray dryer to prepare chitosan microparticles for the oral delivery of metoclopramide. In this study formaldehyde was used as the cross-linking agent, which greatly influenced retardation of drug by the microparticle. In this investigation, the ratio of polymer to drug was fixed at 5:1. Two starting chitosan concentrations were selected for investigation; 1% w/v and 2% w/v. The amount of glutaraldehyde added to the aqueous phase was 0.0%, 0.5% and 5.0% of the dry weight of chitosan (g). Higher concentrations of glutaraldehyde led to rapid gelation of the aqueous phase, which was unsuitable for spray drying.

Chitosan microparticles without glutaraldehyde cross-linking recovered from the spray-drying process appeared white in colour and exhibited good flow properties. As the amount of glutaraldehyde increased, the colour of the product changed to slightly pink colour and the amount retrieved from the production process was slightly reduced. The spray-dried microparticles produced aggregated powders, which might be due to the residual moisture content or surface characteristics of the particles.

4.3.3.2 W/O chitosan microparticles

Microparticles were produced using a W/O emulsion solvent evaporation technique, modified from previously described methods (Kockisch *et al.*, 2003; Lim *et al.*, 2000), to examine the effect of processing on the characteristics of microparticles. W/O techniques tend to produce particles of a larger size than spray drying, which may result in improved drug retardation. However, the time required to dry the particles is significantly longer than the previous technique, which may alter the surface properties of the particles. In addition to sodium fluoride, sodium monofluorophosphate was incorporated into W/O microparticles to investigate whether the use of a divalent fluoride ion would improve particle properties. The highest polymer:drug ratio that could be adopted when using sodium monofluorophosphate was 20:1, as lower ratios induced chitosan precipitation.

Chitosan microparticles produced by a W/O solvent evaporation technique exhibited a significantly improved production yield and good flow properties. Microparticles were off-white in colour and did not resemble the product obtained from the spray drying technique; in particular the powder retained its flow properties and did not aggregate.

4.3.3.3 Particle size

Spray-dried microparticles typically exhibited a narrow particle size distribution with mean particle sizes no greater than 6 μm (Figure 4.8). W/O microparticles produced mean particle sizes that were approximately 10 times those produced in the spray drying process with a much wider size distribution (Figure 4.9). Spray-dried microparticles prepared from a 1% w/v chitosan starting concentration did not demonstrate any significant differences in particle size ($P > 0.05$). This was also true for the particles

prepared from the 2% w/v chitosan dispersion ($P > 0.05$). This suggests that the addition of glutaraldehyde did not have an effect on the particle size. ANOVA was unsuitable to analyse the data collected from all spray-dried microparticles due to an unequal variance. The student's unpaired two-tailed *t*-test assuming unequal variance was used to examine statistical differences between particles prepared using the same percentage constituents, for example HCMF II was compared with HCMF V. Significant differences ($P < 0.05$) were found between HCMF II and V and HCMF III and VI. No significant difference was found between HCMF I and IV ($P > 0.05$) although this may be due to an erroneous value obtained for HCMF I, which resulted in a particularly high standard deviation (Figure 4.8). This suggests that the starting concentration had a significant effect on the particle size, with a higher starting concentration resulting in a larger particle size.

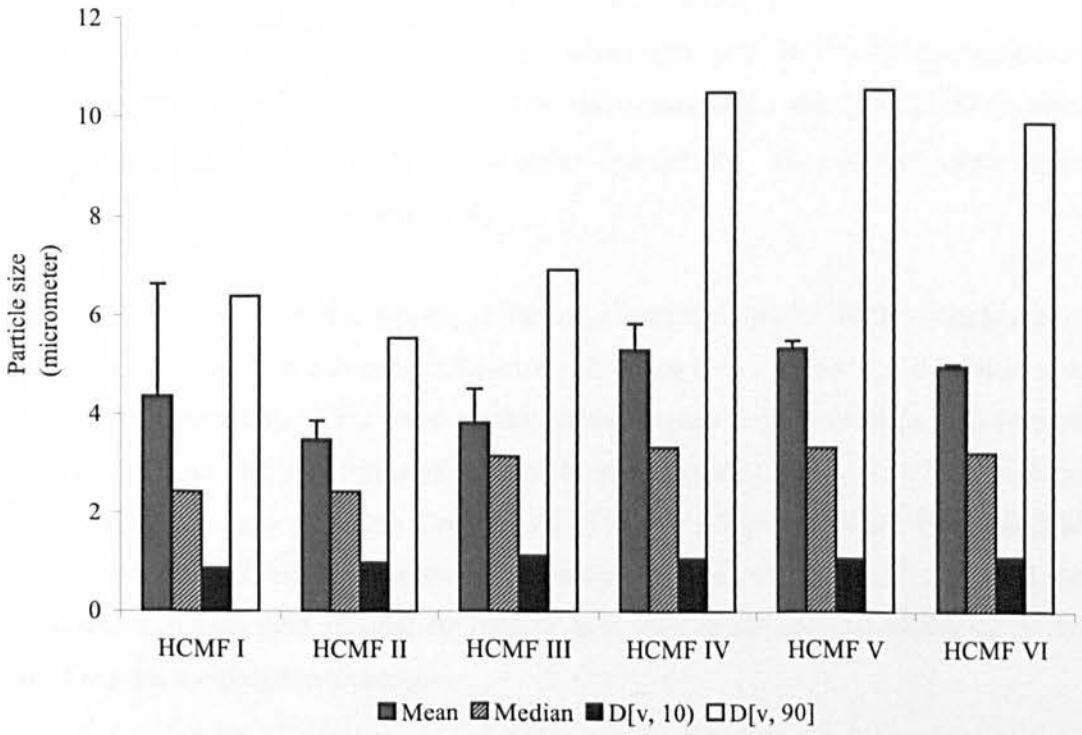

Figure 4.8 Particle size of chitosan microparticles prepared by spray-drying. The values for D[v, 10] and D[v, 90] represent the size (μm) at which 10% and 90% of the measured particles fall under respectively. Mean (±SD) and median particle sizes are also expressed (n = 4).

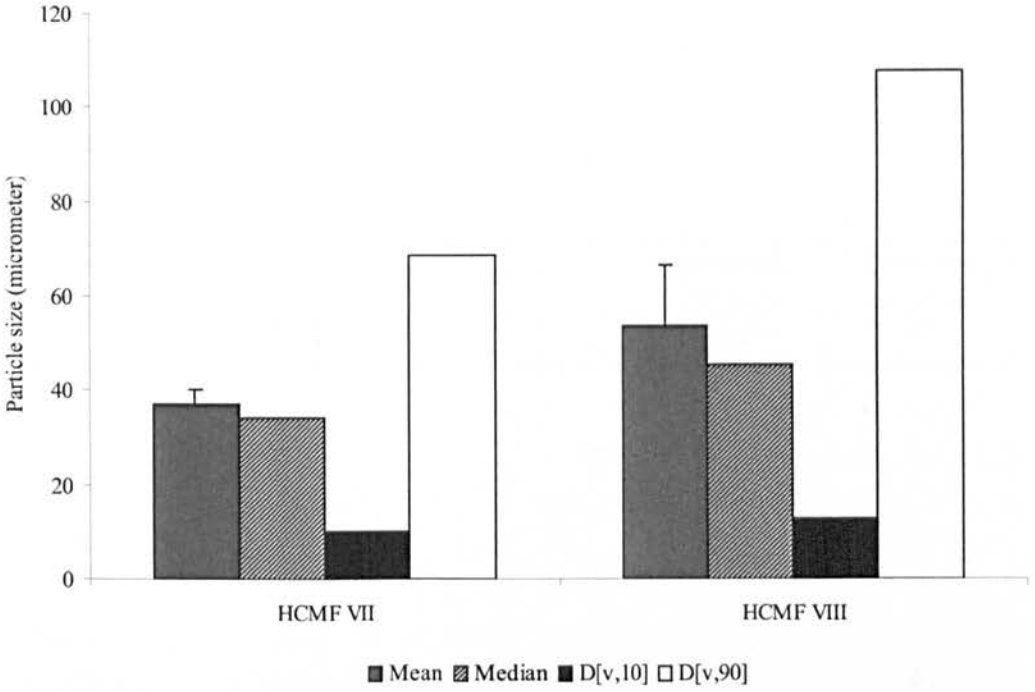

Figure 4.9 Particle size of chitosan microparticles prepared by W/O solvent evaporation technique. The values for D[v, 10] and D[v, 90] represent the size (μm) at which 10% and 90% of the measured particles fall under respectively. Mean (±SD) and median particle sizes are also expressed (n = 4).

The W/O particles were significantly different in particle size ($P < 0.05$), with particles prepared from chitosan and sodium fluoride exhibiting both a higher mean particle size and wider distribution. This could be due to the greater amount of drug incorporated into the sodium fluoride formulation, which was limited in the case of the sodium monofluorophosphate particles. Comparison of HCMF VIII with HCMF IV resulted in a highly significant difference between the particle sizes ($P < 0.001$), indicating that the production process used affected the particle size, with larger particles produced by the W/O solvent evaporation technique.

4.3.3.4 Fluoride loading

The fluoride content of the microparticles produced by spray drying and W/O solvent evaporation technique is given in Table 4.3. HCMF IX, which contains no fluoride and was produced using W/O technique was used to determine the matrix effects of dissolved chitosan on the measurement of fluoride with a fluoride ion selective

electrode. The amount of fluoride was below detectable levels indicating that chitosan itself did not interfere with the fluoride ion selective electrode measurement.

Table 4.3 Fluoride content of chitosan microparticles (n = 6).

Sample	Actual F^- content ($\mu g\ mg^{-1}$)		Theoretical F^- content[a] ($\mu g\ mg^{-1}$)	Entrapment efficiency[b] (%)
	Mean	SD		
HCMF I	59.2	1.7	76.5	77.4
HCMF II	56.9	0.0	74.9	76.0
HCMF III	54.3	1.2	73.5	73.9
HCMF IV	61.7	0.0	75.7	81.5
HCMF V	62.8	1.0	74.9	83.8
HCMF VI	60.5	0.0	71.9	84.1
HCMF VII	49.9	0.2	71.9	69.4
HCMF VIII	3.6	0.1	6.3	57.1

[a] Theoretical contents are calculated based on the quantity of F^- in the aqueous phase assuming homogenous distribution in microparticles.

[b] Entrapment efficiency: mean actual F^- content /theoretical F^- content x 100

The fluoride content and entrapment efficiency of the spray-dried microparticles was improved when the starting concentration of chitosan was increased from 1 to 2% w/v. This is most likely due to the increase in chitosan viscosity when the starting concentration is increased. The addition of glutaraldehyde to the formulation has no significant effect on the fluoride content of the spray-dried microparticles ($P > 0.05$) although a slight reduction can be observed as the amount of glutaraldehyde added increases (Table 4.3). The microparticles prepared using the W/O technique had a significantly lower entrapment efficiency when formulated with sodium monofluorophosphate. It is possible that fluoride is lost from the surface of these microparticles during the washing stage of preparation. This may be exacerbated by the presence of sodium monofluorophosphate at the surface as a consequence of particle drying time. *In vitro* fluoride release and scanning electron microscopy will help to determine the distribution of fluoride within these particles.

4.3.3.5 In vitro fluoride release

The rate of fluoride release from the chitosan microparticles was measured in isotonic 1.5 M calcium chloride/sodium chloride solution at pH 5.5. The volume of isotonic solution utilised for the experiment had to be minimal, due the significant dilution factor that accompanies sample preparation. Fluoride release was monitored over 6 h as samples removed after this time did not produce reliable fluoride ion selective electrode readings due to fluoride concentrations below the limit of detection. Microparticles prepared from chitosan only were used to determine any residual content of fluoride within HCMF. Fluoride remained under detectable levels when analysing the chitosan-only microparticles (Figure 4.10). The percentage release of fluoride from spray-dried microparticles prepared from 1% w/v and 2% w/v starting chitosan concentrations are shown in Figure 4.10 and 4.11 respectively. Chitosan microparticles generally exhibited similar fluoride release profiles, with a maximum release of 77.4% ± 3.9 after 6 h (HCMF II). The highest amount of fluoride released from the particles was detected after the first 10 min, which suggests a significant proportion of the fluoride is at the particle surface, or the formed particles are highly porous. Between 10 and 360 min, microparticles formulated without glutaraldehyde released the largest amount of fluoride. Specifically, the fluoride released increased by 20.0 and 25.8% for HCMF I and IV respectively (Figure 4.10 and 4.11). Microparticles containing 5% glutaraldehyde exhibited the lowest fluoride release regardless of the starting chitosan concentration. The density of polymer cross-links induced by this concentration of glutaraldehyde may effectively entrap sodium fluoride within the microparticle by restricting hydration. Interestingly these particles also demonstrated limited solubility in the release medium and a large amount of particulate debris was remaining after 360 min. Conversely, spray-dried microparticles prepared with either 0.0% or 0.5% glutaraldehyde formed gels upon the addition of isotonic solution. It is the formation of these gels and their subsequent behaviour that most likely accounts for the observed release of fluoride.

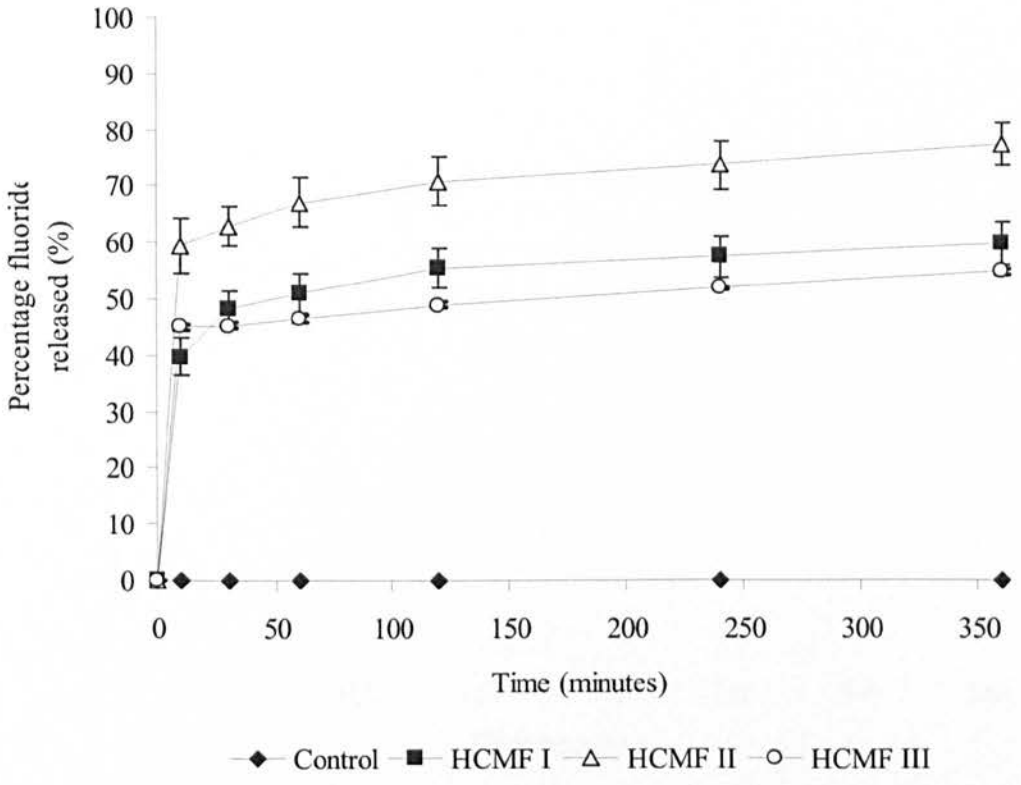

Figure 4.10 Cumulative mean percentage fluoride released from spray-dried chitosan microparticles prepared from a 1% w/v starting chitosan concentration. Spray-dried HCMF without sodium fluoride was used as the experimental control. (n = 3, ±SD)

The release of fluoride was not complete after 360 min, which suggests a significant amount of fluoride remains associated with either the insoluble chitosan products or within the microparticle gels. The microparticles and solution remaining were prepared for fluoride determination by adding hydrochloric acid and 80/20 diluent as per the protocol for sample preparation. Following this, approximately 90% of the total fluoride is recovered from particles prepared with 0.0% and 0.5% glutaraldehyde, while approximately 82% is recovered from the particles prepared with 5% glutaraldehyde. It is possible that this extraction procedure was not able to completely release all of the fluoride from the chitosan debris.

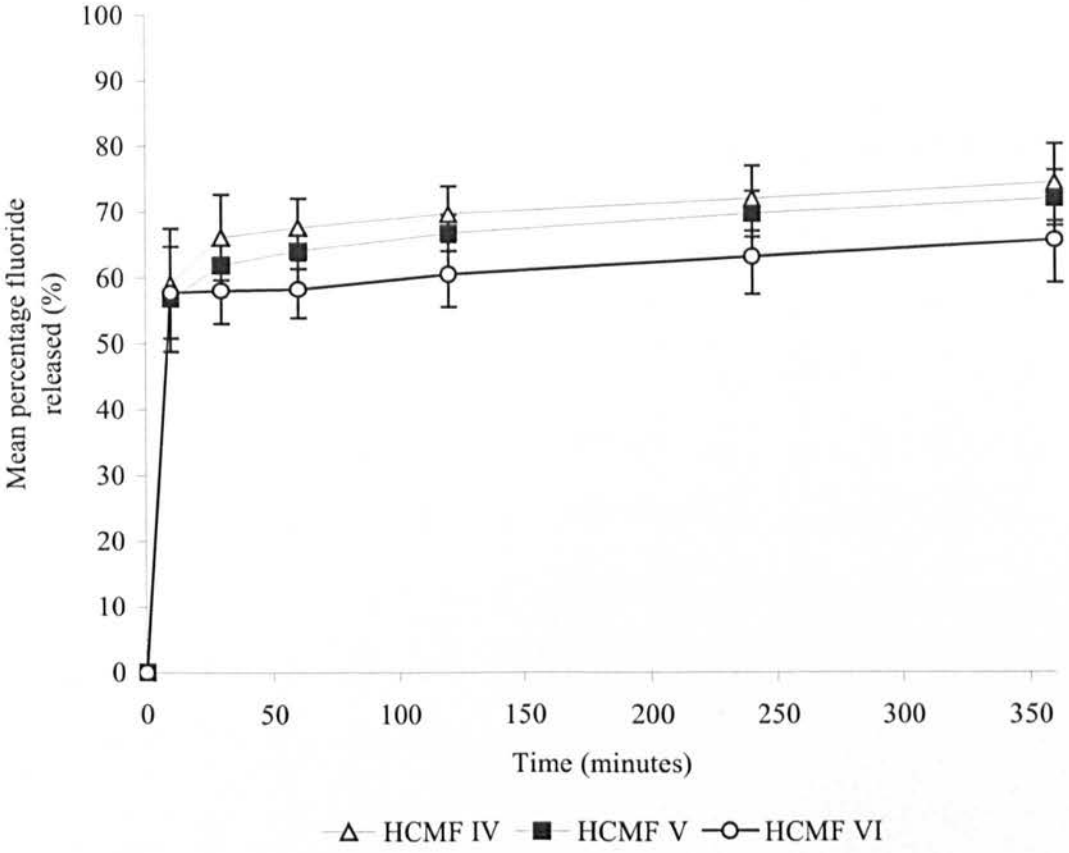

Figure 4.11 Cumulative mean percentage fluoride released from spray-dried chitosan microparticles prepared from a 2% w/v starting chitosan concentration. Spray-dried HCMF without sodium fluoride was used as the experimental control. (n = 3, ±SD)

The percentage release of fluoride from the chitosan microparticles prepared by W/O solvent evaporation technique is shown in Figure 4.12. Upon addition of the isotonic solution, the microparticles did not form a gel and instead dispersed evenly, unlike the spray-dried particles. This behaviour greatly affected the rate of fluoride release from the particles. Chitosan-sodium monofluorophosphate particles released almost 100% of total fluoride within the first 10 min, suggesting that fluoride is mostly distributed at the surface. This may also explain the lack of particle aggregation and gel formation after suspension in the isotonic solution. After 60 min, the release of fluoride was below detectable levels, although the stability of the fluoride ion selective electrode readings after the initial 10-minute measurement was reduced. This may account for possible inaccuracy in measuring the latter samples resulting in the apparent release above 100% (Figure 4.12). The release of fluoride from the chitosan-sodium fluoride microparticles

exhibited an initial "burst" release with only 5% of total fluoride released after this time (Figure 4.12). After 360 min, the release of fluoride was not complete. This release profile is similar to the spray-dried microparticles. Measurement of fluoride at the experimental endpoint resulted in the recovery of 99% of total fluoride indicating that chitosan does not interfere with the measurement of fluoride with the fluoride ion selective electrode.

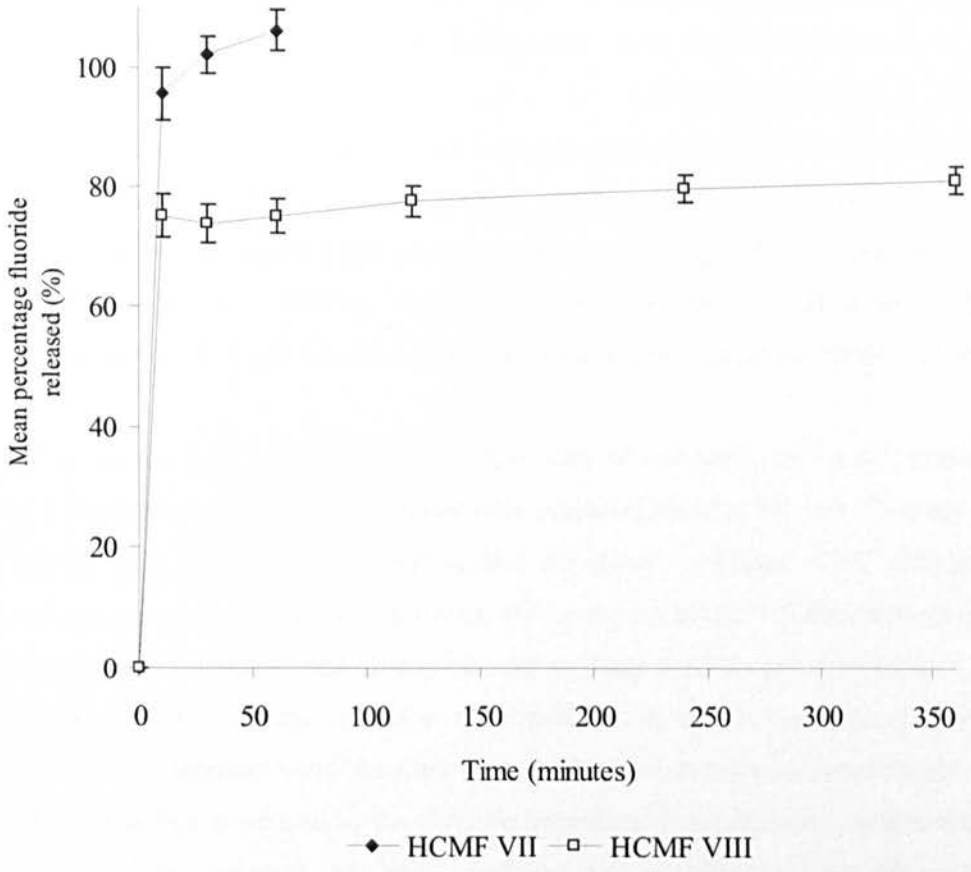

Figure 4.12 Cumulative mean percentage fluoride released from chitosan microparticles prepared from a W/O solvent evaporation technique. (n = 3, ±SD)

4.3.3.6 Texture probe analysis

Microparticles prepared from 1% w/v and 2% w/v chitosan dispersions have demonstrated similar properties, although the latter does exhibit improved entrapment efficiency. Therefore, adhesion of the particles to porcine oesophageal mucosa was carried out on the microparticles prepared from the 2% w/v chitosan dispersion only.

Initially, particles prepared using the W/O solvent evaporation technique were to be investigated for bioadhesive properties. However, the preparation of sample disks using compression was unsuccessful as W/O microparticles did not adhere to each other. This was also observed during the *in vitro* fluoride release studies. Increasing the compression and the weight of microparticles used to prepare the samples has no effect. In an effort to overcome the preparatory problems encountered, W/O microparticles were weighed (10 mg) and spread thinly on the surface of the probe, which was covered in double sided tape. This methodology has been previously adopted in particle adhesion studies carried out by Kockisch *et al.* (2003) and Govender *et al.* (2005). However, results obtained from the texture probe analysis were deemed unreliable upon examination of the force-distance graphs, which showed large adhesion forces that could only be explained by the presence of the underlying adhesive used to secure the W/O particles. In addition, results obtained were not reproducible. Therefore bioadhesion of W/O particles to a model mucosal surface could not be determined.

The maximum detachment force (mN) and work of adhesion (mN mm^{-1}) produced by the adhesion of spray-dried microparticles prepared from a 2% w/v chitosan starting concentration, to a model mucosal surface are shown in Figure 4.13. Ethylcellulose produced no measurable adhesive forces, indicating the validity of the protocol (data not shown). Spray-dried HCMF alone was used to determine the effect of sodium fluoride and glutaraldehyde on the bioadhesive performance of the chitosan microparticles. No significant differences were detected between the maximum detachment force and the work of adhesion produced by the chitosan microparticles containing sodium fluoride ($P > 0.05$). This suggests that glutaraldehyde had no effect on the adhesive forces exhibited by the microparticles. All fluoride-containing microparticles however displayed adhesive forces that were significantly different from the control particles ($P < 0.05$). Together, this data suggests that it is the addition of sodium fluoride that disrupts the bioadhesive properties of the microparticles rather than the density of cross-linking. Slight reduction in the mean adhesive forces can be observed as the concentration of glutaraldehyde is increased in the fluoride-containing microparticles, although this is not statistically significant (Figure 4.13). This may be due to the variation inherent in texture probe analysis measurements using a model mucosal surface. Any reduction in the adhesion of microparticles cross-linked with glutaraldehyde is likely due to reduced polymer hydration. Despite the massive

reduction in adhesive strength, which is approximately 81.1% and 73.0% for maximum detachment force and work of adhesion respectively for HCMF IV compared to the control, the forces produced by the microparticles are comparable to those observed in other studies (Kockisch *et al.*, 2003; Martinac *et al.*, 2005).

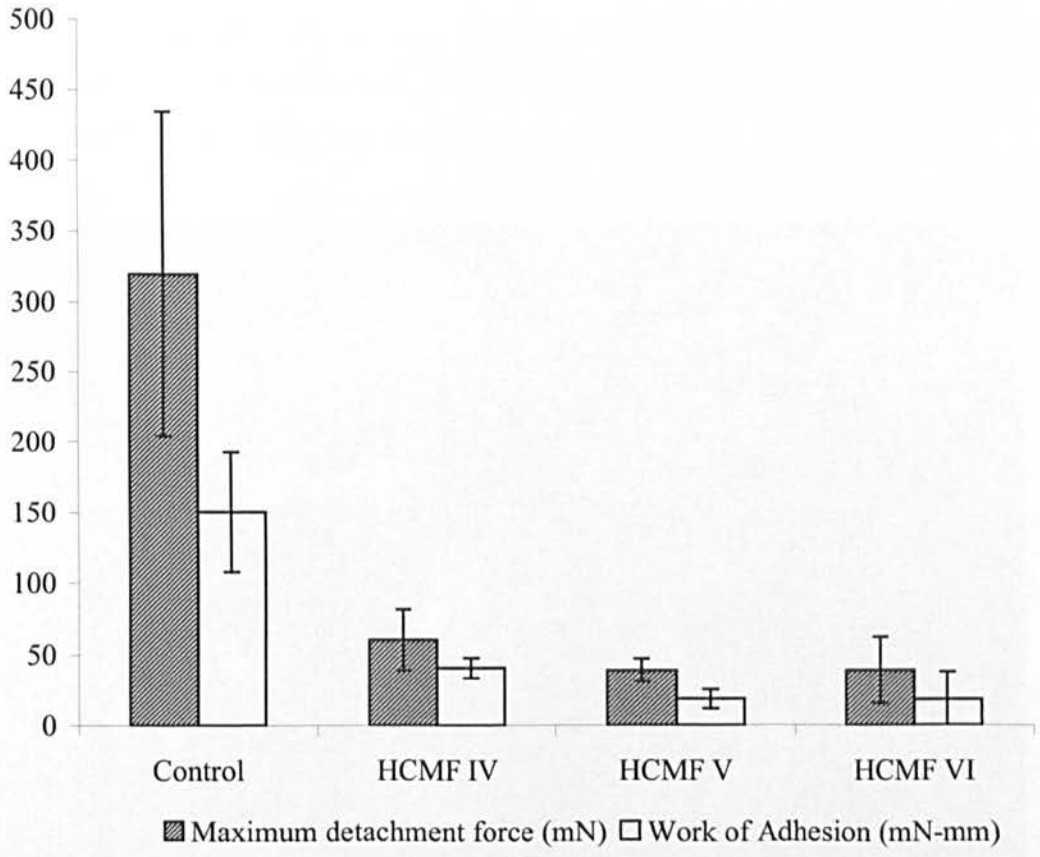

Figure 4.13 Adhesion of spray-dried microparticles prepared from 2% w/v chitosan dispersions to porcine oesophageal tissue in artificial saliva. Spray-dried HCMF without fluoride were used as the experimental control (n = 3, ±SD).

4.3.3.7 Scanning electron microscopy

Scanning electron microscopy was used to examine the morphology of spray-dried microparticles prepared with 2% w/v chitosan dispersions and chitosan-only and chitosan-sodium fluoride particles prepared using the W/O solvent evaporation technique. Chitosan-only microparticles prepared by spray drying (Figure 4.14) and W/O solvent evaporation technique (Figure 4.15, *top*) exhibit significantly different

morphologies. Spray-dried particles were spherical in shape but multiple surface indentations were evident, regardless of sodium fluoride content (Figure 4.14, 4.16 and 4.17). Conversely, W/O microparticles exhibited a smooth spherical shape. However, incorporation of sodium fluoride into the formulation resulted in the formation of large crystals on the particle surface (Figure 4.15, *bottom*). This supports the observations made when analysing the *in vitro* fluoride release of W/O fluoride-containing microparticles. The characteristic initial burst release most likely results from the dissolution of these crystals from the particle surface.

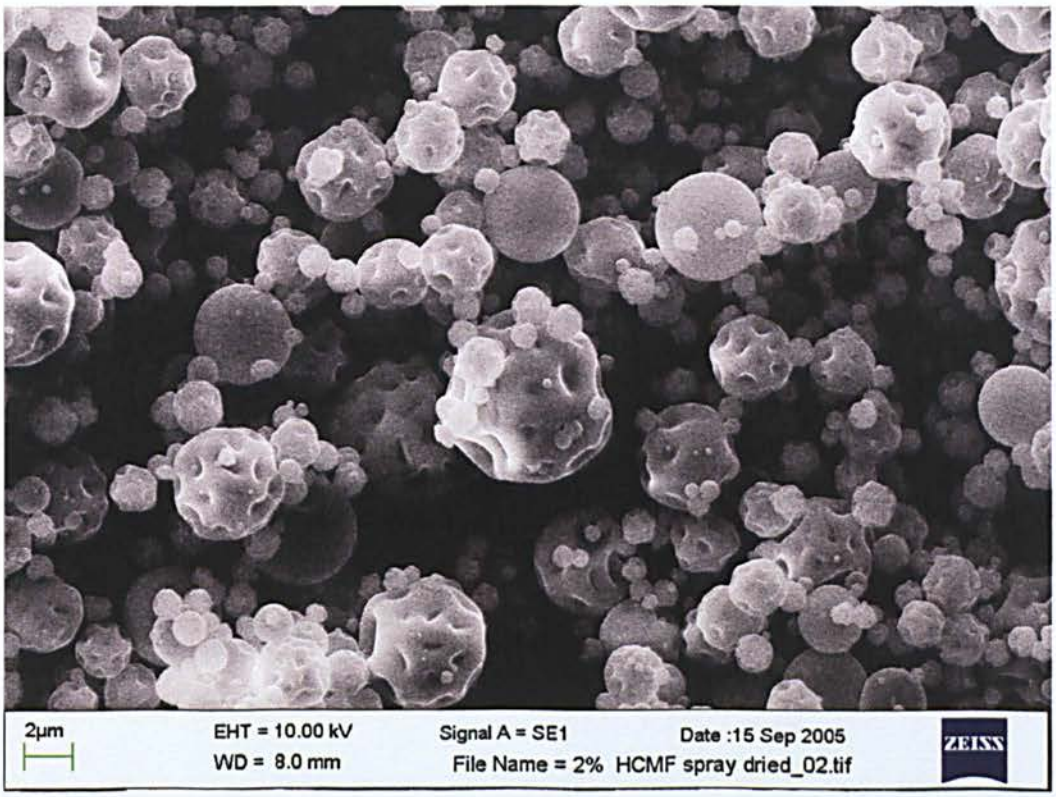

Figure 4.14 Chitosan-only microparticles produced by spray-drying 2% w/v HCMF dispersions.

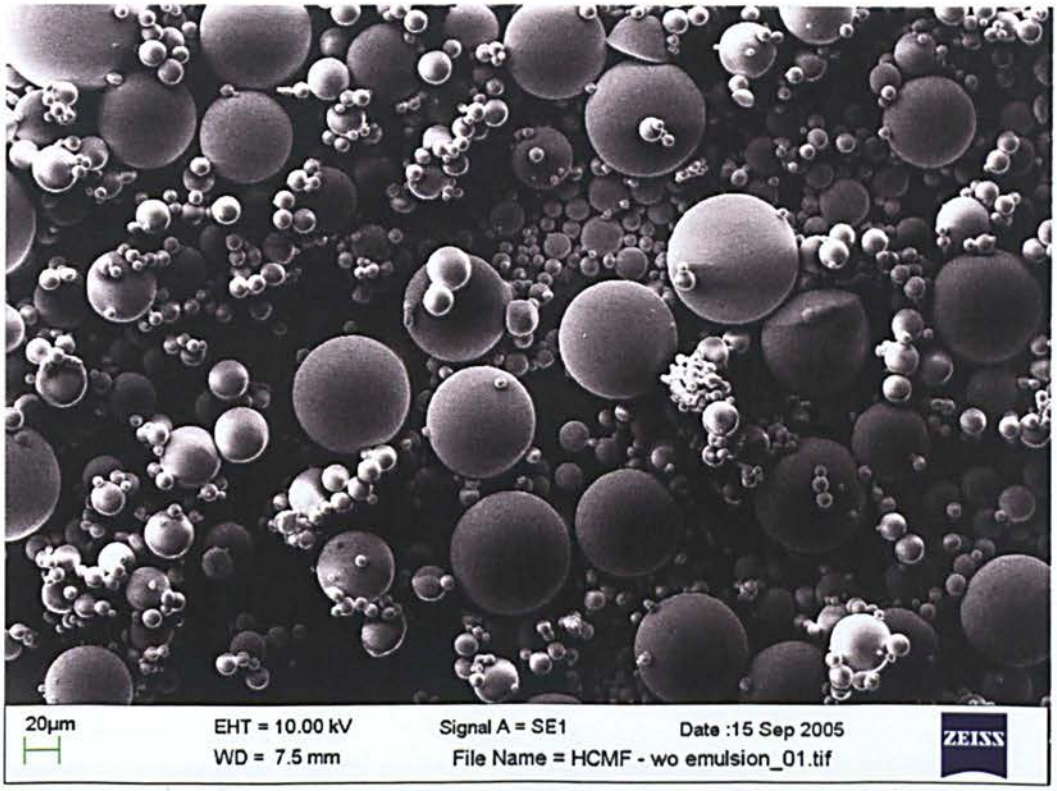

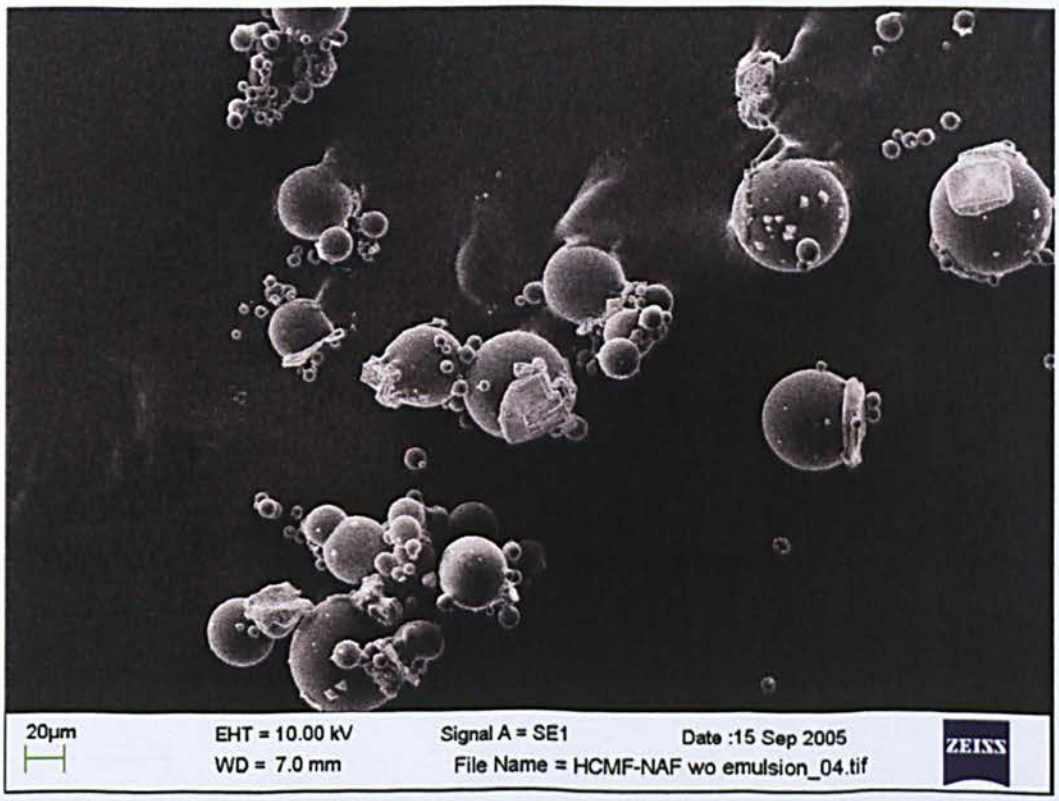

Figure 4.15 Chitosan-only microparticles (*top*) and chitosan-sodium fluoride microparticles (*bottom*) produced using a W/O solvent evaporation technique.

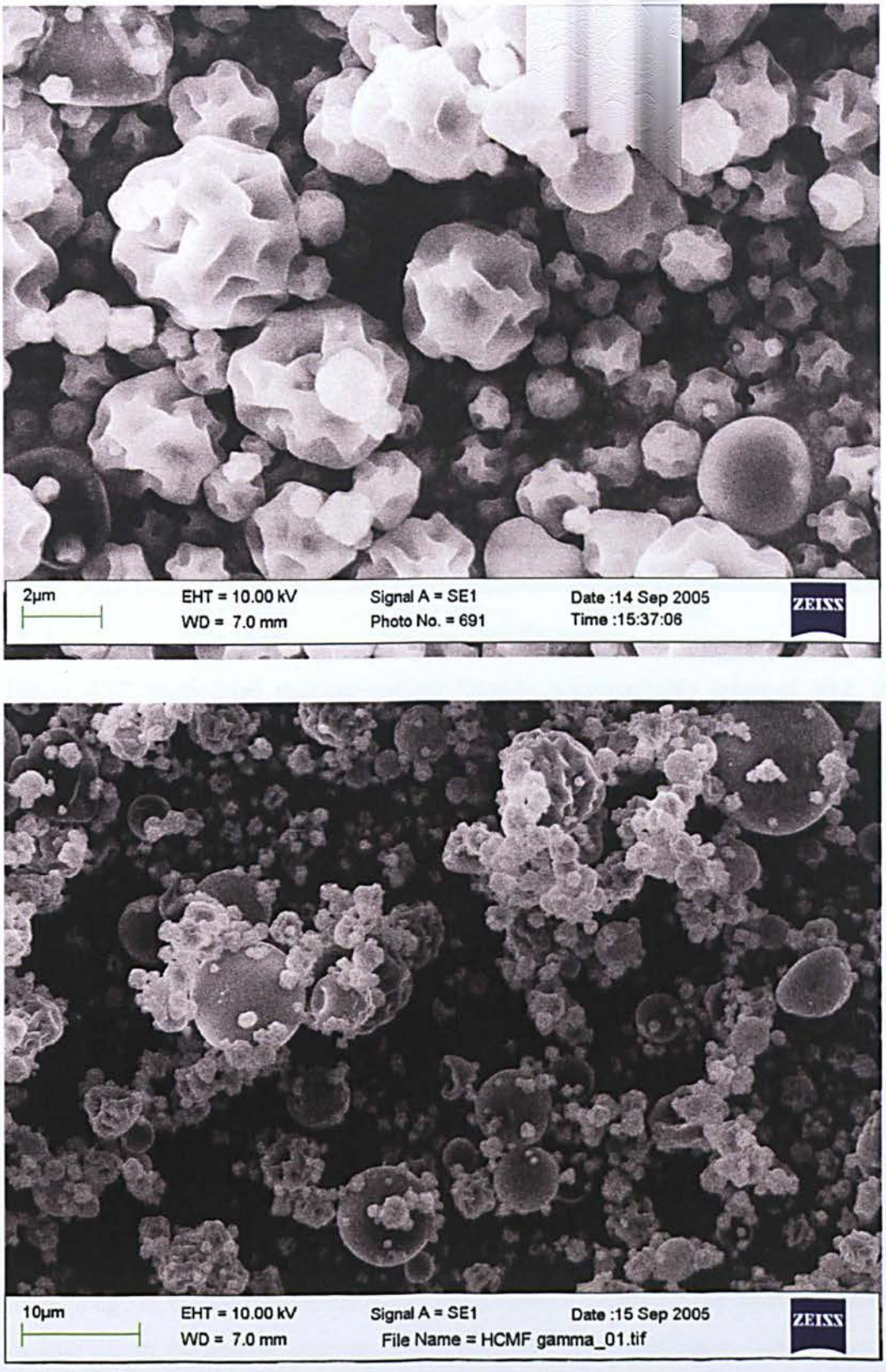

Figure 4.16 Spray-dried chitosan-sodium fluoride microparticles prepared with 0.0% (top) and 0.5% glutaraldehyde (bottom) based on the dry weight of chitosan.

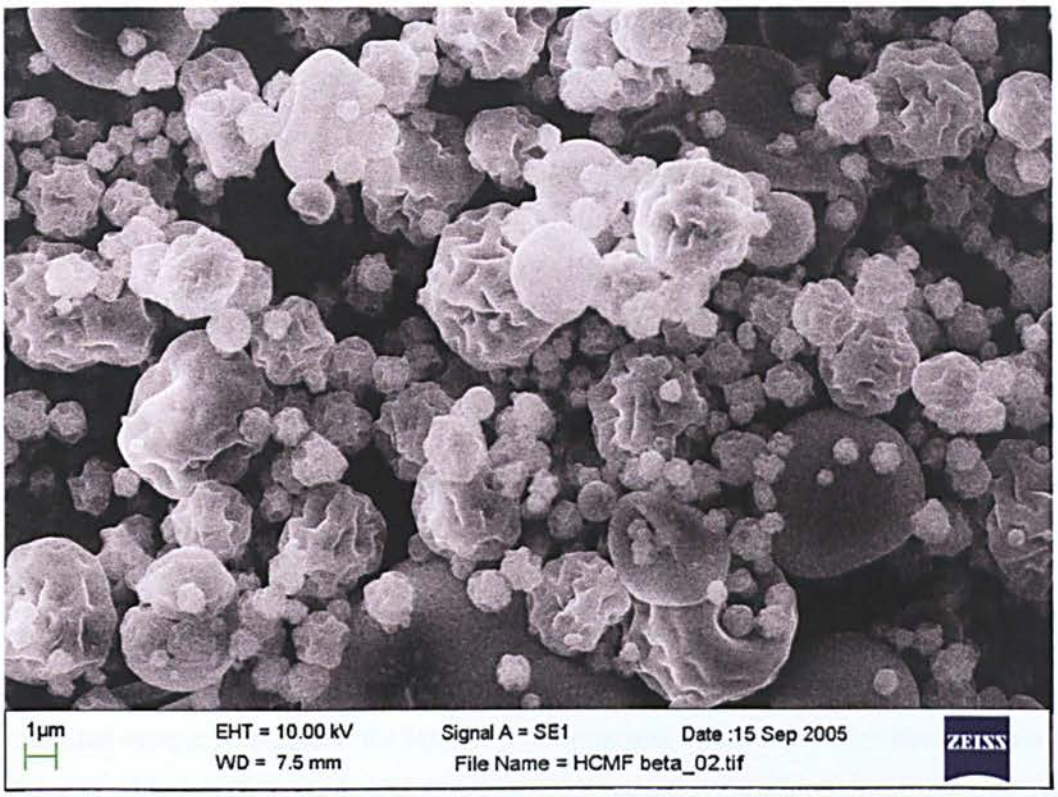

Figure 4.17 Spray-dried chitosan-sodium fluoride microparticles prepared with 5% glutaraldehyde based on the dry weight of chitosan.

Examination of the scanning electron micrographs of spray-dried chitosan-sodium fluoride microparticles confirmed that drug crystals were not evident at the surface. This suggests that sodium fluoride is distributed throughout the microparticle. The length of time required for drying is most likely responsible for the presence of sodium fluoride at the surface of particles prepared using W/O solvent evaporation. In spray drying, as soon as droplets come into contact with the drying air in the spray cylinder, evaporation occurs quickly from the droplet surface. This results in the formation of saturated vapour film. Moisture is then removed from the particle as it passes through the drying chamber. The surface indentations evident on particles prepared using this technique is the result of this drying process and has been observed previously by Martinac *et al.* (2005) when spray drying chitosan dispersions. They attributed the morphology to the subsequent shrinking of the particle following the rapid removal of moisture from the particle interior. Corrigan *et al.* (2006) and Ganza-Gonzalez *et al.* (1999) also found surface indentations on the surface of spray-dried chitosan. The drying process that occurs during the W/O solvent evaporation technique occurs over a

significantly longer period of time and at lower temperatures. Moisture is drawn slowly from the centre of the droplet, rather than the intense heat and mass transfer that occurs during spray drying. As a result, the water soluble sodium fluoride is drawn with the solvent to the particle surface, where it is dried forming salt crystals.

4.3.4 Further investigation of optimised fluoride-containing microparticles

Based on the characterisation of the various microparticles, the spray-dried formulation comprising 2% w/v HCMF as the starting chitosan concentration with 0.2 g sodium fluoride and no added cross-linker was selected as optimum for the purpose of this study. W/O particles demonstrate surface properties that caused an initial "burst" release of fluoride followed by a period of little significant release. In addition, these particles did not form a gel upon hydration and instead exhibited surface properties that inhibited sample preparation for texture probe analysis. The effect of glutaraldehyde on the spray-dried particle characteristics was minimal and certainly not significant enough to warrant its inclusion in the final formulation. In addition the solubility of particles prepared with glutaraldehyde (5% of the dry weight of chitosan) was significantly reduced. Increasing the starting chitosan concentration resulted in higher entrapment efficiency when compared to the use of 1% w/v chitosan dispersions. Hence, the optimum formulation was selected and three batches of fluoride-containing microparticles (HCMF-sodium fluoride) and chitosan-only microparticles (HCMF) were produced for further investigation.

The fluoride content of the microparticles is given in Table 4.4 together with the production yields of the spray drying process. Low production yield have often been identified by other authors when utilising the spray-drying techniques due to powder adhering to the cyclone walls and the loss of the smallest and lightest particles through the exhaust of the spray dryer apparatus (Giunchedi *et al.*, 2002; Martinac *et al.*, 2005). It is apparent that a low yield of HCMF-only microparticles was recovered following spray-drying, which is significantly improved when sodium fluoride was added to the formulation. Poor yields following spray drying have been previously reported by other authors and may account for the observations made in this study (Giunchedi *et al.*, 2002; Martinac *et al.*, 2005). Furthermore, it is possible that the difference between the

yields of spray-dried HCMF-only and HCMF-sodium fluoride is due to the physicochemical properties of the dispersions. For instance the viscosity of the 2% w/v HCMF dispersion may result in less efficient atomisation, causing larger, heavier droplets of chitosan to deposit on the surface of the spray cylinder. The addition of sodium fluoride significantly reduces the viscosity of chitosan due to relaxation of the extended polymer conformation, which occurs in the presence of salts (Singla and Chawla. 2001). In addition, the amount of chitosan within the atomised droplets will be reduced when sodium fluoride is included in the formulation. It is also possible that the inlet air temperature utilised throughout this study is insufficient to fully evaporate the solvent, resulting in liquid deposition within the spray cylinder (He *et al.*, 1999). This suggests that the production of spray-dried microparticles generates some heterogeneity between different batches.

Table 4.4 Fluoride content of chitosan-sodium fluoride and chitosan-only microparticles prepared using a spray dryer. Mean values are based on repeat measurements from three batches of microparticles (n = 9).

Sample	Actual F^- content (μg mg^{-1})		Theoretical F^- content (μg mg^{-1})	Entrapment efficiency (%)	Production yield[a] (%)
	Mean	SD			
HCMF	Bdl	-	0.0	-	18.7
HCMF-sodium fluoride	65.2	2.3	71.9	90.7	41.7

[a] Production yield: amount of material within the aqueous phase /amount of material retrieved following spray drying x 100

Particle size determinations of HCMF and HCMF-sodium fluoride microparticles are displayed in Figure 4.18. The mean particle size of the spray-dried microparticles was significantly different, with HCMF-sodium fluoride particles larger than those produced from chitosan only dispersions ($P < 0.001$). This was accompanied by an increase in the particle size distribution, which may be due to the change in polymer hydration and sodium fluoride content within the droplets. The evaporation of solvent from the

droplets produced by the atomisation of chitosan-only dispersion may not be complete, particularly when droplets are of a larger size. Therefore it is likely that an optimum droplet size travelling through the spray dryer undergoes complete solvent evaporation and achieves deposition in the collecting vessel. Hence, the observed particle size distribution is most likely limited by the initial droplet size. This may also be the reason for the lower median value when compared to the mean (Figure 4.18). Upon addition of sodium fluoride to the dispersion, chitosan hydration and viscosity are reduced, resulting in efficient atomisation and lower solvent content within the droplets. Therefore larger initial droplet sizes can undergo complete solvent evaporation during transit through the spray dryer. Although based on the observed median values (Figure 4.18), it is still likely that large droplets are less likely to be dried and retrieved in the collecting vessel.

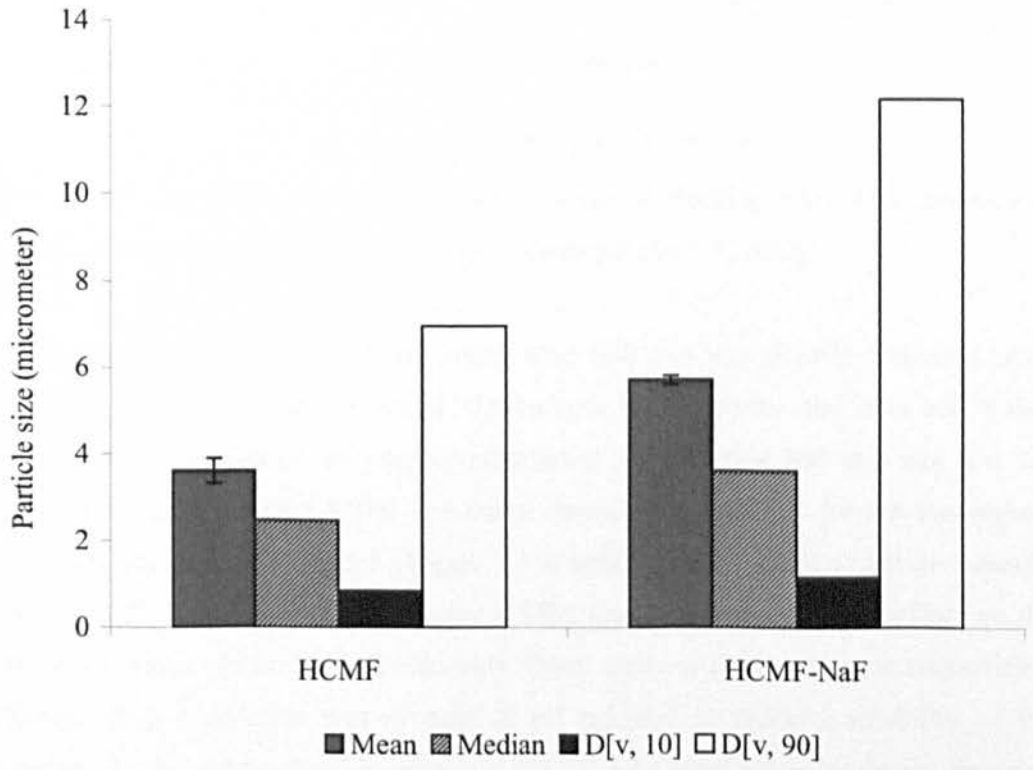

Figure 4.18 Particle size measurements of spray-dried microparticles prepared from chitosan- and chitosan-sodium fluoride aqueous dispersions (n = 9).

The *in vitro* release of fluoride from the HCMF-sodium fluoride microparticles at different pHs did not elicit any significant changes in the release profile (Figure 4.19).

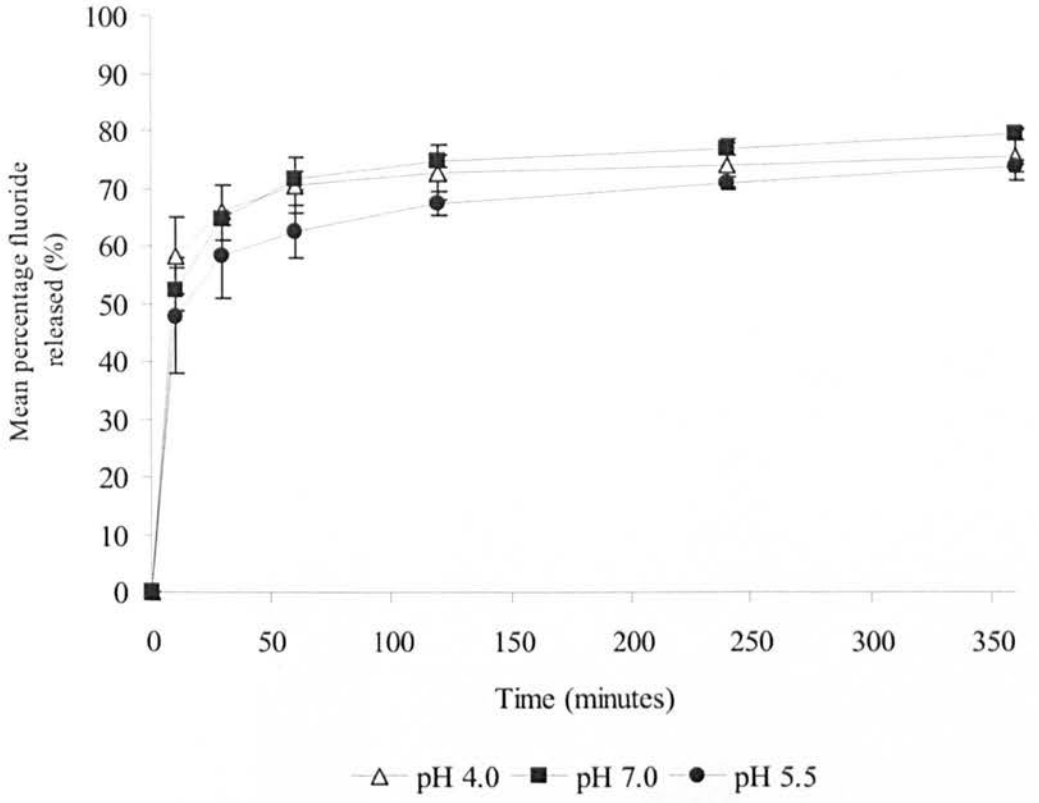

Figure 4.19 Cumulative mean percentage release of fluoride from chitosan-sodium fluoride microparticles at physiologically relevant pHs (n = 3, ±SD).

Although the amount of fluoride recovered after 360 min was slightly increased when the pH of the isotonic solution was pH 7.0 and pH 4.0. However, the latter was within one standard deviation of the amount released at pH 5.5 after 360 min and was not statistically significant ($P > 0.05$). The initial fluoride released after 10 min was highest at pH 4.0 and lowest at pH 5.5 (Figure 4.19) although this was also not statistically significant ($P > 0.05$). Ganza-Gonzalez (1999) found that pH had little effect on the release of metoclopramide hydrochloride from spray-dried chitosan microparticles, although drug retardation was evident at pH 6.8 due to reduced solubility of the polymer. In this study, fluoride release at pH 7.0 was expected to be slower than that observed at pH 4.0 and 5.5. However, this was not evident (Figure 4.19). Drug release by diffusion from chitosan microparticles involves three steps; 1) swelling of the particle matrix upon penetration of water, 2) gel formation by the particles, and 3) diffusion of drug from the swollen polymer gel matrix (Agnihotri *et al.*, 2004). This occurs after drug found near the particle surface has been released, which is often observed as an initial "burst" effect, seen after 10 min in Figure 4.19. Swelling of the

microparticles in isotonic solution may be reduced when compared to deionised water due to interaction of salt with the outer surface of the chitosan microparticle. It is this effect that most likely accounts for the release profile of fluoride from the particles rather than the solution pH.

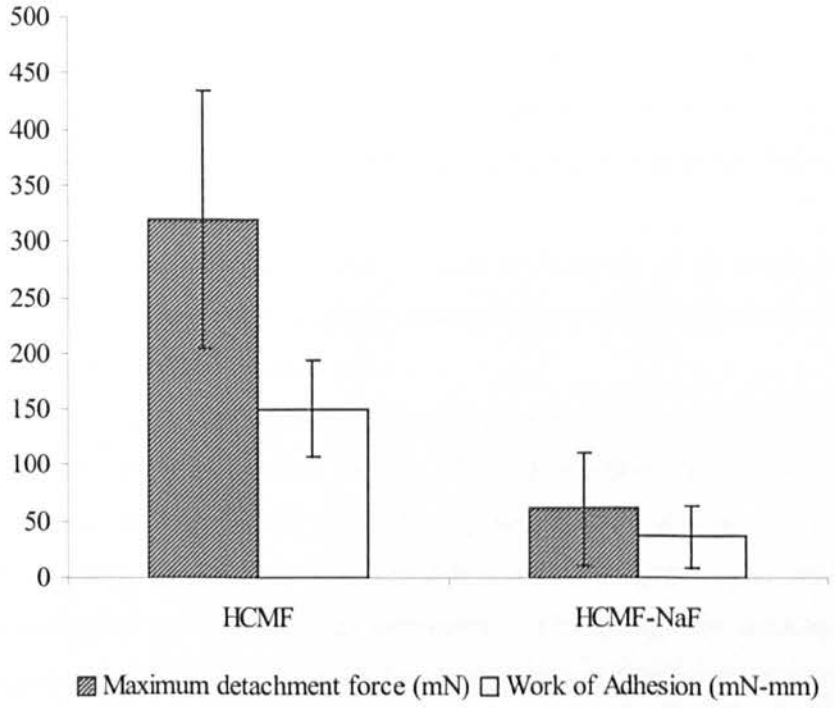

Figure 4.20 Adhesion of spray-dried chitosan- and chitosan sodium fluoride microparticles to porcine oesophageal tissue in artificial saliva (n = 6, ±SD).

The bioadhesion of HCMF and HCMF-sodium fluoride microparticles to model mucosal tissue is shown in Figure 4.20. As previously indicated, the addition of sodium fluoride to the formulation significantly reduced the measured adhesive forces when compared to the HCMF-only microparticles ($P < 0.01$). This may be the result of the drug:polymer ratio utilised within this study. Previous studies have observed a significant reduction in bioadhesive bond strength as the drug:polymer ratio is increased (Ganza-Gonzalez *et al.*, 1999; Govender *et al.*, 2005; Martinac *et al.*, 2005). This is particularly relevant as sodium fluoride may reduce the positive charge density exhibited by chitosan, which has previously been identified as crucial to the interaction with the mucosal surface (Grabovac *et al.*, 2005). This would be exacerbated by the counter-ions present in artificial saliva.

4.4 Conclusions

- Aqueous chitosan dispersions mixed with an equal volume of 23.6 mM sodium monofluorophosphate produce solution that exhibit a limited degree of interaction when dialysed against deionised water.
- Aqueous chitosan dispersions do not exhibit significant interaction with sodium fluoride, evident by the absence of polymer precipitation upon mixing of high concentrations of sodium fluoride and lack of fluoride retention during dialysis against deionised water.
- Dialysis against an isotonic solution results in removal of possible interactions between sodium monofluorophosphate and aqueous chitosan dispersions, which was not influenced by release medium pH.
- Freeze-dried chitosan- sodium monofluorophosphate mixtures were not bioadhesive.
- Microparticles with a narrow particle size distribution and high entrapment efficiency can be produced by spray drying aqueous dispersions of chitosan and sodium fluoride. The addition of glutaraldehyde as a polymer cross-linker had no significant effect on particle characteristics. Increasing the starting chitosan concentration significantly increased the particle size and entrapment efficiency. *In vitro* fluoride release follows a similar release profile regardless of starting chitosan concentration or glutaraldehyde cross-linking. This is characterised by an initial "burst" release of fluoride followed by a slower release that was not complete after 360 min. The surface of the particles were characterised by surface indentations. Inclusion of sodium fluoride into the formulation resulted in a significant reduction in adhesive strength.
- Microparticles with a wide particle size distribution can be produced using a W/O solvent evaporation technique. Mean particle sizes were significantly higher than those produced using the spray-drying technique. The entrapment efficiency was lower than that observed for spray-dried particles, particularly when sodium monofluorophosphate was utilised as the fluoride source. *In vitro* fluoride release was also characterised by an initial "burst" release. In the case of HCMF- sodium monofluorophosphate particles, almost all fluoride was released within 10 min. HCMF-sodium fluoride microparticles exhibited similar release profiles to the spray-dried particles, although less fluoride was released between 10 and 360 min. Release

from these particles was not complete after 360 min. These particles could not be analysed for bioadhesive strength.

- Microparticles prepared by spray-drying an aqueous dispersion composed of 2% w/v HCMF and 0.2 g sodium fluoride were selected for further investigation.
- Particle size was increased when the aqueous phase contained sodium fluoride when compared to chitosan-only dispersions. This may be due to an inadequate inlet temperature and the hydration of the polymer in the presence of sodium fluoride.
- Fluoride content of the microparticles exhibited variation when prepared as three different batches.
- *In vitro* fluoride release from the particles was unaffected by changing the release medium pH.
- Bioadhesion to porcine oesophageal tissue was significantly reduced when compared to the chitosan-only microparticles and may be due to the high drug:polymer ratio utilised in this study.

Chapter 5
Antimicrobial assessment of polymer complexes

5.1 Introduction

5.1.1 Background

Throughout the previous chapters, the bioadhesive properties and *in vitro* release of antimicrobials from a polymeric platform have been investigated as potential sustained release formulations designed to modulate the growth of bacteria within the oral cavity. In this section a variety of planktonic and sessile (biofilm) bacterial techniques will be used to evaluate the antimicrobial activity of the prepared formulations. The ability of the complexes to prevent the growth of key bacterial species found within dental plaque is the main factor to be investigated.

Planktonic studies can give important preliminary information regarding the potential antimicrobial activity of the bioadhesive formulations *in vivo*. Planktonic tests are relatively easy to perform and provide rapid results regarding the effect of an antimicrobial on individual bacterial species. These tests have been used extensively throughout the literature in the development of bioadhesive antimicrobial drug delivery formulations (Shani *et al.*, 1998; Senel *et al.*, 2000; Giunchedi *et al.*, 2002; Arora *et al.*, 2003; Govender *et al.*, 2005). Typically, the minimum inhibitory concentration (MIC) and/or the minimum bactericidal concentration (MBC) are characterised for individual bacterial species using either an agar-based technique, such as zone of growth inhibition (Govender *et al.*, 2005), or a broth dilution technique (Giunchedi *et al.*, 2002). However, to improve the predictive power of these tests they should preferably be supported by data obtained from a sessile study. Organisms grown in a biofilm tend to exhibit different phenotypes when compared to planktonic organisms and this can confer a greater resistance to antimicrobial agents (Marsh, 2003).

In this particular work, bioadhesive complexes have been designed to persist within the oral cavity through interactions with the salivary pellicle and mucosal epithelium. In addition, a therapeutic dose of the active compound must be maintained to reduce bacterial numbers, and hence the formation of a bacterial biofilm; plaque. Conventional antimicrobial activity tests and polymer-complex characterisation both provide

important means for predicting *in vivo* performance, however, simultaneous investigation of these properties may more accurately reflect conditions for which such preparations are intended. For this reason, a bioavailability model designed and validated at GlaxoSmithKline R&D (Weybridge, UK) was used to support initial planktonic studies for selected compounds. Biofilm techniques that have previously been used to characterise the antimicrobial efficacy of anti-plaque agents classically involve the application of the agent to a biofilm surface with subsequent cell viability measurements following biofilm disruption (Robinson *et al.*, 2001; Phan *et al.*, 2004). Some methods such as LIVE/DEAD® Baclight™ viability staining (Jabbour *et al.*, 2005) and luminescence assays that do not require disruption have also been developed (Merritt *et al.*, 2005).

The delivery of bioadhesive complexes to the oral cavity is likely to be in the form of a paste or rinse; therefore oral biofilms have often undergone rigorous mechanical removal prior to application through the process of tooth brushing. In accordance with this, antimicrobial efficacy should focus on biofilm formation and growth rather than the eradication of established biofilms. Microtitre plate assays have been used to monitor the development of biofilms in the presence of plaque-control agents using both spectroscopic techniques (Roberts *et al.*, 2002) and confocal microscopy (Jabbour *et al.*, 2005). In addition, methods to assess the adhesion of bacteria to model oral surfaces, such as hydroxyapatite, have become of interest, particularly in the presence of anti-plaque agents (Rozen *et al.*, 2001; Jabbour *et al.*, 2005).

5.1.2 Detecting bacterial growth: alamarBlue™

AlamarBlue™, also known as resazurin, is soluble, stable in culture medium, non-toxic and has application as a fluorimetric/colorimetric growth indicator based on the detection of metabolic activity (Serotec. 2003). Proliferating cells exhibit a different internal environment to non-proliferating cells. In particular, the ratios of reduced nicotinamide adenine dinucleotide phosphate/nicotinamide adenine dinucleotide phosphate (NADPH/NADP), reduced flavin adenine dinucleotide/flavin adenine dinucleotide (FADH/FAD), and reduced nicotinamide adenine dinucleotide/ nicotinamide adenine dinucleotide (NADH/NAD) increase during proliferation to

produce a more reduced internal environment. Once alamarBlue™ has been taken up into the cell, it can be reduced by these metabolic intermediates which cause a measurable shift in colour. In its oxidised form, alamarBlue™ is non-fluorescent and indigo blue in colour. Upon reduction, alamarBlue™ becomes resorufin, a fluorescent compound that is pink in colour. An example of alamarBlue™ reduction, as it might occur in cells, is given in Figure 5.1.

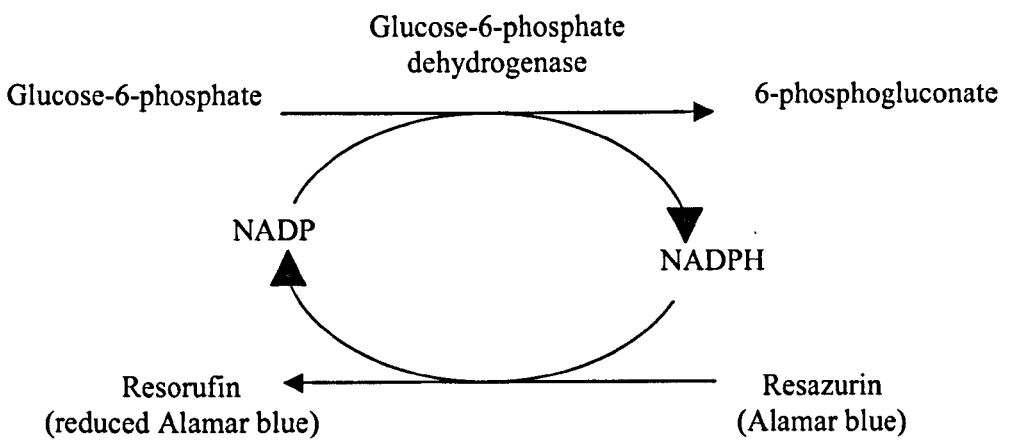

Figure 5.1 Reduction of alamarBlue™ upon uptake into a proliferating cell (Serotec. 2003).

The reduction of alamarBlue™ can be followed in two ways; by measuring absorbance spectrophotometrically or by measuring fluorescence, the latter technique being used in this study. Resorufin, the reduced form of alamarBlue™, absorbs radiation within the range of 530-560 nm (excitation wavelength), and re-emits radiation at 590 nm (emission wavelength). The bioavailability model utilised within this chapter determines the fluorescence of reduced alamarBlue™ to quantify biofilm growth and will be described in the next section (5.1.3). The method of measuring alamarBlue™ reduction by fluorescence has also been used to screen the anti-trichomonas activity of nitroimidazole derivatives (Campos *et al.*, 2005) and to assess the antidermatophytic activities of a range of antimycotics (Okeke *et al.*, 2000). One disadvantage to the use of alamarBlue™ is that it may become further reduced from resorufin to form a colourless, non-fluorescent product known as hydroresorufin. However, systematic

optimisation of cell density, incubation time and media composition can minimise this. In planktonic bacterial studies, alamarBlue™ produced accurate MIC determinations using broth microdilution susceptibility testing against staphylococci and enterococci (Baker and Tenover, 1996). In these studies, neither absorbance nor fluorescence measurements are used to quantify the growth of organisms. Typical broth microdilution techniques rely on the visual detection of turbidity to ascertain the growth of organisms at the concentration of antimicrobial tested. The use of alamarBlue™ provides a colorimetric aid to confirm bacterial proliferation and the MIC value can be assigned to the highest concentration of antimicrobial agent, which remains blue, showing no indication of a shift toward pink.

5.1.3 The bioavailability model: GlaxoSmithKline Research & Development

The bioavailability model developed at GlaxoSmithKline (Weybridge, UK) is a modified version of the technique described by Martin *et al.* (2005). In this method, biofilms grown from a salivary inoculum on hydroxyapatite-coated microtitre plate wells were exposed to actives formulated in prototype pastes. The anti-bacterial effect of these formulations was evaluated by measuring the fluorescence of alamarBlue™ using a plate reader to determine cell viability without the need for biofilm disruption. The percent reduction of mean relative fluorescence of reduced alamarBlue™ following treatment of the biofilm with the test formulation was expressed relative to the fluorescence produced from untreated biofilms (positive growth control). This technique proved successful in assessing the efficacy of antimicrobial formulations against established oral biofilms.

The modified technique, the bioavailability model, utilised within this study is used to determine the substantivity of oral formulations and their subsequent inhibition of biofilm growth. Hydroxyapatite-coated microtitre plates incubated with artificial saliva were used to simulate a model oral surface with a salivary pellicle. The substantivity of many agents is largely due to their interaction with salivary mucins (Scheie, 1989; Doyle, 1989; Eley, 1999). Hence, porcine stomach mucin was included in the artificial saliva to more accurately represent the salivary pellicle formed on oral surfaces *in vivo*. Antimicrobial formulations designed to exhibit substantivity were then applied to the

surface for a pre-determined contact time following which the wells were washed. Saliva-derived inoculum was then incubated with the treated surface and allowed to develop into a biofilm, the growth of which was detected by the addition of alamarBlue™. Growth controls involved treatment of the surface with sterile water and caused 100% reduction of alamarBlue™. All formulations were compared to chlorhexidine as a positive control. This is an agent known to have superior substantivity within the oral cavity (Addy. 1994), which if applied at the appropriate concentration will kill all the bacterial cells (therefore allowing no reduction of alamarBlue™). Successful formulations would exhibit a significant decrease in alamarBlue™ reduction relative to the growth control due to inhibition of bacteria present in the saliva-derived inoculum, thereby preventing the formation of a biofilm on the hydroxyapatite surface.

5.1.4 Quantifying biofilm formation using alamarBlue™: Fluorescence spectroscopy

Fluorescence is a type of luminescence in which a molecule absorbs high-energy radiation and re-emits it as lower-energy radiation. Fluorescent molecules at an electronic ground state require radiation of a particular wavelength, usually within the ultraviolet range, to excite electrons to a higher electronic energy level. Electrons can return rapidly to the ground state by emitting a photon of radiation, causing the molecule to fluoresce. Fluorescence will persist only as long as the stimulating radiation is continued. Resonance fluorescence occurs if the absorbed radiation is re-emitted without a change of frequency, however, for many fluorescent molecules there is a shift towards lower energies (longer wavelengths), which is known as the Stokes shift (Skoog *et al.*, 1997). There is a wide range of applications for fluorescence, for example the visualisation of DNA fragments separated by agarose gel electrophoresis is achieved with the use of ethidium bromide, a compound that, when bound to DNA, fluoresces intensely.

Fluorescence can be measured with a fluorometer or spectrofluorometer (Figure 5.2). Generally, these instruments have components analogous to spectrophotometers. In brief, radiation is emitted from the source as a beam, which is split into a reference beam and a sample beam. The sample beam passes through an excitation filter or

monochromator, which transmits radiation at wavelengths required for excitation. When the beam hits the sample it emits fluorescent radiation, which can be observed at right angles from the specimen. Emitted radiation passes through an emission filter or second monochromator, which isolates the fluorescence for measurement. Meanwhile the reference beam is passed through a beam attenuator, which reduces intensity to approximately that of the fluorescence radiation. Both beams then pass through a transducer, typically a photomulitplier tube, which enhances the signal intensity and produces an electrical output. Outputs from both the reference and sample beam then pass through a difference amplifier which calculates the ratio of the sample to reference intensities (Skoog *et al.*, 1997).

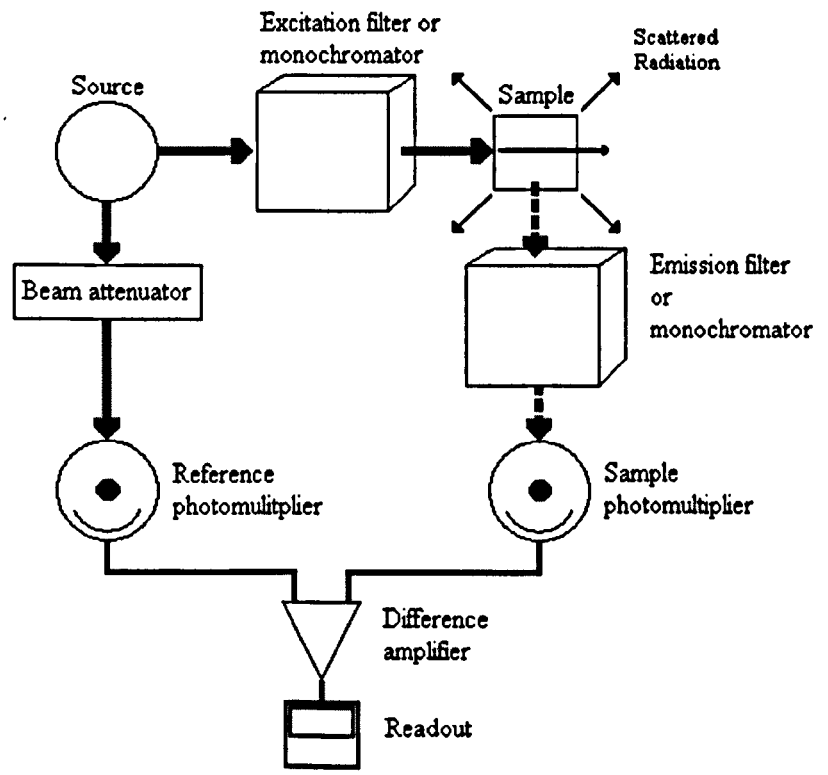

Figure 5.2 Components of a fluorescent spectrometer (adapted from Skoog *et al.*, 1997)

The sensitivity and detection limits of fluorometry are dependant on both instrumentation and analyte variables. Selection of appropriate environmental conditions together with adequate instrumentation can result in detection limits lower than absorption spectroscopy (Wehry, 1997). As with most spectroscopy, the measurement of fluorescent intensities can be adversely affected by interferences. Background fluorescence and scattering are a consequence of other sample constituents

or fluorescent contaminants present within the sample cell or solvent. This type of interference can often be easily avoided e.g. separating the fluorescent component from the remainder of the sample or selecting wavelengths at which other sample constituents do not absorb/fluoresce. Inner-filter effects can be caused by the presence of interferants that absorbs radiation in; a) the same wavelength as the analyte, thus decreasing the radiant power required to excite the analyte, or b) the same wavelength at which the analyte fluoresces, reducing the photons emitted from the sample.

In this chapter, planktonic studies based on broth dilution techniques were used to evaluate the antimicrobial activity of chitosan-fluoride microparticles and zinc-, silver- and copper-Carbopol 971P complexes *in vitro*. From this initial investigation, complexes were selected for investigation using the bioavailability model developed at GlaxoSmithKline R&D (Weybridge, UK). AlamarBlue™ was used to detect changes in bacterial numbers relative to appropriate experimental controls. In the planktonic studies, the colour change of alamarBlue™ was used to confirm bacterial growth together with visual inspection. In the bioavailability model, the fluorescence of alamarBlue™ was determined using a fluorimeter to quantify biofilm growth.

5.2 Materials and Methods

5.2.1 Materials

Optimised chitosan-fluoride and chitosan-only microparticles prepared by spray-drying sodium fluoride (Sigma-Aldrich company, Gillingham, UK) and/or HCMF (Cognis, Illertissen, Germany) (Chapter 4) were utilised in this study. Carbopol 971P was kindly donated by Noveon Inc (Cleveland, USA). AlamarBlue™ was purchased from Serotec (Oxford, UK) and stored immediately at 4^0C until use as per the manufacturer's instructions. Zinc sulphate heptahydrate (ACS reagent), copper sulphate (ACS reagent) porcine stomach mucin, potassium chloride and chlorhexidine digluconate were purchased from Sigma-Aldrich Company Ltd, Gillingham, UK. Silver nitrate (certified analytical reagent), D-glucose, purified water (electrochemical grade) and sodium hydroxide were purchased from Fisher Scientific UK Ltd (Loughborough, UK). Sodium chloride, calcium chloride dihydrate and absolute ethanol were purchased from VWR International (Lutterworth, UK). Granulated brain heart infusion (BHI) broth was purchased from Merck KGaA, (Darmstadt, Germany). All other microbiological media were purchased from Oxoid Ltd (Basingstoke, UK).

All microbiological media and agar were prepared in distilled water and sterilised prior to use by autoclaving at 121°C for 15 min. All work described in the following sections was carried out under sterile conditions in a class II microbiological safety cabinet unless otherwise stated.

5.2.2 Methods

5.2.2.1 Preparation of planktonic bacteria

5.2.2.1a Test bacteria and culture conditions

Individual bacterial strains used in the planktonic studies were as follows; *Staphylococcus aureus* (NCTC 10788), *Streptococcus sanguinis* (NCTC 10904) and

Actinomyces naeslundii (NCTC 10301) (National Collection of Type Cultures, Health Protection Agency, London UK), and *Streptococcus mutans* (NCIMB 702062; National Collection of Industrial, Marine and Food Bacteria Ltd, Aberdeen UK). Working cultures of each bacterial species were stored at 4°C on tryptone soya agar (TSA), except for *Actinomyces naeslundii*, which was grown and stored on anaerobic blood agar (Oxoid Ltd). Working cultures were replaced every two weeks. Single colonies were grown aerobically in 10 mL sterile tryptone soya broth (TSB) with shaking (Denley Orbital Shaker) at 100 rpm for 24 h at 37°C. TSA or anaerobic blood agar plates were then inoculated from the bacterial cultures using an inoculating loop and incubated for a further 24 h at 37°C before being stored at 4°C.

5.2.2.1b Preparation of optical density calibration curves

To obtain the appropriate starting inoculum of *Staphylococcus aureus*, *Streptococcus mutans* and *Streptococcus sanguinis* for planktonic studies, optical density curves were prepared. TSB (10 mL) was inoculated with a single pure colony removed from the working culture and grown for 24 h at 37^0C with shaking at 100 rpm. After this period, the culture was transferred to a 50 mL centrifuge tube (Fisher) and centrifuged at 1300 g for 15 min (Sorvall RT6000B). Excess TSB was decanted and the resultant cell pellet was re-suspended in 20 mL sterile PBS by vortexing for a minimum of 5 min. This process was repeated three times to fully remove any residual TSB and a final bacterial cell suspension was obtained in PBS (10 mL). Serial dilutions of 1:10, 1:8, 1:6, 1:4, and 1:2 were prepared in PBS and the optical density of these dilutions was measured at 540 nm using a Helios Unicam spectrophotometer (Cambridge UK).

Serial 1:10 dilutions were then prepared from the 1:10, 1:6, and 1:2 dilutions in sterile PBS to obtain a final dilution factor of 10^8. Viable counts were made on the four highest dilutions (10^5-10^8) by spreading 100 µL of bacterial cell suspension on TSA plates and incubating for 24 h at 37^0C with shaking at 100 rpm (Denley Orbital Shaker). Three plates were prepared from each dilution. Following the incubation period, the plates that displayed bacterial numbers between 30-300 colony forming units (cfu) were counted and the cfu mL^{-1} of the original suspension calculated. This process was repeated three times for each bacterial species and calibration curves of optical density at 540 nm against cfu mL^{-1} were prepared.

5.2.2.1c Calculating *Actinomyces naeslundii* inoculum size

Due to the filamentous form of *Actinomyces naeslundii*, calculating the cfu mL^{-1} from optical density measurements would be an unreliable method. The presence of filaments would increase the absorbance of the PBS bacterial suspension and prevent accurate dilutions of cell numbers. Therefore the starting inoculum of *Actinomyces naeslundii* was derived by performing viable counts on cultures grown for 24 h and 48 h at 37°C with shaking at 100 rpm. Following incubation, cultures were centrifuged at 1300 g for 15 min to obtain a cell pellet which was then re-suspended in sterile PBS. The cell pellet was washed three times before ten serial 1:10 dilutions were prepared from the final cell suspension in sterile PBS. Aliquots (100 µL) removed from the highest four dilutions were spread on anaerobic blood agar and incubated at 37°C for 24 h. Plates were prepared in triplicate. The plates displaying counts of between 30-300 colonies were used to calculate the cfu mL^{-1} of the original cultures. The mean growth over 24 h and 48 h was then calculated and used to derive dilution factors to obtain the starting inoculum of *Actinomyces naeslundii* for planktonic studies.

5.2.2.2 Antimicrobial activity of chitosan-fluoride microparticles

5.2.2.2a Preparation of microtitre plates and test solutions

Prior to the preparation of test solutions, microparticle samples and sodium fluoride were sterilised under an ultraviolet lamp for a minimum of 30 min. Chitosan-fluoride microparticles (16 mg) were suspended in 10% v/v ethanol (2 mL) to produce a concentration of 480 µg fluoride mL^{-1}. Chitosan-only microparticles (13.9 mg) were suspended in 10% v/v ethanol (2 mL) to produce a concentration of chitosan identical to the amount present in the chitosan-fluoride microparticle suspension (1.5% w/v). Sodium fluoride was prepared in 10% v/v ethanol at a concentration equivalent to 480 µg fluoride mL^{-1} (0.025 M sodium fluoride).

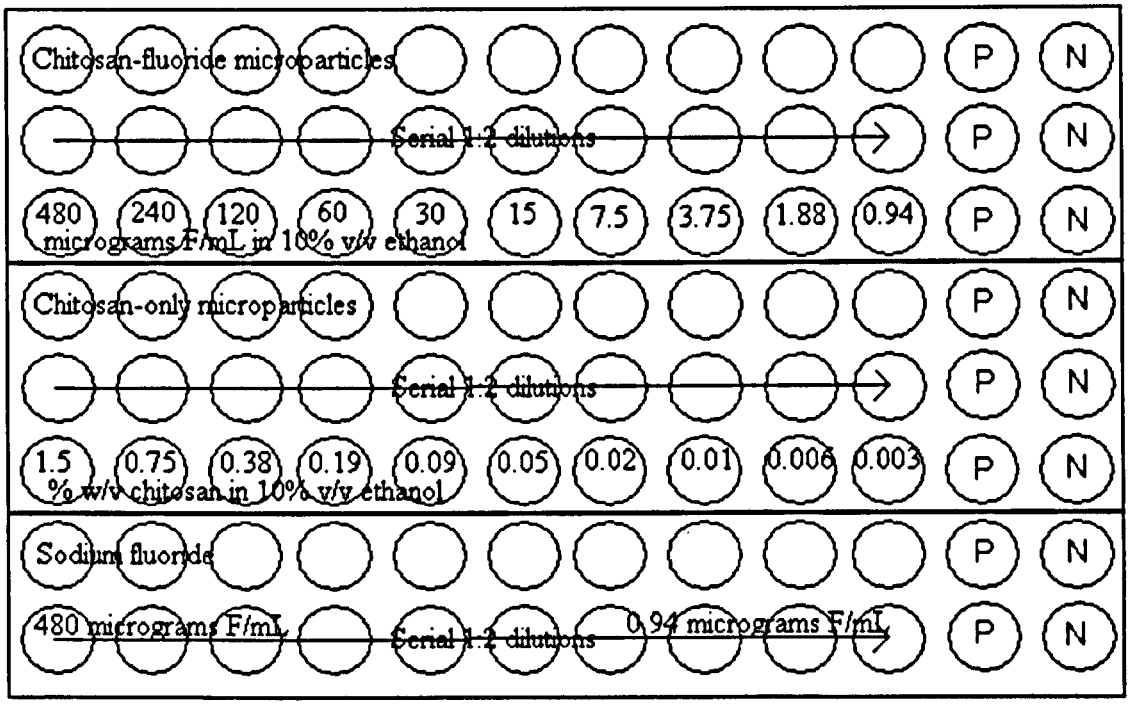

Figure 5.3 Schematic representation of the 96-well microtitre plate used to assess the antimicrobial activity of chitosan-fluoride microparticles, chitosan-only microparticles and sodium fluoride prior to the addition of starting bacterial inoculum. The positive and negative controls are denoted as P and N respectively.

Sterile 96-well, flat bottom microtitre plates (Corning) were used to assess the MIC of chitosan-fluoride microparticles against the four bacterial species (Figure 5.3). Working solutions of chitosan-fluoride microparticles, chitosan-only microparticles, and sodium fluoride (100 μL) were added to the wells of column 1 in rows A-C, D-F, and G-H respectively. Wells in columns 2-10 of each row were used to make serial 1:2 dilutions of the working solutions. Sterile 10% v/v ethanol (100 μL) was dispensed into these wells (Eppendorf Research®). The use of ethanol was necessary to ensure chitosan microparticle dispersion, however the presence of alcohol is known to influence the growth of bacteria. Preliminary experiments determined that 10% v/v ethanol did not adversely affect the growth of the test species. However, to ensure experimental observations were due to the effects of the test compound only i.e. chitosan-fluoride microparticles, chitosan-only microparticles and sodium fluoride, rather than the presence of ethanol, all wells contained 10% v/v ethanol. To all the wells of column 2 in each row, the appropriate working solution (100 μL) was dispensed and mixed with

the 10% v/v ethanol using a pipette to produce a 1:2 dilution of the working solution in 200 µL. 100 µL was then transferred to the subsequent well and the process repeated to produce a range of serial 1:2 dilutions in wells of each row. Wells in columns 11 and 12 were used for the positive and negative control respectively. The positive control was used to check the normal growth of the bacteria under the experimental conditions and was therefore composed of the starting bacterial inoculum in double strength TSB (100 µL) and 10% v/v ethanol (100 µL). The negative control (well 12) was used to assess any bacterial growth originating from the test solutions and was therefore composed of the master test solution in 10% v/v ethanol (100 µL) in sterile double strength TSB (100 µL) without inoculation.

5.2.2.2b Preparation of starting bacterial inoculum

Sterile TSB (10 mL) was inoculated with a single pure colony from the working culture and incubated for 24 h at 37°C with shaking at 100 rpm. After incubation, the cultures were transferred to a centrifuge tube and centrifuged at 1300 g for 15 min. The resultant cell pellet was washed three times in sterile PBS and a bacterial inoculum of 2 x 10^6 cfu mL^{-1} was prepared. In the case of *Staphylococcus aureus, Streptococcus sanguinis*, and *Streptococcus mutans*, the concentration of the starting inoculum was achieved by using the optical density calibration curve to obtain a bacterial cell suspension containing approximately 2 x 10^8 cfu mL^{-1}. Once an appropriate optical density was achieved the suspension was centrifuged at 1300 g for 15 min and the PBS removed and replaced with an equal volume of sterile double strength TSB. Two 1:10 dilutions in TSB were then used to obtain a starting bacterial inoculum of 2 x 10^6 cfu mL^{-1}. *Actinomyces naeslundii* was prepared by re-suspending the cell pellet in sterile double strength TSB at the dilution factor calculated in section 5.2.2.1c.

5.2.2.2c Broth microdilution technique

Starting bacterial inoculum (100 µL) was added to each well (1-10) to produce a final inoculum of 1 x 10^6 cfu mL^{-1} in single strength broth and final working concentrations of the test solutions ranging from 240-0.47 µg fluoride mL^{-1} and chitosan concentrations of 0.75-0.0015% w/v. Starting bacterial inoculum (100 µL) was also added to wells in column 11 to prepare the positive growth control. Sterile double strength TSB (100 µL)

was added to wells in column 12 to prepare the negative control to check for working solution sterility. The plate was sealed with parafilm and incubated for 24 h at 37°C with shaking at 100 rpm.

After the incubation period elapsed, AlamarBlue™ (20 μL) was added to each of the wells and the plate incubated under the same conditions for a further 15 min. Following this the plate was examined for a colour change from dark blue to pink, which indicated bacterial growth. The lowest concentration of test solution that did not cause a colour change was considered the MIC value. Two microtitre plates were used for each bacterial species.

5.2.2.3 Antimicrobial activity of Carbopol 971P-metal ion formulations

5.2.2.3a Preparation of test solutions

Electrochemical grade water (Fisher) sterilised by autoclaving at 121°C for 15 min was used to prepare all test solutions. Carbopol 971P was sterilised under ultraviolet light for a minimum of 30 min prior to use. Aqueous Carbopol 971P dispersions were prepared by adding 0.2 g to 40 mL sterile water under magnetic stirring at 300 rpm for 4 h (Stuart Heat-Stir CB192). The resultant dispersion was adjusted to pH 7.0 using 0.1 M sodium hydroxide prepared in sterile water and made up to volume (100 mL) to obtain a final concentration of 0.2% w/v. Zinc sulphate heptahydrate for use in section 5.2.2.3c was prepared in sterile water at a concentration of 2.78 mM. Copper sulphate, zinc sulphate heptahydrate and silver nitrate were prepared at concentrations of 1.39 mM, 1.39 mM and 2.78 mM respectively for use in section 5.2.2.3d. All metal salt solutions were autoclaved at 121°C for 15 min to ensure sterility.

5.2.2.3b Preparation of bacterial inoculum

Staphylococcus aureus and *Streptococcus mutans* were the only species that exhibited adequate growth in peptone water supplemented with 2.5 g L^{-1} glucose over 24 h and were therefore used to analyse the antimicrobial efficacy of metal salt solutions and Carbopol 971P formulations. Cultures were prepared by inoculating peptone water supplemented with 2.5 g L^{-1} glucose (10 mL) with a single pure colony removed from

the working culture and incubated for 24 h at 37°C with shaking at 100 rpm. Cells were then washed three times in sterile PBS and adjusted to a concentration of 2 x 10^6 cfu mL^{-1} using the technique described in 5.2.2.2b. PBS was removed by centrifugation and the final cell pellet re-suspended in double-strength peptone water containing 5 g L^{-1} glucose.

5.2.2.3c Antimicrobial activity of Carbopol 971P-zinc sulphate solution

The antimicrobial activity of Carbopol 971P-zinc sulphate solutions were assessed using a microtitre plate technique. Rows 1-4 were used to test the antimicrobial activity of 0.695 mM zinc sulphate heptahydrate, 0.05% w/v Carbopol 971P, Carbopol 971P-zinc sulphate solution and a positive growth control respectively. Columns 1-6 were used to assess the growth of the bacteria in the presence of the corresponding test solutions while columns 7-12 were used to confirm the test solution sterility. Test solutions (50 µL), except Carbopol-zinc sulphate solutions, were dispensed into each well of columns 1-12 in rows 1 and 2 and sterile water (50 µL) were added to achieve concentrations of 1.39 mM zinc sulphate heptahydrate and 0.1% w/v Carbopol 971P. Sterile water (100 µL) was dispensed into row 4 for the positive growth control. Bacterial inoculum (100 µL) or sterile double strength peptone water supplemented with 5 g L^{-1} glucose (100 µL) were then added to wells in columns 1-6 and 7-8 respectively to achieve the final test concentrations of 0.695 mM zinc sulphate heptahydrate (row 1) and 0.05% w/v Carbopol 971P (row 2) and the positive growth control (row 4). Carbopol-zinc sulphate solutions with bacterial inoculum or sterile double strength peptone water with 5 g L^{-1} were prepared externally in centrifuge tubes. In brief, double strength peptone water supplemented with 5 g L^{-1} glucose (2 mL), either containing bacterial inoculum (test) or sterile (negative control) was added to 0.2% w/v Carbopol 971P (1 mL) and vortexed for 1 minute to ensure adequate mixing. Zinc sulphate heptahydrate at a concentration of 2.78 mM (1 mL) was then added to the mixture to achieve a final concentration of 0.05% w/v Carbopol 971P and 0.695 mM zinc sulphate. The final solution was then dispensed (200 µL) into wells of columns 1-6 (test solution) and 7-12 (negative control) of row 3 in the microtitre plate.

The microtitre plate was then sealed with parafilm and incubated for 24 h at 37°C with shaking at 100 rpm Following this the plate was removed from the incubator and

Alamarblue™ (20 μL) was added to each well and the incubated for a further 15 min. Bacterial growth was indicated if a colour change from dark blue to pink was observed. Three microtitre plates were used for each bacterial species.

5.2.2.3d Antimicrobial activity of metal salt solutions

The antimicrobial efficacy of zinc sulphate heptahydrate, silver nitrate, and copper sulphate were assessed against *Staphylococcus aureus* and *Streptococcus mutans* using a broth microdilution technique. Three final concentrations of each metal salt were tested depending on the starting concentration within the Carbopol 971P formulation. The microtitre plate was prepared as described in Figure 5.4. Final concentrations of each metal salt at a volume of 100 μL were achieved by performing two 1:2 dilutions of the master metal salt solution (described in section 5.2.2.3a) in sterile water. Hence for zinc sulphate and copper sulphate; the concentrations tested were 0.695 mM, 0.35 mM, and 0.17 mM. For silver nitrate, the concentrations tested were 1.39 mM, 0.695 mM and 0.35 mM. The negative control was used to confirm the sterility of the metal salt solutions and was therefore composed of master metal salt solution (100 μL) and sterile double strength peptone water supplemented with 5 g L^{-1} glucose (100 μL). Sterile water was dispensed into the well assigned for the positive growth control.

Starting bacterial inoculum (100 μL) was added to each well except the negative control and the microtitre plate sealed with parafilm. The plate was then incubated for 24 h at 37°C with shaking at 100 rpm. After this time, the plate was removed and alamarBlue™ (20 μL) was added to each well and incubated for a further 15 min. The wells were then inspected visually to determine whether a colour change from dark blue to pink had occurred. Three microtitre plates were carried out for each bacterial species tested.

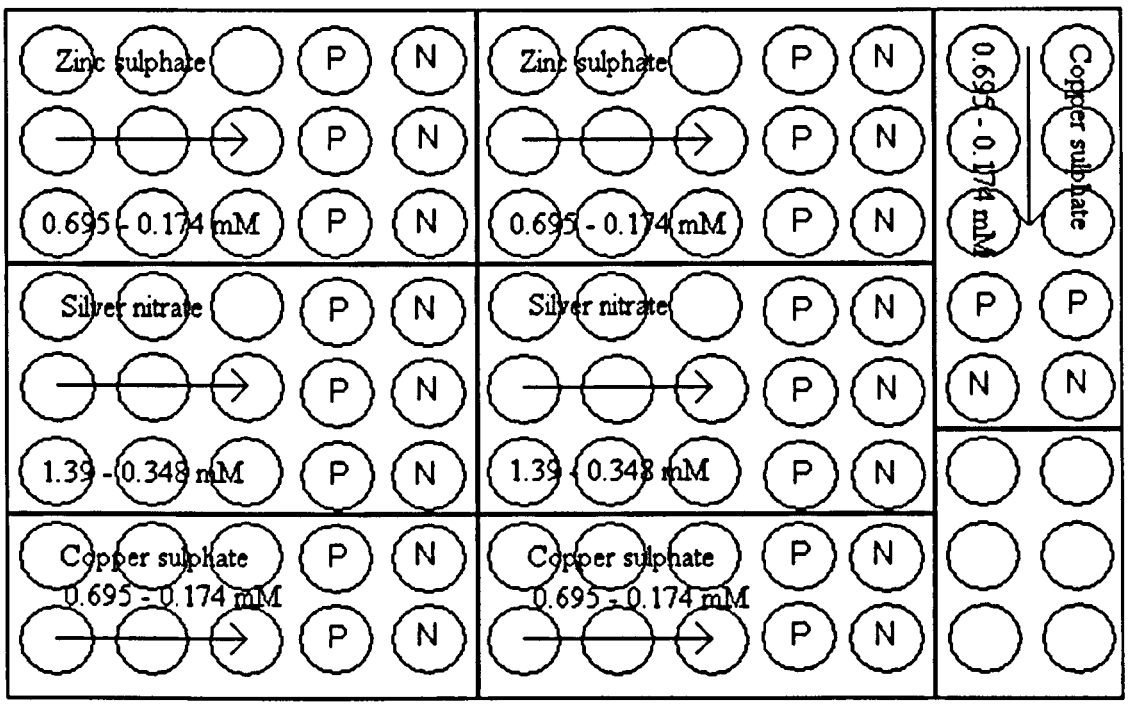

Figure 5.4 Schematic representation of the 96-well microtitre plate used to assess the antimicrobial activity of metal salt solutions used to prepare Carbopol 971P formulations. The positive and negative controls are denoted as P and N respectively.

5.2.2.4 Bioavailability model

This technique was carried out in the New Product Research laboratories based within the GlaxoSmithKline Research and Development site at Weybridge, UK.

5.2.2.4a Preparation of saliva derived inoculum

Fresh saliva was collected without stimulation from three individuals and stored at 4°C until use. No oral care or eating was permitted 3 h before donation and saliva was used within a minimum of 2 h. An example of the declaration required by every individual prior to donation is given in Appendix 4. Aliquots (1 mL) were removed from each salivary sample and added to 250 mL sterile BHI broth. Two BHI broths were prepared in this way. Inoculated BHI broth was incubated overnight at 37°C both aerobically (LABheat incubator) with shaking (Denley Orbital Shaker) and anaerobically (Concept 400 anaerobic work station) without shaking.

Following an overnight incubation, 0.5 mL of the inoculated BHI broth was added to fresh pre-warmed BHI broth (10 mL). This was carried out for each salivary culture and incubated for a further 3 h to obtain early exponential growth at 37°C both aerobically and anaerobically.

5.2.2.4b Preparation of test agents

Carbopol 971P-zinc sulphate and Carbopol 971P-silver nitrate complexes were assessed using the bioavailability model following information gained during the planktonic studies. Carbopol 971P (0.10 g) was weighed into a sterile 150 mL filtrate container (Nalgene) and 5 mL ethanol was added in order to sterilise the powder. The polymer sample was left overnight at 37°C to ensure complete evaporation of ethanol. Sterile water (50 mL) was added to the polymer and stirred using a magnetic stirrer (Stuart heat-stir CB192) at 300 rpm until dispersed. The pH of the aqueous polymer dispersion was adjusted to 7.0 using 0.1 M sodium hydroxide prepared in sterile water. The volume was made up to 100 mL using sterile water and the container sealed and stored overnight at 4°C. Zinc sulphate (0.695 mM and 1.39 mM) and silver nitrate (1.39 mM and 2.78 mM) were prepared in deionised water and autoclaved at 121°C for 15 min to ensure solution sterility.

5.2.2.4c Preparation of artificial saliva

Artificial saliva with mucin was prepared in 1 L deionised water both with and without calcium chloride dihydrate. The composition was as follows: porcine stomach mucin (2.5 g), sodium chloride (0.35 g), potassium chloride (0.2 g), calcium chloride dihydrate (0.2 g), yeast extract (2.0 g), lab lemco powder (1.0 g), and proteose peptone (5.0 g). The artificial saliva was autoclaved at 121°C for 15 min and stored in bottles covered with tinfoil to prevent a reaction with light. Urea (40% w/v) was prepared in deionised water and sterilised using a 0.45 μm syringe filter (Nalgene). Aliquots (1.25 mL) were added to autoclaved artificial saliva (both with and without calcium chloride dihydrate) and stirred for 15 min using a magnetic stirrer to ensure adequate mixing. Artificial saliva was stored in a cool dark environment for a maximum of two weeks.

Test agents to be used in the bioavailability model were mapped out on a 96-well plate prior to test initiation to allow rapid transfer to the test plate. The effect on biofilm growth caused by the polymer complexes was compared to sterile deionised water, 0.695 mM zinc sulphate, 1.39 mM silver nitrate and 0.05% w/v Carbopol 971P (prepared by adding 10 mL sterile water to 10 mL 0.10% w/v Carbopol 971P) to determine the efficacy of the formulation relative to individual components and a growth control (sterile water). Chlorhexidine digluconate (2.0% v/v) prepared in sterile water was used as a positive control as this concentration had previously been found to inhibit biofilm growth (Martin *et al.*, 2005). Carbopol 971P-zinc sulphate and Carbopol 971P-silver nitrate complexes were prepared by adding 1.39 mM zinc sulphate (10 mL) or 2.78 mM silver nitrate to 0.10% w/v sterile Carbopol 971P (10 mL) and mixed for 15 min on an orbital shaker at 100 rpm (Denley Orbital Shaker). Samples were dispensed (200 µl) into all of the wells of the corresponding column, which were assigned as follows; column 1- 2% v/v chlorhexidine digluconate, column 2- Carbopol 971P-zinc sulphate, column 3- Carbopol 971P-silver nitrate, column 9- 0.695 mM zinc sulphate, column 10- 1.39 mM silver nitrate, column 11- 0.05% w/v Carbopol 971P, and column 12- sterile deionised water.

5.2.2.4d Plate wash preparation

For each plate, TSB (500 mL) was prepared in a 1 L flask fitted with a screw cap (feed flask). The screw cap had a feed line and an inlet port fitted with a 0.45 µm air filter (Whatman) connected by silicone rubber tubing. The outlet valve of a Nunc-Immunowash 12 manual plate washer was connected by means of silicone rubber tubing (effluent line) to a 10 L effluent bottle, 0.45 µm air filter and a 6 L h^{-1} vacuum pump. The feed flask was attached to the inlet valve of the plate washer via the feed line. The plate washer was primed by turning on the vacuum pump and running through approximately 20 mL TSB.

5.2.2.4e Bioavailability model

The bioavailability of the polymer complexes was assessed on 96-well microtitre plates coated with hydroxyapatite as described in section 5.1.3. All hydroxyapatite-coated

plates were provided by GlaxoSmithKline R&D (Weybridge, UK). Artificial saliva (200 µl) was dispensed into each test well on the hydroxyapatite-coated plate and incubated at 37°C for 30 min with gentle shaking at 100 rpm to allow the development of a pellicle. Artificial saliva was removed from the plate using the plate washer set-up described in the previous section. In brief, the contents of each well were removed using the Nunc Immunowash 12 manual plate washer and discarded into the effluent bottle. Sterile TSB was then dispensed into each well until full and removed with the plate washer. This was repeated three times to remove excess artificial saliva from the hydroxyapatite-coated plate.

The test agents prepared in the 96-well plate prior to the experiment were transferred to the artificial saliva treated hydroxyapatite-coated plate using a Transtar pipettor (Costar) allowing the transfer of all test agents at the same time and enabling contact times to be closely regulated. The plates were incubated for 2 min at 37°C with shaking at 100 rpm. The plate washer was then used to remove the test agents from the hydroxyapatite surface and the wells were washed three times with TSB from the feed flask. Sterile BHI broth (180 µl) was added to the test wells followed by saliva-derived inoculum (20 µl) prepared as described in section 5.2.2.4a. The plates were incubated at 37°C with shaking at 100 rpm for either 4 or 24 h to allow adhesion of microbial species.

The effect of Carbopol 971P-zinc sulphate and Carbopol 971P-silver nitrate on biofilm formation after a contact time of 2 min was assessed at 4 h and 24 h using hydroxyapatite-coated plates. In total, four plates were prepared for each time point; 2 were treated with artificial saliva containing calcium chloride dihydrate, and 2 were treated with artificial saliva without calcium chloride dihydrate. In addition, a further four plates were used to investigate the effect of an increased contact time on the performance of the polymer complexes in artificial saliva, both with and without calcium chloride dihydrate after 4 h. The total number of replicates for each parameter was 16.

5.2.2.4f Quantification of biofilm formation

Following incubation of the hydroxyapatite-coated plates, the wells were washed three times with sterile TSB from the feed flask using the plate washer in order to remove any planktonic bacteria not attached to the surface. AlamarBlue™ (10% v/v) was prepared in sterile BHI broth not more than 30 min before use and 200 µl was dispensed into the test wells. The plate was then incubated for 30 min at 37°C with shaking at 100 rpm. The fluorescence of all test wells was measured using a plate reader (Biotek Synergy HT-1) fitted with a 530 nm excitation filter and a 590 nm emission filter. Plate reader settings were as follows: sensitivity setting- 25, pre-heat temperature- 37°C, intensity- 1, fluorescent probe position- top.

5.2.3 Statistical analysis

Data obtained from the MIC determinations of chitosan-fluoride microparticles were expressed as the median. The relative fluorescence units generated by the reduction of alamarBlue™ in the bioavailability model were expressed as the mean (±SD). The Kolmogorov-Smirnov test revealed that the data was not normally distributed. Therefore statistical differences between the fluorescence emitted from the wells treated with bioadhesive polymer complexes and metal salts were calculated using Kruskal-Wallis one-way analysis of variance at the 5% probability level. Where significant differences within the data sets were indicated, the Mann-Whitney U test was used to identify which paired locations were significantly different. The percentage reduction of reduced alamar blue™ was expressed relative to the positive and negative controls; where the fluorescence emitted from the positive control (chlorhexidine digluconate) was equal to 100% reduction in reduced alamar blue™ i.e. no alamar blue™ reduction and no metabolising bacteria, and the fluorescence emitted from the negative control (deionised water) equal to 0% reduction i.e. complete alamar blue reduction™. The percentage reduction data was expressed as the mean (± SD) of 16 replicates. The effect of calcium chloride within artificial saliva and increasing contact times on the percentage reduction of alamarBlue™ reduction caused by the test solutions was evaluated using Student's *t* test assuming unequal variance for unpaired samples. All calculations were performed using SPSS v.13 software.

5.3 Results and Discussion

5.3.1 Calculating the starting inoculum

5.3.1.1 Optical density calibration curves

In order to derive the starting inoculum for use in the assessment of chitosan-fluoride microparticle antimicrobial efficacy, optical density calibration curves based on the measurement of pure bacterial cultures in PBS were prepared. This process was completed for *Staphylococcus aureus* (Figure 5.5), *Streptococcus sanguinis* (Figure 5.6) and *Streptococcus mutans* (Figure 5.7). Optical density measurements have been used in previous studies investigating antimicrobial efficacy to determine the starting inoculum (Sondi and Sondi, 2004; Jabbour *et al.*, 2005). It is assumed that within limits a linear relationship exists between the number of bacterial cells in suspension and absorbance at 540 nm. The presence of extracellular material and the possibility of obtaining an inadequate suspension are sources of possible error in measuring the absorbance of cell suspensions.

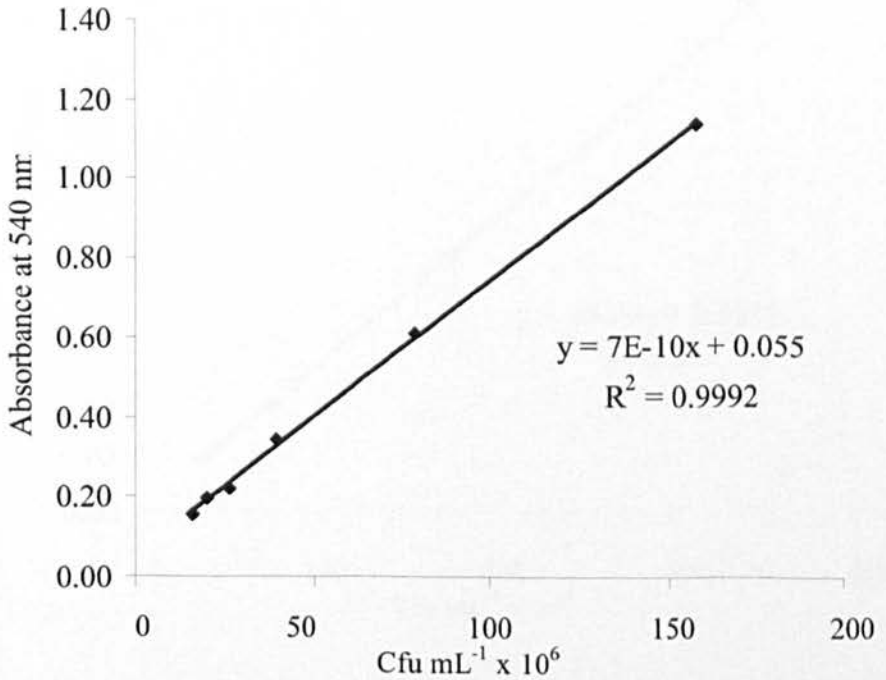

Figure 5.5 Optical density calibration curve for *Staphylococcus aureus* (n= 3 ± SD).

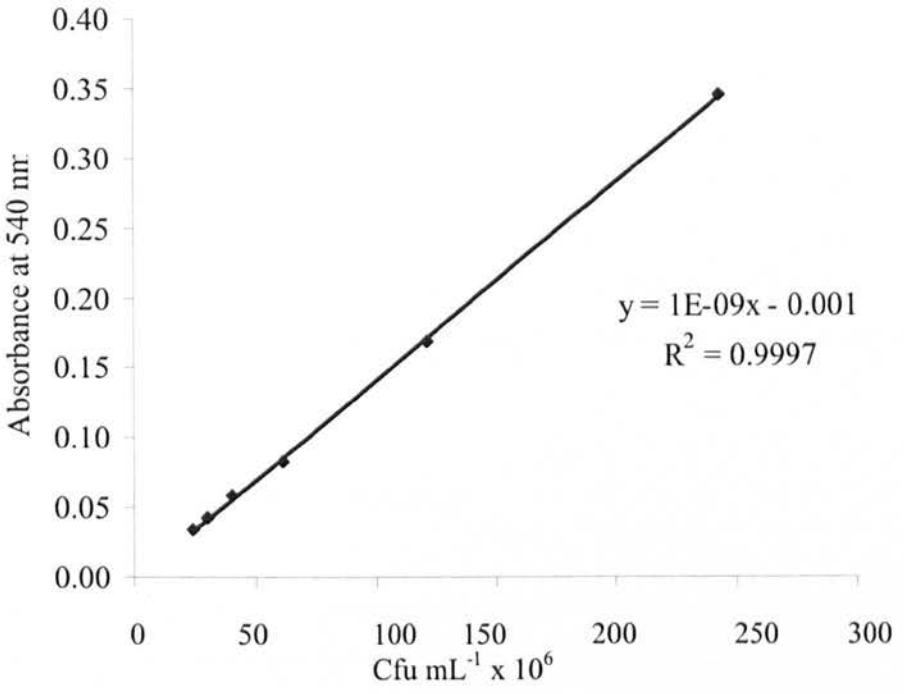

Figure 5.6 Optical density calibration curve for *Streptococcus sanguinis* (n= 3 ± SD).

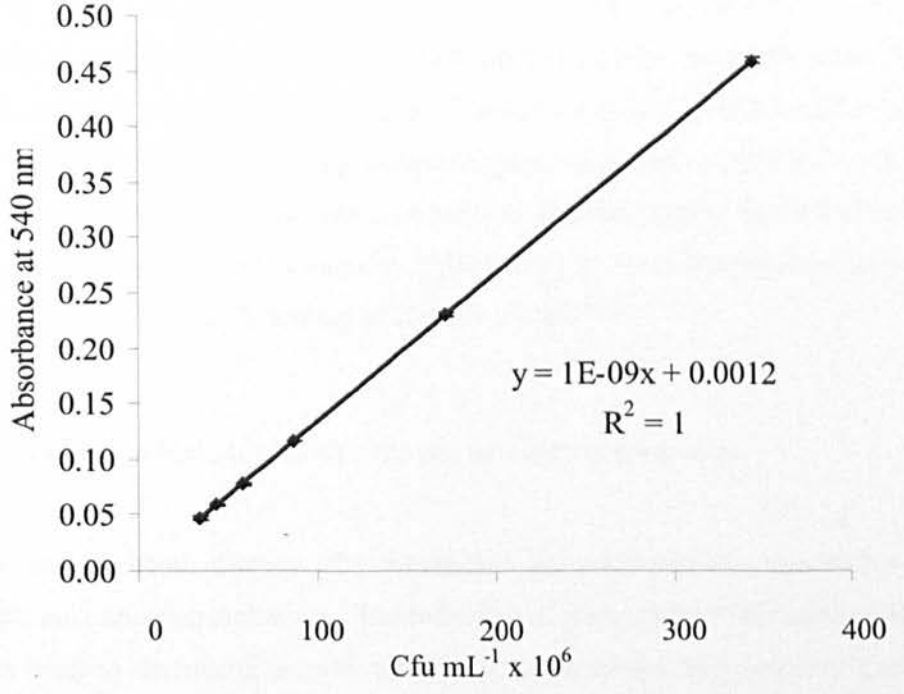

Figure 5.7 Optical density calibration curve for *Streptococcus mutans* (n= 3 ± SD).

Staphylococcus aureus, *Streptococcus sanguinis*, and *Streptococcus mutans* are not known to produce extracellular material under the experimental conditions employed and cell suspensions were vortexed for a minimum of five min prior to measuring absorbance to minimise error. A starting cell suspension containing approximately 2 x 10^8 cfu mL^{-1} was used to achieve a final starting inoculum of 2 x 10^6 cfu mL^{-1} required for testing antimicrobial efficacy. For suspensions of *Staphylococcus aureus*, *Streptococcus sanguinis*, and *Streptococcus mutans* in sterile phosphate buffered saline, an absorbance of 0.195, 0.199, and 0.201 was required at 540 nm to achieve the desired bacterial cell suspension.

5.3.1.2 *Growth of Actinomyces naeslundii*

Actinomyces naeslundii suspensions contain filamentous material, which renders measurements of absorbance inaccurate. Therefore a series of cultures were set up for 24 h and 48 h in order to estimate the starting inoculum. Cultures were plated out on anaerobic blood agar following serial tenfold dilutions. The mean (± SD) viable count of *Actinomyces naeslundii* after 24 h incubation was 6.83 x 10^8 cfu mL^{-1} (± 1.08 x 10^8). After 48 h, mean viable count was 6.10 x 10^8 cfu mL^{-1} (± 5.0 x 10^7). The number of viable bacteria remaining after 48 h had reduced slightly during the latter 24 h period, presumably due to a lack of nutrients. Therefore cultures grown for 24 h were used in the planktonic studies assuming an approximate viable cell count of 6.83 x 10^8 cfu mL^{-1} to prepare the bacterial inoculum. After washing the cells in sterile PBS, two tenfold dilutions of the bacterial suspension, followed by a 1 in 3 dilution was used to obtain a final bacterial starting inoculum of 2 x 10^6 cfu mL^{-1}.

5.3.2 Antimicrobial efficacy of chitosan-fluoride microparticles

The antimicrobial efficacy of chitosan-fluoride microparticles was assessed using a broth microdilution technique. The reduction of alamarBlue™ by metabolising bacteria was used to determine growth within the wells as has been reported previously by Campos Aldrete *et al.* (2005). Okeke *et al.* (2000) and Baker and Tenover (1996) have also used alamarBlue™ to detect micro-organism growth although the techniques used were slightly different. The reduction of alamarBlue™ can be used to determine the

number of viable micro-organisms, as was described by Campos Aldrete *et al.* (2005). The eligibility of alamarBlue™ as a redox indicator for this purpose has been questionable due to the over-reduction of resorufin into the colourless, non-fluorescent product; hydroresorufin (O'Brien *et al.*, 2000). Planktonic bacteria metabolise at a rapid rate and the cell concentrations achieved after 24 h growth begin to over-reduce alamarBlue™ after 20 min. Therefore, to avoid potential error in the fluorescent determination of cell numbers, qualitative data was collected in the planktonic studies.

Table 5.1 Median MIC of chitosan-fluoride microparticles compared to individual components against a panel of oral bacteria (n = 6)

	Staphylococcus aureus	*Streptococcus mutans*	*Streptococcus sanguinis*	*Actinomyces naeslundii*
Chitosan-only microparticles	> 0.75% w/v	0.75% w/v	0.38% w/v	> 0.75% w/v
Chitosan-fluoride microparticles	> 0.75% w/v > 240 μg mL^{-1}	0.19% w/v 60 μg mL^{-1}	> 0.75% w/v > 240 μg mL^{-1}	0.38% w/v 120 μg mL^{-1}
Sodium fluoride	> 240 μg mL^{-1}	240 μg mL^{-1}	240 μg mL^{-1}	> 240 μg mL^{-1}

The growth of each bacterial species was not affected by the presence of 10% v/v ethanol used to disperse chitosan microparticles, indicated by the reduction of alamarBlue™ in the growth controls; which consisted of 100 μL 10% v/v ethanol and 100 μL double strength TSB containing starting inoculum (5.2.2.2b). MIC values were determined for the microparticles themselves and compared to chitosan-only microparticles and sodium fluoride (Table 5.1). The highest concentration of fluoride tested using this technique was 240 μg fluoride mL^{-1} (13.0 mM) while the highest concentration of chitosan tested was 0.75% w/v. Chitosan-fluoride microparticles, chitosan-only microparticles and sodium fluoride had no effect on *Staphylococcus aureus*, as indicated by a MIC greater than the highest concentration tested (Table 5.1). This was also evident when chitosan-only microparticles and sodium fluoride were tested against *Actinomyces naeslundii* and chitosan-fluoride microparticles against

Streptococcus sanguinis. The lowest MIC (60 μg mL^{-1}) was caused by chitosan-fluoride microparticles when tested against *Streptococcus mutans*. Interestingly, both chitosan-only microparticles and sodium fluoride inhibited the growth of *Streptococcus mutans* only at the highest concentration, which suggests a degree of synergism between the two when formulated together. This was also evident from the results obtained for *Actinomyces naeslundii*, where growth was inhibited at 120 μg mL^{-1} fluoride from chitosan-fluoride microparticles, but not at the highest concentrations of chitosan-only microparticles and sodium fluoride. Conversely, antagonistic effects were indicated from the results obtained with *Streptococcus sanguinis* (Table 5.1).

Chitosan at higher molecular weights has demonstrated inhibitory effects against a range of Gram negative and Gram positive bacteria at concentrations as low as 0.08% w/v (No *et al.*, 2002). In general however, Gram negative bacteria are less susceptible to chitosan than gram positive species, which may account for reduced activity against *Actinomyces naeslundii* (No *et al.*, 2002). In this study, *Staphylococcus aureus* and *Actinomyces naeslundii* were not susceptible to chitosan at concentrations as high as 0.75% w/v. In the study by No *et al.* (2002), a concentration ranging between > 0.1-0.05% w/v depending on molecular weight, was found as the MIC for chitosan when tested against *Staphylococcus aureus*, which does not agree with this study. However, the molecular weight of chitosan used in this study was 500-10,000 kDa, which is greater than the molecular weights tested in the study by No *et al.* (2002) and may therefore produce different activity. The highest concentration of sodium fluoride used in this study was inhibitory against *Streptococcus mutans* and *Streptococcus sanguinis*, whereas no effect was seen at these concentrations for the other species tested. Fluoride exhibits a range of inhibitory effects on oral bacteria and it has been suggested that the cariostatic activity observed from the use of fluoridated dentifrices and water may be mediated by this activity (Marquis *et al.*, 2003). In particular, glycolysis impairment by means of enolase inhibition occurs in bacterial species including oral streptococci (Zameck and Tinanoff, 1987; Balzar Ekenback *et al.*, 2001). This effect may explain why the streptococci were susceptible to sodium fluoride alone in this study. In combination, the effect of chitosan and fluoride on *Streptococcus mutans* and *Actinomyces naeslundii* were additive. The presence of chitosan may act to decrease the pH of the media and increase the permeability of the bacterial cell wall. The inhibitory effects of fluoride increase as the pH of the environment decreases due to the formation

of hydrofluoric acid (Marquis *et al.*, 2003). Hydrofluoric acid acts to convey protons across the bacterial membrane, which disturbs the intracellular pH. The maintenance of intracellular pH consumes bacterial energy produced by glycolysis and reduces availability for the growth process. In addition, the inhibition of glycolysis by fluoride occurs at lower concentrations in acidified environments (Marquis *et al.*, 2003). The antagonistic effects observed when assessing antimicrobial efficacy against *Streptococcus sanguinis* are unexpected, but may be due to a reduction in the charge density of chitosan induced by the presence of fluoride. The antimicrobial activity of chitosan is mediated by ionic interactions with the cell wall, which disrupt the barrier properties and allow leakage of intracellular material (Helander *et al.*, 2001; Liu *et al.*, 2004). *Streptococcus sanguinis* exhibited the greatest susceptibility to chitosan alone (Table 5.1), which may explain why this effect was only observed in this bacterial species.

In general, spray-dried chitosan-fluoride microparticles do not demonstrate adequate antimicrobial efficacy against the panel of oral bacteria and were therefore not selected for further investigation using the bioavailability model. Investigating higher concentrations of the chitosan-only and chitosan-fluoride containing microparticles was limited by the formation of precipitates in TSB, probably through ionic interactions with the negatively charged proteins present in the media. In addition, the viscosity of the chitosan dispersions at concentrations greater than those tested within this study were difficult to manipulate accurately at the small concentrations required for the technique.

5.3.3 Antimicrobial efficacy of Carbopol 971P-metal salt solutions

5.3.3.1 Carbopol 971P-zinc sulphate activity using a microtitre plate technique

To investigate whether planktonic studies using the polymer-metal salt solutions would be suitable for antimicrobial susceptibility testing, an experiment using only Carbopol 971P-zinc sulphate was utilised. Peptone water supplemented with 2.4 g L^{-1} glucose was selected as the microbiological medium to conduct the study. The use of TSB had previously resulted in the precipitation of zinc sulphate due to ionic interactions between anionic functional groups on peptides and proteins and cationic zinc ions.

Peptone water is formed by the hydrolysis of proteins and has previously been used to neutralise the activity of zinc ions in antimicrobial assays (Phan *et al.*, 2004). Therefore it can be assumed that some interaction still occurs although at no point during the investigation was precipitation evident. Peptone water supplemented with 2.5 g L^{-1} glucose supported the growth of *Staphylococcus aureus* and *Streptococcus mutans* only. Therefore these bacterial species were used to assess the antimicrobial activity of 0.695 mM zinc sulphate, 0.05% w/v Carbopol 971P, and Carbopol 971P-zinc sulphate solution. Difficulties were encountered when attempting to test the Carbopol 971P-zinc sulphate solution at the concentration intended for use; 0.05% w/v Carbopol 971P and 0.695 mM zinc sulphate. This was due to the unavoidable 1:2 dilution that occurs upon addition of the sterile or inoculated TSB to achieve final concentrations of the test solutions and bacterial inoculum. Adding 2.78 mM zinc sulphate to 0.2% w/v Carbopol 971P results in precipitation due to the ionic cross-linking of the polymer by divalent zinc ions (see 3.3.1). To avoid this, sterile or inoculated double strength peptone water supplemented with 2.5 g L^{-1} glucose was initially added to 0.2% w/v Carbopol 971P. The dilution of the Carbopol 971P aqueous dispersion allowed the addition of 2.78 mM zinc sulphate without precipitation. It was assumed that zinc ions bound to ionised Carbopol 971P to a greater extent than the amino acids present in the microbiological media. This was confirmed later by the activity of Carbopol 971P-zinc sulphate solution, which had no effect on the growth of *Staphylococcus aureus* or *Streptococcus mutans*. This was also observed in the presence of 0.05% w/v Carbopol 971P alone. Conversely, 0.695 mM zinc sulphate was able to prevent the growth of both *Staphylococcus aureus* and *Streptococcus mutans*, indicated by an absence of alamarBlue™ reduction. In all instances, test solutions did not result in the reduction of alamarBlue™ and the positive growth control indicated proliferation of the bacteria under experimental conditions in the presence of deionised water.

These observations resulted in no further testing of Carbopol 971P-metal salt solution using this technique. It was assumed that the interaction of zinc sulphate with Carbopol 971P reduced the bioavailability of the zinc ions to the bacteria and therefore no activity was observed. The hypothesis regarding the antimicrobial activity of the Carbopol 971P-metal salt solutions centres on an ionic exchange mechanism resulting in the slow release of metal ions from ionised carboxyl groups through competition with other cations present in saliva. Therefore, selection of Carbopol 971P-metal salt solutions for

assessment using the bioavailability model was based on the activity of metal salts alone on *Staphylococcus aureus* and *Streptococcus mutans*.

5.3.3.2 Antimicrobial activity of metal salt solutions

Three concentrations of zinc sulphate, copper sulphate, and silver nitrate relative to the starting concentrations in Carbopol 971P formulations were used to determine compounds to be tested using the bioavailability model. Metal salt solutions that inhibited the growth of *Staphylococcus aureus* and *Streptococcus mutans* at one or more of the concentrations tested were selected for further investigation. Zinc sulphate inhibited the growth of *Staphylococcus aureus* and *Streptococcus mutans* at 0.695 mM and 0.35 mM respectively (median, n = 18). Silver nitrate inhibited the growth of both *Staphylococcus aureus* and *Streptococcus mutans* at all the concentrations tested. Copper sulphate however did not inhibit the growth of either bacterial species at any of the concentrations tested. Therefore, Carbopol 971P-zinc sulphate and Carbopol 971P-silver nitrate were selected for assessment using the bioavailability model.

5.3.4 Bioavailability model

The substantivity and antimicrobial efficacy of bioadhesive Carbopol 971P-zinc sulphate and Carbopol 971P-silver nitrate solutions were assessed using the bioavailability model designed and validated at GlaxoSmithKline R&D (Weybridge, UK). In this study, the determination of biofilm formation using alamarBlue™ gave consistent results with low variability, which indicates a lack of over-reduction to hydroresorufin, observed previously by other authors (Pettit *et al.*, 2005). The technique used was modified from the method described by Martin *et al.* (2005). Hydroxyapatite is the predominant constituent of tooth enamel and has been shown to promote the attachment of bacteria to a greater extent than polystyrene surfaces, indicating the importance of its use in models predictive of adhesion *in vivo*. Hydroxyapatite plates used within this study were pre-prepared by GlaxoSmithKline R&S (Weybridge, UK). Scanning electron microscopy of coated wells demonstrates the complete coverage of the polystyrene surface with hydroxyapatite crystals

confirming the efficiency of the coating technique performed at GlaxoSmithKline (Figure 5.8).

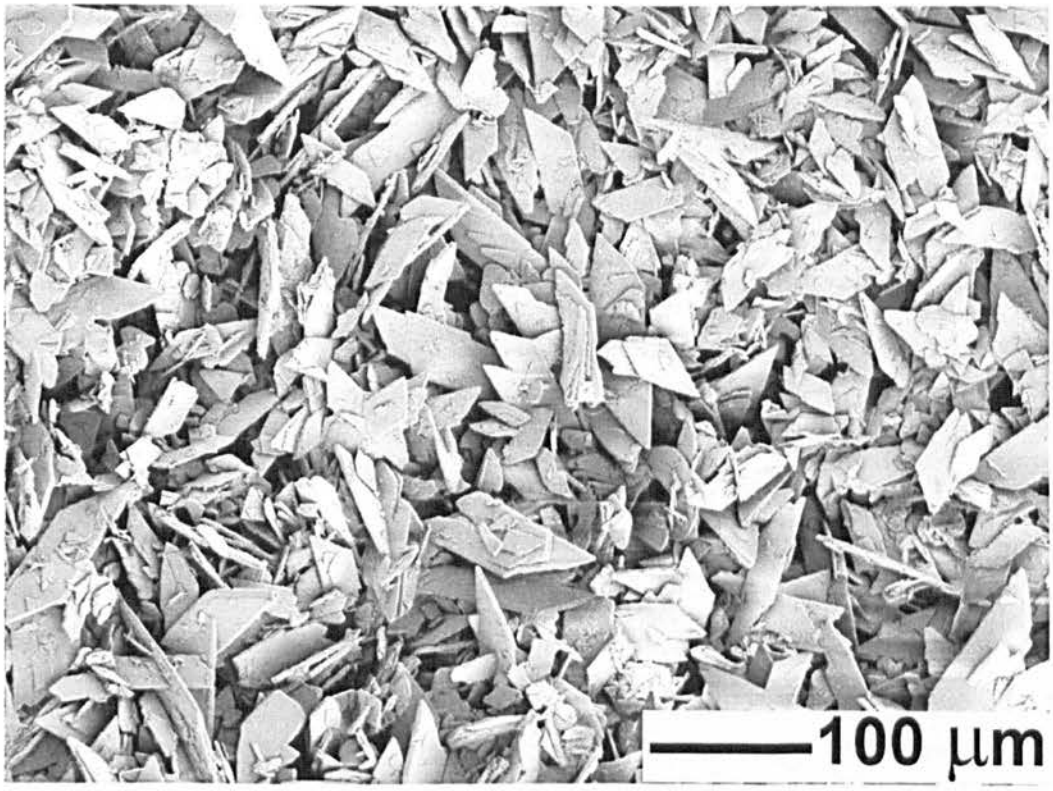

Figure 5.8 Scanning electron micrograph of an untreated hydroxyapatite-coated microtitre plate well. Picture courtesy of Miss L Tait, MPharm student, University of Brighton 2005.

5.3.4.1 Biofilm growth after four hours

5.3.4.1a Two minute contact time

In each experiment, 2% v/v chlorhexidine digluconate inhibited the growth of a bacterial biofilm on the treated hydroxyapatite-coated microtitre plate. This was indicated by a mean relative fluorescence of fewer than 500 relative fluorescent units (RFU) in hydroxyapatite-coated wells treated with artificial saliva with and without calcium chloride. This was confirmed following visual inspection of the microtitre plates; wells treated with 2% v/v chlorhexidine showed no colour change from blue to

pink, indicating that metabolic activity within the wells was not able to reduce alamarBlue™. At this concentration, chlorhexidine is retained at the site of application and prevents biofilm growth on the hydroxyapatite surface after 4 h incubation with saliva-derived inoculum. Chlorhexidine (2% v/v) was therefore suitable for use as the experimental positive control to which all other treatments were compared. Biofilm growth within the wells treated with deionised water was used to confirm the formation of a bacterial biofilm under the experimental conditions. The reduction of alamarBlue™ in these wells yielded approximately 3500 RFU under both artificial saliva conditions after 4 h incubation with the saliva-derived inoculum. Treatment with deionised water was therefore utilised as the negative control and was used to determine "normal" biofilm growth to which the test solutions were compared. These values were statistically different to the positive control ($P < 0.001$).

Application of 0.05% w/v Carbopol 971P to the treated hydroxyapatite-coated surfaces caused an increased mean RFU relative to the negative control after 4 h incubation with the saliva-derived inoculum (Figure 5.9). In wells pre-treated with artificial saliva without calcium chloride, the 18% increase in mean RFU relative to the experimental controls was highly significant ($P < 0.001$). In wells pre-treated with artificial saliva containing calcium chloride, only a 3% increase in mean RFU was observed ($P > 0.05$). This suggests that bacterial attachment and biofilm formation are increased in the presence of 0.05% w/v Carbopol 971P. These results suggest that Carbopol 971P is being retained at the site of application, probably as a consequence of interactions with the artificial salivary pellicle, which is presumed to be formed on the hydroxyapatite surface following pre-treatment with artificial saliva, and is acting as a bioadhesive. No significant difference was observed between the percentage increase in mean RFU caused by Carbopol 971P exposure under the different artificial saliva conditions ($P > 0.05$).

Carbopol 971P-zinc sulphate solution had no inhibitory effect on the growth of a bacterial biofilm after 4 h incubation under both artificial saliva conditions (Figure 5.9). Mean RFU values were consistently higher than the negative control, which may indicate biofilm promotion rather than inhibition; however this difference was only significant in surfaces pre-treated with artificial saliva without calcium chloride ($P < 0.001$). The increased mean RFU relative to the negative control observed in response

to 0.695 mM zinc sulphate exposure was also highly significant in wells pre-treated with artificial saliva without calcium chloride ($P < 0.001$) but not artificial saliva containing calcium chloride ($P > 0.05$). In both instances, the effects caused by each test solution were not significantly different to each other ($P > 0.05$) and were not significantly different to values produced following 0.05% w/v Carbopol 971P ($P > 0.05$), indicating that the co-application of Carbopol 971P and zinc sulphate had no additive effect.

Both Carbopol 971P-silver nitrate and 1.39 mM silver nitrate caused a significant reduction in mean RFU after 4 h when compared to the negative control under both artificial saliva conditions (Figure 5.9) ($P < 0.001$). The application of silver nitrate alone to the treated hydroxyapatite surface caused a greater percentage reduction of mean RFU when compared to Carbopol 971P-silver nitrate (Table 5.2). The difference between the mean RFU was statistically highly significant under both artificial saliva conditions ($P < 0.001$). It is probable that Carbopol 971P is counteracting the activity of silver by promoting the growth of bacteria on the treated hydroxyapatite surface.

5.3.4.1b Ten-minute contact time

Under both experimental conditions, 2% v/v chlorhexidine inhibited the growth of a bacterial biofilm on the treated hydroxyapatite surface (Figure 5.10). However, an increase in mean RFU was observed for hydroxyapatite surfaces treated with the negative control when compared to the previous experiment (5.3.4.1a). It is probable that day-to-day variation accounts for these differences rendering direct mean RFU value comparisons with other experiments inaccurate. For this reason, the percentage reduction or increase of alamarBlue™ was calculated for each test solution relative to the positive (2% v/v chlorhexidine) and negative (deionised water) control to standardise the data obtained from fluorescence measurements (5.2.3). The values obtained were then used to compare the effect of increasing the contact time of the test solutions on the subsequent growth of bacterial biofilms on the treated surfaces (Table 5.2).

As observed with the previous experiments, application of 0.05% w/v Carbopol 971P to treated hydroxyapatite surfaces caused a highly significant increase ($P < 0.001$) in mean

RFU following 4 h incubation with saliva-derived inoculum when compared to the negative control (Figure 5.10). At both contact times, Carbopol 971P has been retained on the treated hydroxyapatite surface. The development of a bioadhesive bond between the Carbopol 971P dispersion and the porcine mucin contained within the artificial saliva is likely to improve with increasing contact time. However, a significant increase in the mean percentage increase of reduced alamarBlue™ was only evident in surfaces pre-treated with artificial saliva containing calcium chloride ($P < 0.001$). Conversely, surfaces pre-treated with artificial saliva without calcium chloride resulted in a significant reduction in the percentage increase of alamarBlue™ reduction when the contact time was increased ($P < 0.05$).

Table 5.2 Effect of test solutions on the mean (± SD) percentage reduction of reduced alamarBlue™ fluorescence on treated hydroxyapatite surfaces relative to the positive and negative control after 4 h incubation. Negative values indicate a percentage increase in relative fluorescence (n = 16).

	2 minute contact time		10 minute contact time	
	Artificial saliva with calcium chloride	Artificial saliva without calcium chloride	Artificial saliva with calcium chloride	Artificial saliva without calcium chloride
2% v/v chlorhexidine	100%	100%	100%	100%
Carbopol 971P-zinc sulphate	-6% (± 8.59)	-15% (± 10.60)	-14% (± 8.83)	2% (± 8.65)
Carbopol 971P-silver nitrate	14% (± 6.72)	19% (± 14.60)	6% (± 8.41)	9% (± 4.89)
0.695mM zinc sulphate	-3% (± 8.63)	-20% (± 15.12)	-8% (± 6.17)	-7% (± 8.30)
1.39mM silver nitrate	28% (± 7.69)	32% (± 15.01)	4% (± 12.76)	6% (± 10.06)
0.05% Carbopol 971P	-3% (± 6.54)	-18% (± 10.73)	-19% (± 14.18)	-9% (± 8.95)
Deionised water	0%	0%	0%	0%

Following a ten-minute contact time, Carbopol 971P-zinc sulphate caused a significant increase of mean RFU relative to the negative control on surfaces pre-treated with artificial saliva containing calcium chloride ($P < 0.01$) but not on surfaces treated with

artificial saliva without calcium chloride ($P > 0.05$). This is evident in the results obtained for percentage reduction data, in which Carbopol 971P-zinc sulphate caused a 2% reduction in mean RFU on surfaces pre-treated with artificial saliva without calcium chloride compared to a 14% increase on surfaces pre-treated with artificial saliva containing calcium chloride (Table 5.2). Increasing the contact time to 10 min resulted in a significant increase ($P < 0.05$) and a highly significant decrease ($P < 0.001$) in the percentage increase of alamarBlue™ reduction of surfaces exposed to Carbopol 971P-zinc sulphate following pre-treatment with artificial saliva with and without calcium chloride respectively. This observation is similar to that observed when increasing the contact time of 0.05% w/v Carbopol 971P. The mean RFU on surfaces exposed to 0.695 mM zinc sulphate was significantly different to the negative control following pre-treatment with artificial saliva without calcium chloride only ($P < 0.05$). However, the percentage increase of mean RFU produced by biofilms grown on hydroxyapatite surfaces exposed to zinc sulphate alone was similar under each artificial saliva condition ($P > 0.05$).

Mean RFU measured from Carbopol 971P-silver nitrate and 1.39 mM silver nitrate exposed surfaces were consistently lower than the negative control (Figure 5.10). The percentage reduction of fluorescence was much less than anticipated, especially when compared to values obtained for the previous experiments (Table 5.2). Increasing the contact time to 10 min resulted in a significant reduction in the percentage reduction of alamarBlue™ caused by 1.39 mM silver nitrate and Carbopol 971P-silver nitrate under both artificial saliva conditions ($P < 0.05$). Therefore, increasing the contact time has caused a detrimental effect on the activity of silver ions despite the probable increased retention of Carbopol 971P at the surface. This is particularly evident on surfaces pre-treated with artificial saliva containing calcium chloride, where there was no significant difference in mean RFU between Carbopol 971P-silver nitrate, 1.39 mM silver nitrate, and the negative control ($P > 0.05$).

After 4 h, the increase in alamarBlue™ reduction rises significantly with 0.05% w/v Carbopol, 0.695 mM zinc sulphate or Carbopol 971P-zinc sulphate 2-minute exposure when calcium chloride is omitted from the artificial saliva ($P < 0.05$). This may be indicative of improved retention of these test solutions in the absence of calcium chloride. However, a contact time of 10-minutes on surfaces pre-treated with artificial

saliva containing calcium chloride caused a significant reduction in the percentage increase of alamarBlue™ reduction ($P < 0.05$). Calcium chloride may therefore aid the retention of these test solutions when longer contact times are used.

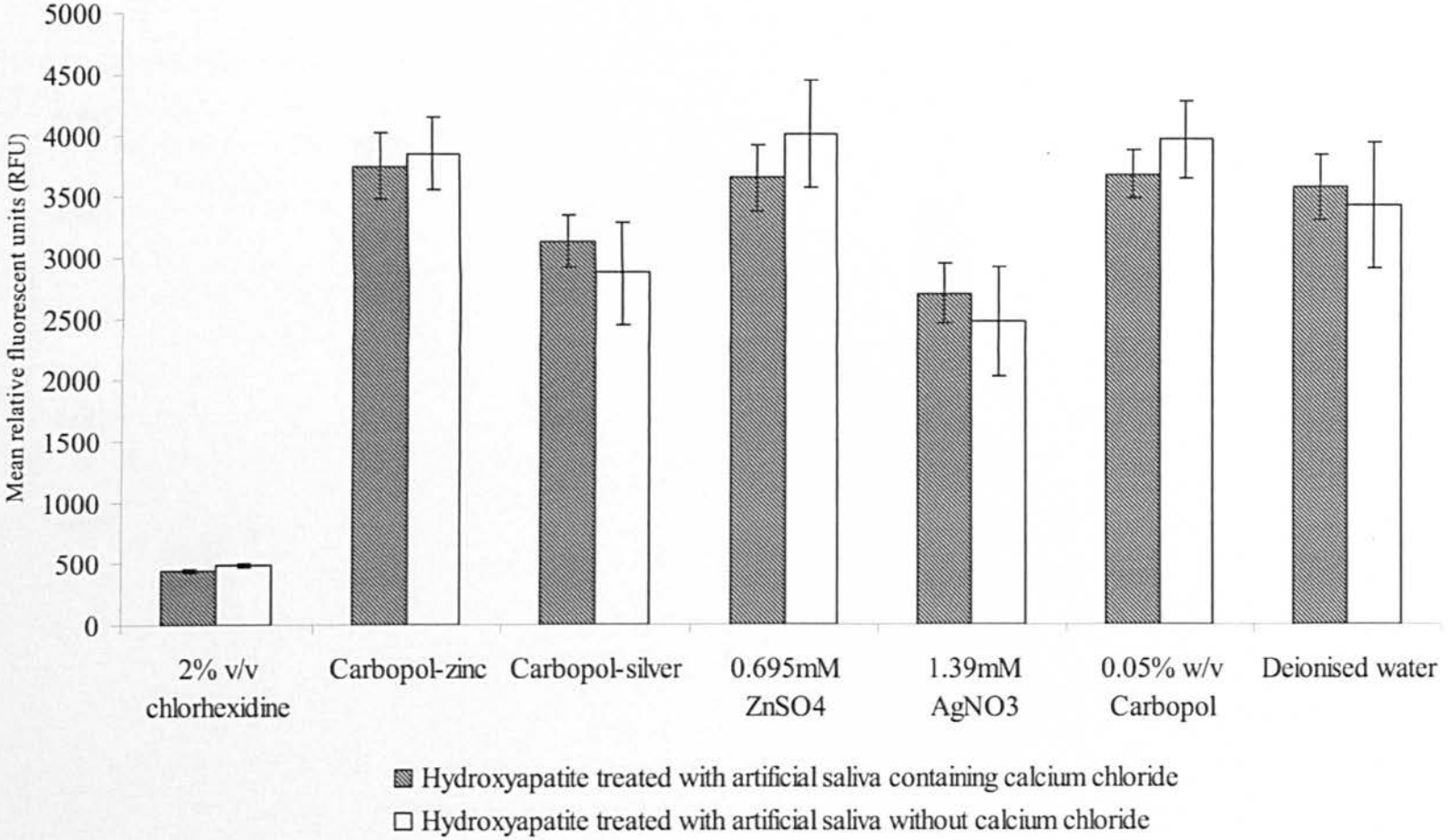

Figure 5.9 Reduction of alamarBlue™ by bacterial biofilms grown on artificial saliva-treated hydroxyapatite surfaces incubated for 4 h with saliva-derived inoculum following a 2 minute contact time of different treatments (n=16, ± SD).

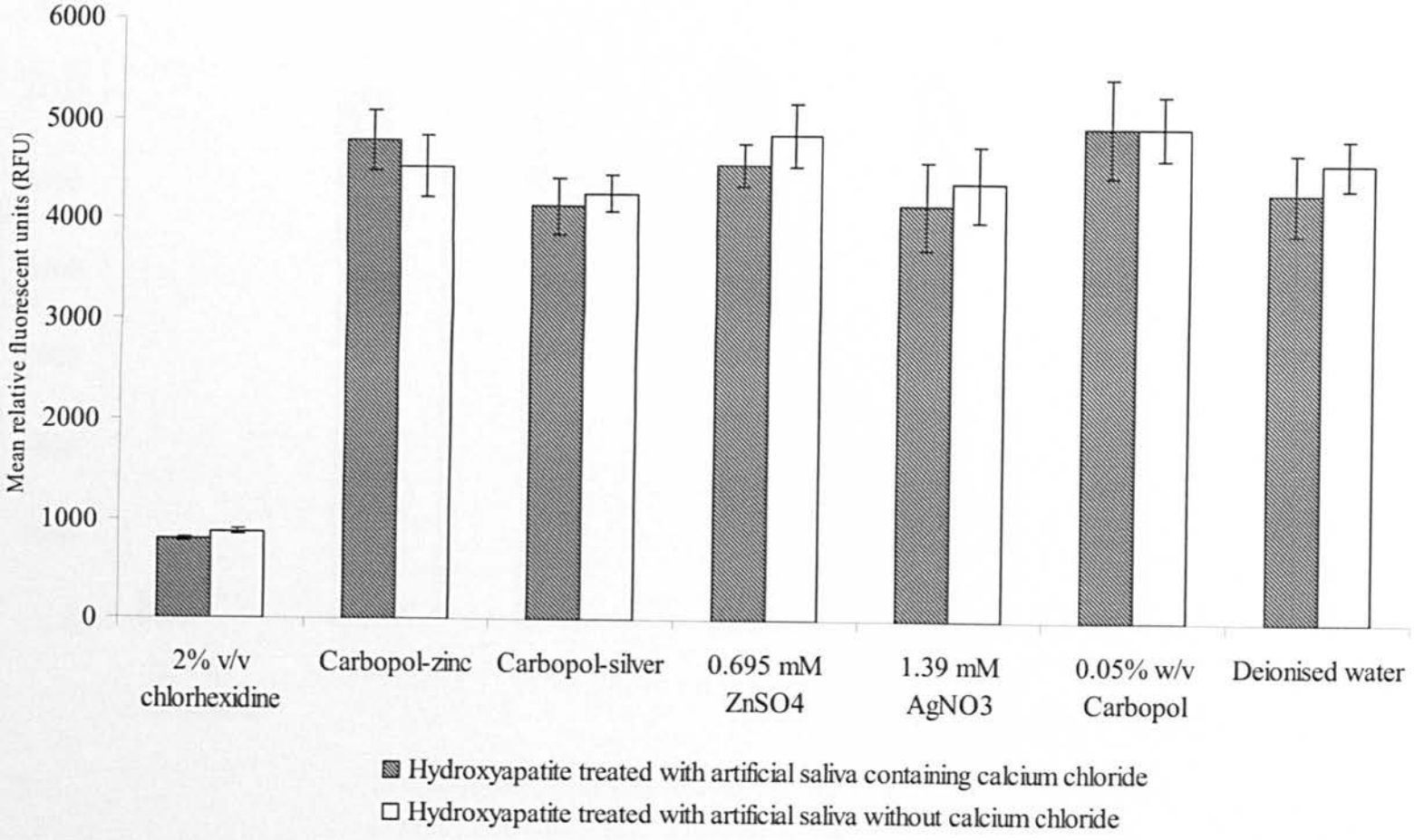

Figure 5.10 Reduction of alamarBlue™ by bacterial biofilms grown on artificial saliva-treated hydroxyapatite surfaces incubated for 4 h with saliva-derived inoculum following a 10 minute contact time of different treatments (n=16, ± SD)

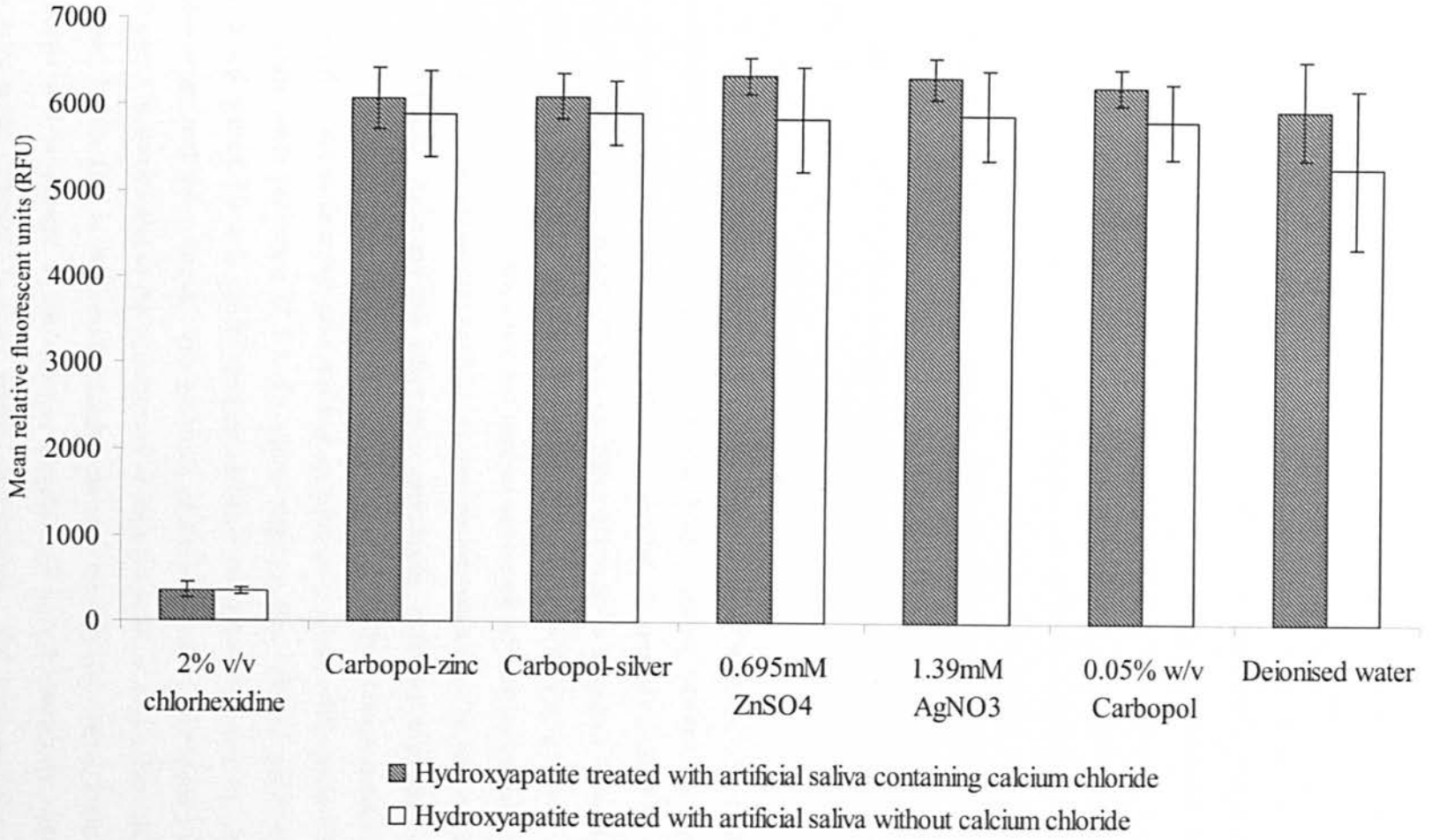

Figure 5.11 Reduction of alamarBlue™ by bacterial biofilms grown on artificial saliva-treated hydroxyapatite surfaces incubated for 24 h with saliva-derived inoculum following a 2 minute contact time of different treatments (n=16, ± SD)

5.3.4.2 Biofilm growth after twenty-four hours

No colour change was observed in wells treated with 2% v/v chlorhexidine, indicating an inhibitory effect on biofilm formation, and mean RFU was below 500 RFU under both artificial saliva conditions (Figure 5.11). Biofilm growth characterised by high RFU values with an accompanying alamarBlue™ colour change, was clearly evident in the negative control. High standard deviations following this treatment were most likely due to the natural variability of live models. Only contact times of two min were examined for biofilm growth after 24 h, as this produced more favourable reductions in fluorescence after 4 h than a contact time of ten min and more accurately represents the clinical situation. There was no significant difference between the mean RFU values obtained for each test solution and the negative control under both artificial saliva conditions ($P > 0.05$). This suggests that after 24 h, biofilm growth within the wells treated with the test solutions is not significantly different from the wells treated with deionised water.

The overall results from this investigation suggest that Carbopol 971P promotes the attachment and growth of bacteria on the hydroxyapatite surface pre-treated with mucin-containing artificial saliva. This was evident on surfaces treated for 2 and 10 minute contact times with 0.05% w/v Carbopol 971P and incubation with saliva-derived inoculum for 4 h. The reason for enhanced biofilm formation in the presence of Carbopol 971P alone is unknown, but may be associated with an improved adhesion of bacteria to the hydroxyapatite surface. Further investigation into this observation would be of interest. Although this effect was undesirable, it further supports claims that aqueous Carbopol dispersions can adhere quickly to an orally relevant surface. Polymer retained on the surface was also resistant to repeated washing with sterile TSB during the plate wash procedure (5.2.2.4e), which suggests that adhered polymer may be retained within the oral cavity despite repeated disruption induced by fluid flow, movement and shear forces. The presence of calcium and other cations in saliva is likely to be detrimental to the bioadhesion of aqueous polymer dispersions (Kriwet and Kissel, 1996). Due to the extended conformation of the polymer chains, fewer carboxyl groups will be present at the adhesive interface for initial interaction with salivary mucins when compared to more viscous preparations. The presence of cations can potentially reduce or enhance the ability of the polymer to interact with the salivary

mucins present on the test surfaces. The diffusion of cations into the aqueous polymer dispersion would reduce the distance between adjacent chains by reducing the negative charge density, which could have one of two effects, 1), increase the potential for ionic cross-linking, and/or 2) allow more functional groups to gather at the adhesive interface. Interestingly, calcium chloride was found to be important in improving the retention of Carbopol 971P when the contact time was increased from 2 to 10 min. This suggests that divalent calcium ions may in this case act to bridge negative charges on the polymer backbone and mucin glycoproteins, improving the retention of the polymer when longer contact times are employed.

Both 0.695 mM zinc sulphate and Carbopol 971P-zinc sulphate had little or no activity against the formation of a biofilm on the treated hydroxyapatite surface. Neither treatment elicited a significant reduction in fluorescence relative to the experimental controls under any experimental condition. A reduction in biofilm growth was observed on hydroxyapatite surfaces treated with calcium deficient saliva when treated with Carbopol 971P-zinc sulphate for 10 min; but this was not significant. It was anticipated that zinc ions would be retained at the surface during the experiment, associated with either the hydroxyapatite coating or mucins present in the artificial saliva. Other investigators have demonstrated that zinc is retained within the oral cavity after delivery via a dentifrice or mouthrinse, where elevated salivary zinc concentrations and increased plaque-associated zinc have both been reported (Harrap *et al.*, 1984; Gilbert, 1987). The adsorption of zinc onto hydroxyapatite has also been demonstrated experimentally (Ingram *et al.*, 1992). Carbopol 971P was incorporated to increase the amount of zinc retained and to maintain elevated concentrations through an ion-exchange mechanism with other cations present in the artificial saliva. It is likely that both zinc sulphate and Carbopol 971P-zinc sulphate is retained at the surface following exposure and concentration, rather than substantivity, is the activity-limiting factor. Phan *et al.* (2004) found that concentrations of 20 mM zinc sulphate were inadequate for bactericidal activity against oral streptococci while Harrap *et al.* (1983) found that this concentration was sufficient to cause 50% inhibition of plaque growth. Discrepancies such as these are common throughout the literature and are possibly due to the different measurements of activity (bacteriocidal and bacteriostatic), and the wide range of techniques used to elucidate zinc efficacy. Although concentrations as high as 20 mM are not attainable through the application of the Carbopol 971P complex due to

polymer precipitation, a reduced rate of biofilm growth through bacteriostatic mechanisms was predicted. Clinical investigations have concluded that the major effect of zinc is on existing plaque, in which the rate of bacterial proliferation is reduced (Moran *et al.*, 2001). In addition, inhibition of acid production through glycolysis can be achieved with as little as 0.01 mM zinc sulphate, which may be efficient at reducing the incidence of dental caries (He *et al.*, 2002; Phan *et al.*, 2004). On the other hand, zinc has been shown to be an essential requirement for bacterial growth (Hughes and Poole. 1989). The concentration of zinc required by bacterial cells was found to be in the region of 0.4 μM (Aranha *et al.*, 1982). The small, but significant increase in biofilm growth evident after exposure to zinc-containing test solutions may suggest that zinc bioavailability is as low as this value under the experimental conditions. In the case of Carbopol 971P-zinc sulphate solution, it is possible that a significantly higher amount of zinc is retained at the surface but due to the effects of Carbopol 971P alone on bacterial growth, is insufficient enough to prevent biofilm formation. The effect of Carbopol 971P alone on the growth of bacteria may also account for the observations made in the planktonic investigation of antimicrobial activity of Carbopol 971P-zinc sulphate solution (5.3.3.1). Future investigation into the effects of Carbopol 971P-zinc sulphate on plaque acidogenesis and established biofilms may improve the efficacy of this bioadhesive complex.

Results obtained in this investigation suggest that both 1.39 mM silver nitrate and Carbopol 971P-silver nitrate exhibit some activity against biofilm formation and growth, demonstrated by a reduction in mean RFU relative to the negative control. This effect can be appreciated 4 h after application, although no differences can be observed after 24 h unlike the responses detected following 2% v/v chlorhexidine exposure. In most instances, activity is not improved when formulating silver nitrate with Carbopol 971P, as no significant differences were detected between the data obtained for each treatment. It is probable that the presence of Carbopol 971P is detrimental to the activity of silver nitrate at this concentration, as its antimicrobial activity does not counteract the growth supporting properties observed in Carbopol 971P only treatments. Silver is an effective antimicrobial and the nitrate salt has been used extensively in the prophylaxis of *Pseudomonas* infections and burns (Hughes and Poole, 1989). Gallagher and Cutress (1977) demonstrated that 30 μg mL^{-1} silver (0.27 mM silver nitrate) was sufficient to prevent the growth of oral *Actinomyces* and some *Streptococci*, while the

same concentration caused a significant reduction in the growth of *Streptococcus mutans* plaques. Spacciapoli *et al.* (2001) found that concentrations as low as 25 μg mL^{-1} silver (0.225 mM silver nitrate) were effective at reducing periodontal pathogens in simulated gingival crevicular fluid. Silver activity against single species biofilms grown from non-oral bacteria was consistently found to be one of the three most toxic metal compounds after mercury and tellurite in a study conducted by Harrison *et al.* (2004). The claims surrounding the toxicity of silver to micro-organisms suggest that Carbopol 971P is responsible for the reduction of antimicrobial activity when compared to silver nitrate only. The substantivity of silver nitrate has not been previously reported in the literature but it can be concluded from this investigation that silver is retained at the surface. Shirkhanzadeh *et al.* (1995) found that silver could be incorporated into hydroxyapatite crystals and that the mechanism for this was likely to be ion exchange. It is also possible that silver ions are retained through interaction with mucin glycoproteins. Higher percentage reductions of alamarBlue™ were often observed in wells exposed to 1.39 mM silver nitrate when compared to Carbopol 971P-silver nitrate. This may be due to the bioavailability of silver nitrate in each test solution. Aqueous silver nitrate alone may bind to hydroxyapatite or mucin glycoproteins to a greater extent than silver delivered within the Carbopol 971P dispersion, which results in greater retention after the test solution has been removed. In the latter instance, negatively charged sites within the polymer dispersion and binding sites on hydroxyapatite and/or mucin glycoprotein may compete effectively for silver binding, which may reduce the bioavailability of silver for retention at the surface when compared to the aqueous silver nitrate salt. Interestingly, increasing the contact time of both silver nitrate and Carbopol 971P-silver nitrate caused a decrease in the percentage reduction of fluorescence relative to the experimental controls. Increasing the contact time was predicted to improve the retention of Carbopol 971P-silver nitrate at the treated hydroxyapatite surface, thereby increasing the local concentration of silver ions. In reality, this caused a detrimental effect on the antimicrobial activity of both test solutions. It is possible that insoluble silver chloride is being formed during an extended contact period, which could be easily removed while rinsing the surface with sterile TSB during the plate wash procedure. The extent of chloride diffusion within the aqueous polymer dispersion may increase with time, allowing the formation of silver chloride. Although this probably occurs to some extent during a contact time of 2 min, a longer contact time may increase the diffusion of silver out of the aqueous Carbopol

971P dispersion while simultaneously increasing the diffusion of chloride into the dispersion. These effects may explain why slightly higher percentage reductions were observed in experiments where calcium chloride was not incorporated into the artificial saliva, giving an overall reduced concentration of chloride ions. Increasing the concentration of silver in Carbopol 971P aqueous dispersions may improve the antimicrobial efficacy of the formulation, as silver does appear to be a promising candidate for reducing bacterial numbers within the oral cavity. Specific investigations into the mode of substantivity could be useful in determining future delivery strategies.

5.4 Conclusions

- Spray-dried microparticles prepared from chitosan only or chitosan-sodium fluoride aqueous dispersions exhibited little antimicrobial activity against planktonic bacteria representative of commonly isolated species from the oral cavity.
- The use of planktonic studies to assess the antimicrobial activity of Carbopol 971P-metal salt solutions was deemed unsuitable due to bacterial growth in the presence of zinc concentrations that are known to be capable of inhibition, along with difficulties associated with sample preparation.
- Both zinc sulphate and silver nitrate inhibited the growth of *Staphylococcus aureus* and *Streptococcus mutans* at one or more of the concentrations tested.
- Copper sulphate had no effect on *Staphylococcus aureus* and *Streptococcus mutans* growth.
- The bioavailability model developed at GlaxoSmithKline is a rapid high-throughput technique, which enables the evaluation of antimicrobial compounds designed to be retained within the oral cavity against biofilm formation.
- Carbopol 971P increases the formation and growth of a biofilm on the pre-treated hydroxyapatite coated surface relative to a deionised water treated surface, suggesting polymer retention at the surface after both a 2 and 10 min contact time.
- Both zinc sulphate and Carbopol 971P-zinc sulphate solution did not produce any significant reduction in fluorescence under any experimental condition. This is most likely due to a sub-minimum inhibitory concentration at the treated-hydroxyapatite surface, which was not improved when contact time of the treatment was increased from 2 to 10 min.
- Both silver nitrate and Carbopol 971P-silver nitrate solution caused a significant reduction in biofilm formation after 4 h when compared to the negative control. However, this activity was not improved with the formulation of silver with Carbopol. Activity of these compounds was still not comparable with that of chlorhexidine.
- Increasing the contact time of silver compounds decreased antimicrobial efficacy possibly due to the formation of insoluble silver chloride.
- After 24 h, none of the tested compounds except chlorhexidine had caused a significant reduction in biofilm formation and growth.

Chapter 6
General Discussion

This project aimed to investigate the use of bioadhesive, Food and Drug Agency (FDA) approved polymers as platforms for the local delivery of non-covalently bound antimicrobial compounds to the oral cavity. The desired outcomes were to achieve sustained localised activity of the antimicrobial compound at effective concentrations for bacteria associated with dental disease, without compromising the bioadhesion of the polymer to orally relevant surfaces. In addition, altered release of the antimicrobial compounds in response to environmental pH changes, particularly lower pHs which favour the growth of acidophilic bacteria such as *Streptococcus mutans*, was a favourable outcome for potentially improving oral antimicrobial delivery above those currently achieved in modern healthcare products.

High molecular weight, cross-linked poly(acrylic acid) and chitosan polymers were selected for investigation in this study for a number of reasons. These included; current FDA approval status; the presence of a high density of charged functional groups to allow non-covalent drug:polymer interactions; proven bioadhesive properties; and, previously reported successful formulation into drug delivery systems as the primary bioadhesive component. A wide range of polymer grades are available commercially, each exhibiting different molecular weights, cross-linking density, viscosity, salt and degree of deacetylation (chitosans only). These characteristics can each influence the bioadhesive properties of the polymer. The selection of an appropriate grade and a suitable method of assessing bioadhesive performance formed the basis for the second chapter. Due to the previous observation (Vivien-Castioni *et al.*, 2000) that generally patients are less tolerant of using solid dosage forms within the oral cavity, the decision was made to utilise a semi-solid or liquid dosage form, either as a paste or mouthrinse formulation. For this reason, a method was required that could appropriately assess bioadhesion from these dosage forms. By modifying an *in vitro* staining technique it was possible to visualise poly(acrylic acid) polymers; Carbopol 971P, Carbopol 974P and polycarbophil AA-1, on the surface of buccal cells following incubation with aqueous dispersions and utilising artificial saliva to pre-treat and wash the cells. This clearly demonstrated the adsorption of the polymer from solution onto the cell surface in the presence of multiple cations, which has previously been shown to affect bioadhesion. Unfortunately, this technique could not provide any accurate information regarding the adsorption/adhesion of high molecular weight chitosans. Texture probe analysis was used to assess the bond strength formed between a moistened mucosal

surface and dry polymer compacts. Using this technique provided numerical data on the relative adhesiveness of the polymers that could be easily interpreted, in order to identify the differences between polymer grades, and the changes in bioadhesive performance following the inclusion of an antimicrobial compound. Texture probe analysis supported the bioadhesion of poly(acrylic acid) polymers to a mucosal surface and demonstrated that little difference existed between the three polymer grades when coupled with the data collected from the *in vitro* staining technique. Carbopol 971P was selected for further investigation due to the highest mean value for work of adhesion and the information provided by the manufacturers regarding the suitability of this polymer grade for oral applications (Noveon. 2002c). Numerous attempts to modify and develop methods to assess the adsorption/adhesion of aqueous chitosan failed; therefore assessment was based on results obtained from texture probe analysis alone. Chitosans that performed poorly; Protasan G113, G213 and CMFP (Cognis), were immediately excluded from the study. All other grades performed similarly to each other and were therefore kept for future consideration. Performance may have been related to the type of chitosan salt used e.g. glutamate, and molecular weight. A major disadvantage of using texture probe analysis was the large variation in repeat measurements, which made statistical comparisons difficult. The use of a model mucosa such as dialysis tubing has previously been found to provide a uniform surface that gave more consistent results; however the utilisation of a mucosal surface was deemed to have more *in vivo* relevance, and therefore important in the predictive power of this technique.

Measuring bond strength has regularly been used as the sole technique to quantify and assess bioadhesion in the development of bioadhesive formulations within the oral cavity (Govender *et al.*, 2005; Owens *et al.*, 2005). In general, tensile testing is predominantly applicable to solid dosage forms such as tablets, compacts and films, designed for buccal or gingival application in oral drug delivery. These tests have been extensively used when evaluating a rank order of adhesiveness among a range of polymer samples (Grabovac *et al.*, 2005; Eouani *et al.*, 2001; Wong *et al.*, 1999). More recently tensile strength methods have been designed to assess the adhesion of hydrogels to either mucin (Jones *et al.*, 1997a) or model mucosa (Hagerstrom and Edsman. 2001). In this instance, successful interpretation of tensile testing often involves the measurement of cohesion and therefore preparations are typically prepared

at high concentrations of polymer (> 0.75% w/v for Carbopol) to obtain a sufficient level of cohesiveness. The concentration of aqueous polymer dispersion used in this study could not be applied to these techniques hence dry polymer compacts were employed. Previous investigations of sodium alginate liquid dosage forms have involved *in vitro* mucosal retention models utilising porcine oesophagus (Batchelor *et al.*, 2002; Richardson *et al.*, 2005). Detection has been based on fluorescent labelling (Batchelor *et al.*, 2002) or direct scraping and subsequent dye complexation assay (Richardson *et al.*, 2005). This principle has also been applied to the retention of fluorescein-loaded microparticles prepared from Carbopol and chitosan (Kockisch *et al.*, 2004). The use of fluorescent labelling is an efficient method of detecting adhered polymer and is easily quantifiable. However labelling often involves attachment of the fluorescent tag to functional groups crucial to secondary bond formation i.e. carboxyl groups in sodium alginate (Batchelor *et al.*, 2002). Polymer functional groups (e.g. carboxyl groups in poly(acrylic acid) polymers) were intended in this study for ionic interactions with charged antimicrobial compounds and therefore fluorescent labelling may have limited the availability of these binding sites. The *in vitro* staining technique in this study is rapid and allows visualisation of adsorbed polymer on the surface of buccal cells. Effects due to a labelling procedure altering the physicochemical properties of the bioadhesive are avoided. Using this test in conjunction with tensile testing, an effective method for evaluating liquid dosage forms has been achieved. Visualisation of polymer adsorption confirms the adhesive properties of liquid formulation while the tensile testing of dry polymer compacts allows the rank order of adhesiveness to be quantified. It is interesting to note that the two techniques, although involving quite different procedures, are both able to detect bioadhesion for the polymers of interest.

The identification of the polymer grades for use as the bioadhesive component and the development of an appropriate means of assessing bioadhesion led to the investigation of selected antimicrobial compounds and their interaction with aqueous polymer dispersions (Chapters 3 and 4). Ionic interactions based on the poly(acrylic acid) Carbopol 971P were likely to be formed with the high density of carboxyl groups located within the polymer structure. The formation of an ionic complex between cationic antimicrobial compounds and negatively charged carboxyl groups at appropriate pHs could potentially exhibit substantivity within the oral cavity. Zinc,

silver and copper were selected for investigation in this study as they are unlikely to induce cross-resistance among bacterial species, are generally non-toxic in humans unless high concentrations are achieved, and have previously been included in a range of topical consumer products (Chapter 3). The retention of zinc, silver and copper by Carbopol 971P during dialysis in deionised water supported the hypothesis that these metal cations were interacting with negatively charged carboxyl groups on the polymer backbone. Gradual displacement of zinc from negatively charged sites on the polymer was achieved in artificial saliva, exhibiting a faster rate of release at lower pHs. Silver however, was released at a rate equal to that of the silver salt alone. The difference in the behaviour of zinc- and silver-polymer complexes was attributed to the different valance of each ion, divalent and monovalent respectively, and their affinity for negatively charged carboxyl groups. Copper was not displaced in artificial saliva and instead caused the gradual formation of blue precipitates, indicative of the formation of inter- and intrapolymer bonds. This may have been prompted by the diffusion of other cations into the dialysis tubing and altered interactions between copper and Carbopol 971P. Copper has previously demonstrated higher affinity for polyelectrolytes than zinc, and may form different complexes under the experimental condition e.g. coordinate bonds (Francois *et al.*, 1997; Heitz and Francois. 1999; Tomida *et al.*, 2001). In later work, copper was found to affect the adsorption of the complex onto buccal cells and significantly reduced the strength of the adhesive bond while both zinc- and silver-Carbopol 971P complexes exhibited bioadhesion comparable to Carbopol 971P alone.

The local delivery of metal ions from solid dosage forms within the oral cavity to achieve antimicrobial action has been previously reported (Bromberg *et al.*, 2000) although relatively few studies have been carried out. In this study, sustained release formulations were not designed to be bioadhesive but to exhibit prolonged delivery of silver nitrate directly into periodontal pockets following professional application. Preventative strategies that utilise sustained antimicrobial delivery to modulate the daily accumulation of plaque, thereby reducing the risk of developing periodontal diseases, are uncommon in the literature. Since bioadhesive therapy directly to the periodontal pocket can achieve high local concentrations, bioadhesive formulations applied to the entire oral cavity i.e. via a liquid dosage form, have the potential to achieve high local concentrations of antimicrobial compounds at multiple sites. This strategy for

preventative therapy has been successfully applied in Colgate™ toothpastes, where co-formulation of the bioadhesive polymer gantrez® with triclosan significantly improved antimicrobial activity (Volpe. 1996). Typically the use of metal ions in oral healthcare formulations has focused on the inclusion of zinc, most notably for its additive effects on the antiplaque activity of triclosan (Bradshaw *et al.*, 1993; Marsh. 1991). This is surprising considering the well-documented antiplaque activity of metal ions on oral bacterial species (Scheie. 1989). Carbopol polymers have been used frequently as the bioadhesive component of formulations intended for local oral drug delivery, although these have primarily been based on buccoadhesive tablets, films and patches, in which sustained release is achieved though the swelling and erosion of the preparation (Perioli *et al.*, 2003; Kohli *et al.*, 2003; Arora *et al.*, 2003; Llabot *et al.*, 2002). Aqueous dispersions of Carbopol 971P were shown to adsorb/adhere onto buccal cells in the previous chapter and therefore this polymer demonstrates ideal properties for use as a bioadhesive drug delivery platform in liquid dosage forms. Ungphaiboon and Maitani (2001) have also explored this possibility for the local delivery of corticosteroid. In particular the ionic interactions that are achievable between cationic drugs and poly(acrylic acid) polymers such as Carbopol allow formulations to be based on ionic, rather than covalent interactions, which are specific criteria within this study. Examples of successful ionic drug delivery complexes have been reported in ophthalmic formulations (Sandri *et al.*, 2006; Lele and Hoffman. 2000). The gradual release of cationic drugs into artificial tear fluid, which has a similar ionic composition to the artificial saliva utilised in this study, demonstrated superior retention when compared to the drug alone both *in vitro* (Lele and Hoffman, 2000) and *in vivo* (Sandri *et al.*, 2006). The problems encountered in ophthalmic drug delivery i.e. reduced residence time due to constant flow of tear fluid and low tolerance of solid dosage forms, are similar to those in oral drug delivery.

Following on from the successful observations with Carbopol 971P and cationic metal salts, fluoride ions in the form of sodium fluoride or sodium monofluorophosphate, known to have therapeutic activity in the oral cavity, were investigated for interactions with chitosan (Chapter 4). Chitosan is a cationic polymer and it was hypothesised that positively charged amine groups would interact with negatively charged fluoride or monofluorophosphate ions. Fluoride is included in a range of oral healthcare products for its anticaries activity, which is due to its interaction with enamel (Vivien-Castioni *et*

al., 1998) and oral bacteria (Marquis *et al.*, 2003). Chitosan exhibits antimicrobial activity against a range of bacteria and has demonstrated antiplaque activity *in vivo* (Sano *et al.*, 2003). The behaviour of chitosan-sodium fluoride solutions during dialysis suggested that no ionic interactions had occurred between the fluoride ions and the protonated amine groups. Sodium monofluorophosphate was retained by chitosan in deionised water, possibly due to weak ionic interactions. However, in artificial saliva no retention was observed. Freeze-dried chitosan-sodium monofluorophosphate solutions were not bioadhesive, possibly due to effects of the fluoride salt on the hydration and ionisation of the chitosan compact.

Chitosan microparticles have demonstrated suitable properties for sustained release local delivery to the oral cavity in previous studies (Kockisch *et al.*, 2003, 2005). Chitosan microparticles prepared by two techniques were therefore investigated as potential bioadhesive carriers for sustained fluoride release (Chapter 4). The use of a water-in-oil solvent evaporation technique produced microparticles with larger particle size distribution that exhibited rapid fluoride release. This was probably due to the deposition of fluoride compounds at the particle surface, which may have also prevented bioadhesive assessment. The use of a spray-drying technique produced chitosan microparticles with higher fluoride loading and entrapment efficiencies. Fluoride release occurred rapidly within the first 10 min and slowed thereafter and was unaffected by pH and glutaraldehyde inclusion. Rapid gelation and the interaction of the chitosan with other ions could account for these observations and may have been the cause of incomplete fluoride release after 8 h. Spray-dried microparticles containing sodium fluoride did exhibit significantly decreased bioadhesive bond strength when compared to chitosan-only microparticles using texture probe analysis. The forces produced were however comparable to other studies in which microparticles have been designed for a bioadhesive application (Kockisch *et al.*, 2003; Martinac *et al.*, 2005). The use of spray drying improved the dispersion of sodium fluoride within the chitosan microparticle when compared to water-in-oil solvent evaporation due to the absence of drug crystals at the particle surface, although significant fluoride is still located near the surface as indicated by fluoride release characteristics. The fluoride loading achieved by spray drying the particles were slightly greater than the solvent evaporation process, however the yield of dry product collected was significantly reduced. This may have

been the result of low drying temperatures used for spray-drying aqueous dispersions as moisture-containing product was deposited on the glass interior of the drying chamber.

The characteristics exhibited by the spray-dried chitosan-sodium fluoride particles were of particular interest due to the potential sustained fluoride release at low concentrations. This has been the target of numerous drug delivery strategies to prevent the development of caries. Fluoride-releasing dental restoratives such as glass-ionomer cements, composites and amalgams demonstrate long-term fluoride release, antibacterial activity and cariostatic properties (Wiegand *et al.*, 2007). These restoratives can maintain low local levels of fluoride for prolonged periods of 250 days and more (Chan *et al.*, 2006). This type of fluoride delivery could potentially reduce the incidence of secondary caries; although at present clinical evidence is not available (Wiegand *et al.*, 2007). The use of bioadhesive polymers to release low concentrations of fluoride over extended periods has been described in previous studies (Owens *et al.*, 2005 and Vivien-Castioni *et al.*, 2000). Both used bioadhesive tablets for prolonged release of fluoride *in-vitro* and *in-vivo*. Microparticles could be formulated into pastes and rinses to improve fluoride retention and antiplaque activity. Chitosan microparticles achieve prolonged retention on a mucosal surface (Kockisch *et al.*, 2004) and chitosan itself has demonstrated antiplaque activity *in vivo* following the application of chitosan-containing mouthrinse (Sano *et al.*, 2003) and more recently chitosan-containing gum (Hayashi *et al.*, 2007). Chitosan-fluoride microparticles that exhibit prolonged fluoride release and adhere to mucosal surfaces could exhibit anticaries activity through the combined effect on bacterial numbers in addition to the effects of fluoride on enamel. Such formulations could achieve low local fluoride concentrations, which are considered to have optimal anticaries effects.

Antimicrobial assessment of the polymer-based formulations was the final component to the project and both planktonic and sessile studies were utilised (Chapter 5). Planktonic studies are regularly used to assess the antimicrobial activity of drug delivery formulations (Nurkeeva *et al.*, 2004; Jumaa *et al.*, 2002; Bromberg *et al.*, 2000). Chitosan-sodium fluoride microparticles did demonstrate some activity against a panel of orally relevant bacteria, although the concentrations required were typically around the highest values tested with some species not inhibited at all. Carbopol-zinc complexes did not inhibit the growth of *Streptococcus mutans* or *Staphylococcus*

aureus, although the zinc salt alone did show activity possibly due to a higher bioavailability. Both silver nitrate and zinc sulphate inhibited bacterial growth when tested alone, while copper sulphate did not exhibit any activity. Based on observations made in the planktonic studies, Carbopol 971P-silver and Carbopol 971P-zinc complexes were further assessed by their ability to prevent biofilm formation using the bioavailability model. Carbopol 971P treatment alone caused a significant increase in biofilm growth at the test surface, which suggests retention after short contact times to orally relevant surfaces. The effect of Carbopol 971P on bacterial growth has not been previously reported and probably accounts for the lack of antimicrobial activity exhibited by Carbopol-zinc complexes in planktonic studies. The polymer may have provided a carbon-rich nutrient source that encouraged bacterial growth and/or enhanced the attachment of bacteria at the hydroxyapatite surface. Zinc salts alone also had growth-potentiating effects on biofilm formation, which may be related to quantity of zinc retained at the surface and its role as an essential nutrient. Silver salts alone did have a significant effect on biofilm formation; however this was not improved by formulating the compound with Carbopol 971P, which may have masked any inhibitory effects. Calcium chloride may have influenced the retention of Carbopol 971P at the hydroxyapatite surface, possibly due to ionic cross-linking with surface-associated mucins. However no effects were observed on Carbopol 971P-zinc complexes, which were predicted to release more zinc in the presence of divalent cations.

The antimicrobial assessment of oral formulations designed to exhibit sustained local drug concentrations in this study identified specific problems that could be associated with their use *in vivo*, in particular the behaviour of the Carbopol 971P in the antimicrobial assays does not support a role for Carbopol 971P in antimicrobial applications. The growth-enhancing effects observed in this study may relate to the physicochemical properties of Carbopol and the dosage form of the formulation. Previous investigations evaluating the use of poly(acrylic acid)-streptomycin sulphate polycomplexes for oral systemic drug delivery did not indicate a reduction in antimicrobial activity of the drug compound (Nurkeeva *et al.*, 2004). This may be directly related to the potent antimicrobial action of streptomycin when compared to metal ions used in this study but it is important to note that this study found that poly(acrylic acid) alone did not cause any bacterial inhibition. Other studies using poly(acrylic acid)-based polymers such as Carbopol have focused on the sustained

release of antimicrobials from a solid matrix i.e. tablets and are typically composed of more than one polymer (Llabot *et al.*, 2002). Delivery in this way may prevent the growth-enhancing effects of Carbopol 971. The use of different microbiological methods to assess the activity of both metal-containing and fluoride-containing formulations may have demonstrated some reduction of bacterial metabolic activity rather than growth inhibitory effects. In particular, the reduction of acid production and glycolysis may significantly alter the growth of bacteria within plaque resulting in reduced cariogenicity *in vivo*. Eradication of all bacteria upon application of antimicrobials to the oral cavity is not desirable as many resident species provide natural protection against more pathogenic species, therefore these types of effects should be a target for preventative oral healthcare formulations.

With hindsight, the chitosan-fluoride microparticles may have performed better than the Carbopol 971P-based formulations in the biofilm model. Particularly since fluoride is known to have an effect on bacterial attachment and plaque formation (Busscher *et al.*, 2006) and chitosan is unlikely to enhance the growth of bacteria. Chitosan microparticles containing an antimicrobial compound have been previously investigated and demonstrate substantial antimicrobial activity (Cevher *et al.*, 2006; Qi *et al.*, 2004). Interestingly, chitosan microparticles intended for local antimicrobial delivery to the oral cavity through retentive properties have not been previously reported although the use of chitosan as an antiplaque agent is well documented and demonstrates *in vivo* efficacy when applied as an aqueous dispersion (Sano *et al.*, 2003). The use of viscous chitosan gels as an adjunct to scaling and root planing has also proved effective (Akincibay *et al.*, 2007). The lack of substantial antimicrobial activity in this study may be the result of the type of chitosan used and could be addressed in future studies. The benefits of sustained fluoride delivery can be partially attributed to its effect on bacterial metabolism; however these effects may not have been obvious from the planktonic tests used to evaluate the chitosan-fluoride microparticles. With further development, chitosan-fluoride microparticles may exhibit greater anticaries activity than could be ascertained in this study and represent a novel idea for sustained fluoride delivery in oral healthcare products.

Conclusions

- Carbopol 971P aqueous dispersions are suited to bioadhesive formulations in which semi-solid or liquid dosage forms are desired.
- Ionic interactions between negatively charged carboxyl groups and cationic metal ions are stable in deionised water but undergo displacement in the presence of other cations. The rate of release is dependent on the valance of the metal ion and its affinity for the polyelectrolyte and can be affected by pH.
- Bioadhesion is unaffected by the inclusion of metal salts provided low drug:carboxyl ratios are maintained and ionic interactions do not result in extensive intrapolymer bond formation.
- Antimicrobial assessment of the Carbopol 971P-based formulations demonstrated no apparent enhancement of antimicrobial activity due to the effect of Carbopol 971P on biofilm formation.
- Aqueous chitosan dispersions did not interact ionically with fluoride compounds.
- Chitosan-sodium fluoride microparticles may benefit current oral healthcare products by enhancing anticaries activity. High fluoride loading and *in vitro* fluoride release were obtained with spray-drying aqueous chitosan dispersions although bioadhesion was significantly reduced.

Further work

The *in vitro* staining technique was suitable for the analysis of aqueous polymer dispersions although it lacked the sensitivity of other methods used to quantify bioadhesion. Further modification of the protocol to obtain quantitative data for polymer adsorption may significantly improve its use in the assessment of future non-solid bioadhesive dosage forms. The use of conventional light microscopy to obtain images for analysis prevented the use of high magnifications due to the depth of field. The use of confocal imaging, which is capable of "Z" stacking to obtain 3D images, may allow better interpretation of the structure of adsorbed polymer at the buccal cell surface. Confocal imaging requires fluorescent labels for visualisation. Preliminary investigation into this technique using Carbopol 971P labelled with fluorescein was

carried out during this study. The use of fluorescent labels may adversely affect bioadhesion and limit the formation of ionic polymer:drug complexes. Utilising a fluorescent stain that binds to carboxyl groups in a similar fashion to Alcian blue would enable staining after polymer adhesion has occurred. Cationic fluorescent stains may be capable of staining anionic polymers in this way. More sensitive quantification of the polymer on the cell surface may then be achievable by analysing the 3D area occupied by fluorescent material.

The adsorption of chitosan from solution should be confirmed before future semi-solid or liquid applications are investigated. One potential technique may be application of aqueous chitosan dispersion to the surface of oral epithelial cell lines cultured in microtitre plates. The retention of chitosan at the surface could be detected with eosin Y, which has a ultra-violet absorption maximum in the region of 514 nm, allowing quantification through the measurement of fluorescence. This would allow quantification of the material adhered to the cells although it is probable that chitosan would adsorb onto all microtitre plate surfaces. Method development may be able to minimise this effect, resulting in a rapid, quantitative technique for the bioadhesive assessment of aqueous chitosan.

The interaction between Carbopol 971P and cationic metal ions may represent an important development in the delivery of cationic drugs for bioadhesive applications. In particular, the characteristic release of divalent zinc in artificial saliva suggests that other multivalent compounds may be displaced from the polymer at rates influenced by environmental pH. This may be relevant to other drug delivery targets that require therapeutic dosing at low pH, such as the oesophagus during gastric reflux. Further characterisation of the precipitated material formed after the addition of high concentrations of metal salt may lead to the development of microparticles, or solid formulations. In particular, the concentration of metal contained within the precipitated material, the type of interaction between the polymer and the metal, *in vitro* metal release and bioadhesive characteristics could be easily clarified. This may also help to explain the interaction of copper with Carbopol 971P in artificial saliva. Precipitated material could potentially contain much higher concentrations of metal than those achievable in aqueous polymer dispersions and may exhibit a significantly enhanced antimicrobial activity.

Chitosan did show some promise as a bioadhesive carrier for oral antimicrobial delivery and has demonstrated antiplaque activity in other studies. Investigating the interaction between aqueous chitosan dispersions and other anionic antimicrobials may exhibit similar characteristics to Carbopol 971P-metal complexes, which were not apparent with fluoride compounds. In addition, chitosan has demonstrated the capacity to chelate metal ions through the formation of coordinate bonds between metal cations and unprotonated amine and hydroxyl groups present within the chitosan structure at pH 7.0 (Qin *et al.*, 2006; Wang *et al.*, 2006). This phenomenon has been previously been investigated for potential application in adsorption, metal ion separation and waste water treatment. Coupled with the antimicrobial activity exhibited by chitosan, metal ions may be retained by the polymer and maintained at active concentrations. By avoiding the use of Carbopol 971P, the metal ions released may exhibit greater antimicrobial activity. Furthermore, bioadhesive chitosan-metal complexes for oral drug delivery have not been reported. Further studies should also focus on the potential for sustained fluoride delivery using chitosan, in terms of both antimicrobial and anticaries action. Development of the protocol used in the spray-drying technique, particularly the use of different operating parameters, may substantially improve the dry product obtained. Increasing the inlet and outlet air temperatures may have decreased the amount of aqueous material deposited on the surface of the drying chamber and influenced the distribution of fluoride within the microparticle. In depth investigations into the aqueous phase used to prepare the particles may also have significantly improved the *in vitro* characteristics. For example, decreasing the initial starting concentration of sodium fluoride added to the aqueous phase may have significantly improved the bioadhesion of the particles, which was reduced when compared to the chitosan-only particles. Although chitosan-fluoride microparticles did not show potent toxicity against the panel of oral bacteria, further analysis of other effects on bacterial metabolism may have shown some beneficial activities, as discussed in the previous paragraph. The planktonic studies did suggest that chitosan and fluoride may have had some synergistic activity against the bacteria and analysis of this observation may enable greater understanding of the antimicrobial action and how it may be harnessed for use in the oral cavity. The antimicrobial activity of chitosan was less than expected and future investigations using this polymer for antimicrobial applications should investigate a range of different chitosans as well as structural modifications that can improve the activity, such as those reported by Avadi *et al.* (2006).

References

Accili D, Menghi G, Bonacucine G, Di Martino P, Palmieri GF, Mucoadhesion dependence of pharmaceutical polymers on mucosa characteristics, *Eur. J. Pharm. Sci.* 2004; **22**: 225-234

Addy M, Local delivery of antimicrobial agents to the oral cavity, *Adv. Drug Deliv. Rev.* 1994; **13**: 123-134

Adult dental health survey: Oral health in the United Kingdom 1998, Office of National Statistics, available from:
http://www.statistics.gov.uk/downloads/theme_health/DHBulletinNew.pdf
Date accessed: 01/05/2005

Afseth J, Helgeland K, Bonesvoll P, Retention of Cu and Zn in the oral cavity following rinsing with aqueous solutions of copper and zinc salts, *Scand. J. Dent. Res.* 1983; **91**: 42-45

Agnihotri SA, Mallikarjuna NN, Aminabhavi TM, Recent advances on chitosan-based micro- and nanoparticles in drug delivery, *J. Control. Release* 2004; **100**: 5-28

Ahuja A, Khar RK, Ali J, Mucoadhesive drug delivery systems, *Drug Dev. Ind. Pharm.* 1997; **23**: 489-515

Aiello AE and Larson E, Antibacterial cleaning and hygiene products as an emerging risk factor for antibiotic resistance in the community, *Lancet Infect. Dis.* 2003; **3**: 501-506

Akincibay H, Senel S, Ay, ZY, Application of chitosan gel in the treatment of chronic periodontitis, *J Biomed Mater Res Part B: Appl Biomater* 2007; **80B**: 290-296

Aksungur P, Sungur A, Unal S, Iskit AB, Squier CA, Senel S, Chitosan delivery systems for the treatment of oral mucositis: *in vitro* and *in vivo* studies, *J. Control. Release* 2004; **98**: 269-279

Ali J, Khar R, Ahuja A, Kalra R, Buccoadhesive erodible disk for the treatment of oro-dental infections: design and characterisation, *Int. J. Pharm.* 2002; **283**: 93-103

Aranha H, Strachan RC, Arceneaux JE, Byers BR, Effect of trace metals on the growth of *Streptococcus mutans* in a Teflon chemostat, *Infect. Immun.* 1982; **35**: 456-460

Arora S, Kohli K, Ali A, Microbiological evaluation of mucoadhesive buccal tablets of secnidazole against anaerobic strains for the treatment of periodontal diseases, Presented at: *Controlled Release Society 30th Annual Meeting* 2003, Glasgow, UK: Abstract #376

Atkins PW, Physical chemistry, 4th Ed, Oxford university press, Oxford 1990: 684-686

Avadi MR, Sadeghi AMM, Tahzibi A, Bayati K, Pouladzadeh M, Zohuriaan-Mehr MJ, Rafiee-Tehrani M, Diethylmethyl chitosan as an antimicrobial agent: Synthesis, characterisation and antibacterial effects, *Eur. Polym. J.* 2004; **40**: 1355-1361

Baker CN and Tenover FC, Evaluation of Alamar colorimetric broth microdilution susceptibility testing method for staphylococci and enterococci, *J. Clin. Microbiol.* 1996; **34**: 2654-2659

Balzar Ekenback S, Linden LE, Sund M-L, Lonnies H, Effect of fluoride on glucose incorporation and metabolism in biofilm cells of *Streptococcus mutans*, *Eur. J. Oral Sci.* 2001; **109**: 182-186

Batchelor HK, Banning D, Dettmar PW, Hampson FC, Jolliffe IG, Craig DQM, An *in vitro* mucosal model for prediction of the bioadhesion of alginate solutions to the oesophagus, *Int. J. Pharm.* 2002; **238**: 123-132

Batchelor H, Dettmar P, Hampson F, Jolliffe I, Craig D, Microscopic techniques as potential tools to quantify the extent of bioadhesion of liquid systems, *Eur. J. Pharm. Sci.* 2004; **22**: 341-346

Bhargava HN and Leonard PA, Triclosan: Applications and safety, *Am. J. Infect. Control* 1996; **24**: 209-218

Birudaraj R, Mahalingam R, Li X, Jasti BR, Advances in buccal drug delivery, *Crit. Rev. Ther. Drug Carrier Sys.* 2005; **22**: 295-330

Bloom W and Fawcett DW, A textbook of histology, WB Saunders Co, Philadelphia 1975: 598-613

Boackle RJ, Dutton SL, Robinson WL, Vesely J, Lever JK, Su HR, Chang NS, Effects of removing the negatively charged *N*-terminal region of the salivary acidic proline-rich proteins by human leucocyte elastase, *Arch. Oral Biol.* 1999; **44**: 575-585

Bodde HE and Leiden NL, Principles of bioadhesion, In: Bioadhesion- possibilities and future trends, ed., Gurny R and Junginger HE, Wissenschaftliche Verlagsgesellschaft mbH, Stuttgart 1990: 44-63

Bradley RM, Essentials of oral physiology, Mosby, St. Louis 1995: 161-186

Bradshaw DJ, Marsh PD, Watson GK, Cummins D, The effects of triclosan and zinc citrate, alone and in combination, on a community of oral bacteria grown *in vitro*, *J. Dent. Res.* 1993; **72**: 25-30

Bromberg LE, Temchenko M, Alakhov V, Hatton TA, Bioadhesive properties and rheology of polyether-modified poly(acrylic acid) hydrogels, *Int. J. Pharm.* 2004; **282**: 45-60

Bromberg LE, Braman VM, Rothstein DM, Spacciapoli P, O'Connor SM, Nelson EJ, Buxton DK, Tonetti MS, Friden PM, Sustained release of silver from periodontal wafers for treatment of periodontitis, *J Control. Rel.* 2000; **68**: 63-72

Buchi, Training papers: Spray drying, Buchi Labortechnik AG, Flawil, Switzerland 2002

Busscher HJ, White DJ, Atema-Smit J, van der Mei HC, Efficacy and mechanisms of non-antibacterial, chemical plaque control by dentifrices- An *in vitro* study, *J Dentistry* 2006; Ahead of print DOI:10.1016/j.dent.2006.10.001

Campos Aldrete ME, Salgado-Zamora H, Luna J, Melendez E, Meraz-Rios MA, A high-throughput colorimetric and fluorometric microassay for the evaluation of nitroimidazole derivatives anti-trichomonas activity, *Toxicol. In Vitro* 2005; **19**: 1045-1050

Carreno-Gomez B and Duncan R, Evaluation of the biological properties of soluble chitosan and chitosan microspheres, *Int. J. Pharm.* 1997; **148**: 231-240

Cevher E, Orhan Z, Mulazimoglu L, Sensoy D, Alper M, Yildiz A, Ozsoy Y, Characterisation of biodegradable chitosan microspheres containing vancomycin and treatment of experimental osteomyelitis caused by methicillin-resistant *Staphylococcus aureus* with prepared microspheres, *Int. J. Pharm.* 2006; **317**: 127-135

Chan WD, Yang L, Wan W, Rizkalla AS, Fluoride release from dental cements and composites: A mechanistic study, *Dent. Mater.* 2006; **22**: 366-373

Chapman JS, Disinfectant resistance mechanisms, cross resistance and co-resistance, *Int. Biodet. Biodeg.* 2003; **51**: 271-276

Chatterjee S, Chatterjee S, Chatterjee BP, Das AR, Guha AK. Adsorption of a model anionic dye, eosin Y, from aqueous solution by chitosan hydrobeads. *J. Colloid Interface Sci.* 2005: 30-35

Cilurzo F, Minghetti P, Selmin F, Casiraghi A, Montanari L, Polymethacrylate salts as new low-swellable mucoadhesive materials, *J. Control. Release* 2003; **88**: 43-53

Cilurzo F, Selmin F, Minghetti P, Montanari L, The effects of bivalent inorganic salts on the mucoadhesive performance of a polymethylmethacrylate sodium salt, *Int. J. Pharm.* 2005; **301**: 62-70

Collins YE and Strotzky G, Factors affecting the toxicity of heavy metals to microbes, In: Metal ions and bacteria, ed., Beveridge TJ, Doyle RJ, John Wiley & Sons Inc, New York 1989: 31-71

Corne SJ, Morrissey SM, Wood RJ. A method for quantitative estimation of gastric barrier mucosa. *J. Physiol.* 1974; **242**: 116-117

Corrigan DO, Healy AM, Corrigan OI, Preparation and release of salbutamol from chitosan and chitosan co-spray dried compacts and mulitparticulates, *Eur. J. Pharm. Biopharm.* 2006; **62**: 295-305

Cowan FF, Dental Pharmacology, 2nd Ed, Lea and Febiger, Philadelphia 1992; 146-157

Cox SD, Lassiter MO, Taylor KG, Doyle RJ, Fluoride inhibits the glucan-binding lectin of *Streptococcus sobrinus*, *FEMS Microbiol. Lett.* 1994; **123**: 331-334

Debon SJJ and Tester RF, *In vitro* binding of calcium, iron and zinc by non-starch polysaccharides, *Food Chem.* 2001; **73**: 401-410

Diarra M, Pourroy G, Boymond C, Muster D, Fluoride controlled release tablets for intrabuccal use, *Biomaterials* 2003; **24**: 1293-1300

Di Martino A, Sittinger M, Risbud MV, Chitosan: A versatile polymer for orthopaedic tissue-engineering, *Biomaterials* 2005; **26**: 5983-5990

Diaz del Consuelo I, Jacques Y, Guy RH, Falson F, Evaluation of pig eosphageal tissue as a model for "*in vitro*" buccal mucosa permeability studies, presented at: Controlled release society 30th annual meeting and exposition 2003, Glasgow, UK; Abstract #514

Dittgen M, Durrani M, Lehmann K, Acrylic polymers: A review of pharmaceutical applications, *STP Pharma Sci.* 1997; **7**: 403-437

Dowd FJ, Saliva and dental caries, *Dent. Clin. North Am.* 1999; **43**: 579-597

Doyle RJ, How cell walls of gram-positive bacteria interact with metal ions, In: Metal ions and bacteria, ed., Beveridge TJ and Doyle RJ, John Wiley & Sons Inc, New York 1989; 275-289

Duchene D, Touchard F, Peppas NA, Pharmaceutical and medical aspects of bioadhesive systems for drug administration, *Drug Dev. Ind. Pharm.* 1988; **14**: 283-318

Dyvik K and Graffner C, Investigation of the applicability of a tensile testing machine for measuring mucoadhesive strength, *Acta Pharm. Nord.* 1992; 4: 79-84

Edgar WM and O'Mullane DM, Saliva and oral health, 2nd Ed. Bristish dental association publications: London 1996.

Edlund C, Hedberg M, Nord CE, Antimicrobial treatment of periodontal diseases disturbs the human ecology: a review, *J. Chemother.* 1996; **8**: 331-341

Eley BM. Antibacterial agents in the control of supragingival plaque- a review, *Br. Dent. J.* 1999; **186**: 286-296

Eouani C, Piccerelle P, Prinderre P, Bourret E, Joachim J, *In vitro* comparative study of buccal mucoadhesive performance of different polymeric films, *Eur. J. Pharm. Biopharm.* 2001; **52**: 45-55

Eshel G, Levy GJ, Mingelgrin U, Singer MJ, Critical evaluation of the use of laser diffraction for particle-size distribution analysis, *Soil Sci. Soc. Am. J.* 2004; **68**: 736-743

Esposito P, Colombo I, Lovrecich M, Investigation of surface properties of some polymers by a thermodynamic and mechanical approach: possibility of predicting mucoadhesion and biocompatibility, *Biomaterials* 1994; **15**: 177-182

Fine DH, Furgang D, Barnett ML, Comparative antimicrobial activities against isogenic planktonic and biofilm forms of *Actinobacillus actinomycetemcomitans*, *J. Clin. Periodontol.* 2001; **28**: 697-700

Francois J, Heitz C, Mestdagh MM, Spectroscopic study (u.v.-visible and electron paramagnetic resonance) of the interactions between synthetic polycarboxylates and copper ions, *Polymer* 1997; **38**: 5321-5332

Friedman M and Steinberg D, Sustained-release delivery systems for treatment of dental diseases, *Pharm. Res.* 1990; **7**: 313-317

Gaffar A, Afflitto J, Nabi N, Chemical agents for the control of plaque and plaque microflora: An overview, *Eur. J. Oral Sci.* 1997; **105**: 502-507

Gallagher IHC and Cutress TW, The effect of trace elements on the growth and fermentation by oral *Streptococci* and *Actinomyces*, *Archs. Oral Biol.* 1977; **22**: 555-562

Ganza-Gonzalez A, Anguiano-Igea S, Otero-Espinar FJ, Blanco MJ, Chitosan and chondroitin microspheres for oral administration controlled release of metoclopramide, *Eur. J. Pharm. Biopharm.* 1999; **48**: 149-155

Gilbert P and McBain AJ, Potential impact of increased use of biocides in consumer products on prevalence of antibiotic resistance, *Clin. Microbiol. Rev.* 2003; **16**: 189-208

Gilbert RJ, The oral clearance of zinc and triclosan after delivery from a dentifrice, *J. Pharm. Pharmacol.* 1987; **39**: 480-483

Giunchedi P, Juliano C, Gavini E, Cossu M, Sorrenti M, Formulation and *in vivo* evaluation of chlorhexidine buccal tablets prepared using drug-loaded chitosan microspheres, *Eur. J. Pharm. Biopharm.* 2002; **53**: 233-239

Gomez-Carracedo A, Alvarez-Lorenzo C, Gomez-Amoza JL, Concheiro A, Glass transitions and viscoelastic properties of Carbopol® and Noveon® compacts, *Int. J. Pharm.* 2004; **274**: 233-243

Govender S, Pillay V, Chetty DJ, Essack SY, Dangor CM, Govender T, Optimisation and characterisation of bioadhesive controlled release tetracycline microspheres, *Int. J. Pharm.* 2005; **306**: 24-40

Grabovac V, Guggi D, Bernkop-Schnurch A, Comparison of the mucoadhesive properties of various polymers, *Adv. Drug Del. Rev.* 2005; **57**: 1713-1723

Gu JM, Robinson JR, Leung SHS, Binding of acrylic polymers to mucin/epithelial surfaces: structure-property relationships, *Crit. Rev. Ther. Drug Carrier Sys.* 1988; **5**: 21-67

Hagerstrom H and Edsman K, Interpretation of mucoadhesive properties of polymer gel preparations using a tensile strength method, *J. Pharm. Pharmacol.* 2001; **53**: 1589-1599

Hancock EB and Newell DH, Preventative strategies and supportive treatment, *Periodontol. 2000* 2001; **25**: 59-76

Hand AR, Pathmanathan D, Field RB, Morphological features of the minor salivary glands, *Arch. Oral Biol.* 1999; **44**: S3-S10

Hannig M, Fiebiger M, Guntzer M, Dobert A, Zimehl R, Nekrashevych Y, Protective effect of the *in situ* formed short-term salivary pellicle, *Arch. Oral Biol.* 2004; **49**: 903-910

Harrap GJ, Saxton CA, Best JS, Inhibition of plaque growth by zinc salts, *J. Periodont. Res.* 1983; **18**: 634-642

Harrap GJ, Best JS, Saxton CA, Human oral retention of zinc from mouthwashes containing zinc salts and its relevance to dental plaque control, *Archs. Oral Biol.* 1984; **29**: 87-91

Harrison JJ, Ceri H, Stremick CA, Turner RJ, Biofilm susceptibility to metal toxicity, *Environ. Microbiol.* 2004; **6**: 1220-1227

Hayashi Y, Ohara N, Ganno T, Yamaguchi K, Ishizaki T, Nakamura T, Sato M, Chewing chitosan-containing gum effectively inhibits the growth of cariogenic bacteria, *Arch. Oral Biol.* 2007; **52**: 290-294

He G, Pearce EIF, Sissons CH, Inhibitory effect of $ZnCl_2$ on glycolysis in human oral microbes, *Archs. Oral. Biol.* 2002; **47**: 117-129

He P, Davis SS, Illum L, Chitosan microspheres prepared by spray drying, *Int. J. Pharm.* 1999; **187**: 53-65

Heitz C and Francois J, Poly(methacrylic acid)-copper ion interactions Phase diagrams: light and X-ray scattering, *Polymer* 1999; **40**: 3331-3344

Helander IM, Nurmiaho-Lassila E-L, Ahvenainen R, Rhoades J, Roller S, Chitosan disrupts the barrier properties of the outer membrane of gram-negative bacteria, *Int. J. Food Microbiol.* 2001; **71**: 235-244

Herrera JL, Lyons MF, Johnson LF, Saliva: Its role in health and disease, *J. Clin. Gastroenterol.* 1988; **10**: 569-578

Hicks J, Garcia-Godoy F, Flaitz C, Biological factors in dental caries: role of saliva and dental plaque in the dynamic process of demineralisation and remineralisation (part 1), *J. Clin. Pediatr. Dent.* 2003; **28**: 47-52

Hoang T, Jorgensen MG, Keim RG, Pattison AM, Slots J, Povidone-iodine as a periodontal pocket disinfectant, *J. Periodon. Res.* 2003; **38**: 311-317

Hughes MN and Poole RK, Metals and micro-organisms, Chapman and Hall Ltd, London 1989; 252-297

Humphrey SP and Williamson RT, A review of saliva: normal composition, flow and function, *J. Prosthet. Dent.* 2001; **85**: 162-169

Ikinci G, Senel S, Akincibay H, Kas S, Ercis S, Wilson CG, Hincal AA, Effect of chitosan on a periodontal pathogen *Porphyromonas gingivalis*, *Int. J. Pharm.* 2002; **235**: 121-127

Ingram GS, Horay CP, Stead WJ, Interaction of zinc with dental mineral, *Caries Res.* 1992; **26**: 248-253

Itota T, Carrick TE, Rusby S, Al-Naimi OT, Yoshiyama M, McCabe JF, Determination of fluoride ions released from resin-based dental materials using ion-selective electrode and ion chromatograph, *J. Dent.* 2004; **32**: 117-122

Issa MM, Koping-Hoggard M, Artursson P, Chitosan and the mucosal delivery of biotechnology drugs, *Drug Discov. Today* 2005; **2**: 1-6

Jabbour A, Srebnik M, Zaks B, Dembitsky V, Steinberg D, Evaluation of oxazaborolidine activity on *Streptococcus mutans* biofilm formation, *Int. J. Antimicrob. Agents* 2005; **26**: 491-496

Johnson DR and Moore WJ, Anatomy for dental students, 3rd Ed, Oxford University Press, Oxford 1997: 181-193

Johnson MF, Comparative efficacy of NaF and SMFP dentifrices in caries prevention: A meta-analysis overview, *Caries Res.* 1993; **27**: 328-336

Jones DS, Woolfson AD, Djokic J. Texture profile analysis of bioadhesive polymeric semisolids: mechanical characterisation and investigation of interactions between formulation components. *J. App. Polym. Sci* 1996; **61**: 2229-2234

Jones DS, Woolfson D, Brown AF, Textural, visoelastic and mucoadhesive properties of pharmaceutical gels composed of cellulose polymers, *Int. J. Pharm.* 1997a; **151**: 223-233

Jones DS, Woolfson AD, Brown AF, Textural analysis and flow rheometry of novel, bioadhesive antimicrobial oral gels, *Pharm. Res.* 1997b; **14**: 450-457

Jones DS, Woolfson AD, Brown AF, O'Neill MJ, Mucoadhesive, syringeable drug delivery systems for the controlled application of metronidazole to the periodontal pocket: *In vitro* release kinetics, syringeability, mechanical and mucoadhesive properties, *J. Control. Release* 1997c; **49**: 71-79

Jones DS, Woolfson AD, Brown AF, Coulter WA, McClelland C, Irwin CR, Design, characterisation and preliminary clinical evaluation of a novel mucoadhesive topical formulation containing tetracycline for the treatment of periodontal disease, *J. Control. Release* 2000; **67**: 357-368

Jumaa M, Furkert FH, Muller BW, A new lipid emulsion formulation with high antimicrobial efficacy using chitosan, *Eur. J. Pharm. Biopharm.* 2002; **53**: 115-123

Kerec M, Bogataj M, Mugerle B, Gasperlin M, Mrhar A, Mucoadhesion on pig vesical mucosa: influence of polycarbophil/calcium interactions, *Int. J. Pharm.* 2002; **241**: 135-143

Kockisch S, Rees GD, Young SA, Tsibouklis J, Smart JD, A direct-staining method to evaluate the mucoadhesion of polymers from aqueous dispersion, *J. Control. Release* 2001; **77**: 1-6

Kockisch S, Rees GD, Young SA, Tsibouklis J, Smart JD, Polymeric microspheres for drug delivery to the oral cavity: An *in vitro* evaluation of mucoadhesive potential, *J. Pharm. Sci.* 2003; **92**: 1614-1623

Kockisch S, Rees GD, Young SA, Tsibouklis J, Smart JD, *In situ* evaluation of drug-loaded microspheres on a mucosal surface under dynamic test conditions, *Int. J. Pharm.* 2004; **276**: 51-58

Kockisch S, Rees GD, Tsibouklis J, Smart JD, Mucoadhesive, triclosan-loaded polymer microspheres for application to the oral cavity: Preparation and controlled release characteristics, *Eur. J. Pharm. Biopharm.* 2005; **59**: 207-216

Kohli K, Puri A, Arora A, Baboota S, Design and characterisation of novel buccoadhesive film of doxycyclin for the treatment of pyorrhea, Presented at: *Controlled Release Society 30th Annual Meeting* 2003, Glasgow, UK: Abstract #445

Koryta J. Ion-selective electrodes, Cambridge University Press, Cambridge, UK 1975

Kriwet B and Kissel T, Interactions between bioadhesive poly(acrylic acid) and calcium ions, *Int. J. Pharm.* 1996; **127**: 135-145

Lee JW, Park JH, Robinson JR, Bioadhesive-based dosage forms: the next generation, *J. Pharm. Sci.* 2000; **89**: 850-866

Lehr CM, Bodde HE, Bouwstra JA, Junginger HE, A surface energy analysis of mucoadhesion II. Prediction of mucoadhesive performance by spreading coefficients, *Eur. J. Pharm. Sci.* 1993; **1**: 19-30

Leke N, Grenier D, Goldner M, Mayrand D, Effects of hydrogen peroxide on growth and selected properties of *Porphyromonas gingivalis*, *FEMS Microbiol. Lett.* 1999; **174**: 218-225

Lele BS and Hoffman AS, Insoluble ionic complexes of poly(acrylic acid) with a cationic drug for use as a mucoadhesive, ophthalmic drug delivery system, *J. Biomater. Sci. Polym. Edn.* 2000; **11**: 1319-1331

Lentner C, Geigy Scientific Tables, Volume 1: Units of measurement, body fluids, composition of the body, nutrition, 8th Ed, Ciba-Geigy Ltd, Basle 1981: 114-122

Liebana J, Castillo AM, Alvarez M, Periodontal diseases: microbiological considerations, *Med. Oral Patol. Oral Cir. Bucal* 2004; **9**: 75-91

Lim ST, Martin GP, Berry DJ, Brown MB, Preparation and evaluation of the *in vitro* drug release properties and mucoadhesion of novel microspheres of hyaluronic acid and chitosan, *J. Control. Release* 2000; **66**: 281-292

Liu H, Du Y, Wang X, Sun L, Chitosan kills bacteria through cell membrane damage, *Int. J. Food Microbiol.* 2004; **95**: 147-155

Listgarten MA, The structure of dental plaque, *Periodontol. 2000.* 1994; **5**: 52-65

Llabot JM, Manzo RH, Allemandi DA, Double-layered mucoadhesive tablets containing nystatin, *AAPS PharmSciTech* 2002; **3**: 1-6

Llabot JM, Manzo RH, Allemandi DA, Drug release from carbomer:carbomer sodium salt matrices with potential use as mucoadhesive drug delivery system, *Int. J. Pharm.* 2004; **276**: 59-66

Loftsson T, Leeves N, Bjornsdottir B, Duffy L, Masson M, Effect of cyclodextrins and polymers on triclosan availability and substantivity in toothpastes *in vivo*, *J. Pharm. Sci.* 1999; **88**: 1254-1258

Ludwig A, The use of mucoadhesive polymers in ocular drug delivery, *Adv. Drug Del. Rev.* 2005; **57**: 1595-1639

Lund W, The pharmaceutical codex: Principles and practice of pharmaceutics, 12th Ed, The Pharmaceutical Press, London 1994: 244-245

Mager DL, Ximenez-Fyvie LA, Haffajee AD, Socransky SS, Distribution of selected bacterial species on intraoral surfaces, *J. Clin. Periodontol.* 2003; **30**: 644-654

Malvern, MasterSizer: Instruction manual, Malvern Instruments Ltd, Worcester, UK 1992: Issue 3.2

Mandel ID and Wotman S, The salivary secretions in health and disease, *Oral Sci. Rev.* 1976; **8**: 25-47

Marcotte H and Lavoie MC, Oral microbial ecology and the role of salivary immunoglobulin A, *Microbiol. Mole. Biol. Rev.* 1998; **62**: 71

Marquis R, Clock SA, Mota-Meira M, Fluoride and organic weak acids as modulators of microbial physiology, *FEMS Microbiol. Rev.* 2003; **26**: 493-510

Marsh PD, Dentifrices containing new agents for the control of plaque and gingivitis: microbiological aspects, *J. Clin. Periodontol.* 1991; **18**: 462-467

Marsh PD and Martin MV, Oral Microbiology, 4th Ed, Wright, Edinburgh 1999.

Marsh PD, Plaque as a biofilm: pharmacological principles of drug delivery and action in the sub- and supra-gingival environment, *Oral. Dis.* 2003; **9** (Suppl. 1): 16-22

Marshall P, Snaar JEM, Ng YL, Bowtell RW, Hampson FC, Dettmar PW *et al*, Localised mapping of water movement and hydration inside a developing bioadhesive bond, *J. Control. Release* 2004; **95**: 435-446

Martin GC, Flanagan AJ, Embleton J, McNab R, A microtitre plate screening method for oral biofilm disinfection, Presented at: *83rd Meeting of the International Association of Dental Research* 2005, Baltimore, USA: Abstract #3471

Martin L, Wilson CG, Koosha F, Uchegbu IF, Sustained buccal delivery of the hydrophobic drug denbufylline using physically cross-linked palmitoyl glycol chitosan hydrogels, *Eur. J. Pharm. Biopharm.* 2003; **55**: 35-45

Martinac A, Filipovic-Grcic J, Voinovich D, Perissutti B, Franceschins E, Development and bioadhesive properties of chitosan-ethylcellulose microspheres for nasal delivery, *Int. J. Pharm.* 2005; **291**: 69-77

Merritt J, Kreth J, Qi F, Sullivan R, Shi W, Non-disruptive, real-time analyses of the metabolic status and viability of *Streptococcus mutans* cells in response to antimicrobial treatments, *J. Microbiol. Methods* 2005; **61**: 161-170

Minami S, Suzuki H, Okamoto Y, Fujinaga T, Shigemasa Y, Chitin and chitosan activate complement via the alternate pathway, *Carbohydr. Polym.* 1998; **36**: 151-155

Mombelli A. Periodontitis as an infectious disease: specific features and their implications, *Oral Dis.* 2003; **9** (Suppl. 1): 6-10

Moran J, Addy M, Corry D, Newcombe RG, Haywood J, A study to assess the plaque inhibitory action of a new zinc citrate toothpaste formulation, *J. Clin. Periodontol.* 2001; 28: 157-161

Mori T, Okumura M, Matsuura M, Ueno K, Tokura S, Okamoto Y *et al*, Effects of chitin and its derivatives on the proliferation and cytokine production of fibroblasts *in vitro*, *Biomaterials* 1997; **18**: 947-951

Mortazavi SA and Smart JD, An investigation into the role of water movement and mucus gel dehydration in mucoadhesion, *J. Control. Release* 1993; **25**: 197-203

Mortazavi SA, An *in vitro* assessment of mucus/mucoadhesive interactions, *Int. J. Pharm.* 1995; **124**: 173-182

Mortazavi SA and Smart JD, An investigation of some factors influencing the *in vitro* assessment of mucoadhesion, *Int. J. Pharm.* 1995; **116**: 223-230

Needleman IG, Martin GP, Smales FC, Characterisation of bioadhesives for periodontal and oral mucosal drug delivery, *J. Clin. Periodontol.* 1998; **25**: 74-82

Nishihara T and Koseki T, Microbial etiology of Periodontitis, *Periodontol 2000.* 2004; **36**: 14-26

No HK, Park NY, Lee SH, Meyers SP, Antibacterial activity of chitosans and chitosan oligomers with different molecular weights, *Int. J. Food Microbiol.* 2002; **74**: 65-72

Noveon Inc, Bulletin 3: Nomenclature and chemistry, 2002a, available from: www.pharma.noveoninc.com/literature; date accessed: 01/05/2005

Noveon Inc, Bulletin 4: Toxicology studies, 2002b, available from: www.pharma.noveoninc.com/literature; date accessed: 01/05/2005

Noveon Inc, Bulletin 2: Product and regulatory guide, 2002c, available from: www.pharma.noveoninc.com/literature; date accessed: 01/05/2005

Nurkeeva ZS, Khutoryanskiy VV, Mun GA, Sherbakova MV, Ivaschenko AT, Aitkhozhina NA, Polycomplexes of poly(acrylic acid) with streptomycin sulfate and their antibacterial activity, *Eur. J. Pharm. Biopharm.* 2004; **57**: 245-249

Nuttall NM, Bradnock G, White D, Morris J, Nunn J, Dental attendance in 1998 and implications for the future, *Br. Dental J.* 2001; **190**: 177-182

O'Brien J, Wilson I, Orton T, Pognan F, Investigation of the Alamar blue (resazurin) fluorescent dye for the assessment of mammalian cell cytotoxicity, *Eur. J. Biochem.* (2000); **267**: 5421-5426

Okeke CN, Tsuboi R, Kawai M, Ogawa H, Fluorometric assessment of *in vitro* antidermatophytic activities of antimycotics based on their keratin-penetrating power, *J. Clin. Microbiol.* 2000; **38**: 489-491

Owens TS, Dansereau RJ, Sakr A, Development and evaluation of extended release bioadhesive sodium fluoride tablets, *Int. J. Pharm.* 2005; **288**: 109-122

Park K and Robinson JR, Bioadhesive polymers as platforms for oral-controlled drug delivery: method to study bioadhesion, *Int. J. Pharm.* 1984; **19**: 107-127

Park H and Robinson JR, Physicochemical properties of water insoluble polymers important to mucin/epithelial adhesion, *J. Control. Release* 1985; **2**: 47-57

Park CR and Munday DL, Development and evaluation of a biphasic buccal adhesive tablet for nicotine replacement therapy, *Int. J. Pharm.* 2002; **237**: 215-226

Patel D, Smith AW, Grist N, Barnett P, Smart JD, An *in vitro* mucosal model predictive of bioadhesive agents in the oral cavity, *J. Control. Release* 1999; **61**: 175-183

Patel D, Smith JR, Smith AW, Grist N, Barnett P, Smart JD. An atomic force microscopy investigation of bioadhesive polymer adsorption onto human buccal cells. *Int. J. Pharm.* 2000; **200**: 271-277

Peppas NA and Sahlin JJ, Hydrogels as mucoadhesive and bioadhesive materials a review, *Biomaterials* 1996; **17**: 1553-1561

Peppas NA and Huang Y, Nanoscale technology of mucoadhesive interactions, *Adv. Drug Del. Rev.* 2004; **56**: 1675-1687

Perioli L, Ambrogi V, Rubini D, Giovagnoli S, Ricci M, Rossi C, Novel mucoadhesive topical formulation containing metronidazole for the treatment of periodontal disease, Presented at: *Controlled Release Society 30th Annual Meeting* 2003, Glasgow, UK: Abstract #464

Pettit RK, Weber CA, Kean MJ, Hoffman H, Pettit GR, Tan R *et al*, Microplate alamarBlue method for *Staphylococcus epidermidis* biofilm susceptibility testing, *Antimicrob. Agents. Chemother.* 2005; **49**: 2612-2617

Phan T-N, Buckner T, Sheng J, Baldeck JD, Marquis RE, Physiologic actions of zinc related to inhibition of acid and alkali production by oral streptococci in suspensions and biofilms, *Oral Microbiol. Immunol.* 2004; **19**: 31-38

Prescott LM, Harley JP, Klein DA, Microbiology, 4th Ed, WCB McGraw-Hill, Boston 1999: 805-808

Qaqish RB and Amiji MM, Synthesis of a fluorescent chitosan derivative and its application for the study of chitosan-mucin interactions, *Carbohydr. Polym.* 1999; **38**: 99-107

Qi LF, Xu ZR, Jiang X, Hu CH, Zou XF, Preparation and antibacterial activity of chitosan nanoparticles, *Carbohydr. Res.* 2004; **339**: 2693-2700

Qin YM, Zhu CJ, Chen J, Chen YZ, Zhang C, The absorption and release of silver and zinc ions by chitosan fibers, *J. Appl. Polym. Sci.* 2006; **101**: 766-771

Quirynen M, Teughels W, van Steenberghe D, Microbial shifts after subgingival debridement and formation of bacterial resistance when combined with local or systemic antimicrobials, *Oral Dis.* 2003; **9** (Suppl. 1): 30-37

Rango Rao KV and Buri P, A novel *in situ* method to test polymers and coated microparticles for bioadhesion, *Int. J. Pharm.* 1989; **52**: 265-270

Reynolds EC, Contents of toothpaste- safety implications, *Aust. Prescr.* 1994; **17**: 49-51

Richardson JC, Dettmar PW, Hampson FC, Melia CD, Oesophageal bioadhesion of sodium alginate suspensions: particle swelling and mucosal retention, *Eur. J. Pharm. Biopharm.* 2004; **23**: 49-56

Richardson JC, Dettmar PW, Hampson FC, Melia CD, Oesophageal bioadhesion of sodium alginate suspensions: suspension behaviour on oesophageal mucosa, *Eur. J. Pharm. Sci.* 2005; **24**: 107-114

Risbud MV, Hardiker AA, Bhat SV, Bhonde RR, pH-sensitive freeze-dried chitosan-polyvinyl pyrrolidone hydrogels as controlled release system for antibiotic delivery, *J. Control. Release* 2002; **68**: 23-30

Roberts SK, Wei GX, Wu CD, Evaluating biofilm growth of two oral pathogens, *Lett. Appl. Microbiol.* 2002; **35**: 552-556

Robinson AM, Bannister M, Creeth JE, Jones MN, The interaction of phospholipid liposomes with mixed bacterial biofilms and their use in the delivery of bactericide, *Colloids and Surf., A,* 2001; **186**: 43-53

Rozen R, Bachrach G, Bronshteyn M, Gedalia I, Steinberg D, The role of fructans on dental biofilm formation by *Streptococcus sobrinus*, *Streptococcus mutans*, *Streptococcus gordonii* and *Actinomyces viscosus*, *FEMS Microbiol. Lett.* 2001; **195**: 205-210

Russell AD, Biocide use and antibiotic resistance: the relevance of laboratory findings to clinical and environmental situations, *Lancet Infect. Dis.* 2003; **3**: 794-803

Sandri G, Bonferoni MC, Chetoni P, Rossi S, Ferrari F, Ronchi C, Caramella C, Opthalmic delivery systems based on drug-polymer-polymer ionic ternary interaction: *In vitro* and *in vivo* characterisation, *Eur. J. Pharm. Biopharm.* 2006; **62**: 59-69

Sano H, Shibasaki KI, Matsukubo T, Takaesu Y, Effect of chitosan rinsing on reduction of dental plaque formation, *Bull. Tokyo dent. Coll.* 2003; **44**: 9-16

Sbordone L and Borkolaia C, Oral microbial biofilms and plaque related diseases: microbial communities and their role in the shift from health to disease, *Clin. Oral Invest.* 2003; **7**: 181-188

Scheie A, Modes of action of currently known chemical anti-plaque agents other than chlorhexidine, *J. Dent. Res.* 1989; **68**: 1609-1616

Schwach-Abdellaoui K, Vivien-Castioni N, Gurny R, Local delivery of antimicrobial agents for the treatment of periodontal diseases, *Eur. J. Pharm. Biopharm.* 2000; **50**: 83-99

Schwender N, Huber K, Al Marrawi F, Hannig M, Ziegler C, Initial bioadhesion on surfaces in the oral cavity investigated by scanning force microscopy, *Appl. Surf. Sci.* 2005; **252**: 117-122

Senel S, Ikinci G, Kas S, Yousefi-Rad A, Sargon MF, Hincal AA, Chitosan films and hydrogels of chlorhexidine gluconate for oral mucosal delivery, *Int. J. Pharm.* 2000; **193**: 197-203

Serotec Ltd, Serotec product datasheet: AlamarBlue™ (BUF012B), 2003, available from: http://www.serotec.com/asp/datasheet.asp?code=BUF012B&vers=NA; date accessed: 01/05/2005

Shani S, Friedman M, Steinberg D, *In vitro* assessment of the antimicrobial activity of a local sustained release device containing amine fluoride for the treatment of oral infectious diseases, *Diagn. Microbiol. Infect. Dis.* 1998; **30**: 93-97

Shirkhanzadeh M, Azadegan M, Liu GQ, Bioactive delivery systems for the slow release of antibiotics: incorporation of Ag^{+} ions into micro-porous hydroxyapatite coatings, *Mater. Lett.* 1995; **24**: 7-12

Singla AK, Chawla M, Singh A, Potential applications of Carbomer in oral mucoadhesive controlled drug delivery system: a review, *Drug Dev. Ind. Pharm.* 2000; **26**: 913-924

Singla AK and Chawla M, Chitosan: some pharmacological and biological aspects- an update, *J. Pharm. Pharmacol.* 2001; **53**: 1047-1067

Skoog DA, Holler FJ, Nieman TA, Principles of instrumental analysis, 5th Ed, Saunders College Publishing, Philadelphia, 1998.

Slomiany BL, Murty VLN, Piotrowski J, Slomiany A, Salivary mucins in oral mucosal defense, *Gen. Pharmac.* 1996; **27**: 761-771

Smart JD, Recent developments in the use of bioadhesive systems for delivery of drugs to the oral cavity, *Crit. Rev. Ther. Drug Carrier Sys.* 2004a; **21**: 319-344

Smart JD, Bioadhesion, In: Encyclopaedia of biomaterials and biomedical engineering, ed., Wnek GE and Bowlin GL, Marcel Dekker, New York 2004b: 62-71

Smart JD, The basics and underlying mechanisms of mucoadhesion, *Adv. Drug Del. Rev.* 2005a; **57**: 1556-1568

Smart JD, Buccal drug delivery, *Expert Opin. Drug Deliv.* 2005b; **2**: 507-517

Smith ME and Morton DG, The digestive system: Basic science and principles, Churchill Livingstone, Edinburgh 2001: 22-37

Smith JMB, Laboratory evaluation of antimicrobial agents, In: Pharmaceutical microbiology, 7th Ed, ed., Denyer SP, Hodges NA, Gorman SP, Blackwell Publishing Oxford 2004: 187-201

Sondi I and Salopek-Sondi B. Silver nanoparticles as antimicrobial agent: a case study on *E.coli* as a model for gram-negative bacteria, *J. Colloid Interface Sci.* 2004; **275**: 177-182

Southard GL and Godowski KC, Subgingival controlled release of antimicrobial agents in the treatment of periodontal disease, *Int. J. Antimicrob. Agents* 1998; **9**: 239-253

Spacciapoli P, Buxton D, Rothstein D, Friden P, Antimicrobial activity of silver nitrate against periodontal pathogens, *J. Periodont. Res.* 2001; **36**: 108-113

Squier CA and Wertz PW, Structure and function of the oral mucosa and implications for drug delivery, In: Oral mucosal drug delivery, ed., Rathbone MJ, Marcel Dekker Inc, New York 1996: 1-26

Sreenivasan P and Gaffer A, Antiplaque biocides and bacterial resistance: a review, *J. Clin. Periodontol.* 2002; **29**: 965-974

Steinberg D and Rothman M, Antibacterial effect of chlorhexidine on bacteria adsorbed onto experimental dental plaque, *Diagn. Microbiol. Infect. Dis.* 1996; **26**: 109-115

Steinberg D and Friedman M, Dental drug-delivery devices: Local and sustained release applications, *Crit. Rev. Ther. Drug Carrier Syst.* 1999; **16**: 425-459

Stevens A and Lowe J, Human histology, 2nd Ed, Mosby, Barcelona 1997: 177-190

Stookey GK, DePaola PF, Featherstone JDB, Fejerskov O, Moller IJ, Rotberg S *et al*, A critical review of the relative anticaries efficacy of sodium fluoride and sodium monofluorophosphate dentifrices, *Caries Res.* 1993; **27**: 337-360

Suzuki Y, Okamoto Y, Morimoto M, Sashiwa H, Saimoto H, Tanioka S *et al*, Influence of physico-chemical properties of chitin and chitosan on complement activation, *Carbohydr. Polym.* 2000; **42**: 307-310

Takeuchi H, Thongborisute J, Matsui Y, Sugihara H, Yamamoto H, Kawashima Y, Novel mucoadhesion tests for polymers and polymer-coated particles to design optimal mucoadhesive drug delivery systems, *Adv. Drug Del. Rev.* 2005; **57**: 1583-1594

Tamburic S and Craig DQM, A comparison of different *in vitro* methods for measuring mucoadhesive performance, *Eur. J. Pharm. Biopharm.* 1997; **44**: 159-167

Theilade E, Factors controlling the microflora of the healthy mouth, In: Human microbial ecology, ed., Hill MJ and Marsh PD, CRC Press, London 1990: 1-9

Tobyn MJ, Johnson JR, Dettmar PW. Factors affecting in vitro gastric mucoadhesion I. Test conditions and instrumental parameters. *Eur. J. Pharm. Biopharm* 1995; **41**: 235-241

Tobyn MJ, Johnson JR, Dettmar PW. Factors affecting in vitro gastric mucoadhesion I. Influence of polymer addition on the observed mucoadhesion of some materials. *Eur. J. Pharm. Biopharm.* 1996; **42** 1996: 331-335

Tobyn MJ, Johnson JR, Dettmar PW. Factors affecting in vitro gastric mucoadhesion I. Influence of tablet excipients, surfactants and salts on the observed mucoadhesion of polymers. *Eur. J. Pharm. Biopharm.* 1997; **43**: 65-71

Tomida T, Hamaguchi K, Tunashima S, Katoh M, Masuda S, Binding properties of a water-soluble chelating polymer with divalent metal ions measured by ultrafiltration. Poly(acrylic acid), *Ind. Eng. Chem. Res.* 2001; **40**: 3557-3562

Tur KM and Ch'ng HS, Evaluation of possible mechanism(s) of bioadhesion, *Int. J. Pharm.* 1998; **160**: 61-74

Ugwoke MI, Agu RU, Verbeke N, Kinget R, Nasal mucoadhesive drug delivery: Background, applications, trends and future perspectives, *Adv. Drug Del. Rev.* 2005; **57**: 1640-1665

Ungphaiboon S and Maitani Y, *In vitro* permeation studies of triamcinolone acetonide mouthwashes, *Int. J. Pharm.* 2001; **220**: 111-117

Vilches AP, Jimenez-Kairuz A, Alovero F, Olivera ME, Allemandi DA, Manzo RH, Release kinetics and up-take studies of model fluoroquinolones from carbomer hydrogels, *Int. J. Pharm.* 2002; **246**: 17-24

Vivien-Castioni N, Baehni PC, Gurny R, Current status in oral fluoride pharmacokinetics and implications for the prophylaxis against dental caries, *Eur. J. Pharm. Biopharm.* 1998; **45**: 101-111

Vivien-Castioni N, Gurny R, Baehni P, Kaltsatos V, Salivary fluoride concentrations following applications of bioadhesive tablets and mouthrinses, *Eur. J. Pharm. Biopharm.* 2000; **49**: 27-33

Volpe AR, Petrone ME, De Vizio W, Davis RM, Proskin HM, A review of plaque, gingivitis, calculus and caries clinical efficacy studies with a fluoride dentifrice containing triclosan and PVM/MA copolymer, *J. Clin. Dent.* 1996; **7**: S1-S14

Vyas SP, Sihorkar V, Mishra V, Controlled and targeted drug delivery strategies towards intraperiodontal pocket diseases, *J. Clin. Pharm. Ther.* 2000; **25**: 21-42

Wang X, Du YM, Liu H, Preparation, characterisation and antimicrobial activity of chitosan-Zn complex, *Carbohydr. Res.* 2004; **56**: 21-26

Watson DG, Pharmaceutical analysis, Churchill Livingstone, Edinburgh 1999.

Weatherell JA, Robinson C, Rathbone MJ, Site-specific differences in the salivary concentrations of substances in the oral cavity- implications for the aetiology of oral disease and local drug delivery, *Adv. Drug Del. Rev.* 1994; **13**: 23-42

Weatherell JA, Robinson C, Rathbone MJ, The flow of saliva and its influence on the movement, deposition and removal of drugs administered to the oral cavity, In: Oral mucosal drug delivery, ed., Rathbone MJ, Marcel Dekker Inc, New York 1996

Wehry EL, Molecular fluorescence and phosphorescence spectrometry, In: Handbook of instrumental techniques for analytical chemistry, ed., Settle F, Prentice Hall, New Jersey USA 1997: 507-538

Weyant RJ. Seven systematic reviews confirm topical fluoride therapy is effective in preventing dental caries, *J. Evid. Based Dent. Pract.* 2004; **4**: 129-135

Wiegand A, Buchalla W, Attin T, Review on fluoride-releasing restorative materials-Fluoride release and uptake characteristics, antibacterial activity and influence on caries formation, *Dent. Mater.* 2007; **23**: 343-362

Willard HH, Merritt LL, Dean JA, Settle FA, Instrumental methods of analysis, 7th Ed, Wadsworth Publishing Company, California 1988: 243-255

Wilson CG and Nottingham GB, *In vivo* testing of bioadhesion, In: Bioadhesion-Possibilities and future trends, ed., Gurny R and Junginger HE, Wissenschaftliche Verlagsgesellschaft mbH, Stuttgart 1990: 93-107

Wong CF, Yuen KH, Peh KK, An *in vitro* methods for buccal adhesion studies: importance of instrument variables, *Int. J. Pharm.* 1999; **180**: 47-57

Zameck RL and Tinanoff N, Effects of NaF and SnF_2 on growth, acid and glucan production of several oral streptococci, *Archs. Oral Biol.* 1987; **32**: 807-810

Zeelie JJ and McCarthy TJ, Effects of copper and zinc ions on the germicidal properties of two popular pharmaceutical antiseptic agents cetylpyridinium chloride and povidone-iodine, *Analyst* 1998; **123**: 503-507

Zhang H, Zhang J, Streisand JB, Oral mucosal drug delivery: Clinical pharmacokinetics and therapeutic application, *Clin. Pharmacokinet.* 2002; **41**: 661-680

Appendix 1

Justification of statistics employed within the study.

- Descriptive statistics.

Throughout this thesis data has been presented as the mean and standard deviation (SD) or standard error (SE) of the mean. These statistics are used to describe the distribution of data. The mean is a measure of location within the distribution and is the sum of all values divided by the number of observations (n). Both the SD and SE of the mean are measures of the spread of data and describe how widely values are dispersed about the mean. Further to this, the SE is sensitive to the number of measurements that make up the sample and transforms the SD with a bias that gives advantage to a larger sample size. The SE has only been utilised within this thesis in the presentation of data collected from the *in vitro* staining technique, described in 2.2.2.2, as n = 60 for each treatment.

- Goodness of fit: The Kolmogorov-Smirnov test.

Statistical analysis utilises tests that can determine the significance of data relative to a probability level. These tests can be either parametric; which assumes that the data set is normally distributed, and non-parametric; in which no assumptions are made about the distribution of data. Selection of the type of test undertaken will affect the result obtained. For instance, if a parametric test is utilised for a data set that is not normally distributed then inaccuracies can arise in the statistical interpretation. Non-parametric tests can be utilised to assess the significance of data that may not be normally distributed, however these tests lack power that can be obtained when using a parametric test, provided the data is normally distributed. Therefore it is important to assess whether the data is normally distributed before selection of the appropriate test.

The Kolmogorov-Smirnov test is used to decide whether a sample comes from a population with a specific distribution. Throughout this project, data sets were first analysed for normality using this technique before subsequent tests were initiated. The statistics package SPSS v.14 for Windows (Copyright SPSS Inc. 1989-2005) was utilised for data analysis when using the Kolmogorov-Smirnov test and an example of the output is given in Table 1.

Table 1 One-sample Kolmogorov-Smirnov test to assess the normality of the data set obtained from the texture analysis of spray-dried microparticles described in chapter 4 (4.3.3f).

		Detach	Work
N		15	15
Normal Parameters(a,b)	Mean	155.5333	75.8667
	Std. Deviation	155.49454	69.31076
Most Extreme Differences	Absolute	.291	.251
	Positive	.291	.251
	Negative	-.181	-.143
Kolmogorov-Smirnov Z		1.127	.972
Asymp. Sig. (2-tailed)		.158	.302

a Test distribution is Normal.
b Calculated from data.

In the Kolmogorov-Smirnov test, the null hypothesis states that the data set follows a specified distribution, in this case, a normal distribution. The test examines the largest difference between two cumulative distribution functions, one calculated from the data and one from a theoretical mathematical model. The difference between the distributions is shown in Table 1 under the most extreme differences, in which the absolute value represents the largest difference between the distributions. In the example shown in Table 1, the absolute difference is positive in both instances. The Z statistic represents the square root of the sample size, divided by the largest absolute difference between the distributions. To interpret the output given by SPSS the value given below the Z statistic represents the significance of the data. In this instance, the values are both above 0.05, which indicates that the normal distribution is a good fit for the maximum detachment force and the work of adhesion of the spray-dried microparticles.

- Comparing two data sets: Student's *t*-test

The *t*-test is a parametric test that is used to compare two sample populations to determine whether they are significantly different. The workbook function available in Microsoft Excel 2003 (Copyright Microsoft corporation 1985-2001) was used to calculate the probability associated with Student's *t*-test. Within this project, all *t*-tests were based on independent data sets typically with equal variance; hence the two-

sample *t*-test assuming equal variance was used. The variance is obtained by squaring the SD and is another measure of spread. The method used to assess equal variance is described in the following section. When unequal variance was evident between two data sets, the two-sample *t*-test assuming unequal variance was used. In either case, the probability associated with the *t*-test was derived using a two-tailed distribution.

Table 2 Kolmogorov-Smirnov test to check the suitability of Student's *t*-test in analysing percentage increase data obtained from the *in vitro* staining technique in artificial saliva.

		increase
N		360
Normal Parameters(a,b)	Mean	56.9440
	Std. Deviation	21.36221
Most Extreme Differences	Absolute	.032
	Positive	.032
	Negative	-.030
Kolmogorov-Smirnov Z		.600
Asymp. Sig. (2-tailed)		.864

a Test distribution is Normal.
b Calculated from data.

In chapter 2, the *in vitro* staining technique was used to compare the adhesion of Carbopol 971P only and Carbopol-metal complexes to buccal cells in artificial saliva. The Kolmogorov-Smirnov test confirmed that the data collected from this technique was normally distributed (Table 2). Therefore, the *t*-test was used to determine whether the percentage increase in relative stain intensity induced by Carbopol 971P and the Carbopol-metal complexes were significantly different to each other. An example data set and subsequent analysis is given in Table 3. The probability value (located under T-test in Table 3) is returned from the two-sample equal variance (note the near identical SD) *t*-test. The value obtained is less than 0.001, indicating that the inclusion of copper in the polymer sample caused a highly significant difference in relative stain intensity when compared to the polymer alone.

Table 3 Percentage increase data sets obtained from the in vitro staining technique of Carbopol 971P only (positive control) or Carbopol 971P-copper complex (test) in artificial saliva described in chapter 3 (3.3.5.2).

Positive Control	Test		Positive control cont.	Test cont.
19.87	22.82		79.47	48.40
43.83	52.59		78.15	16.22
43.03	71.51		69.36	84.90
94.35	65.86		27.51	86.37
68.89	57.70		87.45	15.93
67.13	49.87		61.79	99.56
35.48	85.32		47.49	29.33
67.00	54.29		26.09	29.37
34.85	33.74		89.03	111.47
90.92	54.58		52.46	73.29
119.45	51.22		33.55	70.87
52.12	50.16		80.46	67.74
78.87	8.38		48.05	42.77
103.39	37.02		48.49	60.24
87.76	32.69		1.43	28.55
72.59	39.52		88.17	50.48
93.31	32.75		62.65	22.20
106.14	56.23		74.59	65.97
66.09	43.34		95.87	48.90
41.18	62.49		65.37	93.58
44.76	31.92		93.38	56.93
55.30	80.00		63.44	74.54
78.97	23.43		72.70	88.83
51.25	35.52		94.98	32.91
84.85	50.56		89.91	46.37
53.31	35.28		81.34	43.83
76.82	30.44	**Mean**	**67.58**	**50.96**
73.76	63.79	**SD**	**23.20**	**22.22**
83.71	44.75	**SE**	**3.00**	**2.87**
84.48	31.08			
60.83	55.99			
63.59	57.07			
70.48	35.80		**T-Test**	
73.15	30.39		**0.000108198**	

- Comparing more than two data sets: One-way Analysis Of Variance (ANOVA)

Comparing the means of multiple data sets can be achieved using *t*-test for all the pairs of locations. For example, for 7 sets of data there would be 21 different paired comparisons. However, multiple *t*-tests performed on a range of data sets leads to inaccuracies in the analysis. Once a large number of comparisons are required the normal 5% probability level loses significance and is subject to errors derived from

false significant differences, which may be due to chance alone. To avoid this, one-way ANOVA can be used to determine whether a significant difference exists between the data as a whole. An important assumption underlying the ANOVA is that all data sets must have similar variance, like the two-sample *t*-test assuming equal variance. Due to the importance of this assumption, equal variance was assessed prior to analysis by calculating the variance ratio. This value was obtained by dividing the highest value of variance by the lowest in a range of data sets. This value was then compared to the maximum variance ratio table (known as an F_{max} table, an example of which can be found at http://helios.bto.ed.ac.uk/bto/statistics/tress6.html) for the number of treatments to be analysed and the degrees of freedom (number of replicates per treatment – 1). In chapter 4 (4.3.3c) for example, one-way ANOVA was unsuitable for the analysis of particle size data collected from the spray-dried particles prepared from both 1% w/v and 2% w/v starting chitosan concentrations due to a high variance ratio. Therefore, *t*-tests were used to compare 3 paired locations. To assess the effect of glutaraldehyde on the size of spray-dried microparticles, the variance ratio was below the value obtained from the F_{max} value and the ANOVA test was deemed suitable for analysis. The data collected from particle size measurements for microparticles prepared from 1% w/v starting chitosan concentrations was suitable for parametric analysis (Table 4).

Table 4 Kolmogorov-Smirnov test to determine the goodness of fit of the normal distribution to particle size data collected from spray-dried microparticles prepared with a 1% w/v starting concentration of chitosan.

		Size
N		12
Normal Parameters(a,b)	Mean	3.8967
	Std. Deviation	1.31270
Most Extreme Differences	Absolute	.323
	Positive	.323
	Negative	-.277
Kolmogorov-Smirnov Z		1.117
Asymp. Sig. (2-tailed)		.165

a Test distribution is Normal.
b Calculated from data.

One-way ANOVA was carried out using SPSS v.14. This test is based on assessing the amount of overall variation in the data that can be attributed to 1) differences between group means and comparing that with 2) the amount of variation that can be assigned to the difference between individuals within the same group. An example of the output from SPSS is given in Table 5 for the particle size data discussed above. The F statistic is derived by dividing the mean square between groups by the mean square within groups. The SPSS output returns the significance of the F statistic at the 5% probability level. In the example (Table 5), this value is greater than 0.05, indicating no significant difference in particle size as a result of glutaraldehyde.

Table 5 ANOVA of particle size data obtained from spray-dried microparticles prepared from 1% w/v starting chitosan concentration to determine whether glutaraldehyde causes an effect on measured size.

	Sum of Squares	df	Mean Square	F	Sig.
Between Groups	1.547	2	.774	.400	.682
Within Groups	17.408	9	1.934		
Total	18.955	11			

- Non parametric tests to compare multiple data sets: The Kruskal-Wallis ANOVA

In instances where data to be analysed does not fulfil the criteria for the parametric ANOVA test, a non-parametric alternative can be utilised. The Kruskal-Wallis ANOVA makes no assumptions about the data i.e. the data does not have to be normally distributed and unequal variance is acceptable. This test is a one-way ANOVA by ranks. It tests the null hypothesis that multiple independent samples come from the same population. The Kruskal-Wallis statistic measures how much the group ranks differ from the average rank of groups. The chi-squared value is obtained by squaring each groups distance from the average of all ranks according to the sample size, summing across groups and multiplying by a constant (SPSS v.14). This test was carried out using SPSS v.14 and returns a significance value which describes the probability of achieving a chi squared value greater than, or equal to the value obtained relative to the degrees of freedom of the data set. If the significance value is less than 0.05 then the

null hypothesis is rejected and the multiple independent samples originate from different populations. Analysis of the maximum detachment forces of chitosan polymers in chapter 2 (2.3.2) revealed a non-normal distribution according to the Kolmogorov-Smirnov test, shown in Table 6. Due to this, the Kruskal-Wallis ANOVA instead of the parametric one-way ANOVA was used to assess any significant difference between the data obtained and is given in Table 7.

Table 6 Kolmogorov-Smirnov test indicating that the normal distribution is not a good fit for texture probe analysis data collected on the maximum detachment force of chitosan polymers.

		detach
N		66
Normal Parameters(a,b)	Mean	349.1818
	Std. Deviation	358.92754
Most Extreme Differences	Absolute	.169
	Positive	.159
	Negative	-.169
Kolmogorov-Smirnov Z		1.371
Asymp. Sig. (2-tailed)		.047

a Test distribution is Normal.
b Calculated from data.

Table 7 Kruskal-Wallis ANOVA to determine the presence of any significant difference between the maximum detachment force measured from the chitosan samples. Initially, the samples are ranked (a) and the Kruskal-Wallis statistic is then derived (b).

a)

	chitosan	N	Mean Rank
detach	Carbopol 974P	6	25.33
	Ethylcellulose	6	3.50
	G213	6	27.92
	G113	6	16.50
	CL213	6	48.67
	CL113	6	41.25
	HCMF	6	42.58
	DCMF	6	42.25
	CMFP	6	18.83
	Fluka Med	6	48.75
	Fluka High	6	52.92
	Total	66	

b)

	detach
Chi-Square	41.699
df	10
Asymp. Sig.	.000

a Kruskal Wallis Test
b Grouping Variable: chitosan

In this instance, the probability returned by the test indicated that a significant difference existed between the maximum detachment forces produced during the assessment of chitosan adhesion.

- Non-parametric tests to compare two data sets: The Mann-Whitney U test.

Once a significant difference has been established for non-parametric data using the Kruskal-Wallis ANOVA, the specific location of the significant difference must be assessed. This can be done with the Mann-Whitney U test for two independent samples. The null hypothesis states that the difference between the median of the two data sets is no greater than can be explained by random sampling. This test, like the Kruskal-Wallis test, is based on the ranks of the original values, rather than the values themselves. The Mann-Whitney U test was used to examine the location of significant differences in maximum detachment forces between the chitosan polymers and an example is given in Table 8.

Table 8 Mann-Whitney U test carried out using SPSS v.14 to detect a significant difference between high viscosity chitosan and CMFP. The data is first ranked (a) and the U statistic is then calculated (b).

a)

	chitosan	N	Mean Rank	Sum of Ranks
detach	CMFP	6	3.83	23.00
	Fluka High	6	9.17	55.00
	Total	12		

b)

	detach
Mann-Whitney U	2.000
Wilcoxon W	23.000
Z	-2.562
Asymp. Sig. (2-tailed)	.010
Exact Sig. [2*(1-tailed Sig.)]	.009(a)

a Not corrected for ties.
b Grouping Variable: chitosan

The U statistic is derived by counting the number of values in the second data set which exceed the each rank in the first data set and vice versa. The Mann-Whitney U statistic displayed in the table is the smaller of these two values. SPSS v.14 also returns the Wilcoxon W statistic, which denotes the smaller of the two rank sums displayed for each group in the rank table; in this case it is the rank sum of CMFP. The significance returned by the test estimates the probability of obtaining a Z statistic equal to or greater than the one displayed, if the data sets are derived from the same population. In this instance, the significance is less than 0.05, which indicates that the maximum detachment force produced by CMFP is significantly different to those produced by high viscosity chitosan. Although the use of multiple comparisons using a two-sample statistical test is not typically recommended, it is assumed that any bias toward false significant differences is eliminated by first utilising a multiple test, such as the Kruskal-Wallis ANOVA, to indicate the presence of a significant difference within the data sets.

Appendix 2

Theory and practise of Atomic absorption spectroscopy (AAS),

AAS can be divided into two stages: 1) the production of free atoms from the sample, and 2) the absorption of radiation from an external source by these atoms (Willard *et al.*, 1988). It is on the production of uncombined and un-ionised atoms in an atomic vapour that the success of an atomic absorption analytical procedure depends. This process is known as atomisation and is commonly achieved using flame or electrothermal techniques. Other more specialist techniques exist; these include glow discharge and hybride atomisation. In flame atomisation (Figure 1), a solution of the sample is nebulized by a flow of gaseous oxidant (e.g. air, oxygen, nitrous oxide), mixed with a gaseous fuel (e.g. natural gas, hydrogen, acetylene), and carried into a flame where atomisation occurs (Skoog *et al.*, 1997). The flame temperature can be varied using different fuel and oxidant combinations. The use of air as the oxidant typically produces flame temperatures of 1700°C to 2400°C, which is suitable for the atomisation of easily decomposed samples. Atoms that resist atomisation through the formation of refractory oxides require oxygen or nitrous oxide as the oxidant, which can achieve flame temperatures of 2500°C to 3100°C. Flame atomisation remains an effective technique for the analysis of liquid samples. Electrothermal atomisation achieves enhanced sensitivity as the entire sample is atomised within a short period of time and atoms remain in the optical path for longer (flame $\approx 10^{-4}$ s, electrothermal ≈ 1 s). A few microlitres of sample are evaporated at low temperatures and then ashed at higher temperatures in an electrically heated graphite tube. The temperature in the tube is then raised rapidly to 2000°C to 3000°C by increasing the electrical current; atomisation of the sample occurs in a period of a few milliseconds to seconds (Skoog *et al.*, 1997). Absorption is then measured immediately above the heated surface. Solids introduced as fine powders can be measured using this atomisation technique.

In AAS, the radiation required to elevate ground state free atoms to the excited state is achieved using a specialised external source, which passes through the atomised sample. Analytical methods based on atomic absorption are highly specific because atomic absorption lines are narrow (0.002 to 0.005 nm) and because electronic transition energies are unique for each element (Skoog *et al.*, 1997). The external source must emit radiation at a bandwidth narrower than the atomic absorption peaks in order to

obey the Beer-Lambert law, which states that in order for there to be a linear relationship between the analytical signal (absorbance) and concentration, it is necessary that the bandwidth of the source must be narrow relative to the absorption peak. This is achieved using radiation emitted from excited atoms of the element to be analysed. The most common source used in AAS is a hollow cathode lamp, although others e.g. electrodeless discharge lamps, are also in use. The hollow cathode lamp consists of a tungsten anode and a cylindrical cathode sealed in a glass tube that is filled with neon or argon. The cathode is constructed from the element to be determined. The ionisation of some gas atoms occurs by applying a potential difference between the anode and the cathode (300-400 mV). These gaseous ions bombard the cathode, causing some metal atoms to be ejected, known as sputtering. Some of the sputtered atoms are in the excited electronic state and as they return to ground state they emit radiation. The cathode concentrates the radiation into a beam, which is passed through a quartz window, and the sputtered atoms are redeposited on the cathode.

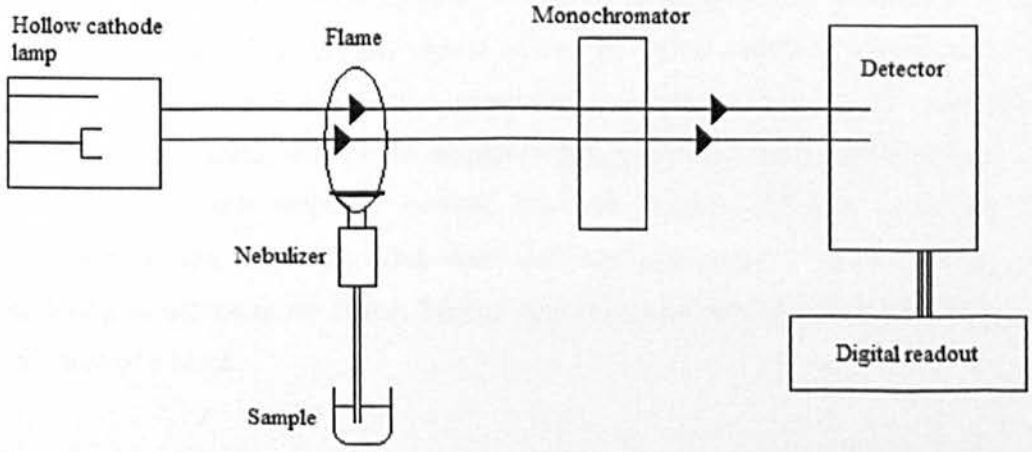

Figure 1: Schematic representation of an atomic absorption spectrometer using a hollow cathode lamp as the external radiation source and a flame atomiser.

An atomic absorption spectrophotometer consists of the following critical components: external radiation source e.g. hollow cathode lamp, atomiser e.g. flame, monochromator, and a detector (Figure 1). Free atoms are generated by atomisation of the sample and radiation emitted from the external source passes through the free atoms, either within the interzonal region of the flame, or above the heated surface in the graphite furnace. The monochromator isolates the desired wavelength needed to reach

the detector. Interferences caused by radiation emitted by the flame is often removed by the monochromator e.g. emission from atoms other than the analyte. However excitation and emission by analyte atoms within the flame will have wavelengths corresponding to the monochromator setting. Modulating the output of the external source so that its intensity fluctuates at a constant frequency eliminates these effects. The detector then receives two signals; an alternating one from the external source, and a continuous one emitted by the flame. The detector consists of a photomultiplier tube, which produces an electrical signal proportional to the light intensity. The unmodulated signal is then removed and the modulated signal continues for amplification.

There are two types of interference encountered in atomic absorption methods (Skoog *et al.*, 1997): 1) *spectral interferences* which arise when the absorption or emission of an interfering species either overlaps or lies so close to the analyte absorption or emission that resolution by the monochromator becomes impossible or; 2) *chemical interferences* resulting from various chemical processes occurring during atomisation that alter the absorption characteristics of the analyte. The most common spectral interference occurs when components of the sample matrix absorb or scatter radiation emitted from the source, although these effects are generally rare when using flame atomisation techniques. Substances with broad absorption bands such as metal oxides and hydroxyl radicals may absorb radiation emitted from the source, although increasing the temperature of the flame can often cause their decomposition. Where the source of interfering substance is the flame, background absorption can be measured during the aspiration of a blank.

Chemical interferences are generally more common than spectral interferences. Anions that form compounds of low volatility with the analyte may reduce the rate of atomisation, decreasing absorbance. Sulphate and phosphate ions have both been shown to cause a decrease in calcium absorbance. The use of releasing agents (cations which preferentially react with the interfering anion), protective agents (substances which preferentially react with the analyte to form volatile species) and increasing the flame temperature are all effective measures of reducing this type of interference. The equilibrium between associated and undissociated atoms ($NaCl \Leftrightarrow Na + Cl$) and neutral and ionised atoms ($M \Leftrightarrow M^+ + e^-$) can shift in the presence of other species in the

sample or fuel. This can alter the atomic concentration of atoms and thereby lower the measured absorbance.

Calibration,

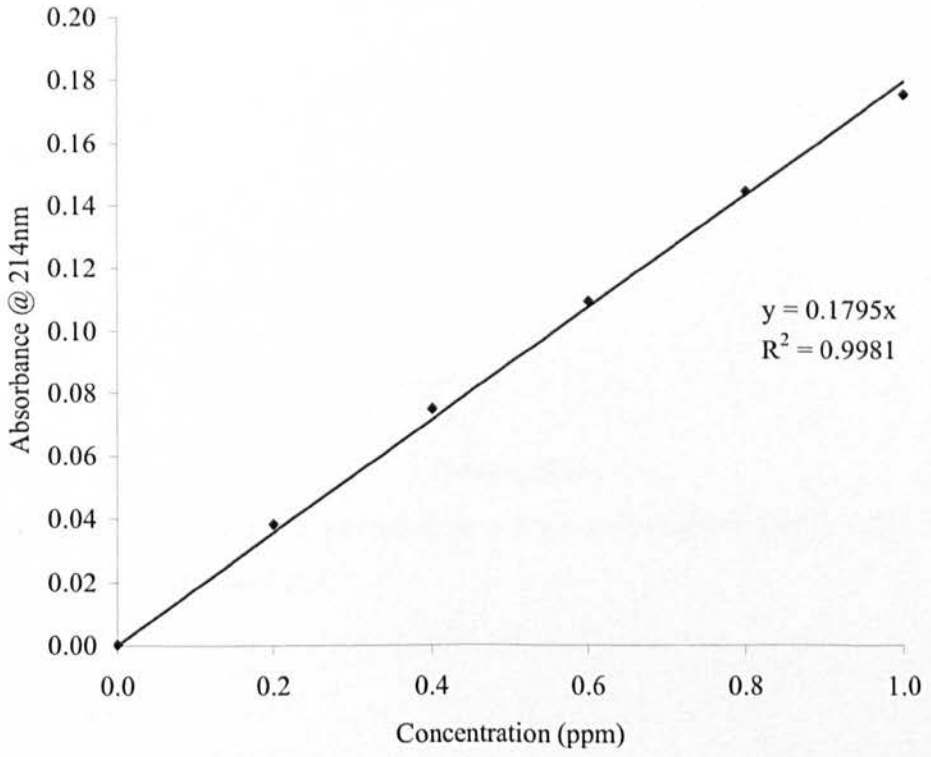

Figure 2: Calibration curve plotted from atomic absorption measurements of known concentration zinc standards.

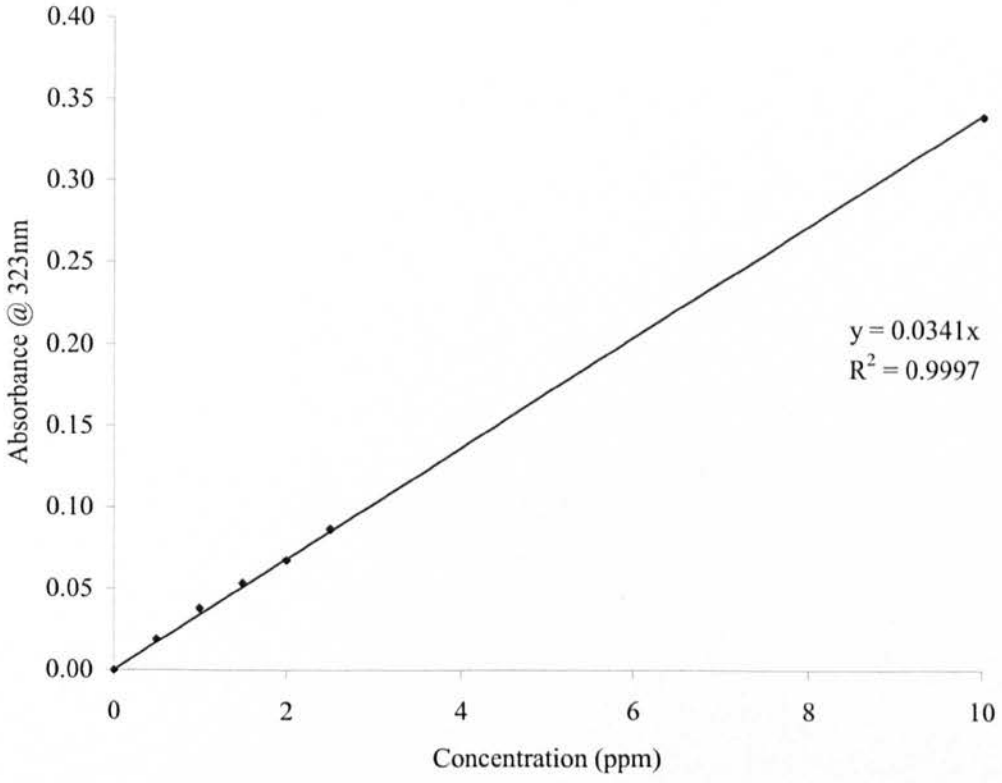

Figure 3: Calibration curve plotted from atomic absorption measurements of known concentration silver standards.

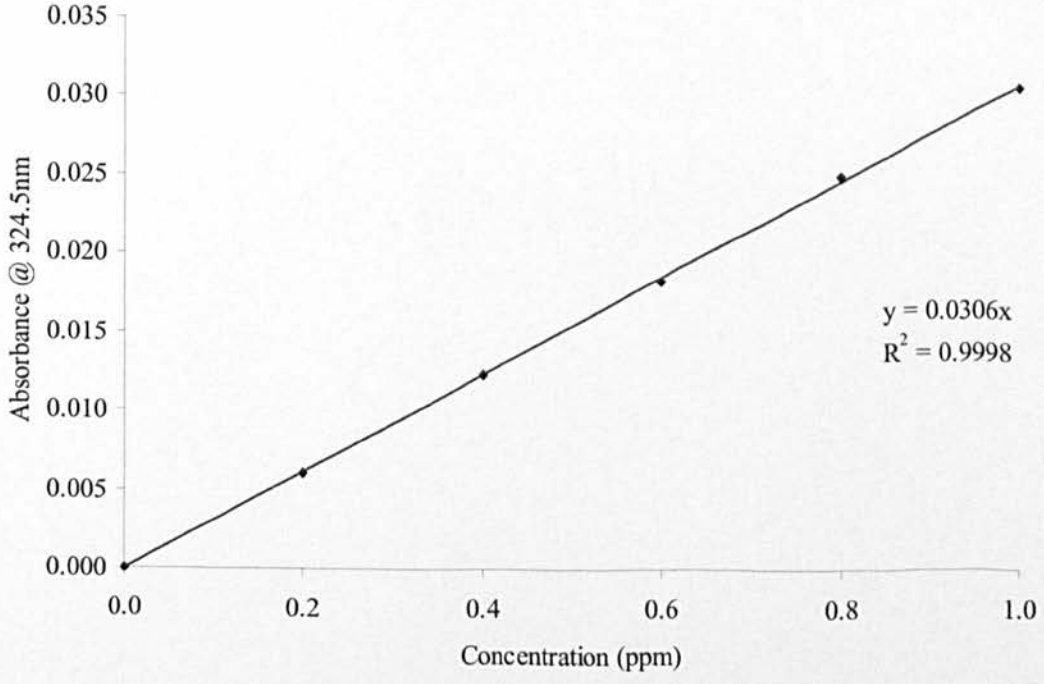

Figure 4: Calibration curve plotted from atomic absorption measurements of known concentration copper standards.

Appendix 3

- Fluoride ion selective electrode calibration

Table 1 Measurement of the calibration standards prepared in 80/20 diluent with corresponding values for fluoride concentration and $\log^{10}$ fluoride concentration to prepare the calibration graph.

Standard (ppm)	mV	F^- conc. (mM)	Log (10) F^- conc.
100	8.7	5.27	0.72181
50	26.9	2.635	0.42078
10	68.1	0.527	-0.27819
5	85.7	0.2635	-0.57922
1	122.8	0.0527	-1.27819

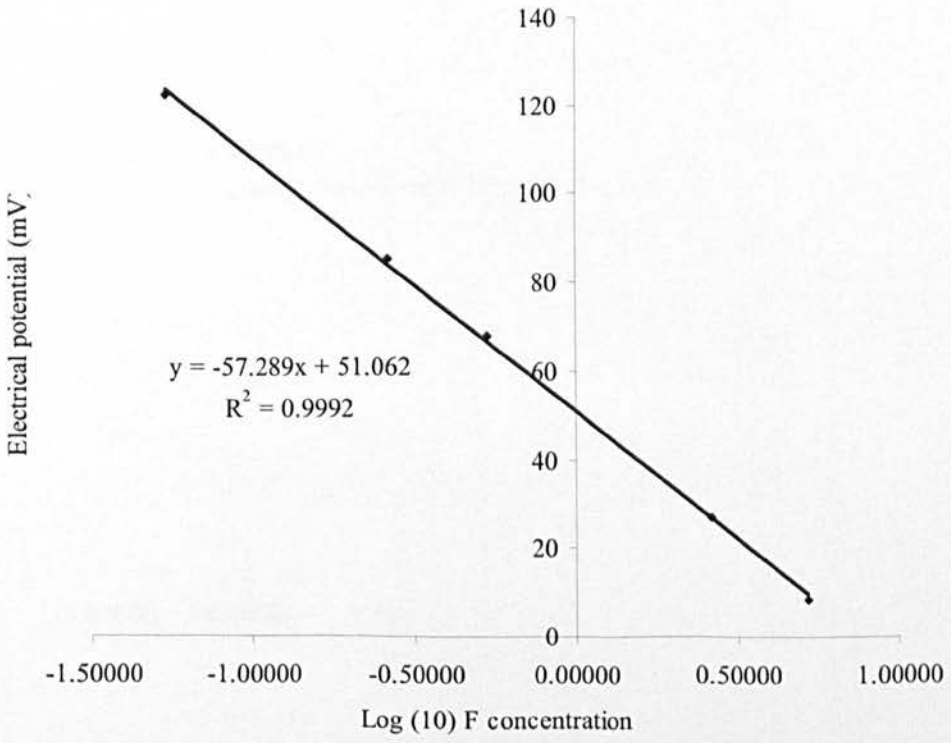

Figure 1 Calibration curve showing the linear relationship between $\log^{10}$ fluoride concentrations in the calibration standards and the electrical potential (mV) measured by the fluoride ion selective electrode.

- Measuring the limit of detection

Table 2 Measurement of the calibration standards prepared in 80/20 diluent with corresponding values for fluoride concentration and log^{10} flouride concentration to detect the limit.

Standard (ppm)	Conc (mM)	Log (10) conc	mV
100	5.27	0.72181	5
50	2.635	0.42078	23
5	0.2635	-0.57922	82
1	0.0527	-1.27819	123
0.1	0.00527	-2.27819	168
0.05	0.002635	-2.57922	175
0.01	0.000527	-3.27819	174

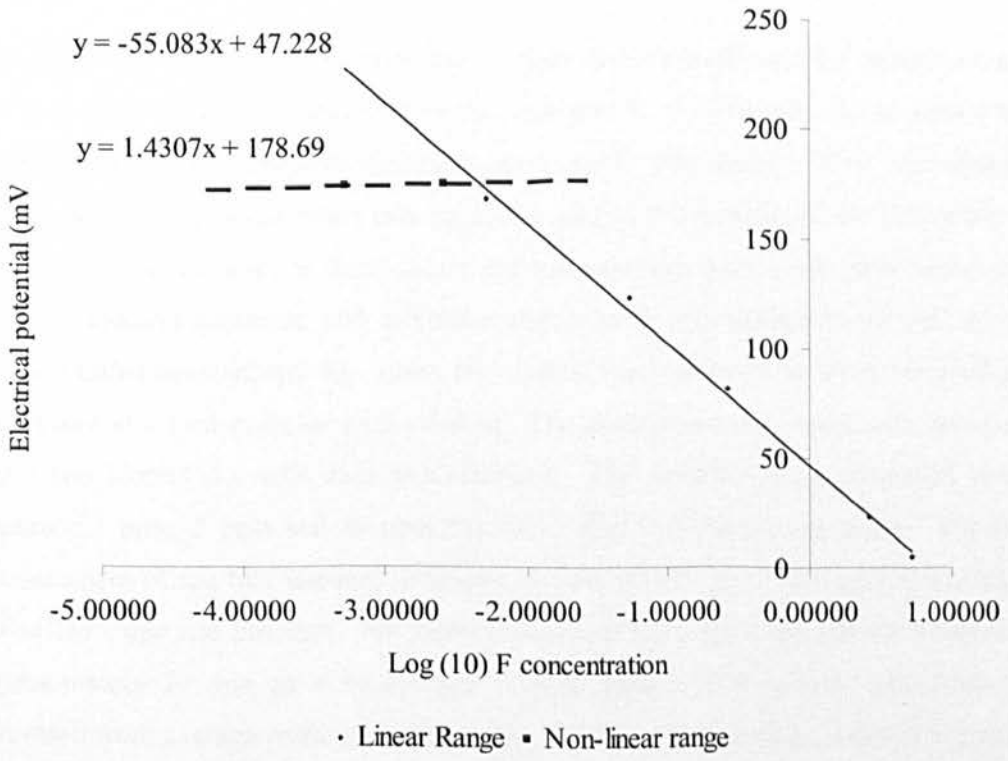

Figure 2 Linear and non-linear range of calibration standards measured with the fluoride ion selective electrode.

The values of mV determined for the standards equal to and below 0.05 ppm did not fit with the linear relationship displayed for the standards of a higher fluoride concentration; therefore the limit of detection must be greater than 0.05 ppm. The limit

of detection of the fluoride ion selective electrode can be determined by calculating the point at which the linear and non-linear regions of the calibration curve intercept. This can be achieved by calculating the point at which the equations of the linear and non-linear lines are equal to each other.

$1.4307x + 178.69 = -55.083x + 47.228$ (subtract 47.228)

$1.4307x + 131.46 = -55.083x$ (subtract 1.4307x)

$131.46 = -56.514x$

Therefore: $x = \frac{131.46}{-56.51} = -2.326$

Limit of detection = 0.0047 mM or 0.090 ppm

- Accuracy and precision of the fluoride ion selective electrode

Standard solutions containing 1 ppm and 10 ppm fluoride were used for calibration and a 5 ppm fluoride solution was used as the test sample to determine the accuracy and precision of the ion selective electrode used within this study. This was deemed necessary as the instrumentation was regularly used by the students of the University of Brighton. Measurements of the standard and test solutions were made after immersing the ion selective electrode and reference electrode in approximately 80 mL of the solution under constant stirring. Once the reading had stabilised for 10 s, ten readings were taken at 1 s intervals for each solution. The electrodes were rinsed with deionised water and blotted dry with each measurement. The solutions were measured in the sequence 1 ppm, 5 ppm and 10 ppm fluoride. This was repeated 6 times. The first measurement of the two standard solutions (1 ppm and 10 ppm fluoride) was used to define the slope and intercept. Six measurements of the 5 ppm test sample taken over approximately 30 min gave an average of 4.80 ppm ± 0.08 (SD). The slope, as measured from average readings of the 1 ppm and 10 ppm standards, showed a gradual drift downwards during the course of the experiment (-57.05, -57.05, -57.24, -57.23, -57.94, -56.44). This is expected when using a fluoride ion selective electrode and can be compensated by increasing the frequency of calibration. The accuracy of the probe was adequate, with the average reading of the 5 ppm test sample 0.2 ppm lower than that expected. The variation over 30 min was 0.08 ppm, which is an error of less than 2% indicating the ion selective electrode recorded precise measurements.

Appendix 4

Example of saliva donation declaration form required prior to donation:

SALIVA DONATION DECLARATION

All saliva donors must read and understand the exclusion criteria and give consent to participate in the study.

Please sign to confirm you have read and understood the exclusion criteria and to confirm you do not fall under that criteria.

The exclusion criteria for saliva donation is:

- known Hepatitis carrier;
- currently suffering any viral/bacteria infection, including common colds and coughs;
- currently being treated with antibiotics;
- suffered glandular fever in the previous 6 months;
- currently suffer from tender or bleeding gums;

If none of the above criteria apply please sign and fill in the details below.

- Study details;
- .....
  .....
  .....
  .....
- Any donation criteria, for example, no tooth brushing prior to collection.
- .....
  .....
  .....

Signature ..... **Date** .....

Name (Print) .....